UNIVERSITY OF BIRMINGHAM

The role of Mucosal-associated Invariant T cells in children with Autoimmune liver disease

A Thesis by

Suzan Shou Ying Warner

Submitted for the degree of DOCTOR OF PHILOSOPHY

Centre for Liver and

Gastrointestinal Research

Institute of Immunology and

Immunotherapy

College of Medical and Dental Sciences

University of Birmingham

CLGR

CENTRE FOR LIVER AND GASTROINTESTINAL RESEARCH

This thesis is dedicated to my amazing husband, Justin Steven Warner,

whom I owe the biggest thanks to.

Justin, you have been my rock, sounding board and biggest source of comfort throughout. I could not have completed this work without your unwavering support and understanding. Thank you for always making me laugh and seeing the funny side of things. I am eternally grateful for your love and belief in me.

Abstract

Mucosal-associated invariant T (MAIT) cells, defined as CD3+ Valpha7.2+ CD161++ T lymphocytes, are central in the immunosurveillance and maintenance of mucosal integrity.

Transcriptomic studies has revealed a tissue repair signature and in health, MAIT cells adopts a regenerative role, releasing antifibrotic cytokines like interleukin-22 at steady state.

In chronic liver disease, intrahepatic MAIT cells predominantly localizes to the fibrotic septae and peribiliary regions, most notably in Primary sclerosing cholangitis (PSC).

Autoimmune liver disease (AILD), including PSC, are lifelong chronic immune-mediated hepato-biliary disorders that often presents in childhood. There is no cure except for liver transplantation (LT) and even then, the recurrence rate is high.

In adult AILD, intrahepatic MAIT cells displays an activation-induced cell exhaustion state with functional IFNγ and TNFα impairment. Furthermore, polarization to the profibrotic MAIT17 phenotype occurs with chronic stimulation. MAIT cells are therefore speculated to augment biliary epithelial damage and disease progression in AILD.

This project examines the biological characterization of MAIT cells and their functional activity in children with AILD which has not been investigated. Deciphering the early immunopathogenesis of this lifetime condition may provide pathways to explore new treatment options in the future for this debilitating disease. In this research, intrahepatic MAIT cells were confirmed in paediatric liver explants and in terms of function, MAIT cells from children with PSC had preserved TNFα secretion in association with upregulated TNF superfamily activity. These PSC MAIT cells also displayed an early polarization towards the chronic inflammatory MAIT17 phenotype. Findings from my research signify that MAIT cells play an important role in the pathogenesis of paediatric autoimmune liver disease. Deciphering this early immunopathogenesis may provide pathways to explore new treatment options for this debilitating lifelong disease.

Acknowledgements

First of all I would like to thank Professors Deirdre Kelly, David Wraith and Ye Oo for giving me this incredible opportunity to undertake a PhD in Liver Immunology, a field I have wanted to specialize in since starting my career in Paediatric Hepatology.
I am forever grateful for their support and guidance, especially to Professor Kelly who has been a friend and mentor to me throughout my training and research.
I am very thankful for the funding that I have received for my research from Birmingham Children's Hospital Charity and from Supporting Paediatric Liver and Intestinal Transplantation (SPLIT). I am extremely thankful to the patients and parents for giving their consent and allowing for their blood and/or liver tissue to be sampled and used in the experiments of this research work.

My research would not have been possible without the help and assistance from my colleagues at the Centre of Liver and Gastrointestinal Research (CLGR). A tremendous shout out and thanks to the Oo Group postdocs and technicians for their technical support and advice for my MAIT cell coculture and flow cytometry experiments; Hannah Jeffery, Paul Collins, Grace Wootton, Baksho Kaul, Naomi Richardson and Remi Fiancette. A special thanks to Scott Davies, Jagjeet Sodh and Alessandro di Maio for teaching and supervising my immunohistochemistry, immunofluorescence and confocal microscopy work. I owe a great deal of thanks to Naeem Khan from Clinical Immunology for all his help and guidance with my metal conjugation and CyTOF experiments, and to Shahram Golbabapour for his technical support on the Helios mass cytometer. I would like to extend my thanks to Gill Muirhead for teaching me the technique of biliary epithelial cell culture. I want to especially thank Chris Weston and Janine Fear for their sound advice,

encouragement and kindness. Huge thanks to my fellow students who have been a great source of support – it's always so nice to see their friendly faces and hear the banter.
Next, I would like to give a massive thank you to all my consultant, nursing, junior doctor, physician associate, and research administrative colleagues at Birmingham Children's Hospital who have given me their full support and helped me out over the years, particularly with enormous thanks to Khalid Sharif, Alex Brant and Julie Taylor who have gone out of their way to help me obtain blood/tissue samples and lab consumables for my research.

Lastly, I want to thank my amazing friends and family for their support, understanding and boundless faith in me. I owe my deepest gratitude to my wonderful husband Justin Warner who has been there for me through thick and thin. I thank him dearly from the bottom of my heart for all his love, support, patience, and level-headed reasoning during all the ups and downs of my research.

Table of Contents

List of Figures

Chapter 1 – Introduction

Chapter 3 – Assessing the spatial relationship of MAIT cells and Tregs in the paediatric autoimmune liver

Chapter 4 – Examining the biological characteristics and functional capabilities of paediatric blood MAIT cells by CyTOF analysis

Chapter 5 – Functional role of MAIT cells in autoimmune liver disease in children and adults.

List of Tables

List of Abbreviations

ABCB1	Adenosine triphosphate binding cassette subfamily B member 1
αEβ7	Alpha E beta 7 integrin
aGVHD	Acute Graft-Versus-Host-Disease
AIH	Autoimmune hepatitis
AIH type 1	Autoimmune hepatitis type 1
AIH-1	Autoimmune hepatitis type 1
AIH T1	Autoimmune hepatitis type 1
AIH type 2	Autoimmune hepatitis type 2
AIH-2	Autoimmune hepatitis type 2
AIH T2	Autoimmune hepatitis type 2
AILD	Autoimmune liver disease
ALF	Acute liver failure
ALP	Alkaline phosphatase
ALT	Alanine transferase
ANA	Antinuclear antibody
ANCA	Anti-neutrophil cytoplasmic antibody
AST	Aspartate transferase
ASC	Autoimmune sclerosing cholangitis
BA	Biliary atresia
BCH	Birmingham Children’s Hospital
BcL2	B-cell lymphoma 2
BECs	Biliary epithelial cells
BSA	Bovine Serum albumin

C3	Complement protein C3
C4	Complement protein C4
CCL	C-C Motif ligand
CXCL	C-X-C Motif ligand
CD	Cluster of differentiation
CCR	C-C Motif chemokine receptor
CXCR	C-X-C Motif chemokine receptor
CLGR	Centre of Liver and Gastrointestinal Research
CK19	Cytokeratin 19
CAS	Cell acquisition media
Cd	Cadmium
CNS	Central nervous system
COVID-19	Coronavirus disease
CSM	Cell staining media
CTLA-4	Cytotoxic T-lymphocyte associated protein 4
CUDA	Compute Unified Device Architecture
CyTOF	Cytometry by Time Of Flight
DAAs	Direct-acting antivirals
DAB	3,3′-Diaminobenzidine
DAPI	4′,6-diamidino-2-phenylindole
DCs	Dendritic cells
DN	double negative T lymphocytes (CD4- CD8-)
DNA	Deoxyribonucleic acid
DNase	Deoxyribonuclease
DPX	Dibutylphthalate polystyrene xylene mounting medium

Dy	Dysprosium
E.coli	Escherichia coli
EDTA	Ethylenediaminetetraacetic acid
ERCP	Endoscopic retrograde cholangiopancreatography
Er	Erbium
ESLD	End stage liver disease
ESPGHAN	European Society of Paediatric Gastroenterology, Hepatology and Nutrition
Eu	Europium
FACS	Fluorescence-activated cell sorting
FBS	Fetal Bovine Serum
Fc	Fc receptor
FCS	Fetal calf serum
FFPE	Formalin fixed paraffin embedded
FOXP3	Forkhead box P3 protein
GCP	Good clinical practice
Gd	Gadolinium
GGT	Gamma glutamyl transferase
GMCSF	Granulocyte-macrophage colony-stimulating factor
GRZB	Granzyme B
HBRC	Human Biomaterials Resource Centre
HBV	Hepatitis B virus infection
HC	Healthy children cohort
HCC	Hepatocellular carcinoma
HCV	Hepatitis C virus infection

HDV	Hepatitis delta virus infection
HEA	Human epithelium antigen
HIV	Human immunodeficiency virus
HLA-DR	Human leukocyte antigen DR isotype
Ho	Holmium
HSC	Hepatic stellate cells
IAIHG	International autoimmune hepatitis group
IBD	Inflammatory bowel disease
IBR	Institute for Biomedical Research
ICH	Institute of Child Health
ICAM-1	Intercellular adhesion molecule-1
IDA	Industrial denatured alcohol
IDO	Indoleamine dioxygenase
IF	Immunofluorescence
IFNα/β	Interferon α or β (type 1 interferons)
IFNγ	Interferon gamma
IgG	Immunoglobulin G
IgG1	Immunoglobulin isotype G1
IgG2	Immunoglobulin isotype G2
IHC	Immunohistochemistry
IL	Interleukin
IL- R	Interleukin- receptor
In	Indium
iNKT	Invariant natural killer T lymphocytes
ITM	Institute of Translational Medicine

Ki67	Antigen Ki-67, marker of proliferation
LC1	Liver cytosol antibody
LFA-1	Lymphocyte function-associated antigen-1
LI-DC	Liver dendritic cell
LI-MAIT	Liver mucosal-associated invariant T cells
LKM	Liver-kidney microsomal antibody
LLT-1	Lectin-like transcript 1
LMC	Liver mononuclear cell
LSEC	Liver sinusoidal endothelial cells
LT	Liver transplantation
Lu	Lutetium
M1	Phenotype M1 macrophages
M2	Phenotype M2 macrophages
MAIT cells	Mucosal-associated invariant T cells
MAIT17	MAIT cells with Th17 cell characteristics
MAIT1	MAIT cells with Th1 cell characteristics
MCP-1	Monocyte chemoattractant protein-1
MDR2	Multidrug resistance protein 2
MHC	Major histocompatibility complex
MIP-1α	Macrophage inflammatory protein-1 alpha
MIP-1β	Macrophage inflammatory protein-1 beta
MMF	Mycophenolate mofetil
MMI	Median metal intensity
MR1	Major histocompatibility complex class 1-related protein
MRCP	Magnetic resonance cholangiopancreatography

MS	Multiple sclerosis
NAFLD	Non-alcoholic fatty liver disease
NASH	Non-alcoholic steatohepatitis
Nd	Neodymium
NK cells	Natural killer cells
NSAID	Non-steroidal anti-inflammatory drug
PBC	Primary biliary cirrhosis
PBMCs	Peripheral blood mononuclear cells
PBS	Phosphate buffered saline
PCR	Polymerase chain reaction
PD-1	Programmed cell death protein 1
Pen/Strep	Penicillin-Streptomycin
Perm buffer	Permeabilization buffer
PFA	Paraformaldehyde
PHT	Portal hypertension
PLZF	Promyelocytic leukemia zinc finger protein
PMA	Phorbol myristate acetate
Pr	Praseodymium
PSC	Primary sclerosing cholangitis
PT	Prothrombin time
QEH	Queen Elizabeth Hospital, Birmingham
R&D	Research and Development
RORγt	Retinoic acid receptor-related orphan receptor gamma t
RPMI	Roswell Park Memorial Institute medium
Rx	Treatment

SBP	Spontaneous bacterial peritonitis
Sm	Samarium
SMA	Smooth muscle antibody
SOP	Standard Operating Procedure
STAT1	Signal transducer and activator of transcription 1
STIM	Stimulated
Tb	Terbium
Tbet	T-box expressed in T cells
TBX21	T-box transcription factor 21
TCEP	Tris (2-carboxyethyl) phosphine
TCR	T cell receptor
TGFβ	Transforming growth factor β
Th	T helper cells
THP-1	Human monocyte cell line
TIM3	T-cell immunoglobulin and mucin domain 3
Tm	Thulium
TNFα	Tumour necrosis factor alpha
TNFL	Tumour necrosis factor ligand superfamily
TNFR	Tumour necrosis factor receptor superfamily
Total Bili	Total bilirubin
Tregs	Regulatory T cells
TRAJ	T cell receptor alpha joining
TRAV	T cell receptor alpha variable
TRBV	T cell receptor beta variable
tSNE plots	t-distributed stochastic neighbour embedding

UC	Ulcerative colitis
UNSTIM	Unstimulated
Vα7.2	Valpha 7.2 invariant T cell receptor alpha chain
Vβ	T cell receptor variable beta chain
VLA-4	Very late antigen-4 protein
Yb	Ytterbium
γδ	gamma delta T lymphocytes
5-OP-RU	5-(2- oxopropylideneamino)-6-D-ribitylaminouracil
6-FP	6-formyl pterin
7AAD	7-aminoactinomycin D

Chapter 1. Introduction

1.1 Mucosal-associated Invariant T (MAIT cells)

1.1.1 The discovery and definition of human MAIT cells

Mucosal-associated invariant T (MAIT) cells are a type of unconventional T lymphocyte first identified by Porcelli et al in 1993 during the characterization of double negative (CD4-, CD8-) T lymphocytes in which polymerase chain reaction (PCR) amplification of the alpha and beta chains isolated regions of invariant rearrangement of the T cell receptor (TCR) [1] MAIT cells in humans to largely express the TCR α chain, Vα7.2-Jα33 (TRAV1- 2-TRAJ33). Normal variants of the α chain include Vα7.2-Jα12 (TRAV1-2-TRAJ12) and Vα7.2-Jα20 (TRAV1-2-TRAJ20) [2, 3]. These alpha chains are customarily paired with a limited number of beta chains, predominately Vβ2 (TRBV20) and Vβ13 (TRBV6) [3-5].
MAIT cells have the highest expression of the C-type lectin CD161 in comparison to NK cells and conventional T cells. CD161 modulates MAIT cell effector function by the lectin-like transcript 1 (LLT-1) [6, 7]. Therein, MAIT cells have come to be defined as CD3+ Valpha7.2+ CD161++ T lymphocytes [8, 9].

MAIT cells constitute 1-10% of total T cells in the circulation and are found in abundance at epithelial sites like the skin, liver, gut and lung. MAIT cells are considered central in the immunosurveillance, tissue maintenance and repair at mucosal sites [10-12].

Human MAIT cells are predominantly CD8+ and to a lesser degree, double negative (CD8-CD4-) T cells with an effector memory phenotype (CD45RO+ CCR7−) [9, 13, 14]. CD4+

cells make up only a minority of this subpopulation. Adult CD8+ MAIT cells mostly express the CD8αα homodimer, with the CD8αβ heterodimer being present in fewer individuals. Similar chemokine-receptor profiles are expressed by both invariant TCR isoforms, implying similar cell recruitment and effector functions [15, 16] . MAIT cells have been identified in the human fetal liver, gut and lung from the second trimester and were of an effector memory phenotype [14].

1.1.2 TCR Va7.2 restriction by the MR1-related molecule

Conventional $\alpha\wr$ T lymphocytes are classically restricted by peptides presented by the major histocompatibility complex (MHC). The invariant nature of the MAIT cell T cell receptor Vα7.2 is its restriction by metabolic derivatives of bacterial riboflavin and folic acid degradation products presented by the monomorphic MHC class-1 related protein, MR1 [2, 5, 17]. The MR1 protein is present on the cell surface of antigen presenting cells and many tissue cell types including cholangiocytes and hepatocytes [18, 19].
The MR1 α domains are almost identical between humans and mice leading to the inference that this molecule is conserved amongst mammals [9, 20, 21].

Microbial induction of MAIT cells were first described in 2010 by Gold et al and Le Bourhis et al in which Gram-positive and Gram negative bacteria, Mycobacterium and yeast were shown to elicit MAIT cell activation. Le Bourhis et al demonstrated MAIT cell activation by Gram-positive bacteria *Staphylococcus epidermidis, Staphylococcus aureus, Lactobacillus acidophilus* and Gram negative bacteria *Escherichia coli, Klebsiella pneumoniae, Pseudomonas aeruginosa and Mycobacterium abscessus[22, 23].* Gold et al showed MAIT

cell activity to *Staphylococcus aureus, Escherichia coli, Salmonella enterica* and *Mycobacterium tuberculosis* even in previously unexposed individuals [24, 25].
MAIT cells however do not respond to all bacteria. Group A *Streptococcus pyogenes, Enterococcus faecalis,* and *Listeria monocytogenes* for example cannot activate MAIT cells, suggesting these bacteria do not produce the offending ligand or that the ligand lacks specificity to the MR1 binding cleft or to induce TCR Vα7.2 restriction [22, 25].
Whilst bacterial riboflavin (vitamin B2) metabolites are MAIT cell agonists, notably 5-2 (-oxopropylideneamino)-6-D-ribitylaminouracil (5-OP-RU), derivatives of the folic acid (vitamin B9) biosynthetic pathway 6-formyl pterin (6-FP), do not activate these effector cells despite having the ability to bind to the MR1 antigen presenting cleft [17, 26]

Keller et al went on to identify a wide spectrum of small organic molecules, drug and drug metabolites which were capable of binding to the MR1 molecule [27]. Furthermore, the investigators demonstrated MAIT cell TCR Vα7.2 restriction by these drug and drug-like molecular ligands, with some inducing activation whilst others inhibited MAIT cell activity. Fragment-based virtual screening identified 147 compounds which could occupy the same binding site of MR1 as 5-OP-RU, the most potent MAIT cell activating ligands. Of the drugs analyzed, diclofenac, a non-steroidal anti-inflammatory drug (NSAID), showed the greatest potency in activating MAIT cells. This study confirmed MAIT cell modulation by ligands other than bacterial-derived vitamin B metabolites and is of clinical significance when considering drug-mediated effects on MAIT cell activity [27].

1.1.3 MAIT cell activation and function

MAIT cells share effector cytokine profiles as T helper 1 (Th1) and T helper 17 (Th17) cells; upon activation MAIT cells upregulate their expression of the proinflammatory cytokines interferon-gamma (IFNγ) & tumour necrosis factor alpha (TNFα), and interleukin-17 (IL-17) & interleukin-22 (IL-22) respectively [8, 28-30]. Additionally, they possess cytotoxic potential by being able to degranulate and release the lytic cytokines Granzymes and Perforin on activation [10, 30].

Apart from activation by TCR Vα7.2 restriction in a MR1-dependent manner as described above, MAIT cell activation can also occur in a MR1-independent manner by cytokine stimulation [31]. van Wilgenburg et al demonstrated MAIT cell activation with the release of Granzyme B and interferon-gamma (IFNγ) in association with upregulation of the T cell activation marker CD69 when human peripheral blood MAIT cells were co-cultured with dengue virus, hepatitis C or influenza virus [32]. These responses occurred in the absence of TCR Vα7.2 stimulation and were dependent on the presence of interleukin-18 (IL-18) in conjunction with IL-12 and/or IL-15. Viral infections activate MAIT cells via this cytokine dependent/MR1 independent pathway only [31, 32].

MAIT cells express a spectrum of cytokine receptors such as interleukin-12 receptor (IL-12R), IL-18R and IL-23R which enables MAIT cell activation in a cytokine-dependent/MR1-independent manner [12, 31]. Many cytokines can activate MAIT cells in this manner including IL-1b, IL-7, IL-12, IL-15, IL-18 and type 1 interferons (IFNα/β) [33, 34]. These cytokines are released mainly by activated circulating innate immune cells as part of the inflammatory milieu.

Both modes of MAIT cell activation, MR1-TCR Vα7.2 dependent and independent pathways, are often activated together in bacterial infections and are synergistic in their

function. Recent studies have shown MAIT cell TCR activation alone to be insufficient to trigger optimal MAIT cell proinflammatory activity which only occurs in the presence of the aforementioned cytokines [35, 36]. Interestingly, MAIT TCR restriction without cytokine co-stimulation induces an antifibrotic phenotype and adopts a homeostatic tissue repair role which will be discussed further in Chapter 1.3.2.

Of the transcription factors expressed by MAIT cells, three are of particular importance; the T-box transcription factor TBX21, also known as T-box expressed in T cells (Tbet) regulates the function of Th1 cells, and retinoic acid-related orphan receptor γt (RORγt) which regulates the production of IL-17 [37, 38]. Promyelocytic leukaemia zinc-finger (PLZF) is classically a transcription factor of natural killer (NK) cells that has been identified in MAIT cells; the innate-like properties of MAIT cells are enhanced by PLZF activity [38].

Lastly, MAIT cells can be recruited to sites of inflammation due to their expression of a set of homing chemokine receptors. Our group reported a higher expression of the liver homing chemokine receptors C-C chemokine receptor type 6 (CCR6) and C-X-C chemokine receptor type 6 (CXCR6) on intrahepatic MAIT cells from diseased explants and donor livers [19]. The gut homing C-C chemokine receptor type 9 (CCR9) has also been found to be expressed by MAIT cells and has been linked to hepatic stellate cell proliferation in murine models [39]. MAIT cell expression of the monocyte/macrophage chemokine receptors CCR2 and CCR5 has also been reported. CCR2 mediates monocyte chemotaxis via the monocyte chemoattractant protein-1 (CCL2). CCR5 is expressed on conventional T cells, and antigen presenting cells and is a receptor for potent chemoattractants like the macrophage inflammatory protein-1 alpha (MIP-1α, aka CCL3) and MIP-1β (CCL4) [11, 40]. This expression pattern of homing receptors enables MAIT cells to mobilise and contribute to the inflammatory milieu (Figure 1a).

1.2.1 The role of MAIT cells in liver homeostasis and tissue repair

MAIT cells account for ≥30% of total T lymphocytes in the healthy donor liver [10, 38]. Their abundance in the liver and gastrointestinal tract suggests MAIT cells play an important role in maintaining immunity and mucosal integrity at these key sites of potential microbial exposure [38, 41].

The large volume of blood delivered to the liver by the portal vein brings with it an enormous antigenic load of dietary compounds and commensal bacteria [37, 42]. The liver needs to confer tolerance to these physiological 'harmless' compounds but at the same time be able to respond rapidly to an array of pathogenic bacteria [37, 43].

Under 'normal' conditions in the healthy human liver, a steady state low grade exposure to bacterial ligands imported from the portal vein, triggers MAIT cell TCR activity [35, 36]. However, this TCR activity alone induces a partial MAIT cell response which appears to promote tissue repair and wound healing due to their expression of the anti-fibrotic cytokines IFNy and IL-22 [44, 45]. This theory is supported by several recent studies. For example, inferior skin would healing is observed in MR1 knock out mice i.e. in the absence of MAIT cells. Direct application of the TCR Vα7.2 agonist 5-OP-RU ligand onto injured skin promoted MAIT cell expansion and wound healing in another murine model. In an in vitro assay, human blood MAIT cells activated by *E.coli* supernatant, accelerated the tissue repair of intestinal epithelium [46-48]. Recent human peripheral blood MAIT cell transcriptomic studies have revealed TCR Vα7.2/MR1-dependent MAIT cell activation to possess a tissue repair signature. Shared human and murine tissue repair genes includes TNF, PTGES2, TGFB1, CCL3, HMGB1, VEGFB, HIF1A, FURIN, GMCSF and PDGFEB [41, 45, 49].

MAIT cell TCR activation in the absence of cytokines e.g. in the healthy uninflamed, uninjured liver tissue, appears to adopt a homeostatic tissue repair and regenerative role [35, 36, 44].

In disease, gastrointestinal dysbiosis and disruption of gut integrity can give rise to bacterial translocation of potentially harmful bacterial strains [33, 44]. Microorganisms can enter the biliary tract from the duodenum and they can be introduced from translocated gut microbiota in the portal venous system [37, 50]. In the context of liver damage and inflammation, large amounts of the cytokines are generated e.g. by IL-12, IL-18,IL-15, TNF and type 1IFN [33, 44]. These cytokines are strong activators of MAIT cells and as discussed, maximal MAIT cell proinflammatory activity requires the synergistic cytokine and TCR activation. This dual stimulation cancels out the tissue repair mode of steady state TCR activation, enabling optimal MAIT cell driven microbial and target cell destruction [36, 47, 49]. Chronic activation of MAIT cells promotes IL-17A and TNF production which results in hepatic myofibroblast proliferation. The profibrogenic MAIT cell phenotype will reviewed in Chapter 1.3.3.

In the adult human liver, MAIT cells were first described by our group to be predominantly located around the bile ducts in the periportal regions in healthy ‘donor’ livers and in explanted livers from patients with end stage liver disease. These were specifically primary sclerosing cholangitis (PSC), primary biliary cholangitis (PBC), alcoholic liver disease (ALD) and non-alcoholic steatohepatitis (NASH). Periportal MAIT cell frequency was highest in explanted PSC livers [19].

Intrahepatic MAIT cells are now known to take up a more dispersed distribution dependent on the underlying liver condition [18]. A higher concentration of MAIT cells can be found in the sinusoids and parenchyma of healthy donor livers and in acute liver injury [19, 51]. In chronic liver disease, which will be discussed in the next Chapter 1.3.2, intrahepatic MAIT

cells localize to the fibrotic septae as well as the portal tracts.

Our group had further demonstrated cholangiocytes to function as non-classical antigen presenting cells to MAIT cells by expressing MR1 when exposed to *E. coli*, thus activating MAIT cells in a MR1-dependent manner [19]. BECs, aka cholangiocytes, line the bile ducts which are a potential port of entry by microbes from the duodenum. This potential crosstalk between MAIT cells and BECs supports the theory of MAIT cells forming part of the biliary firewall, safeguarding the biliary epithelium against microbial invasion and injury [19, 52, 53].

Lastly, sinusoidal recruitment of MAIT cells can occur through their expression of C-X-C chemokine receptor type 3 (CXCR3), lymphocyte function-associated antigen-1 (LFA-1), very late antigen-4 protein (VLA-4), intercellular adhesion molecule-1 (ICAM-1) and vascular cell adhesion molecule-1 (VCAM-1), which have all been shown to attract lymphocytes during inflammation [54-56]. They also express the gut homing chemokine integrin-αEβ7 which promotes mobilization to gastrointestinal tissue and adherence to VCAM-1 [57, 58]. Intrahepatic MAIT cell expression of the liver homing C-C chemokine receptor type 6 (CCR6) and CXCR6 was identified by our group on diseased explanted and donor livers. It is proposed that intrahepatic MAIT cells expressing CCR6, CXCR6 and integrin-αEβ7 are recruited and retained close to bile ducts, protecting the biliary epithelia and prevents ascending cholangitis from gut derived pathogens [19].

1.2.2 MAIT cells in the context of chronic liver disease

Peripheral blood MAIT cell frequency is reduced in chronic liver disease compared to healthy controls [19, 33, 37]. MAIT cell activation and dysfunction has been described in many conditions including autoimmune diseases, malignancy, bacterial and viral infections [10, 11, 45]. A well-recognised phenomenon is the loss of blood MAIT cell numbers in disease compared to healthy individuals, a finding not described with invariant natural killer T (iNKT) or Gamma delta (γδ) T cells [8, 59]. One study reported an inverse relationship with the frequency of blood MAIT cell numbers and the cell survival marker B-cell lymphoma 2 (BcL2), suggesting reduced survival or activation-induced cell death may be responsible for the depletion of circulating MAIT cells [51]. A second theory for lower circulating MAIT cell numbers is their recruitment to sites of inflammation, for example, higher MAIT cell numbers are found in the inflamed colon of patients with ulcerative colitis, the synovial fluid of patients with active rheumatoid arthritis, and in CNS lesions of multiple sclerosis [60-62]. Aspects of liver and blood MAIT cell function in adult chronic liver disease, specifically viral hepatitis and metabolic (fatty) liver disease and to a lesser degree, autoimmune liver disease will be reviewed here. There are only two MAIT cell studies in children with liver disease, both have reported lower blood and liver MAIT cell numbers compared to healthy controls but MAIT cell function was not investigated [63, 64]. A focused section on autoimmune liver disease will be discussed in Chapter 1.4. There is minimal data on MAIT cell frequency and function in acute liver disease; liver MAIT cells are known to locate around the sinusoids and parenchyma of patients with acute liver injury and failure [19, 51]. Liver MAIT cells, as with their blood counterparts, are described to be of a chronically activated, functionally impaired and cell-exhausted phenotype [33, 51].

Depletion and dysfunction of MAIT cells are reported in chronic viral hepatitis B (HBV) and chronic hepatitis C (HCV) infection. With HBV, more pronounced depletion is seen with

hepatitis delta virus (HDV) co-infection [65]. In HCV, both blood and liver MAIT cell frequencies are reduced, with the lowest reported in HIV/HCV co-infection [66-68]. The lowest frequency however, is observed with end-stage liver disease in both HCV and HBV [66, 67, 69].

Blood MAIT cells from patients with chronic HBV, especially with HDV co-infection, and in HCV have upregulation of the activation markers CD38, CD69, human leukocyte antigen DR (HLA-DR) and the cell exhaustion markers, programmed cell death protein 1 (PD-1) and cytotoxic T lymphocyte-associated protein 4 (CTLA-4) [33, 65, 70]. A positive correlation with HBV DNA levels are reported with PD-1 and CTLA-4. Partial phenotype normalization with a decrease of CD38 is reported with Entecavir antiviral treatment [71]. Some studies reported lower HBV MAIT production of IFNγ and Granzyme B following cytokine induction with IL-12 and IL-18 compared to healthy controls whilst others found no change in function [65].

MAIT cell frequency in HCV correlates negatively with the liver inflammation histological activity index. After treatment with direct-acting antivirals (DAAs), liver MAIT cells in HCV were observed to repopulate although it remained significantly lower than healthy donor levels [72]. One study reported a reduction in CD69 and HLA-DR in blood and liver MAIT cells after 1month of DAA treatment. Functionality however remains impaired despite DAAs, with lower blood MAIT production of IFNγ, TNF and Granzyme B in response to cytokine induction, particularly in patients with severe liver disease [73, 74]. Interestingly, HCV liver MAIT cells displayed greater cell activation and cytotoxicity than their blood counterparts, both of which decreased with DAAs. Although antiviral treatment induces intrahepatic MAIT cell repopulation in HCV and partial reversal of the activation-induced exhausted state in both HBV and HCV, functional restoration does not occur, signifying permanent damage in this important invariant T cell faction [65, 73, 74].

Non-alcoholic fatty liver disease (NAFLD) and non-alcoholic steatohepatitis NASH) are liver manifestations of the metabolic syndrome which consists of obesity, insulin resistance, hypertension and hypertriglyceridaemia [33, 44]. Blood MAIT cells in patients with NAFLD and NASH are depleted but higher concentrations of intrahepatic MAIT cells are described, particularly within areas of lobular inflammation and steatosis [75, 76]. A positive correlation of blood MAIT cell frequency is established with the NAFLD activity score (NAS), indicating greater MAIT cell recruitment or proliferation in areas of fatty liver inflammation.

As with chronic viral hepatitis, MAIT cells in patients with fatty liver disease display an activated, exhausted phenotype with high CD69 and PD-1 levels respectively and functional impairment with reduced IFNγ and TNF production on PMA/Ionomycin stimulation [75].

Of interest, a higher frequency of MAIT cells are found in the adipose tissue of obese patients along with higher IL-17A levels [76]. Chronic MAIT cell stimulation is associated with higher IL-17A production. This MAIT17 phenotype is implicated in many chronic inflammatory and autoimmune conditions, and in indeed IL-17A is considered a profibrogenic cytokine [77-79]. Greater circulating IL-17A levels, perhaps of MAIT cell origin, may contribute to the disease activity and progression of patients with NAFLD and NASH, especially in obese patients.

Lastly, although most MAIT cell studies in human and mice report a negative impact on liver inflammation and fibrosis, one study of MR1 knockout mice fed on a NASH diet showed higher proinflammatory macrophage M1 polarization and lower immunosuppressive M2 ratios, suggesting MAIT cells may play a protective role in fatty liver disease [75].

Autoimmune liver disease (AILD) will be discussed in detail in Chapter 1.4 but as with that

observed in other chronic liver conditions, a reduction in circulating numbers and chronic activation-induced cell exhaustion and dysfunction in residual MAIT cells are described [80, 81]. Higher intrahepatic MAIT cell frequencies with a predilection to localize to the peribiliary and portal areas in AILD, especially in PSC, are shown [11, 19, 44].

There are very few studies of MAIT cells in children with liver disease. A reduction in circulating and liver MAIT cell numbers were reported in one paediatric AIH study [64]. In another study, the MAIT cell composition of total CD3+ cells were reported to average at 10.5% in the liver explants of 10 children compared to blood MAIT cells of 1.4% from 74 children undergoing diagnostic liver biopsies; the indication for liver biopsy and underlying liver disease of explants were not made known [63].

Taken together, the reduction in blood MAIT cell frequency and functional impairment is not disease specific. In chronic liver disease, there appears to be a direct relationship between MAIT cell numbers and progressive liver disease, with the lowest frequency and greatest functional impairment observed in those with end-stage liver disease [44, 69].
Higher intrahepatic MAIT cell numbers may be secondary to recruitment from the peripheral circulation followed by tissue retainment. Notably, in chronic liver disease, as in the case of chronic viral hepatitis, functional impairment persists despite successful treatment [73, 74].

1.2.3 The profibrogenic nature of chronically activated MAIT cells

An inverse relationship exists between the loss of MAIT cells from the circulation and advanced liver disease, irrespective of the underlying liver condition [19, 44, 67]. Chronic inflammation in liver disease induces liver fibrotic change with the abnormal deposition of extracellular matrix proteins and ultimately leads to cirrhosis and end-stage liver failure [33, 44].

Since the initial description of higher MAIT cell numbers in the portal tracts of explanted chronically diseased livers, other investigators have since described MAIT cells to localize not only to periportal areas but also to fibrotic septae [51, 80]. Böttcher et al performed co-culture studies using hepatic stellate cells (HSC) with MAIT cells; HSC proliferation was found to be partially IL-17A dependent. A trans-well separation system did not provoke a response, indicating cell-to-cell contact was necessary in MAIT cell induced HSC proliferation. In the same study, chronic stimulation with IL-12 and IL-18 over a 72 hour period of blood MAIT cells from patients with autoimmune liver disease (AILD) induced higher IL-17A and higher RORγt expression but a reduction in IFNγ, Tbet, and PD-1 expression compared to blood MAIT cells from healthy controls. This upregulation of the Th17 profile and impaired Th1 cytokine function is frequently described in disease. The authors concluded blood MAIT cells from patients with AILD to possess a chronically activated, exhausted and profibrotic phenotype [80].

Another study similarly found higher concentrations of MAIT cells in the fibrous septae and portal tracts of cirrhotic explants from patients with alcoholic liver disease and/or non-alcoholic steatohepatitis (NASH); higher MAIT IL-17 expression was also described [51]. In contrast, MAIT cells mostly localized to sinusoids and parenchyma in healthy donor livers and in acute liver injury [18, 19, 51]. Hedge et al co-cultured MAIT cells with hepatic

myofibroblasts; MAIT cells were also found to enhance hepatic fibrogenic cell proliferation in a cell-to-cell contact fashion which was blunted by MR1-blockade. The same investigators performed murine experiments in parallel and found MR1 knockout mice had less hepatic αSMA and Sirius red staining but MAIT cell transgenic mice had enhanced staining compared to wild type mice. These two elegant studies demonstrated separately the profibrogenic potential of liver MAIT cells, which were characteristically of an activation-induced cell exhausted phenotype [51, 80].

The MAIT17 phenotype of preferential IL-17 production is described with many autoimmune conditions and IL-17 is considered a cytokine of chronic inflammation [62, 77, 78]. Another profibrotic cytokine being increasingly recognised is IL-26 which is also produced by activated MAIT cells and supports the profibrogenic nature of this invariant cell type [82, 83].

MAIT cells are increasingly recognised to possess anti-fibrotic potential. IL-22 and IFNγ are produced by MAIT cells mainly via MR1-dependent activation and both cytokines inhibits HSC proliferation [84-86]. The application of anti-fibrotic cytokines and MR1-antagonists to prevent and even reverse liver disease progression is a very attractive therapeutic option.

In terms of cirrhosis, no discernible difference could be observed in MAIT cell numbers between patients with compensated and decompensated cirrhosis [44]. In ascites however, higher MAIT cell numbers were identified in the ascitic fluid of decompensated cirrhotic patients, particularly in decompensated cirrhotics with spontaneous bacterial peritonitis (SBP) [87, 88]. A reduction in ascitic MAIT cell numbers following antibiotic treatment was observed. This could reflect resolution of inflammation in the peritoneal compartment with MAIT cells repopulating back into the circulation. Modest recovery of blood MAIT cell

numbers is reported in patients on long-term antibiotic treatment and in chronic viral hepatitis patients on antivirals [67].

As with chronic liver disease, blood MAIT cells from patients with cirrhosis display an activated phenotype with high CD38, CD69 and HLA-DR but with preserved and even superior Granzyme B and IL-17 production [44]. The latter is particularly interesting from what we now know of the MAIT17/IL-17 profibrogenic phenotype. Others have reported lower IFNΓ and TNF expression in blood MAIT cells but preserved ascitic MAIT cell function in cirrhotic patients. The exact role and impact of MAIT cell function in liver cirrhosis and end-stage liver disease needs to be further investigated.

Malignant change with the development of hepatocellular carcinoma (HCC) as a result of ongoing inflammation is a risk factor and long-term complication of all chronic liver diseases [89, 90]. As with the liver diseases and cirrhosis, circulating MAIT cell numbers are depleted in patients with HCC [91]. The activation-induced exhausted phenotype with impaired function is reflected in tumour-infiltrating MAIT cells which express higher CD38, HLA-DR, PD-1 and CTLA-4, and lower Granzyme, IFNγ and Il-17 upon TCR stimulation [44, 92]. Higher tumour-infiltrating MAIT cell count is associated with poorer survival in both HCC and colorectal carcinoma [10, 12, 44]. The clinical relevance of these findings, whether MAIT cells possess pro or anti-tumour properties remains to be further clarified.

1.3.1 Autoimmune liver disease in children

The incidence of autoimmune liver disease (AILD) is increasing worldwide. AILD are chronic immune mediated hepato-biliary disorders that damage hepatocyte and biliary epithelial cell

function [93, 94]. They often present in childhood and are usually lifelong [95, 96]. The pattern of presentation differs between children and adults, with primary biliary cholangitis (PBC) remaining in essence an adult disease [97, 98]. However, whilst autoimmune hepatitis (AIH) is the dominant immune mediated disease in childhood, some children present with primary sclerosing cholangitis (PSC) and others will have features of both hepatocyte and biliary targeted injury (“overlap” or “autoimmune sclerosing cholangitis”) [99, 100].

There are two distinct types of AIH as defined by the presence of circulating non-organ specific autoantibodies; antinuclear antibody(ANA) and/or smooth muscle antibody (SMA) in AIH type 1 (AIH-1) and liver-kidney microsomal antibody (LKM) and/or liver cytosol antibody type 1 (LC-1) in AIH type 2 (AIH-2) [96, 101]. Both types of AIH are more prevalent in females with a female to male ratio of 3:1. AIH can occur at any age but classically has two peaks; childhood/adolescence and middle age. Clinical presentation of AIH-1 is heterogenous with some children presenting acutely with hepatitis +/- progression fulminant liver failure, some may have evidence of chronic liver disease +/- complications e.g. portal hypertension and lastly, a proportion of children are asymptomatic and will be diagnosed incidentally [96, 101, 102]. Twenty percent of children will have a personal history of another autoimmune condition and 40% will have a family history of other autoimmune diseases, for example coeliac disease, thyroid disease, idiopathic thrombocytopenia and/or inflammatory bowel disease (IBD) [96, 103].

Children with AIH-2 have well-defined differences compared to AIH-1: younger age at presentation, aggressive clinical phenotype, higher rates of acute liver failure, need for transplantation [96, 101].

Liver biopsy histology is diagnostic in AIH and comprises characteristic features of varying

degrees of interface hepatitis, dense plasma cell-rich lymphocytic infiltrate, hepatocellular rosette formation and emperipolesis [96, 100, 103]. The majority will have an element of bridging fibrosis which equates to stage 2 (moderate) fibrosis at diagnosis An acute hepatitis with high transaminases, elevated immunoglobulins, particularly IgG, reduced levels of complement (C3, C4), non-organ specific autoantibodies as described above are supportive of the diagnosis of AIH [96, 100, 103].

The diagnostic criteria of autoimmune hepatitis in adults is based on the International Autoimmune Hepatitis Group (IAIHG) scoring system which was first formulated in 1993, later revised in 1999 and in 2008, a simplified IAIHG scoring system was devised. However, children with AILD have different disease characteristics compared to adults e.g. lower autoimmune antibody titres and IgG levels at presentation [103-105]. In 2009, a diagnostic criteria for AIH in childhood was proposed which took into consideration the presence of lower autoantibodies levels along with elevated IgG, high transaminases and diagnostic liver biopsy findings. Other forms of hepatitis (e.g. viral hepatitis), drug induced liver injury, inherited and metabolic forms of chronic liver disease (e.g. Wilson's disease) must be excluded. More recently in 2018, the European Society of Paediatric Gastroenterology, Hepatology and Nutrition (ESPGHAN) Hepatology Committee released a position statement to provide guidance on the diagnosis and management of children with autoimmune liver disease by which a scoring criteria for AIH and ASC was created [96].

Primary sclerosing cholangitis (PSC) and the mixed hepatitic/biliary phenotypes of overlap syndrome/ASC are more likely to occur in teenage male patients with IBD, namely ulcerative colitis [99, 106, 107]. The majority of patients will be asymptomatic with abnormal

liver function picked up incidentally e.g. liver function tests in IBD patients which highlights the importance of liver blood screening in IBD patients despite the lack of liver-related symptoms. Indeed 70-80% of patients with PSC will have dual IBD pathology [106, 108]. The autoimmune biliary phenotypes of PSC, overlap and ASC are usually ANA, SMA and/or ANCA (anti-neutrophil cytoplasmic antibody) antibody positive [96, 106, 109]. Diagnosis is with confirmatory findings on histology and/or radiological imaging, specifically biliary dilatation, 'beading' and/or strictures observed in magnetic resonance cholangiopancreatography (MRCP) [96, 110, 111]. Periductal concentric fibrosis, bile duct proliferation and fibrous-obliterative cholangitis are the classic histological lesions [112-114]. Hepatitic features such as interface hepatitis and emperipolesis may be present in patients with overlap syndrome or ASC [103, 104, 115].

PSC is unresponsive to immunosuppression and the mainstay of management is encouragement of bile excretion with Ursodeoxycholic acid, optimizing IBD control and the anticipation and prevention of complications of chronic liver disease [108, 113, 116]. On the other hand, 80% of children with AIH will respond to first line therapy [95, 103, 104]. Relapse or AIH flare is common and will occur in over 40% of children within the first year of treatment [96, 103, 117]. True non-responders (treatment refractory patients) will need to be placed on second-line therapy such as mycophenolate mofetil (MMF) or Tacrolimus [96, 103, 117]. Third line therapy described in case reports of adult patients have shown promising results and include Rituximab, mTOR inhibitors e.g. Sirolimus and tumor necrosis factor alpha (TNAα) monoclonal antibody with Infliximab [118, 119].

Treatment options for autoimmune biliary disease continues to lack the efficacy of AIH management, and often progressive biliary disease ensues [106, 108, 116, 120]. The only cure for both is liver transplantation (LT) which is indicated in children who fail to respond to

therapy, in decompensated cirrhosis/end-stage liver disease, or in the presence of malignant change e.g. hepatocellular carcinoma [112, 120, 121]. Disease recurrence occurs in 30% of AIH and in 20-40% of PSC patients; there are, at present, no biomarkers or predictors of prognosis or disease recurrence [122-124].

1.3.2 MAIT cells in autoimmune hepatitis

MAIT cell frequencies are depleted in patients with autoimmune liver disease (AILD) compared to healthy controls [19, 80, 125]. This is not a disease specific finding as it is observed with all chronic liver conditions and almost all diseases [38, 41, 78].

Renand et al reported a sustained depletion of peripheral blood MAIT cell frequencies from newly diagnosed autoimmune hepatitis (AIH) patients one year after starting treatment; MAIT cell frequencies were similar at diagnosis and in remission, implying a lack of restoration in circulating MAIT cell numbers despite clinical restoration. In the same study, it was shown that intrahepatic MAIT cells from these AIH patients remained in the portal tracts with little difference observed in the diagnostic liver biopsy compared to the biopsy 1year after starting treatment [126]. Authors concluded circulating MAIT cell numbers were depleted but preserved within the portal tracts of the AIH patients possibly as a result of tissue retainment of intrahepatic MAIT cells following recruitment to the inflamed liver. There is only one study in the literature which reviewed MAIT cell frequencies in children with AIH; lower blood and liver MAIT cells were observed in children with AIH. MAIT cells accounted for 0.54% of total CD3+ cells in newly diagnosed AIH children n=5 compared to 2.7% of total CD3+ cells from healthy children n=7 [64]. Absolute intrahepatic MAIT cell %

was also lower in the liver biopsy of children with AIH n=3 compared to a) healthy adult donor liver n=8 and b) paediatric healthy liver biopsy tissue n=3. Sampling of healthy liver tissue was obtained during the partial hepatectomy of children with hepatoblastoma [64].

Böttcher et al investigated MAIT cells from adult patients with AIH, PSC and PBC, collectively referred to as AILD. In this study, the reduction in blood MAIT cell numbers from AILD patients correlated with increasing fibrosis stage estimated by transient elastography [80]. Intrahepatic MAIT cells were identified in the portal tracts and parenchyma in healthy donor livers assessed by immunohistochemistry but were situated in the portal tracts and fibrotic septae in AILD livers. At rest, blood MAIT cells from AILD patients had higher expression of the activation markers CD38, CD69 and cell exhaustion markers CTLA-4, TIM3, including the terminal T cell exhaustion marker CD39. After PMA/Ionomycin stimulation, blood MAIT cells from the AILD patients had marked decrease IFNγ production compared to healthy controls. Although Granzyme B levels were higher at rest in the AILD patients, this failed to upregulate after stimulation compared to healthy controls[80]. Impaired IFNγ production is a consistent finding in AILD but there are variable reports of Granzyme B release with some investigators reporting upregulation on MAIT cell activation [81, 126]. Taken together, these findings implied AILD blood MAIT cells to be chronically activated and functionally impaired [12, 80, 127].

A reduction in MAIT cell IFNγ was also shown with repetitive cytokine stimulation with IL-12 and IL-18 in AILD patients and in healthy controls, suggesting chronic cytokine stimulation drives MAIT cell exhaustion [80]. MAIT cells in the chronically inflamed liver microenvironment as observed in AILD, may be chronically exposed to inflammatory cytokines and bacterial ligands translocated from portal venous blood and the biliary system

[43, 128, 129]. Böttcher et al additionally showed that repetitive stimulation with IL-12 alone induced MAIT cell IL-17A production in AILD and in healthy controls. Importantly, MAIT cells from AILD and healthy controls were able to induce hepatic stellate cell (HSC) activation and proliferation which was interrupted by IL-17A blockade [80]. Investigators concluded chronic cytokine stimulation of MAIT cells induced a profibrogenic IL-17A phenotype which predisposes to HSC mediated liver fibrosis.

1.3.3 MAIT cells in Primary sclerosing cholangitis

MAIT cells from biliary duct brush samples obtained via endoscopic retrograde cholangiopancreatography (ERCP) were fourfold higher in frequency compared to matched peripheral blood MAIT cell numbers [127]. The biliary system in PSC is speculated to be enriched with MAIT cells recruited from the circulation which has retained at the site of inflammation i.e. the biliary mucosa. Circulating MAIT cells from these patients were markedly reduced. Notably, the reduction in MAIT cell numbers were similar in PSC patients with IBD and PSC patients alone, with no link to clinical severity established. With MR1-dependent stimulation, MAIT cells from these patients expressed lower CD107a (marker of degranulation), IFNγ and TNFα compared to healthy controls [127]. Cytokine stimulation only elicited minor changes in lowering TNFα production. Another study in 2014 contrastingly found liver biopsy samples from PSC patients and healthy controls to have similar intrahepatic MAIT cell numbers [130]. These patients' blood MAIT cells also displayed an activated exhausted phenotype with high CD69, CD39, PD-1 and impaired MR1-dependent function of IFNγ and TNFα production by *E.coli* stimulation.

Work from our group showed intrahepatic MAIT cells from PSC and PBC explants

predominantly localised to bile ducts in the portal tracts. These MAIT cells expressed higher liver homing chemokines of CCR6, CXCR6 and αE⟩7 integrin. Importantly, cholangiocytes in addition to macrophages and liver derived B lymphocytes were shown to activate MAIT cells in a MR1-dependent manner with the upregulation of IFNγ, CD107a and CD40L expression [19].

Although PBC is exclusively an adult autoimmune biliary disorder, the finding of correlations between MAIT cell numbers and disease activity is of interest. MAIT cell frequency is associated with a negative correlation with alkaline phosphatase (ALP), a disease activity marker in PBC [125, 131]. Jiang et al demonstrated partial reversal of low blood MAIT cell numbers in PBC patients following 6months of ursodeoxycholic acid therapy. These blood MAIT cells had higher expression of CCR6, CXCR6, annexin and IL-17A levels following PMA/Ionomycin stimulation [132]. MR1-tetramer staining showed higher absolute intrahepatic MAIT cell numbers in PBC compared to healthy controls. Lower intrahepatic MAIT cell numbers however were reported by other investigators. Annexin expression supports the concept of post-activation induced apoptosis which may explain, to an extent, the depletion of MAIT cells from the circulation [44, 132]. Higher expression of CCR6 and CXCR6 suggests homing and recruitment to the liver, providing an alternative for the reduction in blood MAIT cell numbers.

Depletion of MAIT cell numbers from the circulation therefore could be due to reduced survival and/or recruitment to sites of inflammation e.g. bile ducts in PSC, liver parenchyma in AIH. MAIT cells from adult patients with AILD consistently display a chronically activated, functionally impaired and cell exhausted phenotype [10, 80, 132]. Loss of gut integrity, translocation of intestinal bacteria into an already cytokine enhanced inflamed hepatic

environment may be responsible for the chronic MAIT cell activation [133-135].

CD40L is a molecule known to induce BEC apoptosis via CD95/Fas augmentation. MAIT cell CD40L directed biliary epithelial damage may be fundamental in the pathogenesis of biliary conditions like PSC (Figure 1b) [136, 137]. Injured cholangiocytes, as observed in PSC, express fewer tight junction proteins and in MDR2 knock-out mice, a murine model of PSC, disruption of biliary epithelial tight junctions enabled leakage of bile into the portal tracts, perpetuating portal inflammation and fibrosis [138] (Figure 2). Impaired biliary epithelial tight junctions and increased gut permeability leads to microbial colonisation of a largely sterile biliary system [139-141].

1.4 Aims & Objectives

Aims

To explore the phenotypic and functional role of MAIT cells in autoimmune biliary disease.

Objectives

1) Investigate for the presence of MAIT cells within the paediatric autoimmune liver

2) Assess the spatial relation of MAIT cells and Tregs in the periportal regions of the human liver.

3) Deep immunophenotype characterization of peripheral blood MAIT cells from children with Autoimmune liver disease by mass cytometry using Cytometry by time of flight (CyTOF)

4) To examine human liver and blood derived MAIT cell phenotype and function upon activation by *E.coli* primed intrahepatic dendritic cells (DCs).

Chapter 2. Material and Methods

2.1 Ethical approval

This project was granted ethical approval from the Human Biomaterials Resource Centre (HBRC) at the University of Birmingham for the usage of blood and liver tissue from paediatric autoimmune liver disease (AILD) patients. Over the course of my research, I applied for and was granted amendments to our ethics for the use of a) blood from healthy children, b) fresh native liver explants and c) formalin-fixed paraffin-embedded liver tissue from paediatric patients with AILD and non-AILD for comparison. The Ethics code granted from the HBRC was Oo 13-150.

2.2 Antibodies and Reagents

Table 1 – 4 below details all the antibodies used in this research project and includes the experiment type, concentrations used per test and the source (supplier).

Table 1. List of antibodies used for immunohistochemistry and immunofluorescence

Antibody	Host	Isotype	Clone	Primary / Secondary	Technique	Concentration	Source
TCR Vα7.2	Mouse anti-human	IgG1	3C10	Primary	IHC IF	5 µg/mL	BioLegend
FOXP3	Mouse	IgG3	mAbcam 450	Primary	IHC IF	5 µg/mL	Abcam
Granzyme B	Mouse	IgG2a	351927	Primary	IHC IF	1 µg/mL	R&D Systems
CK19	Rabbit	IgG1	EP1580Y	Primary	IHC IF	1 µg/mL	Abcam
AF488	Goat anti-Rabbit	IgG1	N/A	Secondary	IF	0.6 µg/mL	Invitrogen
AF647	Goat anti-Rabbit	IgG1	N/A	Secondary	IF	2 µg/mL	Abcam
AF594	Goat anti-Rabbit	IgG1	N/A	Secondary	IF	2 µg/mL	Invitrogen
AF647	Goat anti-Mouse	IgG1	N/A	Secondary	IF	4 µg/mL	Invitrogen
AF555	Goat anti-Mouse	IgG1	N/A	Secondary	IF	2 µg/mL	Invitrogen
AF647	Goat anti-Mouse	IgG2a	N/A	Secondary	IF	4 µg/mL	Invitrogen
AF488	Goat anti-Mouse	IgG3	N/A	Secondary	IF	0.6 µg/mL	Invitrogen
AF594	Goat anti-Mouse	IgG3	N/A	Secondary	IF	2 µg/mL	Invitrogen

IHC: Immunohistochemistry, IF: Immunofluorescenc; N/A: Not applicable

Table 2. List of antibodies and lanthanide metal isotopes used for CyTOF mass cytometry – surface markers

Antibody	Isotype	Clone	Lanthanide isotype	Volume per test	Source
Surface markers					
TCR Va7.2	IgG1	3C10	147Sm	1 uL	BioLegend
CD45	IgG1	HI30	89Y	1 uL	Fluidigm
CD154 (CD40L)	IgG1	24-31	162dY	1 uL	BioLegend
CD57	IgG1	QA17A04	115In	1 uL	BioLegend
IL-12r	IgG2a	S16020B	169Tm	1 uL	BioLegend
CD56	IgG1	B159	155Gd	1 uL	Fluidigm
CD196 (CCR6)	IgG1	11A9	141Pr	0.8 uL	Fluidigm
CD186 (CXCR6)	IgG2a	K041E5	149Sm	0.8 uL	BioLegend
CD279 (PD1)	IgG1	EH12.2H7	175Lu	0.8 uL	Fluidigm
CD39	IgG1	A1	160Gd	0.8 uL	Fluidigm
IL-18r	IgG1	H44	148Nd	0.6 uL	BioLegend
CD199 (CCR9)	IgG2a	L053E8	168Er	0.6 uL	BioLegend
CD195 (CCR5)	IgG1	NP-6G4	171Yb	0.6 uL	Fluidigm
CD183 (CXCR3)	IgG1	G025H7	156Gd	0.6 uL	Fluidigm
CD161	IgG1	HP-3G10	159Tb	0.6 uL	Fluidigm
CD103	IgG1	BER-ACT8	176Yb	0.6 uL	BioLegend
CD8a	IgG1	RPA-T8	114Cd	0.6 uL	BioLegend
CD95 (Fas)	IgG1	DX2	152Sm	0.5 uL	Fluidigm
CD3	IgG1	UCHT1	154Sm	0.5 uL	Fluidigm
CD38	IgG1	HIT2	145Nd	0.5 uL	BioLegend
CD8b	IgG2a	QA20A40	142Nd	0.5 uL	BioLegend
CD45RO	IgG2a	UCHL1	144Nd	0.5 uL	BioLegend
CD73	IgG1	AD2	151Eu	0.4 uL	BioLegend
CD197 (CCR7)	IgG2a	G043H7	167Er	0.4 uL	Fluidigm
CD4	IgG1	OKT4	116Cd	0.4 uL	BioLegend
CD49d	IgG1	9F10	174Yb	0.4 uL	Fluidigm
CD27	IgG1	O323	112Cd	0.2 uL	BioLegend

Table 3. List of antibodies and lanthanide metal isotopes used for CyTOF mass cytometry – intracellular markers

Antibody	Isotype	Clone	Lanthanide isotype	Volume per test	Source
TGF-B1	IgG2b	TW7-28G11	110Cd	1 uL	BioLegend
IL-10	IgG2a	3F9	209Bi	1 uL	BioLegend
Perforin	IgG2b	dG9	143Nd	1 uL	BioLegend
TNFa	IgG1	MAb11	146Nd	1 uL	Fluidigm
CD152 (CTLA-4)	IgG2a	14D3	170Er	1 uL	Fluidigm
Ki67	IgG1	B66	172Yb	1 uL	Fluidigm
IL-17A	IgG1	N49-653	164Dy	1 uL	Fluidigm
RORgt	IgG1	RORg2	163Dy	0.8 uL	BioLegend
Tbet	IgG1	4B10	161Dy	0.8 uL	Fluidigm
IFNγ	IgG1	B27	165Ho	0.8 uL	BioLegend
Granzyme B	IgG1	GB11	173Yb	0.6 uL	Fluidigm
GMCSF	IgG1	BVD2-21C11	150Nd	0.6 uL	BioLegend
IL-22	Poly Ig	Poly5161	158Gd	0.4 uL	BioLegend
PLZF	IgG2b	W18031A	153Eu	0.2 uL	BioLegend
BcL2	IgG1	100	166Er	0.2 uL	BioLegend

Table 4. List of antibodies used for the MAIT cell cocultures

Antibody	Isotype	Clone	Concentration	Volume per test	Flurophore	Source
IFNg	IgG1	4S.B3	50 µg / mL	2 µL (0.1µg)	BV785	BioLegend
TNFa	IgG1	MAb11	50 µg / mL	1 µL (0.5µg)	PECF594	BioLegend
IL-17A	IgG1	BL168	25 µg / mL	2 µL (0.05µg)	PE/Dazzle 594	BioLegend
Perforin	IgG2b	dG9	100 µg / mL	1.5 µL (0.15µg)	FITC	BioLegend
CD107a (LAMP-1)	IgG1	H4A3	400 µg /mL	1.5 µL (0.6µg)	PE	BioLegend
CD40L	IgG1	24-31	100 µg / mL	2 µL (0.2µg)	PeCy7	BioLegend
Ki67	IgG1	B56	50 tests / 0.25 mL	2 µL (0.4µg)	BV786	BD Biosciences
CD8a	IgG1	RPA-T8	100 µg / mL	1.5 µL (0.15µg)	BV510	BioLegend
TCR Va7.2	IgG1	3C10	100 µg / mL	2 µL (0.2µg)	BV605	BioLegend
CD3	IgG1	UCHT1	100 µg / mL	1.5 µL (0.15µg)	BV650	BioLegend
CD161	IgG1	HP-3G10	50 µg / mL	3 µL (0.15µg)	APC	BioLegend
CD4	IgG1	RPA-T4	200 µg / mL	3 µL (0.6µg)	APC Cy7	BioLegend
7AAD		Viability dye	100Tst / 2mL	2 µL (0.1µg)	PerCP Cy5.5	BD Biosciences

Table 5. List of Reagents and buffers used throughout this research

Application / Procedure	Reagents & Buffers	Source	Concentration and purpose
Immunofluorescence	Tris-Based	Vector Laboratories (H-3301-250)	Ph9.0, 100x (Antigen Unmasking solution)
Immunofluorescence	Tris-Buffered saline TBS) & Tween 20 (TBST)	Sigma-Aldrich	1x Tris-Buffered saline 0.01% Tween 20 (diluent/washer)
Immunofluorescence	Bloxall Blocking solution	Vector Laboratories (SP-6000-100)	Neat, blocking of endogenous peroxidase and Alkaline phosphatase
Immunofluorescence	Casein buffer 10x	(SP-5020-250)	2x solution (200uL in 800uL TBS) (blocking of non-specific proteins)
Immunofluorescence	Impact DAB substrate kit, Peroxidase	Vector Laboratories (SK-4105)	200uL per slide (Substrate staining in Immunohistochemistry)
Immunofluorescence	Haematoxylin (Mayers)	PFM Medical (PRC/R/42)	Neat, nucleated cell staining in Immunohistochemistry
Immunofluorescence	Vector TrueVIEW	Vector Laboratories (SP-8500-15)	Autofluorescence quenching kit with DAPI
Immunofluorescence	VECTASHEILD VIBRANCE	Vector Laboratories (SP-8500-15)	Antifade mounting medium
CyTOF experiments	CytoStim	Miltenyi Biotec (130-092-172)	200uL per cocktail per $10x10^8$ cells
CyTOF experiments	Golgistop	BD Biosciences (554724)	4 µl of BD GolgiStop™ for every 6 mL of cell culture
CyTOF experiments	Dnase	STEMCELL (07900)	1mg/mL (nonspecifically cleaves DNA)
CyTOF experiments	EDTA	ThermoFisher Scientific (invitrogen) (AM9260G)	0.5M / pH8.0(chelating agent, prevents cell clumping)
CyTOF experiments	Fc Blocker	BioLegend (422301)	5uL per $10x10^7$ cells in 100uL staining volume
CyTOF experiments	Cisplatin 194	Standard Biotools (201194)	0.02% (live/dead stain equivalent in CyTOF)
CyTOF experiments	Paraformaldehyde	Fisher Scientific (11586711)	1.6% (cell membrane fixation agent)
CyTOF experiments	Rhodium-103	Standard Biotools (201103A)	0.002% (live/dead stain equivalent in CyTOF)
CyTOF experiments	Maxpar Fix and Perm buffer	Standard Biotools (201067)	Fixation and Permeabilisation agents
CyTOF experiments	Maxpar Cell Acquisition solution (CAS)	Standard Biotools (201240)	Neat, washer/buffer

CyTOF experiments	Maxpar Cell Staining Buffer (CBS)	Standard Biotools (201068)	Neat, diluent/washer
CyTOF experiments	Maxpar X8 Antibody Labelling Kit	Standard Biotools (201146B)	Contains L-buffer, C-buffer, R-buffer and W-buffer for metal conjugation of purified antibodies
CyTOF experiments	TCEP	ThermoFisher Scientific (77720)	Neat, Reducing agent
	Lympholyte	Cedarlane Laboratories (CL5020)	Neat (Cell Separation Media)
MAIT cell coculture	Magnetic cell separation (MACs) buffer	Made from different reagent components	Phosphate buffered saline 0.5% BSA 1mM EDTA
MAIT cell coculture	RPMI	ThermoFisher Scientific (Gibco) (11875093)	n/a (cell culture media component)
MAIT cell coculture	Penicillin-Streptomycin	ThermoFisher Scientific (Gibco) (15140122)	10,000 U/mL (cell culture media component)
MAIT cell coculture	L-Glutamine	ThermoFisher Scientific (Gibco) (25030081)	200mM (cell culture media component)
MAIT cell coculture	FCS	ThermoFisher Scientific (Gibco) (11550356)	10% (cell culture media component)
MAIT cell coculture	Miltenyi Pan T cell isolation kit	Miltenyi Biotec (130-096-535)	10uL Pan T cell Biotin-~Antibody cocktail per $10x10^7$ cells
MAIT cell coculture	Miltenyi CD14 magnetic isolation kit	Miltenyi Biotec (130050201)	20uL CD14 microbeads per $10x10^7$ cells
MAIT cell coculture	Golgistop	BD Biosciences (554724)	4 µl of BD GolgiStop™ for every 6 mL of cell culture
MAIT cell coculture	FACs buffer	PBS + 2% FCS	PBS + 2% FCS (diluent)
MAIT cell coculture	Cytofix	BD Biosciences (554722)	100 µL per well/test tube
MAIT cell coculture	eBioscience Transcription Factor Staining Buffer set (Fixation/Perm Diluent)	ThermoFisher Scientific (invitrogen) (005523-00)	0.1% Permeabilization buffer solution
MAIT cell coculture	Fc Blocker	BioLegend (422301)	5uL per $10x10^7$ cells in 100uL staining volume
Cell culture	DMSO	Merck (D2650)	5% Used as freezing media for cells
Cell culture	Phosphate buffered saline (PBS)_	Sigma-Aldrich (P4417)	Diluent/washer
Cell culture	Type IA Collagenase	Sigma-Aldrich (C9891)	20% solution for BEC isolation
Cell culture	Percoll	VWR International (Cytvia) (17-0891-01)	33% and 77% Percoll solution

Cell culture	HEA125 antibody	2B Scientific (61004)	50uL per biliary epithelial cell isolation experiment
Cell culture	Dynabeads™ Protein G for Immunoprecipitation	ThermoFisher Scientific (10003D)	10uL per biliary epithelial cell isolation experiment
Cell culture	TryplEX1	ThermoFisher Scientific (Gibco) (12605010)	1mL for T25 and 3mL for T75 flasks for passaging of BEC cells
Cell culture	Trypsin-EDTA (0.25%)	ThermoFisher Scientific (Gibco) (25200056)	1mL for T25 and 3mL for T75 flasks for passaging of BEC cells
Cell culture	FCS	ThermoFisher Scientific (Gibco) (11550356)	10% (cell culture media component)
Cell culture	Collagen Type 1 solution	Merck (C3867-1VL)	2.5% solution for coating of T25 and T75 flask for BEC culture
Cell culture	HAMS F12	ThermoFisher Scientific (Gibco) (11765054)	90mL, Neat (per 200mL of BEC culture media)
Cell culture	DMEM	ThermoFisher Scientific (Gibco) (A4192101)	90mL, Neat (per 200mL of BEC culture media)
Cell culture	EGF	Peprotech (100-15)	100ug/mL
Cell culture	HGF	Peprotech (100-39)	100ug/mL
Cell culture	Cholera toxin	Sigma-Aldrich (C8052-1MG)	1ug/mL
Cell culture	Tri-ido-thyronine	Sigma-Aldrich (T5516-1MG)	2mL (per 200mL of BEC culture media)
Cell culture	Heat activated human serum	TCS Biosciences (CS100-100)	20mL (per 200mL of BEC culture media)

2.3 Sampling of paediatric blood and liver tissue

I undertook the Institute of Child Health (ICH) Good Clinical Practice (GCP) module and the HBRC consent training course in preparation for my research. Approval was sought from the Liver Unit Research & Development (R&D) team at Birmingham Children's Hospital (BCH). I set up a new pathway for the collection and transfer of paediatric blood and liver tissue samples from BCH to the HBRC for initial sample handling and research labelling prior to transfer to the Centre for Liver and Gastrointestinal Research (CLGR) at the

Institute for Biomedical Research (IBR) for sample processing by myself.

Help was enlisted from the medical Hepatology team, Liver transplant surgeons, Theatre Nurses, Pathology consultants, Laboratory staff, Phlebotomists and the Nursing team. This included individual face to face meetings and departmental seminar presentations. I designed SOPs (Standard Operating Procedure) each for the obtainment of paediatric blood and liver tissue and placed posters about my research in the departments and theatres to alert staff of the project.

Consent was obtained prior to the sampling of all blood and liver tissue for this project as per ICH GCP and HBRC guidance. All collected blood and liver tissue samples from BCH were anonymised when booked into the HBRC. Parents and children were aware and consented for their demographic and relevant clinical data pertaining to the patient's age, gender, disease status, medications and other related variables e.g. laboratory results, imaging and histology reports to be obtained for correlation of clinical findings.

<u>Blood sampling</u>

I underestimated the amount of blood required for the experiments, having initially applied for approval of 2mL of blood per patient. This was done on the basis that only 1mL of blood is taken for biochemistry analysis routinely and a maximum of 2mL is taken for additional diagnostic tests at BCH.

The peripheral blood mononuclear cell (PBMC) layer was insufficient and therefore an ethics amendment to double the volume of blood to 4mL was applied. The PBMC layer from 4mL of paediatric blood was sufficient for downstream experiments. However, as my research progressed, I wanted to investigate different experimental conditions; cell activation (stimulated) vs. cell resting state (unstimulated). This meant an increase to the volume of blood to allow for 'matched sample' assessments. I applied for ethics approval

for the next size of blood tube which is a 10mL EDTA tube. The PBMC layer from 10mL of blood was sufficient to enable the experimental conditions and 10 mL of whole blood was used per experiment going forward.

Liver tissue

Collaboration and help from the Histopathology team at BCH was crucial to the success of safe liver sampling and transfer to the HBRC.

For fresh native liver samplings, the explant liver tissue was inspected and handled by the pathologist on-call who resected tissue for my research if he/she deemed there to be enough tissue to be taken for research without affecting the formal histopathology examination of the explant.

Formalin-fixed paraffin-embedded liver tissue blocks were selected by the Pathologists who only released them if he/she deemed there to be enough tissue to be taken for research. Ethics approval amendment was awarded for the use of tissue from autoimmune liver disease (autoimmune hepatitis (AIH) Type 1 and Type 2 and Primary sclerosing cholangitis (PSC)) and non-autoimmune liver disease including Biliary atresia and Acute Liver failure (ALF).

2.5 Isolation of human peripheral blood mononuclear cells (PBMCs) from whole blood

Peripheral blood mononuclear cell (PBMC) from whole blood were isolated by density gradient centrifugation using **Lympholyte Separation** Medium. Established protocols from the CLGR were used. Whole blood was layered onto Lympholyte placed into a 50 mL Corning tube at a ratio of 1:1. This is then centrifuged at 800 x *g* for 20 min with an acceleration set at 5 and deceleration at 3. The resultant buffy coat (PBMC layer) was removed using a Pasteur pipette and placed into a 15 mL Corning tube, made up to 14mL

with Phosphate buffered saline (PBS) with 2% Fetal Bovine Serum (FBS). This is then centrifuged at 2000 rpm for 5min with acceleration and deceleration set at 9. The supernatant was discarded and the cell pellet resuspended with PBS & 2% FBS made up to 14 mL. A viability cell count was performed using a haemocytometer and trypan blue stain (dead cells stained blue); 10 uL of the cell suspension was placed between the haemocytometer and cover glass using a P-10 pipette. Cells were counted in all four larger outer squares, then divided by four (mean number of cells/square). The number of cells per square x 10^4 = the number of cells/mL of suspension.

This cell suspension was centrifuged at 2000 rpm for 5 min and the pellet resuspended in 1mL of Cryostor (cryoprotective media) in a cryogenic vial and placed at -80dC for 3 days then stored in liquid nitrogen until the sample is needed for downstream applications.

2.6 Isolation of human liver mononuclear cells from explanted liver

Human explanted or donor liver was manually diced into 0.5 cm^3 pieces using sterile scalpels and equipment. The diced liver was washed in Phosphate buffered solution (PBS) in a sterile beaker until the supernatant ran clear. Cell culture media (10% Fetal Bovine Serum, FBS) in RPMI with Penicillin-streptomycin (Pen/Strep) and L-Glutamine) was added and the contents poured into double bagged sterile ‘Stomacher bags’, heat-sealed and mechanically digested by the Stomacher machine with a setting of 260 rpm for 6 min. The contents were poured into a fine mesh sealed sterile beaker. The filtered supernatant were collected and poured into 50 mL Corning tubes and centrifuged at 2000 rpm for 5 min at an acceleration and deceleration of 9. The supernatant was discarded and the cell layer resuspended with 2 mL PBS using a Pasteur pipette and made up to 50mL with PBS. This is centrifuged at 2000 rpm for 5 min for 3-4 more washes until the supernatant runs clear. The cell layer was then resuspended in 30 mL of PBS before layering onto 20 mL of

Lympholyte Separation Medium in a 50 mL Corning tube and centrifuged at 800 x *g* for 20 min with an acceleration of 3 and deceleration of 0. The resultant liver mononuclear cell layer (LMC) was resuspended in 50mL PBS and centrifuged at 2000 rpm for 5 min. This washing process was repeated two more times. The concentration of cells in the final cell layer was counted using a haemocytometer.

This LMC suspension was centrifuged at 2000 rpm for 5 min and the cell pellet resuspended in 1 mL of Cryostor (cryoprotective media) in a cryogenic vial and placed at -80dC for 3 days then stored in liquid nitrogen until the sample is needed for downstream applications.

2.4 Paraffin Tissue Sample preparation

Human adult and paediatric formalin-fixed paraffin-embedded native liver tissue were used for immunohistochemistry (IHC) and immunofluorescence (IF) staining.

Paediatric liver tissue used were from patients with autoimmune liver disease (autoimmune hepatitis (AIH) Type 1 and Type 2 and Primary sclerosing cholangitis (PSC)) and non-autoimmune liver disease including Biliary atresia and Acute Liver failure (ALF).

Sections (slides) were cut from 1) paediatric liver blocks obtained from Birmingham Children's Hospital (BCH) and 2) adult liver blocks from liver explants from the Queen Elizabeth Hospital (QEH), Birmingham.

Liver tissue from BCH and the QEH were fixed in 100% formalin (4% 51 formaldehyde). A CLGR tissue processing technician cut the liver blocks for immunohistochemistry (IHC) and immunofluorescence (IF) staining for my research. The cut liver tissue were placed in cassettes, then embedded in wax and allowed to set for 24hours. 3 µm-thick sections were then cut using a rotary microtome and floated on 35°C water to remove any tissue

folding. Tissue sections were mounted onto charged glass slides. The slides were then loaded into metal racks and set at 60°C to dehydrate the tissue. These sections were then used for IHC and IF staining.

2.5 Immunohistochemistry of liver tissue

Paraffin embedded liver slides (sections) were labelled and prepared for IHC/IF by first undergoing dewaxing and rehydration;

I. Xylene 3 x 3 min incubations followed by
II. 99% industrial denatured alcohol (IDA) 3 x 3min incubations followed by
III. dd$H_2$0 2 x 3 min incubations for tissue rehydration

Next, the antigen retrieval step was undertaken. A 1000mL 1% tris-based (high pH) antigen unmasking solution was prepared and placed in a microwave oven set at 'High' for 10 min. The dewaxed and rehydrated liver tissue sections were placed in the preheated unmasking solution and microwaved at 'High' for 30 min. The liver tissue sections were cooled for 10 min.

Plastic slide boxes were made into humidified chambers by lining with damp paper towel and parallel glass stripettes (sized to fit) placed inside to act as slide racks.

Slides from the cooled unmasking solution were transferred to the humidified chambers; the tissue sample was outlined using an ImmEDGE Hydrophobic Barrier PAP pen and then placed onto the stripette slide rack. Slides were then washed with TBST for 5 min.

For IHC downstream experiments, tissues were blocked with Vectorlabs Bloxall solution for 10 min to counteract endogenous perioxidase/alkaline phosphatase to prevent non-specific binding. Slides were then washed with TBST for 5 min. Incubation with casein buffer (2X solution) for 10 min was applied to prevent non-specific protein binding.

Primary antibodies were applied without washing off the casein buffer and incubated for 1 hour at room temperature; primary antibody dilution optimisation was performed using adult liver tissue and repeated on paediatric tissue prior to testing on multiple patients/conditions. TBST was used as the diluent for the antibodies. Following the primary antibody incubation, slides were washed with TBST for 5 min. Two drops of the Vector Impress Secondary (anti-mouse/rabbit) antibody was applied for a 30 min incubation as per manufacturer's instructions before being washed off with TBST x 3.

Tissues were then incubated with the chromogen IMMpact DAB (1drop DAB added to 1mL of diluent as per manufacturer's instructions) and incubated for 5 min. The chromogen was washed off with dH_20 and filtered Mayers haematoxylin used as the counterstain for 40-45 sec before being further developed in hot water for 1 min. The slides were put through the following rehydration treatment procedure;

I. ddH_20 2 x 3 min followed by
II. 99% industrial denatured alcohol (IDA) 3 x 3min incubations followed by
III. Xylene 3 x 3min incubations

Glass coverslips were used after the tissues were mounted with DPX mountant.

2.6 Immunofluorescence staining of liver tissue

The treatment of liver tissue slides for immunofluorescence is very similar to preparation for IHC; tissues first underwent dewaxing and rehydration;

I. Xylene 3 x 3 min incubations followed by
II. 99% industrial denatured alcohol (IDA) 3 x 3 min incubations followed by
III. ddH_20 2 x 3 min incubations for tissue rehydration

A 1000mL 1% tris-based (high pH) antigen unmasking solution was prepared and placed in

a microwave oven set at ‘High’ for 10 min for antigen retrieval. The dewaxed and rehydrated liver tissue was placed in the preheated unmasking solution and microwaved at ‘High’ for 30 min. The tissue were cooled for 10 min.

Plastic slide boxes were made into humidified chambers by lining with damp paper towel and parallel glass stripettes (sized to fit) placed inside to act as slide racks.

Slides from the cooled unmasking solution were transferred to the humidified chambers; the tissue was outlined using an ImmEDGE Hydrophobic Barrier PAP pen and then placed onto the stripette slide rack. Slides were then washed with TBST for 5 min.

Tissues were then incubated with casein buffer (2X solution) for 10 min to prevent non-specific protein binding. Primary antibodies were applied without washing off the casein buffer and incubated for a 12 hour period at 4dC; primary antibody dilution optimisation was performed as for IHC. TBST was used as the diluent for the antibodies. Following the primary antibody incubation, slides were washed with TBST for 5 min.

Secondary antibodies were applied to the corresponding primary antibody and incubated e.g. AF555 goat anti-mouse IgG1 secondary antibody for the TCR Valpha 7.2 mouse anti-human IgG1 primary antibody; optimal dilution experiments were performed prior to multiple staining of patients/conditions. TBST was used as the diluent.

Tissues were washed with TBST x 3. The Vector labs TrueVIEW Autofluroescence Quenching kit with DAPI was used and incubated for 5 min; manufacturer’s guidance on reagent volumes and mixing steps were applied. Tissues were washed with TBST and mounted immediately with VECTASHIELD Vibrance Antifde Mounting Medium 50 uL with glass coverslips.

2.7 Confocal microscopy on liver tissue sections

Immunofluorescent (IF) stained liver tissue were imaged using the Zeiss 780 or 900 confocal microscope 24 hrs after application of the mounting medium. Formal training on the Zeiss 780 confocal microscope was undertaken in preparation for the IF work. Later on I was additionally trained on the Zeiss 900 for the experience accrued to enable multiple laser use for the 5 channel imaging set up; AF488, AF594, AF555, AF647 and DAPI.

2.8 Metal conjugation of CyTOF antibodies

I designed a MAIT cell Cytometry by Time Of Flight (CyTOF) panel consisting of 42 markers; 27 cell surface and 15 intracellular markers. Twenty-two of these antibodies were purchased from Fluidigm and 20 were purified antibodies that I metal conjugated in the using the Fluidigm Metal Antibody Labelling protocol.

The technique of metal conjugation to purified antibodies include 1) lanthanide metal polymer pre-loading, 2) metal loaded polymer purification, 3) partial antibody reduction and 4) conjugation of the antibody with the metal loaded polymer;

1) Pre-loading polymer with lanthanide metal;

The polymer and the pre-selected lanthanide metal is centrifuged (pulse spin).

The polymer is resuspended with 95 uL of L-buffer. 5 uL of the selected lanthanide metal e.g. 147Sm, is added to the polymer solution and incubated for 40 min at 37dC.

2) Purification of metal loaded polymer;

200 uL of L-buffer is added to a 3kDa filter followed by 100 uL of the metal loaded polymer

solution from step 1. This is then centrifuged at 12,000 x *g* for 25 min at room temperature. The flow-through is discarded. 400 uL of C-buffer is now added and centrifuged at 12,000 x *g* for 30 min at room temperature.

3) Partial antibody reduction

100 ug of the purified antibody e.g. TCR Valpha 7.2 is added to a 50 kDa filter. R-buffer is added to make a up total volume of 400 uL. This solution is centrifuged at 12,000 x *g* for 10 min at room temperature. The flow-through is discarded. TCEP is diluted in R-buffer to make up a 4 mM solution (8 uL of 0.5 m TCEP is added to 992 uL R-buffer). Then 100 uL of this TCEP/R-buffer solution is added to the centrifuged antibody and mixed by pipetting before incubated for exactly 30 min at 37dC. 300 uL of C-buffer is added to the antibody – TCEP/R-buffer solution and centrifuged for 10 min at 12,000 x *g* at room temperature. The flow-through is discarded and another wash with 400 uL of C-buffer is performed at 12,000 x *g* for 10 min at room temperature.

4) Conjugating the antibody with the metal loaded polymer

The metal polymer from the end of step 2. is resuspended in 60 uL of C-buffer. This is then transferred to the 50 kDa filter containing the partially reduced antibody. The antibody – metal polymer solution is mixed by pipetting and incubated at 37dC for 90 min.

200 uL of W-buffer (Wash buffer) is added and centrifuged at 12,000 x *g* for 10 min at room temperature. The flow-through is discarded and 400 uL of W-buffer is added and centrifuged at 12,000 x *g* for 8 min at room temperature. This 400 uL W-buffer wash step is repeated a further three times, discarding the flow-through each time. 80 uL of the W-buffer is added, pipetted to mix and rinse the walls of the filter, then centrifuged at 12,000 x *g* for 8 min at room temperature. 120 uL of the stabilisation buffer is added, pipetted to mix and rinse the walls of the filter. The 50 kDa filter containing the metal conjugated antibody is inverted into a new collection tube. This is then centrifuged at 1000 x *g* for 2 min and

transferred to a low-bind 1.5mL tube.

A NanoDrop (set at IgG mode) is used to measure the antibody concentration. The low-bind 1.5mL tube is then labelled with the antibody target e.g. TCR Valpha 7.2, clone 3C10, mass-tag 147Sm, antibody concentration and date. The metal labelled antibody is then stored at 4dC, ready for use.

2.9 CyTOF experiments using paediatric blood from AILD patients and healthy control

a) Cell culture media (10% FCS & RPMI, with Pen/Strep and L-Glutamine) was prewarmed at 37dC.

b) PBMCs were thawed and placed in the prewarmed media in a 15 mL Corning tube and then centrifuged at 1500 rpm for 10 min (acceleration and deceleration set at 9).

c) The supernatant is tipped off and the pellet slowly resuspended by pipetting and made up to 7mL of cell culture media. A manual cell count is performed using a haemocytometer. The 7mL cell solution is centrifuged at 2000 rpm at 5 min (acceleration and deceleration set at 9 unless stated otherwise).

d) The supernatant is tipped off and the pellet is resuspended with 2mL of cell culture media, then divided into two wells in a 48 well plate i.e. 1mL per well (4-5million cells per 1mL).

The wells are labelled a) Stimulated (treated) and b) Unstimulated (not treated). In the well labelled ‘Stimulated’, this was treated with 2uL of CytoStim (a cell stimulation cocktail containing polyclonal antibodies, plus protein transport inhibitor) as per manufacturer’s instructions. Golgistop 1uL (protein transport inhibitor) was added to the ‘Unstimulated’ well to account for the protein transport inhibitor already added in the ‘Stimulated’ well. The 48

well plate is then incubated at 37dC for 4 hours.

e) Cells solutions were retrieved from the 48 well plate and placed into FACS tubes labelled ‘Stimulated’ and ‘Unstimulated’ accordingly. Culture media was added to make up 3mL and centrifuged at 500 x *g* for 5min. The centrifuge speed was increased from 350 x *g* to 500 x *g* following troubleshooting and optimization experiments to prevent cell loss by increasing cell pellet compactness.

f) The supernatant is tipped off and 1mL of culture media is added to the cell pellet and mixed by gentle vortex. DNase 50uL is added to the 1mL cell solution 1drop at a time, vortexed and incubated for 15 min at room temperature. The DNase step was added to improve sample preparation; samples were clumped together and viscous particularly with the ‘Stimulated’ patient samples. The ‘stickyness’ of the clumped samples made pipetting and cell preparation more difficult. The risk of cell loss after each centrifuge was greater as noted following acquisition on the Helios mass cytometer. The viscosity of a cell sample usually increases during cell lysis when nucleic acid material is released. Patient samples treated (‘Stimulated’) with CytoStim were expected to produce a higher degree of cell lysis by the nature of the experiment.

DNase successfully reduced cell viscosity and improved cell pelleting in my CyTOF experiments; DNase was used in all subsequent CyTOF experiments. All troubleshooting steps were undertaken in discussion and advice by the Fluidigm team.

g) Whilst the cell suspension is incubated with DNase, the CyTOF surface antibodies are centrifuged at 12,000 x *g* for 8 min. The CyTOF surface antibody cocktail is made up carefully in a 1.5mL Eppendorf by careful pipetting.

h) Once the DNase incubation is complete, top up with culture media to make up 3mL and centrifuge at 500 x *g* for 5min.

i) Tip off the supernatant and add FC blocker 3.2uL to the cell pellet, gently vortex and

incubate for 10 min. Do not wash off the FC blocker. Add the surface antibody cocktail (17.7uL per FACS tube) and incubate for 30 min at room temperature. Dilute cisplatin stock in 100uL of Maxpar PBS. Add 10uL of this Cisplatin solution to the cell solution containing the FC blocker and surface antibodies.

Incubate precisely for 2 min and wash with CSM (Cell Staining Media) made up to 3mL at 500 x *g* for 5min twice.

j) Fix cells with 1.6% Paraformaldehyde (PFA) solution; add 100uL filtered 16% PFA to 900uL Maxpar PBS. Add 1mL of the 1.6% PFA solution to each tube, gently vortex to mix, and incubate for 20 min protected from light at room temperature.

k) During the fixation of cells with 1.6% PFA, centrifuge the CyTOF intracellular antibodies at 12,000 x *g* for 8 min.

l) Make up the intracellular antibody cocktail carefully in a 0.5mL Eppendorf by careful pipetting.

m) Once the cells have been fixed with 1.6% PFA, centrifuge at 1000 x *g* for 5 min (following troubleshooting experiments). The centrifuge speed was increased from 800 x *g* to 1000 x *g* following optimization to prevent cell loss by increasing cell pellet compactness.

n) Make up the Permeabilization solution; add 0.5mL of Permeabilization buffer to 4.5mL de-ionised H_20. Add 2mL of this Permeabilization solution to each FACS tube and centrifuge at 1000 x *g* for 5 min. Resuspend cell pellet in 100uL of the Permeabilization solution. Add the intracellular antibody cocktail and incubate for 30 min protected from light at room temperature. Add CSM 2mL and centrifuge at 1000 x *g* for 5 min.

o) Separately, make up the Intercalation solution by adding 1uL of Rhodium to 600uL of Maxpar Fix & Perm Buffer per FACS tube. Add 500uL of this Intercalation solution per FACS tube and incubate overnight at 4dC.

p) The next day, wash cells by adding 2mL of Maxpar Cell Acquisition Solution (CAS) to

each FACs tube and gently vortex. Centrifuge tubes at 1000 x *g* for 5 min. Repeat wash for a total of 3 washes.

q) Each pellet/sample is resuspended in 300uL of CAS and taken to the Institute of Translational Medicine (ITM) for acquisition by the Helios (CyTOF) mass cytometer.

2.10 Application of the Barcoding technique in CyTOF

I used the technique of barcoding in order to maximise the number of patient samples 'per run' on the Helios mass cytometer. Barcoding increases the number of patient samples acquired 'per run' with up to 8 samples (4 patients with two conditions each) per FACS tube. The barcoding approach involves the addition of two surface antibodies not included in the MAIT cell panel which would allow for separation in the analysis phase. The barcoding antibodies I used were metal conjugated with isotopes of Cadmium (2.11 Metal conjugation). Each patient sample and condition was placed in a separate FACS tube and the barcoding antibodies added e.g. Patient 1 'Stimulated' had Cd106 and Cd 110, Patient 1 'Unstimulated' had Cd112 and Cd115,

Patient 2 'Stimulated' Cd111 Cd113, and Patient 2 'Unstimulated' had Cd114 & Cd116 added etc.

Cell suspensions were incubated with these barcoding antibodies after step e) of '2.10 CyTOF experiment' for 20 min at room temperature. Maxpar Cell Staining Media (CSM) was then added to the FACS tubes to make up 3 mL and centrifuged at 350 x *g* for 5 min. The wash step was repeated once. Following barcoding, the cell suspensions from the four FACs tubes (Patient 1 'Stim', Patient 1 'Unstim', Patient 2 'Stim' and Patient 2 'Unstim') were combined into one FACS tube and centrifuged at 350 x *g* for 5 min.

FC blocker 3.2 uL was added to the FACS tube and incubated for 10 min. The rest of the

experiment follows on identically from i) onwards in ‘2.12 CyTOF experiments’.
At the end of the experiment, one FACs tube containing 300 uL of Cell Acquisition Solution (CAS) and two patient samples (with two conditions each of ‘Stim’ vs ‘Unstim’) is taken to the Institute of Translational Medicine (ITM) for acquisition by the Helios (CyTOF) mass cytometer. I had to stop using the barcoding method for my experiments after several attempts as total MAIT cell number acquired per sample was too low; MAIT cell makes up 0.1 to 10% of total CD3 T lymphocytes and running patient samples separately without barcoding gave higher MAIT cells yields.

2.11 Cell culture and isolation of cholangiocytes

Human explanted or donor liver was manually diced in a petri dish using steril scalpels and placed into a sterile 200 mL beaker. One 5 mL aliquot of collagenase was added to 20 mL sterile PBS. The beaker is incubated at 37dC for 45 min with constant agitation in an Automated Shaking Incubator. The diced liver was then strained through a fine mesh into another sterile beaker. PBS was added to make up to a volume of 200 mL. This was then divided between 8 universal containers and centrifuged for 5 min at 2000 rpm with acceleration and deceleration set at 9. The supernatant was tipped off and the cell pellet resuspended and divided into 4 universal containers then centrifuged at 2000 rpm for 5 min. The wash step was repeated x 2 until the pellet was combined into 1 universal container. PBS was added to make up the volume to 24 mL.
Percoll cell separation gradients were prepared in advance:

- Stock percoll – 99 mL percoll + 11 mL 10x PBS
- 33% percoll – 33 mL stock + 67 mL 1x PBS
- 77% percoll – 77 mL stock +23 mL 1x PBS

3 mL of 33% percoll was added into each 8 x 15 mL conical bottomed tubes. Then 3 mL of 77% percoll was carefully dispensed underneath the 33%, Lastly 3 mL of the cell suspension was layered onto the percoll gradients then centrifuged at 2000 rpm for 25 min with the acceleration set at 3 and deceleration at 0.

The band of cells at the percoll interface was removed; two aliquots were placed into one universal container to fill 4 universal containers in total. Each universal container was made up to a volume of 25 mL with PBS, mixed well and centrifuged at 2000 rpm for 5 min, with an acceleration and deceleration at 9. The supernatant was tipped off and two pellets combined into 1 universal container, the volume made up to 25 mL with PBS and then centrifuged at 2000 rpm at 5 min. The supernatant was tipped off and the pellets this time combined into a 15 mL conical tube, the volume made up to 14 mL with PBS and centrifuged at 2000 rpm at 5 min. The supernatant was tipped off and the pellet resuspended in 500 uL of PBS. 50 uL of HEA 125 (mouse anti-human epithelial cell adhesion molecule (EPCAM))

was added and incubated at 37dC for 30 min. PBS was added to make up the volume to 14 mL and centrifuged at 2000 rpm for 5 min. The pellet was resuspended in 500 uL of ice cold PBS and 10 uL cold dyna beads were added and incubated at 4dC for 30 min with constant agitation in an automated shaking rack.

Magnetic separation was performed next; 6 mL of ice cold PBS was added to the cell suspension-HEA-dyna bead solution, mixed by pipetting and the tube placed in a magnet for 2 min. The supernatant was aspirated off by pipetting whilst the tube remained in the magnet. This process was performed a total of 3 times. Once the supernatant was aspirated off after the 3rd time, 5 mL of BEC media was added, mixed well by pipetting and the contents transferred to a 2.5% collagen pre-coated T25 cm flask and incubated at 37dC to establish cell growth. The flask was labelled (i.e. Oo Group, CLR number, date, passage

number and disease type e.g. AIH). BEC media was changed every two days; 5 mL media removed by pipetting and new 5mL BEC media added.

Once cells have formed a confluent monolayer on the bottom of the flask, they were passaged; all media were removed by pipetting, and the sides washed down with 5 mL of PBS (this removes traces of serum which can inactivate trypsin. The PBS was removed and 1mL of trypsin added to the T25 flask and incubated for 2-5min at 37dC until the cells round up and lifts off the bottom of the flask (assessed by light microscopy). The cells were removed with 2-3mL of PBS and transferred to a 15 mL corning tube containing 1 mL pure FCS which neutralises the trypsin. PBS was added to make up to 14 mL and centrifuged at 2000 rpm for 5 min. The pellet was resuspended in 3 mL of BEC media and placed in a T75 cm flask. 7mL of additional BEC media was added to the T75 flask to make up a total volume of 10 mL. The flask is labelled and incubated at 37dC until needed for downstream applications.

2.12 Paraformaldehyde fixation of E.coli

Under sterile conditions, 50 uL of thawed Escherichia coli (*E.coli)* (DH5a, Invitrogen) was added to 5 mL of microbial growth medium (LB Broth, Miller) in a 15 mL Falcon tube and placed in an Automated Shaking Incubator for 12 hours at 200 rpm at 37dC. A control Falcon tube containing 15 mL of LB Broth (without *E.coli*) was also placed in the incubator. At the end of the 12 hours, the Falcon tubes were centrifuged at 2000 rpm for 5 mins. The Falcon tube containing *E.coli* had a visible pellet compared to the control Falcon tube. The supernatant was discarded and the pellet resuspended with PBS and centrifuged at 2000 rpm for 5 min x 2. The *E.coli* was then fixed with paraformaldehyde (PFA); the pellet was resuspended with 5 mL of 2% PFA (1 mL 10% PFA to 4 mL PBS, prepared under a fume

extraction hood) and incubated for 30 min at room temperature. Centrifugation with 15 mL PBS at 2000 rpm at 5 min x 2. After the second wash, the PFA fixed *E.coli* pellet was resuspended with 10 mL of sterile filtered PBS. The total bacteria count (TBC) was 9.6 x 10^6 *E.coli* per 1 mL of PBS. This TBC of PFA fixed *E.coli* was used for downstream applications (co-culture experiments).

2.13 Tissue culture of THP-1 cells

The human monocyte cell line, THP-1 cells, were purchased from the ECACC, Public Health England. The vial was rapidly thawed in a Lab Armor Bead bath set at 37dC for < 2 min. The contents of the vial was pipetted into a 15 mL Corning tube containing 5 mL of pre-warmed cell culture media (10% FCS in RPMI with Pen/Strep and L-Glutamine) and a viable cell count performed manually with a haemocytometer and trypan blue stain. The cell suspension was then centrifuged at 150 x *g* for 5 min and the pellet resuspended in fresh culture media at a maximum of 1 x 10^6 THP-1 cells per 1 mL in a T75 flask. The flask is incubated at 37dC in a vertical position. The THP-1 cells were pelleted down and resuspended in fresh 5 mL culture media every 3 days, with cell counts maintained 1 x 10^6 per 1 mL for downstream applications.

2.14 Magnetic positive CD14+ selection

Firstly, make up a MACS cell suspension buffer using 95 mL PBS, 5 mL 10% BSA and 200 uL EDTA and pre-cool at 4dC. PBMCs were isolated from whole blood by density gradient centrifugation and a viability cell count performed. The single cell suspension of PBMCs were centrifuged at 300 x *g* for 10 min and the pellet resuspended in 80 uL of MACS buffer for 1 x 10^7 cells. Volumes are given per 1 x 10^7 cells.

CD14+ MicroBeads 20 uL was added, mixed by pipetting and incubated at 4dC for 15 min. The cells were washed with 2 mL of MACS buffer, centrifuged at 300 x *g* for 10 min and the pellet resuspended in 500 uL of MACS buffer.

For the magnetic separation, a MS column was placed into the magnetic field of the MACS Separator and rinsed with 500 uL of MACs buffer. A 15 mL collection tube was placed under the MS column. The 500 uL CD14+ labelled cell suspension was then placed in the MS column followed by MACS buffer 500 uL x 3. The flow-through (effluent) containing the unlabeled cells were collected for later use (for T cell isolation).

The MS column containing the CD14+ labelled cells was removed and placed into a new 15 mL Corning tube. One mL of MACS buffer was pipetted into the MS column and immediately flushed through with the plunger provided. The collected CD14+ cells were centrifuged at 2000 rpm at 5 min and resuspended in cell culture media (10% FCS in RPMI with Pen/Strep and L-Glutamine) at a concentration of 1 x 10^6 cells per 500 uL, ready for downstream applications.

2.15 Magnetic negative CD3+ selection via Pan T cell isolation

Depending on the experiment, either PBMCs or the flow-through from the CD14+ positive magnetic selection were used for Pan T cell isolation. Volumes below are given per 1 x 10^7 cells. The single cell suspension was centrifuged at 2000 rpm for 5 min and resuspended with pre-cooled MACs buffer 40 uL. Pan T cell Biotin antibody cocktail 10 uL was added, mixed by pipetting and incubated for 5 min at 4dC. MACs buffer 30 uL was then added, followed by the addition of 20 uL Pan T cell MicroBead, mixed by pipetting and incubated at 4dC for 10 min. A MS column was placed into the magnetic field of the MACS Separator and rinsed with 500 uL of MACs buffer. Then the magnetically labelled cell suspension was put in the MS column 500 uL at a time and the flow-through containing the unlabeled cells collected in a 15 mL Corning tube (enriched T cells). The enriched T cells were centrifuged at 2000 rpm at 5

min and resuspended in cell culture media (10% FCS in RPMI with Pen/Strep and L-Glutamine) at a concentration of 1 x 10^6 cells per 500 uL, ready for downstream applications.

2.16 In-vitro MAIT cell co-culture with *E.coli* primed cholangiocytes using THP-1 cells as a positive control

a) Cultured cholangiocytes (from donor liver or explanted adult PSC liver) were seeded in a 24 well plate at 50,000 cells per well and incubated at 37dC with paraformaldehyde-fixed *E.coli* (DH5a, Invitrogen) at 200 bacteria per cell. The ratio of lymphocyte to *E.coli* of 1:200 was derived from previous Oo Group experiments (Jeffery et al, J Hepatol, 2016). Media was added to the negative control well to maintain the same total volume.

b) Two positive controls were used for this experiment a) *E.coli* primed THP-1 cells at the same ratio of 200 bacteria per cell and b) treatment with CytoStim (polyclonal TCR antibodies).

c) CD3+ T cells isolated from PBMCs by negative selection Microbeads (Pan T cell isolation kit, Miltenyi Biotec) were added to the co-cultures at a ratio of 1 BEC to 10 CD3+ cells and 1 THP-1 to 1 CD3+ cell (Jeffery et al, J Hepatol, 2016). Monesin was added to all wells (except for those containing Cell Stimulation Cocktail) at a concentration of 1 uL per 1 mL of cell solution as per manufacturer's instructions. These co-cultures (*E.coli* primed BEC & CD3+, *E.coli* primed THP-1 & CD3+, Cell Stimulation Cocktail & CD3+, and their respective negative controls) were incubated for 4 hours (Figure).

d) Contents from the wells were retrieved into pre-labelled FACS tubes corresponding to the test e.g. 'E.coli / BEC / CD3+' and centrifuged at 2000 rpm at 5 min, acceleration 9 and

deceleration 9, with 2 mL PBS. Cell suspension from the FACS tubes were then transferred to a new 96 well round bottom plate and centrifuged with 200 uL FACS buffer at 1500 rpm for 2 min x 2.

e) 7AAD 1 uL per 100 uL (1:100) of cell suspension was added to all wells (except for the 'Unstained' test) and incubated at 4dC for 30 min followed by centrifugation with FACS buffer 200 uL at 1500 rpm for 2 min x 2.

f) FC block 1 uL was added per 100 uL of cell suspension and incubated for 15 min at 4dC, followed by centrifugation with 200 uL FACs buffer at 1500 rpm for 2 min x 1.

g) Staining for surface and intracellular markers were performed next; I designed two MAIT cell panels (MAIT cell panel A and MAIT cell panel B) and one BEC panel (Figure).

A mastermix containing surface antibody markers and 50 uL BV buffer per FACS tube (except for the 'Unstained' test) were added accordingly and incubated for 30 min at 4dC protected from light, followed by centrifugation with FACS buffer 200 uL at 1500 rpm for 2 min x 2. Cell fixation was performed next using 200 uL eBiosciences Fix Buffer (1 mL Fix concentrate was added to 3 mL diluent) and incubated for 45 min at 4dC protected from the light. Centrifugation with FACS buffer 200uL at 1500 rpm for 2 min x 2. Permeabilisation of the cells followed by adding 200 uL Perm buffer (0.5 mL Perm buffer x 10 diluted with 4.5 mL H20) and incubated for 30 min at room temperature, protected from light, followed by centrifugation with FACS buffer 200 uL at 1500 rpm for 2 min x 1. Intracellular antibodies were added to the cell suspension containing 100 uL of Perm buffer and incubated for 30 min at room temperature protected from light. Centrifugation with FACS buffer 200uL at 1500 rpm for 2 min x 2.

h) Cell solutions were resuspended in 300 uL of FACS buffer in the 96 well plate and transferred to pre-labelled FACS tubes. FACS tube samples were acquisitioned on the BD LSR Fortessa X-20 and analyzed using Flow Jo software v10.

2.17 In-vitro MAIT cell co-culture with *E.coli* primed cholangiocytes using CD14+ monocytes as positive control

As in 2.19, cultured cholangiocytes (from donor liver or explanted adult PSC liver) were seeded in a 24 well plate at 50,000 cells per well and incubated at 37dC with paraformaldehyde-fixed *E.coli* (DH5a, Invitrogen) at 200 bacteria per cell. Media was added to the negative control to ensure the total volume per well was the same.
CD14+ monocytes (by magnetic selection of PBMCs) primed with *E.coli* at the same ratio of 200 bacteria per cell was set up as a positive control in place of THP-1 cells. Treatment with CytoStim was used as a second positive control.
Enriched CD3+ T cells isolated from PBMCs by Magnetic negative selection were added to the co-cultures at a ratio of 1 BEC to 10 CD3+ cells and 1 CD14+ to 1 CD3+ cell. Monesin was added to all wells (except for those containing Cell Stimulation Cocktail) at a concentration of 1 uL per 1 mL of cell solution. The co-cultures (*E.coli* primed BEC & CD3+, *E.coli* primed CD14+ & CD3+, Cell Stimulation Cocktail & CD3+, and their respective negative controls) were incubated for 4 hours (Figure). The rest of the experiment proceeds identically to 2.19 d) onwards.

2.18 Statistical analysis

The Kruskal-Wallis H test was the statistical analysis applied to compare three cohorts or more. It is the non-parametric equivalent of the One-Way ANOVA test and does not require results to be normally distributed (Gaussian distribution) and it takes into account of outlying

results which can skew the data. There were several outlying results from my CyTOF data

and hence the Kruskal-Wallis H test, although more restrictive, will ensure the data is not over represented. The Bonferroni multivariate correction was applied to compare intergroup differences (subgroup analysis). Differences between two groups were compared using the Mann Whitney U test which is the non-parametric equivalent of the Student's t-Test to assess differences between two independent groups. All statistical analysis was performed using GraphPad Prism software, with $p < 0.05$ indicative of statistical significance. Statistical significance will be expressed as *≤0.05, **≤0.01, ***≤0.001, and ****≤0.0001.

Chapter 3. Assessing the spatial relationship of MAIT cells and Tregs in the paediatric autoimmune liver

3.1 Demonstrating the presence of MAIT cells in the paediatric autoimmune liver

Confocal image capture of immunofluorescence (IF) stained mucosal-associated invariant T (MAIT) cells was reported by our group in which triple IF staining for the semi-invariant T cell receptor Vα7.2, the C-type lectin CD161 and CD3+ T lymphocytes was performed on formalin fixed paraffin embedded (FFPE) liver tissue. In this previous work, human intrahepatic MAIT cells were shown to be predominately located around the bile ducts of portal tracts in diseased adult liver explants of varying aetiology [19]. The highest frequency of peribiliary and periportal MAIT cells were observed in PSC liver. In contrast, a higher propensity of MAIT cells were identified in the parenchyma of livers explanted for acute liver failure [19].

Aside from our research, there is one other study of adult intrahepatic MAIT cell IF staining in which a higher proportion of MAIT cells were found in PBC livers compared to donor liver controls [125]. There are no reports of IF staining for intrahepatic MAIT cells in paediatric liver tissue to date. There are only three other reports demonstrating IF staining and confocal imaging of tissue MAIT cells, namely from patients with inflammatory bowel disease, and in multiple sclerosis; MAIT cell frequency was found to be higher in active disease e.g. inflamed ileum in Crohn's disease, white matter lesions/plaques in MS patients

[135, 142, 143]. Gargano et al showed Vα7.2+ CD161+ to represent 90% of all TCR Vα7.2 positive cells in their MAIT cell IF staining but accounted for only 36% of total CD161 positive cells. CD3+ cells were shown to have similar co-expression of anti-Vα7.2 antibody and the MR1-antigen tetramer by Torre et al. Other groups have found MAIT cell localization using the MR1-antigen tetramer to be suboptimal and difficult to stain for (Pohl et al, unpublished work).

With this collective evidence of MAIT cell IF staining, I elected to perform MAIT cell IF staining using the anti-TCR Vα7.2 antibody, Clone 3C10, on paediatric liver explant tissue. Following antibody optimization, I performed anti-TCR Vα7.2 antibody IF staining on liver explant tissue from children with autoimmune liver disease (autoimmune hepatitis type 1; AIH T1, autoimmune hepatitis type 2; AIH T2 and Primary sclerosing cholangitis; PSC). Liver explant tissue from children with biliary atresia was used as a disease comparison to the autoimmune group and adult donor liver tissue was used as a control for comparison. Ethics approval was granted and Human Tissue Authority (HTA) guidelines were followed in the conduct of these experiments.

Biliary atresia, a progressive obliterative form of cholangiopathy is the commonest cause of chronic liver disease and liver transplantation in childhood [144, 145]. Due to logistical complexities during the COVID pandemic, greater numbers of liver explant FFPE blocks were available from AIH T1 and biliary atresia patients. Therefore, IF staining and confocal imaging were performed on AIH T1 patients N=4, biliary atresia patients N=5, AIH T2 N=1 and PSC N=1 patient.

Clinical characteristics of the autoimmune liver and biliary atresia patients whose liver explant sections were used for immunofluorescence staining, were consistent with disease characteristics described in the literature for these conditions. Table 6 shows the patient demographics and disease characteristics of the autoimmune liver patients. The median age of the AIH T1 patients were 13years at the time of transplant; 3 were female and of Caucasian descent. The PSC patient was a Caucasian male aged 16years at the time of transplant. The AIH T2 patient in contrast presented much younger at 1.5years and had a more aggressive phenotype with acute liver failure (ALF) requiring transplantation. This AIH T2 patient differs significantly from the AIH T1 and PSC cohorts as she had ALF and had no evidence of chronic liver disease including portal hypertension as suggested by her laboratory parameters. Although no MAIT cell assessment has been reported in the literature for AIH T2, MAIT cell distribution is more disperse and located within the parenchyma in adult ALF as compared to chronic liver disease explants [19, 51]. Moreover, children with AIH T2 have well-defined differences compared to AIH T1. Similar to our AIH T2 patient, most present at a younger age and have a more aggressive clinical phenotype with higher rates of acute liver failure and need for transplantation [96, 101]. Caution must therefore be employed in the interpretation of the results when comparing AIH T2 with AIH T1 and PSC.

The AIH T1 and PSC were transplanted for end-stage liver disease. All AIH type 1 patients were on azathioprine and low dose prednisolone immunosuppressive therapy (Table 7); their liver functions were controlled with treatment although their immunoglobulin G (IgG) were still raised, and all were anti-smooth muscle antibody positive (SMA). The AIH T2 patient had positive anti-liver kidney microsomal (LKM) antibodies. The PSC patient was cholestatic and positive for both antinuclear antibody (ANA) and SMA.

The demographics and clinical characteristics of the biliary atresia (BA) patients at liver transplantation are specified in Table 8; four out of five BA patients were male, all were Caucasian, and diagnosed as a neonate. Four were transplanted for end-stage liver disease (ESLD) and one had a dysplastic liver lesion which was suspicious for hepatocellular carcinoma. Of the four patients transplanted for ESLD, three had evidence of portal hypertension confirmed by the presence of varices, splenomegaly and/or low platelet count. The liver section used for the IF staining in this research was lesion/tumour free.

Table 6. Autoimmune liver disease patient demographics and disease characteristics – immunofluorescence staining and confocal microscopy

	AIH T1 n=4	AIH T2 n=1	PSC n=1
Age at LT (Years)	13 (13-14)	1.5	16
Age at diagnosis (Years)	9 (6-12)	1	15.5
Sex (% Male)	25% (1/4)	0% (0/0)	100% (1/1)
Caucasian	75% (3/4)	100% (1/1)	100% (1/1)
Labs			
Total Bili (µmol/L)	56 (50-78)	63	127
ALP (IU/L)	217 (118-309)	94	988
GGT (IU/L)	24 (14-108)	27	119
ALT (IU/L)	45 (35-48)	37	58
AST (IU/L)	56 (53-66)	58	40
Albumin (g/L)	32 (31-39)	40	31
Total Protein (g/L)	66 (63-73)	66	59
PT (sec)	15 (13-15)	17	15
Platelets ($x10^9$/L)	41 (39-50)	203	76
IgG (g/l)	19.12 (16.21-28.2)	21.05	21.53
Autoantibodies			
ANA	0% (0/4)	0% (0/1)	100% (1/1)
LKM	0% (0/4)	100% (1/1)	0% (0/1)
SMA	75% (3/4)	0% (0/1)	100% (1/1)
ANCA	0% (0/4)	0% (0/1)	0% (0/1)
Disease severity			
*PELD**	n/a	17.6	n/a
*MELD***	15 (15-22)	n/a	22
PHT	75% (3/4)	0% (0/1)	100% (1/1)
Decompensated cirrhosis	100% (4/4)	0% (0/1)	100% (1/1)
Indication for LT			
ESLD	100% (4/4)	0% (0/1)	100% (1/1)
ALF	0% (0/4)	100% (1/1)	0% (0/1)
Disease recurrence			
Patients with disease recurrence	25% (1/4)	0% (0/1)	0% (0/1)

**PELD, Paediatric End-Stage Liver Disease score, a disease severity scoring system for children <12years of age; **MELD, Model for End-stage Liver Disease, a predictor of survival in patients ≥12yrs of age with cirrhosis. AIH T1: autoimmune hepatitis type 1, AIH T2: autoimmune hepatitis type 2, PSC: primary sclerosing cholangitis, LT; liver transplantation, PHT; portal hypertension, ESLD; end-stage liver disease, ALF; acute liver failure.*

Table 7. Immunosuppression treatment for AIH patients

– immunofluorescence and confocal microscopy

	AIH on Rx n=4
Immunosuppressant	
Prednisolone	4
Azathioprine	4
MMF	0
Tacrolimus	0
Sulphasalazine / Mesalazine	0

AIH: autoimmune hepatitis, Rx: treatment, MMF; Mycophenolate mofetil

Table 8. Biliary atresia patient demographics and disease characteristics

– immunofluorescence and confocal microscopy

	BA n=5
Age at LT (years)	1 (0.5-9)
Age at diagnosis (days)	30 (20-35)
Sex (% Male)	80% (4/5)
Caucasian	100% (5/5)
Labs	
Total Bili (µmol/L)	128.5 (12-197)
ALP (IU/L)	1076 (465-1701)
GGT (IU/L)	482 (146-1110)
ALT (IU/L)	137 (91-298)
AST (IU/L)	190 (65-217)
Albumin (g/L)	37 (28-43)
Total Protein (g/L)	67.5 (49-77)
PT (sec)	11 (10-19)
Platelets ($x10^9$/L)	190.5 (119-577)
Disease severity	
*PELD**	15.7 (0-21.5)
PHT	60% (3/5)
Decompensated cirrhosis	80% (4/5)
Indication for LT	
ESLD	80% (4/5)
Suspected HCC	20% (1/5)

**PELD, Paediatric End-Stage Liver Disease score, a disease severity scoring system for children <12years of age, BA: biliary atresia, LT; liver transplantation, PHT; portal hypertension, ESLD; end-stage liver disease, HCC; hepatocellular carcinoma.*

3.2 Confirmation of intrahepatic MAIT cells in paediatric AILD and biliary atresia

Optimization of secondary antibodies were carried out on FFPE liver explant tissue from adult autoimmune liver explants and donor livers. Donor livers deemed unsuitable for transplantation due to suboptimal anatomy e.g. small vessel size and where consent was given for research were used for this work.

After successful optimization of IF MAIT cell anti-Vα7.2 antibody staining on adult liver tissue, I applied the same technique and dilutions of Vα7.2 IF staining on paediatric liver tissue. Confocal microscopy captured clear TCR Vα7.2 IF staining, showing well delineated cell surface membrane TCR Vα7.2 positivity in AIH type 1 (Figure 3a and 3b), AIH type 2, PSC (Figure 3c), biliary atresia and donor liver (Figure 3d). This research demonstrates and confirms the presence of MAIT cells in paediatric liver tissue for the first time. Intrahepatic MAIT cells were not only found within the spectrum of autoimmune liver disease (AILD) but also in biliary atresia, suggesting it is not disease specific.

CD3+ and TCR Vα7.2 dual expression via IF staining was previously confirmed in our group [19]. Adult human intrahepatic MAIT cells are shown to be predominantly CD8+T cells. Double negative MAIT cells (CD8 –, CD4 –) are also present in large numbers but intrahepatic CD4+ cells, although more numerous than their blood counterparts, make up only a small proportion of this T cell subset [9, 14]. Hence, I next performed dual staining with anti-CD8+ and Vα7.2+ antibodies to assess the colocalization of CD8+ Vα7.2+ MAIT cells in the paediatric AILD and biliary atresia liver explant tissue; CD8+ Vα7.2+ colocalization was most clearly demonstrated in an area of interface hepatitis of an AIH T1 paediatric liver where high numbers of CD8+ cells were identified in the inflammatory infiltrate (Figure 3e). In this example, CD8+ Vα7.2+ MAIT cells represented <5% of CD8+ cells. Gargano et al also found CD8+ MAIT cells to represent <5% of the total CD8+ cells in MS lesions and concluded that low CD8+ Vα7.2+ MAIT cell count may represent low total tissue MAIT cell numbers [142].

Next, quantification of MAIT cell numbers were performed on the paediatric livers, in which TCR Vα7.2+ cells were counted and compared in the periportal and hepatic parenchymal regions (Figure 3f (i) and (ii)). The distribution of MAIT cells in these paediatric livers were higher in the periportal regions compared to the hepatic parenchyma, a finding which reflects that described in adult diseased [19, 51, 80]. Moreover, paediatric PSC liver explant had the highest number of MAIT cells identified in the periportal region (Vα7.2+, 23 cells/mm^2) compared to the parenchyma (Vα7.2+, 12 cells/mm^2) (Figure 3f (ii)), again reflecting that described in adult autoimmune liver explants [19, 80].

I next assessed the functional aspect of these MAIT cells by dual staining for Granzyme B in TCR Vα7.2+ cells. Although biliary atresia explanted liver were used as a disease comparison to the paediatric AILD explants, the IF experiments has yielded some interesting results and to date, there is no published data reporting the presence of intrahepatic MAIT cells in biliary atresia (BA). Cytotoxic and IFNγ producing CD8+ T cells are implicated in BA [146, 147]. Additionally, Th-17 cells are known to infiltrate the liver in BA which is associated with a worse prognosis [148]. The majority of MAIT cells in the circulation and the liver are CD8+ and double negative (CD4- CD8-) T lymphocytes [19, 80]. MAIT cells possess Th1 and Th17 cytokine profiles, being able to release IFNγ and Il-17, and has cytotoxic potential with the release of perforin and granzyme upon activation [38, 80]. Interleukin-17 producing MAIT cells are linked to chronic inflammation and fibrosis [60, 78, 80].

I found Granzyme B expression by TCR Vα7.2+ MAIT cells to be most evident in BA liver explant tissue (Figure 3g) in which a rim of Granzyme B is seen enveloping the surface TCR Vα7.2+ of MAIT cells, indicating cytotoxic Granzyme B release into the surrounding tissue. IF staining of interferon gamma (IFNγ) and interleukin-17 (IL-17) expressing MAIT cells has been demonstrated in recent work but not Granzyme B expression [142].

3.3 Localization of MAIT cells and Tregs in paediatric livers

The liver is maintained in an immunotolerant homeostatic state at rest [149, 150]. Regulatory T cells (Tregs) are central in preserving immune health and regulation in the liver [151, 152]. In addition to Treg dysfunction, an imbalance between Tregs and T effector cells are speculated to contribute to the disease process in autoimmune hepatitis (AIH) [151, 153]. The portal tracts of liver biopsy samples from newly diagnosed (treatment naïve) adult AIH patients are enriched with MAIT cells and FOXP3+ Tregs [126].

However, little is known about the presence or localisation of these two immune cell types in paediatric autoimmune livers. I therefore set out to perform dual IF staining for TCR Vα7.2+ MAIT cells and FOXP3+ Tregs to examine the spatial relationship between these two important liver immune cells and assess whether there is a difference in their frequency and location in the paediatric autoimmune liver.

In terms of frequency count, TCR Vα7.2+ MAIT cells were mainly found in the periportal regions of portal tracts in paediatric liver explants. In contrast, FOXP3+ Tregs were predominantly identified in the parenchyma of the biliary cholangiopathies PSC and BA (statistical significance not reached). This is distinctly different from the AIH T1 patients where Treg numbers were generally found to be higher in the periportal region (Figure 3h (i) and (ii)). Paired line plots were chosen to represent the data in Figure 3f (i) and Figure 3h (i) as each paired line plot represents the same patient (tissue section) examined; the cell count is given for the periportal and parenchymal region for each patient (tissue section) reviewed.

In the paediatric AILD and BA tissue, I had difficulty finding the presence of both IF stained TCR Vα7.2+ MAIT cells and FOXP3+ Tregs within the same optical window (view) in the confocal microscope. The presence of TCR Vα7.2+ MAIT cells and a FOXP3+ Treg was captured however, in one confocal image of a paediatric AIH T1 liver explant tissue section (Figure 3i). Furthermore, I was able to capture what appears to be cell-to-cell contact between a TCR Vα7.2+ MAIT cell and a FOXP3+ Treg in the liver explant of a patient with biliary atresia (Figure 3k).

3.4 Cell-in-cell structures in paediatric AILD and biliary atresia

During the course of my confocal microscopy research, I unexpectedly captured cell-in-cell structures, namely the processes of emperipolesis. Emperipolesis, was first defined by Humble et al in 1956, and describes the internalisation and movement of one cell inside another. Suicidal emperipolesis further describes the fate of immune cells, and was first observed in the peripheral deletion (extrathymic) of autoreactive CD8+ cells by hepatocytes via lysosomal degradation,[154, 155]. Enclysis was first described by Davies et al, and specifically refers to the capture and lysis of Tregs by hepatocytes [156, 157].

Vα7.2+ MAIT cells were observed to lie within the cytoplasm of cholangiocytes in the liver explant of a paediatric PSC patient (Figure 3j). Emperipolesis was found to promote BEC apoptosis and bile duct injury in PBC [158]. The finding of emperipolesis in PSC suggests a common pathway may be causing bile duct injury in both these autoimmune cholangiopathies. MAIT cell emperipolesis in PSC has not been reported and this finding in the paediatric PSC liver may be of importance in helping to understand the cause of biliary epithelial damage in AILD.

Along with emperipolesis of Vα7.2+ by BEC, enclysis of FOXP3+ Tregs were also evident in the same PSC patient (Figure 3l). My initial interpretation of this micrograph was that it may represent a FOXP3+ cell captured lying on top of a hepatocyte (surface contact). However, following presentation to the Oo Group and in particular, after image analysis by Dr Scott Davies, our Postdoc who has a specialist interest and expertise in confocal microscopy, Figure 3l was in considered to represent enclysis.

In another PSC liver section from the same paediatric patient, an IF stained FOXP3+ cell was captured on the cell surface of a hepatocyte (Figure 3m). This cell-to-cell contact may

represent crosstalk between the immunosuppressive cell and hepatocyte and/or the onset of enclysis.

In a paediatric AIH T2 liver explant section, an intracellular FOXP3+ IF stained cell appears to be approaching a hepatocyte which may represent the immunosurveillance Treg activity (Figure 3n).

Enclysis (Davies 2019, Borensztejn et al 2021) is observed more frequently in autoimmune hepatitis (AIH) compared to other forms of chronic liver disease e.g. viral hepatitis. Unregulated enclysis is speculated to contribute to the loss of tolerance which leads to autoimmune mediated hepatocyte injury in AILD [159].
Dual staining with CD4 and FOXP3 was performed to confirm these to be CD4+ FOXP3+ Tregs. Clear cell surface IF staining by anti-CD4 antibody can be appreciated along with the independent intracellular FOXP3+ IF staining of the same cell in Figures 3o and 3p which shows a CD4+ FOXP3+ Treg enclysis in the biliary epithelial cell cytoplasm of the biliary ductules in a paediatric AIH T1 liver explant.

3.5 Discussion

3.5.1 Confirmation of intrahepatic MAIT cells in paediatric AILD and Biliary atresia

The detection of mucosal-associated invariant T (MAIT) cells by immunofluorescence (IF) and confocal microscopy in paediatric liver tissue in this research work is unique and novel. There is no published data relating to IF identification of MAIT cells in children, an invariant T cell population which is gaining increasing recognition as important mediators of many autoimmune disease conditions [12, 60, 78]. Autoimmune liver disease (AILD) often starts in childhood and span decades, effectively impacting a patient's entire lifetime [96, 110]. It is crucial to understand the underlying mechanisms of these immune mediated diseases early on in their pathophysiology to enable effective and timely intervention and facilitate targeted therapy development.

MAIT cells are the most abundant invariant T lymphocyte population in the adult liver and are implicated in biliary epithelial damage and fibrosis in AILD [10, 19, 80].
There are two research works in the literature with regards to IF stained MAIT cells in adult liver disease, the first were by the Oo Group in which triple IF staining of the semi-invariant T cell receptor Vα7.2, CD161 and CD3+ T lymphocytes were performed on formalin fixed paraffin embedded (FFPE) liver explant tissue in patients with chronic liver disease including PBC [19]. The second article confirms the higher frequency of intrahepatic MAIT cells in PBC liver explants compared to controls [125].
Neither has shown IF staining of MAIT cells in autoimmune hepatitis (AIH) or Primary sclerosing cholangitis (PSC), conditions with increasing prevalence and childhood presentation.
In my immunofluorescence research, I successfully stained Vα7.2+ MAIT cells in three

types of paediatric autoimmune liver disease (AILD), AIH type 1, AIH type 2 and PSC, and also in biliary atresia (BA). BA is a chronic and progressive cholangiopathy of infancy and the commonest indication for liver transplantation (LT) in childhood [144, 145, 160]. No known aetiology has been found for either AILD or BA for which there is no known cure except for LT [160, 161]. Of concern, AIH and PSC has a disease recurrence rate of 20-40% post LT which poses ethically challenging questions of whether LT and re-grafting are the best management strategies for these patients [96, 115].

My research confirms the presence of MAIT cells in paediatric liver tissue for the first time. My confocal micrographs clearly show well delineated cell surface Vα7.2 IF staining of intrahepatic MAIT cells in AIH type 1 (Fig. 3a), AIH type 2 and PSC (Fig. 3b) and in biliary atresia (Fig. 3c). Following on from the previous Oo group CD3+, TCR Vα7.2 and CD161 colocalization experiments, staining with CD8+ve and Vα7.2+ antibodies were performed on paediatric liver tissue. Figure. 3d. demonstrates this nicely with CD8+ Vα7.2+ MAIT cells observed amongst the inflammatory infiltrate of CD8+ cells in the liver explant of an AIH type 1 patient. This confocal micrograph shows CD8+ Vα7.2+ MAIT cells to account for <5% of total CD8+ cells. Gargano et al found almost all IF stained MAIT cells were CD8+ lymphocytes but CD8+ MAIT cells only represented <5% of the total CD8+ cells in MS lesions [142]. Low CD8+ Vα7.2+ MAIT cell numbers may be related to low total MAIT cells within the liver tissue as opposed to a low proportion of CD8+ MAIT cells.

Given more time, I would like to have performed CD4 dual staining with Vα7.2 antibodies and triple staining with CD4, CD8 and Vα7.2 to assess for CD4+ Vα7.2+ MAIT cells which are slightly more abundant in the adult liver than in the peripheral circulation and for double positive CD4+ CD8+ Vα7.2+ which are seldom described in adult livers [9, 14, 41].

Additionally, triple staining for CD3, CD161 and Vα7.2 would have strengthened my research on these paediatric livers. I had elected to follow on from the previous IF staining with these antibodies carried out by our group and made the assumption that paediatric liver Vα7.2+ cells would be CD3+ lymphocytes that co-express CD161. Gargano et al has since shown Vα7.2+ CD161+ to represent 90% of all TCR Vα7.2 positive cells in their MAIT cell IF staining of white matter lesions in Multiple sclerosis. Lastly, an MR1-antigen tetramer was sourced but the practicality afforded by using the Vα7.2 antibody for which I had already performed optimisation experiments and had success with IF staining, supported its continual use in my experiments. The Vα7.2 antibody of the same clone, 3C10, and the MR1-antigen tetramer has been shown to have similar co-expression on CD3+ cells by Torre et al [143]. MAIT cell localisation using the MR1-antigen tetramer were reported to be suboptimal and difficult to stain by another group (Pohl et al, unpublished work).

3.5.2 A higher propensity of MAIT cells in the periportal areas of PSC and Biliary atresia paediatric liver explants

MAIT cell distribution within the paediatric liver FFPE sections were next assessed (Fig. 3e). Vα7.2+. MAIT cell numbers were higher in the periportal regions of these liver explant samples compared to the hepatic parenchyma in all four conditions. This was the case in all except for one biliary atresia patient in which Vα7.2+ MAIT cell numbers were similar in both the periportal region (5 cells/mm^2) and the parenchyma (6 cells/mm^2).

MAIT cell frequency from these paediatric liver explants were much lower than MAIT cell frequencies found in the portal tracts of adult donor and diseased liver explants [19]. This finding reflects the overall lower circulating MAIT cell numbers in children compared to

adults with liver disease [63, 64].

The child with PSC had the highest number of Vα7.2+ MAIT cells in the periportal region compared to AIH T1, AIH T2 and biliary atresia, a finding which also reflects that found in adult livers [19, 51, 80]. The predominance of intrahepatic MAIT cells in the periportal areas in both AILD and non-AILD (Biliary atresia) suggests this finding is not disease specific. Indeed, a higher concentration of MAIT cells are described in the portal tracts and fibrotic septae in chronic liver disease in adults of different aetiology [19, 51].

In both the Biliary atresia and PSC liver sections, bile ducts were absent due to the end stage nature of these explants in which ductopenia is established. The periportal presence of MAIT cells in PSC is described from adult studies; data on whether MAIT cells are present in the peribiliary regions in these cholangiopathies is important but unfortunately due to the marked ductopenia in these liver sections, this vital information cannot be captured. The assessment of liver sections from biopsy samples at the various stages of liver disease i.e. at disease onset, during a period of disease stability, and in compensated and decompensated cirrhosis in addition to explant data would be a much better and stronger study model in the investigation of MAIT cell presence in the peribiliary, periportal and parenchymal regions.

I would have liked to have performed Vα7.2+ IF staining on different paediatric PSC liver tissue to confirm/dispute this finding but unfortunately there was a lack of tissue availability as, although PSC often starts in childhood, patients who require transplantation usually do so in adulthood e.g. with decompensated liver failure.

The functional aspect of these MAIT cells by dual staining for granzyme B in TCR Vα7.2+ cells was next assessed. IF staining of interferon gamma (IFNγ) and interleukin-17 (IL-17) on Vα7.2+ MAIT cells was demonstrated by Gargano et al, 2022. In addition to Th1 and

Th17 cytokine profiles, MAIT cells possess cytotoxic potential and can release of granzyme and perforin upon activation [11, 12, 80]. Granzyme B expression by Vα7.2+ MAIT cells were confirmed by my experiments which was most evident in biliary atresia liver tissue (Fig. 3f). This confocal image capture of active MAIT cell cytotoxicity adds to our knowledge of functional flow cytometry research. Had I more time, I would have assessed for co-expression of perforin in the Vα7.2+ MAIT cells of these paediatric livers and performed more cytokine IF staining including IFNγ, TNFα, and IL-17A, assessed the surface expression of chemokine markers, such as the liver homing chemokines CXCR6 and CCR6 and investigate for Toll-like receptors in these innate-like T effector cells [19, 129].

3.5.3 Colocalization and interaction of MAIT cells and Tregs

Regulatory T cells (Tregs) are central in preserving immunotolerance within the liver [152, 162] Complex immune cell dynamics exists to enable this frontline immune organ to detoxify harmful ingested substances such as xenobiotics, microbiota and endotoxins whilst being able to recognize and promote tolerance to ‘harmless’ commensal bacteria and dietary compounds [43, 129].

Treg dysfunction and a breakdown in immunotolerance are thought to underly the pathophysiology of AILD [151, 163]. Human clinical trials are underway to establish the efficacy of Treg therapy in AILD. The AUTUMN trial (Autologous T-regulatory cell tracking after InfUsion in AutoiMmuNe Liver Disease) has established Treg infusion to be safe with no serious adverse effects or infusion reactions. An imbalance between Tregs and T effector cells are central in the immunopathogenesis of AIH [153, 164].

AIH T1 patients with active disease were found to have significantly reduced numbers of FOXP3+ Tregs and a high number of T helper 1 (Th1), Th17 and Th22 cells and higher

levels of their respective inflammatory cytokines in the peripheral blood compared to AIH T1 patients in remission and healthy controls [165]. The portal tracts of liver biopsy samples from newly diagnosed (treatment naïve) adult AIH T1 patients were enriched with MAIT cells and FOXP3+ Tregs [126]. Granzyme B expressing MAIT cells were higher in the peripheral circulation in these patients compared to healthy subjects, suggesting activated cytolysis.

The interactions of these two immune cell types have not been investigated but their enrichment at the portal tracts in newly diagnosed AIH patients signifies their importance. In health, these two dynamically distinct immune cells may work synergistically to combat microbial invasion, particularly at the portal tracts where bacteria can gain entry from either the bile ducts or via translocation into the portal venous system [37, 43].

MAIT cell and Treg colocalization demonstrated in this research is a first; there are no published immunohistochemistry or immunofluorescence experiments assessing the presence of these two cell types together. MAIT cells and Tregs colocalization were mainly found around the portal tracts and periportal areas in paediatric AIH (Fig. 3g) and PSC (Fig. 3h).

The frequency of MAIT cells and Tregs are significantly reduced in patients with PSC [19, 80, 127]. As with AIH, the suppressive capabilities of Tregs in PSC appears impaired compared to healthy controls [166, 167]. Reduced FOXP3 expression in PSC intrahepatic Tregs could be linked to increased interleukin-12 (IL-12) signaling in the inflamed hepatic microenvironment [166, 167]. MAIT cells express IL-12 receptors on its cell surface and can be activated by IL-12 in a cytokine dependent manner [31, 32, 34].

A decrease in Treg immunosuppressive function with reduced FOXP3 expression and increased MAIT cell activation in the presence of IL-12 maybe contributory to the pathology in PSC. The colocalization of MAIT cells and Tregs in paediatric PSC supports the concept of cellular interaction amongst these two central immune cell types in AILD.

The physical interaction and colocalization of MAIT cells and Tregs captured in biliary atresia is exciting and novel (Fig. 3j).. There is no published data or confocal microscopy on MAIT cells in biliary atresia (BA). This new appreciation of immune effector and suppressor cell interaction in BA can potentially add to our understanding and knowledge of this common childhood cholangiopathy of uncertain aetiology.

Cytotoxic and IFNγ producing CD8+ T cells are implicated in BA [147, 168]. BA patients were shown to have lower Treg numbers and higher Th1, Th2 and Th17 subsets in the liver and peripheral circulation [165, 169].

Functionally, Tregs block Th1 activity via the STAT1/IFNγ pathway [169]. MAIT cells possess both Th1 and Th17 cytokine profiles and Tregs can possibly suppress the effector functions of MAIT cells via Th1 inhibition [11, 66, 81].

Th-17 cells were also found to infiltrate the liver in BA and is associated with a poorer prognosis (Hill et al, 2015). IL-17 producing MAIT cells are closely linked with chronic inflammation and fibrosis [60, 78].

Adoptive transfer of Tregs in a BA murine model prevented further biliary inflammation and bile duct obstruction, suggesting Tregs suppresses inflammation in BA [170]. Il-17A producing MAIT cells, aka MAIT17 phenotype, may be responsible for the biliary epithelial damage observed.

To take the project further, I would perform IF staining for proinflammatory cytokines of MAIT cells and TGFβ and IL-10 expression in Tregs in the same BA explant in addition to co-culture functional experiments to further investigate the interaction between MAIT cells and Tregs in biliary atresia.

3.5.4 Cell-in-cell structures in paediatric AILD and biliary atresia

During the course of this research I unexpectedly captured cell-in-cell structures, specifically emperipolesis and enclysis. Emperipolesis, was first defined by Humble et al in 1956, and describes the internalisation and movement of one cell inside another. It originates from Greek and literally translates to ‘inside (em), around (peri) and wander about (polemai)’ [158, 171]. Suicidal emperipolesis further describes the fate of immune cells, and was first observed in the peripheral deletion (extrathymic) of autoreactive CD8+ cells by hepatocytes via lysosomal degradation [154]. This process occurs transiently in normal physiology to

maintain immunotolerance within the liver [155]. It's persistence in autoimmune hepatitis suggests defective T cell clearance [157, 172]. More recently, it has been described in Primary biliary cholangitis (PBC), an autoimmune condition of small intrahepatic bile ducts [158]. In this study, internalised CD8+ cells observed in cholangiocytes appeared to advance BEC apoptosis. Suicidal emperipolesis was concluded to aggravate bile duct injury in PBC. Fig. 3k shows Vα7.2+ MAIT cells within the cytoplasm of BECs in paediatric PSC explant. The internalisation of MAIT cells show that emperipolesis occurs in PSC as observed in AIH and PBC, and maybe a common pathway that leads to bile duct injury in AILD.

Within the same paediatric PSC explant, FOXP3+ Tregs were identified to lie within the cytoplasm of hepatocytes, a phenomenon known as enclysis (Fig. 3l). Enclysis was first described by Davies et al, and refers to the capture and lysis of Tregs by hepatocytes. Hepatocytes were shown to preferentially engulf Tregs; Tregs underwent hepatocyte deletion by lysosomal degradation whereas non-Tregs were observed to exit hepatocytes undamaged [156]. Enclysis was observed to be higher in patients with AIH and is thought to contribute to the loss of tolerance observed in AIH [159]. A FOXP3+ Treg was imaged to be moving towards a hepatocyte in a paediatric AIH type 2 liver explant (Fig. 3m) and in the paediatric PSC liver, cell-to-cell contact between a FOXP3+ Treg and a hepatocyte was captured (Fig. 3n).

Dual staining with CD4 and FOXP3 confirmed them to be CD4+ FOXP3+ Tregs. Enclysis by hepatocytes was observed in the cholangiocytes in an AIH type 1 (Fig. 3o and 3p).

Clear and well defined cell CD4 surface IF staining can be appreciated here along with independent intracellular FOXP3+ IF staining of the same cells.

Treg frequencies were higher in the parenchyma of the biliary cholangiopathies; biliary atresia and PSC compared to AIH T1. Treg numbers were higher in the periportal region of all except one AIH T1 patient. This may reflect the area of active disease with high effector cell activity and subsequent Treg ‘expenditure’ or dysfunction accounting for the low Treg numbers i.e. inflammation is concentrated in the periportal regions in biliary atresia and PSC as opposed to AIH, in which interface hepatitis and parenchymal immune cell infiltration dominates. Results were not shown to be statistically significant.

Emperipolesis in PSC and enclysis in AIH paediatric livers is novel and exciting. These findings lend support to the theory of MAIT cell induced biliary epithelial damage as speculated in adult intrahepatic MAIT cell research. The lower Treg frequency in key areas of active inflammation e.g. periportal region in PSC and the parenchyma of AIH T1 may have resulted from enclysis. If so, then the hepatobiliary cellular deletion of Tregs may be a contributing factor in the pathophysiology of AILD.

Chapter 4. Examining the biological characteristics and functional capabilities of paediatric blood MAIT cells by CyTOF

4.1 Paediatric blood MAIT cell analysis by CyTOF mass cytometry

Mucosal-associated invariant T (MAIT) cells, defined as CD3+ Valpha7.2+ CD161++ T lymphocytes, are central in the immunosurveillance, tissue maintenance and repair at mucosal sites [10-12].

MAIT cells are speculated to protect the biliary epithelium from microbiota, effectively acting as a ‘biliary firewall’ due to their predominant location near the periportal areas in health and in disease [10, 19]. It is now better appreciated that MAIT cells localize to the periportal areas and fibrotic septae in chronic liver disease but are found in higher frequency in the sinusoids and parenchyma in healthy donor livers and in acute liver injury [44, 51, 80]. Both cholangiocytes and hepatocytes can activate MAIT cells in an MR1 dependent manner [18, 19]. Once activated, intrahepatic MAIT cells contribute significantly to the hepatic proinflammatory milieu and can polarize to a MAIT17 profibrogenic phenotype with chronic stimulation [44, 80].

Deep immunophenotyping of MAIT cells by mass cytometry has been reported in patients with inflammatory bowel disease and in other autoimmune conditions but not in autoimmune liver diseases (AILD), a life-long immune mediated liver disease which often presents in childhood [173, 174].

The majority of human immune cell research is adult population based, the function and cell status of which may have important differences compared to their paediatric immune cell counterparts [175, 176]. The findings from this focused examination of paediatric MAIT cell populations and function in children with AILD may offer new insights and further our understanding into their immunopathogenesis.

During my PhD fellowship, in order to characterize the deep immunophenotype of MAIT cells in children with AILD, I designed a MAIT cell specific CyTOF (Cytometry by time of flight) panel consisting of 38 metal-conjugated antibodies against cell surface and intracellular markers. Half of the antibodies used in my CyTOF experiments were purchased from Fluidigm and the rest were custom made. I elected to metal-conjugate and custom make the antibodies myself by learning the technique of purified antibody metal-conjugation. I performed this under the supervision of Dr Naeem Khan (PhD), an expert in mass cytometry research from the department of Clinical Immunology at the Institute of Immunology and Immunotherapy, University of Birmingham. The methodology for the metal-conjugation process, the CyTOF antibody panel and CyTOF experiments are detailed in the methods section.

Once the conjugation process was completed and the antibodies tested and optimized, mass cytometry by CyTOF was performed on the peripheral blood mononuclear cells (PBMCs) of:

a) paediatric patients with autoimmune liver disease (AILD);
    i. Autoimmune hepatitis type 1 (AIH) N=8, median age 14yrs (range 9-14)
    ii. Primary sclerosing cholangitis (PSC) N=8, median age 14yrs (range 12-15)
b) Healthy children (HC, control cohort) N=8, median age 12years (range 5-15)

In brief, PBMC samples were incubated for 4hours with CytoStim prior to investigation by CyTOF. CytoStim is a polyclonal antibody-based reagent that induces T lymphocyte activation via TCR stimulation. For each experiment, a control well containing the patient's PBMCs were incubated for 4hours with culture media only (without treatment) and then subjected to investigation by CyTOF. Two conditions per patient were thus examined; stimulated (CytoStim) and unstimulated (PBMC and culture media only (10% FCS + Penstrep + Glutamine)). These CyTOF prepared paired PBMC samples were then processed using the Helios mass cytometer at the Institute of Translational Medicine. Data analysis was performed using the Cytobank platform. Formal Cytobank training was undertaken by myself (Cytobank training modules; basic and advanced).

The demographics and disease characteristics of the children with autoimmune liver disease whose blood was used in the CyTOF experiments are shown in Table 9. Patients were similar in age at presentation and when the blood were drawn for the experiments. Two-thirds of the PSC patients were male and 2/3 of AIH T1 patients were female and the majority of both were of Caucasian descent. The AIH T1 patients had a range of mild-moderate hepatitis with raised transaminases. Cholestasis was not a marked feature of our PSC cohort but 25% experienced recurrent cholangitis and all of the PSC patients had IBD comorbidity. None of the patients had decompensated cirrhosis/end-stage liver disease.

The AIH cohort was further divided into those AIH patients who were newly diagnosed (Rx Naïve) and the AIH patients on maintenance treatment (and in remission) (AIH on Rx) are shown in Table 10. They were of a similar age when blood was drawn for these experiments but the 'AIH on treatment' subgroup were slightly younger at diagnosis. Three quarters of the newly diagnosed AIH patients were male and 50% were Caucasian

compared to the AIH children on treatment who were all female Caucasian patients. The latter is more representative of characteristics described in the literature for AIH. The newly diagnosed patients had moderate to severe acute hepatitis and higher immunoglobulin G (IgG) in contrast to those patients already on treatment who had stable liver function. All AIH treated patients were on azathioprine and low dose prednisolone (Table 11).

Table 9. CyTOF patient demographics and disease characteristics

	PSC n=8	**AIH n=8**
Current Age (Years)	13 (11-16)	13 (9-16)
Age at diagnosis (Years)	11 (8-16)	10 (7-15)
Sex (% Male)	62.5% (5/8)	37.5% (3/8)
Caucasian	90% (7/8)	75% (6/8)
Labs		
Total Bili (µmol/L)	21 (4-177)	16.5 (3-159)
ALP (IU/L)	360 (208-786)	263.5 (73-437)
GGT (IU/L)	16.5 (7-331)	62.5 (19-108)
ALT (IU/L)	18 (9-237)	360 (25-1463)
AST (IU/L)	25.5 (16-141)	100 (7-1197)
Albumin (g/L)	39 (35-46)	40.5 (33-49)
Total Protein (g/L)		75 (67-84)
PT (sec)	12 (11-13)	13 (11-14)
Platelets ($x10^9$/L)	236 (45-441)	173.5 (60-303)
IgG (g/l)	16.47 (13.91-34.23)	20.31 (9.6-35.63)
Autoantibodies		
ANA	75% (6/8)	87.5% (7/8)
LKM	0% (0/8)	0% (0/8)
SMA	0% (0/7)	12.5% (1/8)
ANCA	12.5%(1/8)	50% (4/8)
Disease severity		
*PELD**	0	4.5 (2.8-6.1)
*MELD***	10 (7-18)	9 (9-22)
PHT	25% (2/8)	3/8
Decompensated cirrhosis	0% (0/8)	0% (0/8)
Cholangitis		
Patients with cholangitis	25% (2/8)	0% (0/8)
Recurrent cholangitis	25% (2/8)	0% (0/8)
Non-adherence		
Non-adherent patients	12.5% (1/8)	12.5% (1/8)
IBD		
Total	100% (8/8)	12.5% (1/8)
Ulcerative colitis	37.5% (3/8)	0% (0/8)
Crohn's disease	37.5% (3/8)	0% (0/8)
Indeterminate	25% (2/8)	12.5% (1/8)

**PELD, Paediatric End-Stage Liver Disease score, a disease severity scoring system for children <12years of age; **MELD, Model for End-stage Liver Disease, a predictor of survival in patients ≥12yrs of age with cirrhosis. PSC: primary sclerosing cholangitis, AIH: autoimmune hepatitis, PHT; portal hypertension, IBD; inflammatory bowel disease.*

Table 10. CyTOF AIH patient subgroup demographics and disease characteristics

	AIH type 1 n=8	
	AIH Rx Naïve n=4	**AIH on Rx n=4**
Current Age (Years)	12 (9-16)	13 (11-15)
Age at diagnosis (Years)	12 (9-15)	9.7 (7.5-13)
Sex (% Male)	75% (3/4)	0% (0/4)
Caucasian	50% (2/4)	100% (4/4)
Labs		
Total Bili (µmol/L)	84.5 (21-159)	9,5 (3-12)
ALP (IU/L)	341 (222-437)	232 (73-315)
GGT (IU/L)	80.5 (46-108)	25 (19-86)
ALT (IU/L)	816.5 (360-1463)	44 (25-95)
AST (IU/L)	1011.5 (119-1197)	38 (7-81)
Albumin (g/L)	37.5 (33-41)	42.5 (37-49)
PT (sec)	12.5 (11-14)	13 (11-13)
Platelets ($x10^9$/L)	239.5 (127-303)	156 (60-199)
IgG (g/l)	28.03 (16.84-35.63)	14.52 (9.6-23.78)
Autoantibodies		
ANA	100% (4/4)	75% (3/4)
LKM	0% (0/4)	0% (0/4)
SM	25% (1/4)	0% (0/4)
ANCA	50% (2/4)	50% (2/4)
Disease severity		
*PELD**	2.8-6.1	0
*MELD***	19-22	9 (9-9)
PHT	0% (0/4)	75% (3/4)
Decompensated cirrhosis	0% (0/4)	0% (0/4)
Cholangitis		
Patients with cholangitis	0% (0/4)	0% (0/4)
Recurrent cholangitis	0% (0/4)	0% (0/4)
Non-adherence		
Non-adherent patients	n/a	25% (1/4)
IBD		
Total	0% (0/4)	25% (1/4)
Ulcerative colitis	0% (0/4)	0% (0/4)
Crohn's disease	0% (0/4)	0% (0/4)
Indeterminate	0% (0/4)	25% (1/4)

**PELD, Paediatric End-Stage Liver Disease score, a disease severity scoring system for children <12years of age; **MELD, Model for End-stage Liver Disease, a predictor of survival in patients ≥12yrs of age with cirrhosis. AIH: autoimmune hepatitis Rx: treatment, PHT; portal hypertension, IBD; inflammatory bowel disease.*

Table 11. Immunosuppression treatment for AIH patients

	AIH on Rx n=4
Immunosuppressant	
Prednisolone*	4
Azathioprine	4
MMF	0
Tacrolimus	0
Sulphasalazine / Mesalazine*	0

AIH; autoimmune hepatitis, Rx; treatment, MMF; Mycophenolate mofetil

4.2 Analysis of CyTOF data

Dimensionality reduction analysis was performed using the tSNE-CUDA (t-distributed Stochastic Neighbor Embedding, Compute Unified Device Architecture) technique on Cytobank. This generated tSNE plots for individual patients; cumulative results per condition will be displayed in box-and-whisker plots for total MAIT cells and MAIT cell subsets, and summary dot plots will display the cumulative results for the AIH subgroups. The AIH cohort consists of autoimmune hepatitis type 1 patients who were newly diagnosed and treatment (Rx) naïve (‘AIH Rx Naïve’ N=4) and those patients who are already on treatment ‘AIH on Rx’ N=4.

Heatmaps generated per condition (AIH, PSC, HC) for total MAIT cells and its subsets will be displayed following on from the cumulative results.

Colours assigned to the conditions are shown in the figure legend; please take note of the conditions as the same colours are used in different graphs due to the colour coding system of the Cytobank platform which cannot be changed. Results of each patient’s cell marker expression level, measured as the median metal intensity (MMI) is displayed. The y-axis scale changes per marker as it reflects the range of MMI expression for individual markers.

4.3 Total MAIT cell and subset frequency

MAIT cells are the most numerous invariant T lymphocyte population in humans [41, 44]. Peripheral blood MAIT cell count is quoted to represent 1-10% of total CD3+ T lymphocytes in adults [41, 177]. Paediatric MAIT cell studies are limited but a reduction in circulating MAIT cell numbers are reported in the majority of conditions and overall, are comparatively lower than in adults [178, 179]. In one study, the MAIT cell composition of total CD3+ cells were reported to average 1.4% from 74 children undergoing diagnostic liver biopsies [63]. These circulating MAIT cells are mainly CD8+ T cells and to a lesser degree, double negative MAIT cells (CD4- CD8-). CD4 + T cells make up only a minority of this subset [9, 14]. A greater proportion of the MAIT CD4+ subset is however described in the human liver [10, 38]

Adult MAIT CD8+ cells mostly express the CD8aa homodimer in contrast to CD8αβ heterodimer of conventional CD3+ T lymphocytes [14, 180]. As the same chemokine-receptor profiles are described for both MAIT CD8 isoforms, they are considered to exhibit similar effector functions. Reduced circulating MAIT cell numbers are consistently reported in all disease conditions including AILD, as well as in infections and malignancy [38, 181]. This disease associated reduction in MAIT cell numbers is speculated to result from activation-induced exhaustion and apoptosis [38, 80, 182].

The peripheral blood MAIT cell frequency was assessed from children with autoimmune hepatitis (AIH), primary sclerosing cholangitis (PSC) and in age-matched healthy children (control cohort). Figure 4a. shows the tSNE plots of TCR Vα7.2+ cells gated on CD3+ lymphocytes from a healthy child, a paediatric patient with AIH and one with PSC; larger areas with darker shading of positive Vα7.2+ clustering is observed in the HC, and less dense clustering of the same regions are observed in the AIH and PSC patients.

The highest frequency of MAIT cells was observed in the HC cohort compared to the AIH and PSC at rest (UNSTIM) and post-stimulated (STIM) (p=0.0004); HC total 'MAIT cells' was 0.97 – 5.61% of total CD3+ cells, followed by children with AIH 0.23 – 2.44% and then PSC 0.08 – 2.71% (Figure 4b). An overall reduction in MAIT cell numbers post-STIM was evident in the HC cohort but the median (central grey bar) and the overall distribution of MAIT cells in the AIH and PSC groups were largely unchanged.

On review of the population subsets, a significant difference in subset distribution was observed amongst the patients' MAIT cells and conventional CD3+ cells. The majority of conventional CD3+ cells in our cohorts were CD4+ cells, with the highest frequency detected in children with PSC (p=0.002), then AIH, followed by healthy children (Figure 4c (i). HC also had the most DN CD3+ cells compared to the disease cohorts (p=0.001). The distribution of CD8a+ CD3+ cells were wider but the median cell count amongst the three cohorts were the same. MAIT cells in our AIH, PSC and HC cohorts consisted mostly of double negative (DN) (CD4- CD8-) cells and to a lesser extent CD8a+ cells. The MAIT CD4+ subset, as observed in adults, is negligible and only appreciated in the HC (Figure 4c (ii). As reflected in the overall MAIT cell frequencies in Figure 4a, HC had the highest count in all three MAIT cell subsets. For ease of interpretation, MAIT cell subset cell counts at rest (UNSTIM) are presented.

4.4 Paediatric MAIT cells express a pro-inflammatory phenotype

MAIT cells share effector cytokine profiles as Th1 and Th17 cells; upon activation MAIT cells upregulate production of interferon gamma (IFNγ) and tumour necrosis factor alpha (TNF-α), and interleukin-17A (IL-17A) and interleukin-22 (IL-22) respectively [28, 38, 80]. They also possess cytotoxic potential being able to degranulate the intracellular cytokines Granzyme B and Perforin on activation [32, 181, 183]. MAIT cells express several transcription factors; T-box expressed in T cells (T-bet, aka T-box transcription factor TBX21) which controls Th1 cells, retinoic acid-related orphan receptor gamma t (RORγt) mediates Th17 cells and the promyelocytic leukemic zinc-finger (PLZF), a transcription factor of natural killer T lymphocytes (NKT), which is believed to give MAIT cells their innate-like properties [8, 38, 181].

These cytokines and their respective transcription factors were included in my MAIT cell CyTOF panel. The results will be discussed here and interpretation of the results will be reviewed in the Discussion Chapter.

Comparison of the difference between CD3+ and MAIT cell expression levels of cytokines, cytolytic markers and their respective transcription factors will be reviewed, followed by the expression of cell activation and exhaustion markers, chemokine and interleukin receptors. Results of the MAIT cell subset expression of the same surface and intracellular markers will then presented, followed by subgroup analysis of the AIH cohort (treatment naïve vs. patients already on treatment).

4.4.1 TNFα and IFNγ, and T-bet expression

To start with, I examined the expression levels of the proinflammatory cytokines TNFα and IFNγ and their transcription factor Tbet in MAIT cells and compared them with expression levels from total CD3+ cells.

Higher post-STIM TNFα level expression is observed in the total MAIT cells from all three cohorts (AIH, PSC and HC) compared to the CD3+ T cells from the same patients (Figure 4d (i)). The children with PSC displayed the highest median metal intensity (MMI) compared to the other two cohorts; both the group median result (grey bar) and the distribution of data is highest in the PSC STIM group ($p<0.0001$). Negligible TNFα levels were observed pre-stimulation (UNSTIM) in all three groups.

In contrast, the highest post-STIM IFNγ responses was observed in the HC MAIT cells followed by the PSC and AIH cohorts ($p=0.0003$). UNSTIM baseline levels of IFNγ were negligible in all three as observed with TNFα expression. Similarly, the highest post-STIM Tbet responses was observed in HC MAIT cells followed by the AIH and then the PSC cohorts ($p=0.0002$). A 'zoomed in' image of CD3+ T cell TNFα and IFNγ expression levels are shown in Figure z; a smaller but similar trend is observed in the CD3+ cells (Figure 4d (ii).

Figure 4d (iii) shows the tSNE plot of the post-STIM TNF-α, IFNγ and Tbet expression compared to its paired negative control (UNSTIM) from a paediatric patient with AIH, one with PSC and a healthy child. The conditions are depicted in the rows. Higher post-STIM expression can be appreciated by the 'red to yellow' clustering observed as depicted by the colour scale bar located on the right side of each tSNE plot.

4.4.2 MAIT17 characteristics

MAIT cells with a predominant Th17 phenotype are termed MAIT17 cells [60, 77, 78]. The upregulation of RORγt and its subsequent release of interleukin-17A (IL-17A) upon activation is described in many chronic inflammatory and autoimmune conditions [78, 184]. As observed with TNF-α, the PSC MAIT cell IL-17A post-STIM response was higher than the AIH and HC cohorts (p=0.005). The MMI range of the IL-17A post-STIM response amongst our cohorts is small but statistically significant (Figure 4e (i)) and greater than described in adult MAIT cell short stimulation experiments; prolongation of stimulation over a 72hour period was required to induce MAIT cell IL-17A response in one study [80]. This difference is of importance when considering the MAIT17 potential of chronic inflammation. There is near to no IL-17A post-STIM response from the CD3+ cells.

Quite different from the other three cytokines, there is no observed or statistical difference in the IL-22 post-STIM response between CD3+ and MAIT cells. A similar distribution of RORγt UNSTIM and post-STIM MMI is seen amongst the CD3+ and MAIT cells, with the largest difference in post-STIM activity observed in the HC CD3+ cells (p=0.01).
The IL-22 post-STIM response differs considerably from those of IFNγ, TNFα and IL-17A; the MAIT cell and CD3+ cell plots are almost identical with unchanged median bars except in the HC CD3+ group. Differences were not found to be statistically significant.

Figure 4e (ii) shows the tSNE plot of the post-STIM IL-17A, IL-22 and RORγt expression compared to its paired negative control (UNSTIM) from a paediatric patient with AIH, one with PSC and a healthy child. The conditions are depicted in the rows. Positive IL-17A post-STIM clustering is less dense but higher expression is noted in these regions of red shading.

4.4.3 MAIT cells cytotoxic activity and GMCSF expression

I observed that both MAIT cells and CD3+ cells from healthy children possess higher post-STIM Granzyme B expression than the AIH and PSC cohorts with statistical significance (Figure 4f). Although the distribution (spread) of MMI differs, the median MMI (grey bar) is similar between the AIH and PSC groups. On review of the PLZF transcription factor expression, MAIT cells from children with AIH and HC had higher expression than that of PSC children. CD3+ PLZF expression from all three groups were similar.
MAIT cells secrete GMCSF as part of its proinflammatory responses [185, 186]. GMCSF secretion has not been described in the paediatric MAIT cell setting.

A higher median MMI post-STIM GMCSF (grey bar) response was observed in the PSC CD3+ and MAIT cells and to a lesser extent in the HC group. A wider distribution of data is observed in the AIH group but the median GMCSF MMI was low. These differences in observation was not statistically significant. This study is the first report of GMCSF expression by circulating MAIT cells in children in health and autoimmune liver disease.

4.4.4 MAIT cell activation and proliferation marker expression

In this section, the CD3+ and MAIT cell expression levels of the cell activation marker CD38, proliferation marker Ki67 and the T cell inhibition and exhaustion markers, programmed cell death protein 1, PD-1 (CD279) and the cytotoxic T-lymphocyte-associated protein 4, CTLA-4 (CD152), are reported.

These markers were chosen as activated MAIT cells from adults are reported to be subject to activation-induced exhaustion with the display of CD38, CD69 and PD-1 and CTLA-4 described [38, 80, 182]. Ki67, a marker of cell division and proliferation, was included to assess and correlate MAIT cell activity with cytokine expression [187, 188].

CD38 post-STIM expression is higher in CD3+ cells compared to total MAIT cells in all three cohorts (Figure 4g). Children with PSC had the highest CD38 expression compared to HC and AIH patients in both cell populations but this reached statistical significance with the PSC MAIT cells (p=0.002). In contrast, there was near to no response in CD3+ Ki67 activity and in the MAIT cells, only the AIH patients demonstrated Ki67 expression (p=0.007). PD-1 expression on the other hand was highest in PSC MAIT cells followed by the HC and AIH cohorts, with almost no PD-1 activity registered in the CD3+ cells. CTLA-4 expression in CD3+ and MAIT cells appear similar with the PSC children displaying the highest CTLA-4 levels compared to AIH and HC.

4.4.5 MAIT cell chemokine receptor expression

Liver and gut homing chemokine receptor expression are reported in adult MAIT cell phenotyping. The liver homing chemokine receptors CCR6 and CXCR6 and to a lesser degree, the gut homing chemokine receptor CCR9 has been described in intrahepatic MAIT cells from diseased (chronic liver disease explants) and normal (donor) livers [19, 133, 189]. In our paediatric cohorts, MAIT cell expression levels of all three chemokine receptors are low. No CXCR6 post-STIM expression was detected in CD3+ cells. In the MAIT cells, CXCR6 expression was mostly observed from the HC group (Figure 4h). MAIT cell CCR6 expression was observed in all 3 cohorts but their median MMI were near to zero. Higher CCR9 expression was observed in the AIH group in both the CD3+ (p=0.007) and MAIT cells, with very little expression observed in the PSC and HC cohorts.

The proinflammatory chemokine receptors CXCR3 and CCR5 were also assessed. The AIH patients' CD3+ and MAIT cells expressed significantly higher CXCR3 levels compared to the PSC and HC cohorts. Patients with AIH had higher CCR5 expression compared to HC and PSC patients (p=0.01).

4.4.6 MAIT cell expression of TNF superfamily proteins

The CD40 ligand or CD40L (CD154) is a member of the tumour necrosis factor (TNF) ligand superfamily expressed mostly by CD4+ cells [190, 191]. CD40L binds to CD40 on the surface of antigen presenting cells such as macrophages and B lymphocytes, potentiating their activation and contributing to the inflammatory milieu. It's upregulation on activated intrahepatic MAIT cell was first described in 2016 [19]. This finding has since been described in peripheral MAIT cell work. The CD40L ligation of CD40 present on cholangiocytes is thought to augment FAS (CD95) dependent biliary cell death [136, 137]. This led to the hypothesis of MAIT cell augmented biliary epithelial damage and disease, such as in biliary conditions like PSC [19].

Indeed, I also observed MAIT cells from our paediatric PSC cohort to have the highest expression of CD40L compared to the AIH and HC cohorts (p=0.04). A similar trend but at lower MMIs was observed in the CD3+ cells (p=0.03). In addition, I examined the expression of CD27 which is a costimulatory molecule of the tumour necrosis factor receptor (TNFR) superfamily that promotes T cell activation and proliferation (Takanori 2019, Starzer 2020).

Greater CD27 expression from our disease cohorts compared to HC can be appreciated in both the CD3+ and MAIT cell populations, with the highest expression observed in the PSC CD3+ cells.

4.4.7 MAIT cell cytokine IL-12 and IL-18 receptor expression

MAIT cells can be activated in a cytokine dependent (MR1 independent) manner due to their cell surface expression of cytokine receptors, in particular interleukin-12 receptor (IL-12r) and IL-18r [31, 32].

Interleukin-12 receptor (IL-12r) expression was most marked in the HC MAIT cells compared to the disease cohorts and were near to none in the CD3+ cells (Figure 4k). In contrast, IL-18r expression was highest in the MAIT cells from children with PSC followed by AIH. The median MMI was lowest in the HC MAIT cells. MAIT cell subset cell surface and intracellular marker expression levels

In this section, the post-STIM MAIT cell subset cell surface and intracellular marker expression levels will be reviewed. A comparison between MAIT CD8a+, MAIT DN (double negative) and MAIT CD4+cells will be made and presented alongside total MAIT cell ('MAIT cells') results. The format and order of the cell markers presented is the same as for total MAIT cell vs. CD3+ cells. The median metal intensity (MMI) expression level of each marker per patient is displayed. The Kruskal Wallis H test with Bonferroni correction is applied for multigroup comparison.

4.4.8 MAIT cell subset TNFα and IFNγ, and T-bet expression

Amongst the MAIT cell subsets, activated (STIM) MAIT CD4+ cells of PSC patients had the highest TNFα expression level (Figure 4l). The TNFα median of the MMI (grey bar) expressed by MAIT DN cells were similar amongst the three cohorts despite a slight difference in distribution, and minimal TNFα expression was observed in the MAIT CD8a+ cells. The subset expression levels combined produces an overview of the results displayed in the total MAIT cells (MAIT cells) which mirrors the trend of MAIT CD4+ cells with PSC MAIT cells displaying the highest TNFα expression. No statistical significance was shown. With IFNγ expression, the highest median MMI were in healthy children in all three MAIT subsets and in the total MAIT cells compared to the AIH and PSC cohorts. Statistical significance was observed for MAIT CD4+ (p=0.02) and CD8+ cells (p=0.02). HC also displayed the highest median MMI for Tbet which was followed by the AIH and then PSC cohorts with statistical significance reached for MAIT CD4+ (p<0.001) and CD8+ cells (p=0.02) and total MAIT cells (p=0.004).

4.4.9 MAIT17 characteristics amongst MAIT cell subsets

The median MMI for IL-17A expression were low and similar amongst all three cohorts in all MAIT subsets despite the slight difference in distribution (Figure 4m). Overall, total MAIT and CD8a+ cells from PSC patients displayed the highest IL-17A median MMI compared to the AIH and HC cohorts with no statistical significance reached. The median MMI for IL-22 were similar amongst all three cohorts in all subsets, with the AIH cohort displaying a marginally higher median MMI in MAIT CD4+ and CD8a+ cells. HC had the highest median MMI for RORγt followed by the PSC and then AIH cohorts in MAIT CD4+, DN and in the overall total MAIT cells. MAIT CD4+ cells from all three cohorts had the highest RORγt expression in terms of distribution and median MMI.

4.4.10 MAIT cell subset cytotoxic activity and GMCSF expression

Granzyme B expression was highest amongst healthy children in all MAIT cell subsets followed by the AIH and then PSC cohorts (Figure 4n). Post-STIM PLZF expression was similar in the subsets of all three cohorts, with slightly lower expression levels observed in MAIT cells from PSC children. The reverse is observed in GMCSF expression in which a higher median MMI is seen in the PSC subsets and overall total MAIT cells.

4.4.11 MAIT cell subset activation and proliferation marker expression

Total MAIT cell and subset expression of the cell activation marker CD38, proliferation marker Ki67 and the cell exhaustion markers PD-1 and CTLA-4 are presented (Figure 4o (i)). The PSC cohort had the highest CD38 median MMI expression followed by the AIH and then HC cohorts with statistical significance shown for MAIT CD8a+ (p=0.03), DN (p=0.01) and in total MAIT cells (p=0.002). Ki67 expression on the other hand was highest in the AIH cohort MAIT CD8+ (p=0.04), DN (p=0.04) and total MAIT cells (p=0.007) but minimal in MAIT CD4+ cells. PD-1 expression was also highest in the PSC cohort compared to HC and the AIH patients in MAIT CD4+, DN and total MAIT cells (ns). The MAIT cell subsets' CTLA-4 expression was similar to PD-1 in which the highest median MMI is observed in PSC MAIT CD4+, DN and reflected in the total MAIT cells (ns).
A zoomed in image with adjusted y-axis scales for each marker is shown in Figure 4o (ii).

4.4.12 MAIT cell subset chemokine receptor expression

CXCR6 expression is minimal in the MAIT cell subsets and overall (Figure 4p). CCR6 expression although low, is observed in all three subsets with comparable median MMIs amongst the disease and healthy cohorts. CCR9 was also minimal but higher median MMI is observed in the AIH cohort MAIT cell subsets and overall.

Outlying results skew the data for CXCR3 and CCR5 (Figure 4q (i); a zoomed in image with a lower y-axis scale is shown in Figure 4q (ii). AIH patients had the highest CXCR3 expression in all subsets, with significance reached for MAIT CD8a+ (p=0.04) and overall, in total MAIT cells (p=0.03). CCR5 expression was also highest in the AIH cohort, with significance shown in MAIT CD4+ (p=0.02), DN (p=0.04) and in total MAIT cells (p=0.01).

4.4.13 MAIT cell subset TNF superfamily protein expression

MAIT CD4+ cells from PSC patients displayed the highest expression of CD40L, followed by the AIH and HC cohorts, a trend which is reflected in the total MAIT cells (Figure 4r (i)). A zoomed in image presented on the right (Figure 4r (ii)) shows PSC MAIT CD8+ cells to express the highest level of CD27 followed by the AIH and then HC cohorts.

4.4.14 MAIT cell subset cytokine receptor IL-12r and IL-18r expression

As seen with the above markers, outlying results compress the data for IL-12r and IL-18r due to the broad y-axis scale. Figure 4s (ii) on the right display the zoomed in results which shows MAIT cell subsets from healthy children had higher IL-12r median MMI expression and distribution compared to the autoimmune cohorts (ns). The reverse is observed in IL-18r expression in which higher median MMIs are seen with PSC and AIH MAIT cell subsets compared to HC (ns).

4.5 AIH treatment Naïve vs. AIH on treatment

The autoimmune hepatitis type 1 (AIH) cohort consists of patients who are treatment (Rx) Naïve (N=4) and those who are already on treatment (N=4). The post-STIM expression levels of surface and intracellular markers between these two AIH subgroups will be reviewed here.

4.5.1 AIH Rx Naïve vs. AIH on Rx - Th1 characteristics

The post-STIM TNFα expression is highest in the AIH Rx Naive MAIT cells compared to the patients already on treatment, 'AIH on Rx' (Figure 4t). Minimal difference in IFNγ expression was detected between subgroups despite the varying median MMI observed. The distribution of Tbet expression was more widespread but minimal difference was observed in the median MMI.

4.5.2 AIH Rx naïve vs. AIH on Rx - MAIT17 characteristics

IL-17A expression was higher in the 'AIH Rx Naïve' MAIT cells (Figure 4u). Statistical significance was reached for IL-22 expression in which higher median MMI was observed in the 'AIH Rx Naïve' subgroup. The same trend was seen with RORγt expression (ns).

4.5.3 AIH Rx Naïve vs. AIH on Rx - cytotoxic activity and GMCSF expression

Higher median MMIs and generally a greater spread of data points was observed in the ‘AIH Rx Naive’ subgroup Granzyme B, PLZF and GMCSF expression (ns) (Figure 4v).

4.5.4 AIH Rx Naïve vs. AIH on Rx - activation and proliferation marker expression

Minimal change in post-STIM expression levels of CD38, Ki67, PD-1 and CTLA-4 were detected in the AIH treatment naïve and treated patients (Figure 4w). Slightly higher Ki67 and PD-1 were observed in the AIH Rx Naïve subgroup.

4.5.5 AIH Rx Naïve vs. AIH on Rx - chemokine receptor expression

AIH Rx Naïve patients were observed to have overall higher post-STIM CXCR6 and CCR9 expression compared to AIH on Rx (ns) (Figure 4x). No change was detected in CCR6 expression. Higher CXCR3 expression was observed in the AIH Rx Naive patients compared to the AIH on Rx (ns) (Figure 4y). Minimal difference was observed in CCR5 expression.

4.5.6 AIH Rx Naïve vs AIH on Rx - TNF superfamily protein expression

Total MAIT cells from AIH Rx Naïve patients had higher median MMIs in their post-STIM CD40L compared to AIH on Rx (ns) (Figure 4z). Expression levels of CD27 were variable amongst the AIH subgroups.

4.5.7 AIH Rx Naïve vs. AIH on Rx - cytokine receptor IL-12r and IL-18r expression

There was almost no expression for IL-12r observed in the MAIT cells in the AIH subgroups except for one ‘AIH on Rx’ patient. IL-18r expression in contrast was observed in both AIH subgroups with ‘AIH Rx Naïve’ patients expressing significantly higher IL-18r MMIs (p=0.03) (Figure 4aa).

4.6 Heatmaps of MAIT cell surface and intracellular marker expression

Heatmaps of the MAIT cell CyTOF analysis are presented here to give an overview of the surface and intracellular marker expressions. Heatmaps of total 'MAIT cells', MAIT cell subsets CD4+, CD8+ and DN, and total CD3+ cells are shown.

Measurements are recorded as the median metal intensity (MMI). The colour scale bar, located below the heatmap, is set to a range of 0 – 50 MMI; yellow= strong positive and black = strong negative. The cell markers are arranged in the columns and the conditions (AIH, PSC, HC STIM vs UNSTIM) are in the rows.

MAIT cells show higher expression levels of most markers with a greater proportion of 'yellow' shading than the patients' CD3+ cells (Figure 4ab).

The heatmap confirms the cell population to be MAIT cells with the high expression of CD3+ Va7.2+ CD161++ in the former, and CD3+ in the latter. MAIT cells display an effector memory phenotype, T_{EM} CD45RO+ CCR7-, in all three cohorts. They display a higher expression of the transcription factors Tbet, RORγt and PLZF and the cytokines TNF-α, IFNγ, GMCSF and Perforin than the CD3+ cells. MAIT cells from the negative controls (UNSTIM) had higher Perforin expression than the treated arm (STIM) in all three cohorts. This is thought to be secondary to insufficient Monensin, the protein transport inhibitor, being added and therefore the release of Perforin post-STIM was not captured. Higher Granzyme B levels from the UNSTIM control is also observed.

In terms of surface marker expression, MAIT cells displayed higher immune checkpoint and cell exhaustion markers of CTLA-4 and PD-1 as well as the cell death receptor CD95 (Fas) than CD3+ cells. MAIT cells also had a higher expression of CD27, a costimulatory molecule of the TNF receptor family and CD40L, a member of the TNF ligand family. Of note, treated MAIT cells (STIM) from the PSC patients displayed higher GMCSF and

CD40L compared to MAIT cells from the AIH and HC cohorts and to CD3+ cells.
In terms of chemokine and cytokine receptors, MAIT cells had higher CCR5, a chemokine receptor of the macrophage inflammatory protein (MIP) 1*α* and 1*β* ligands, particularly in the AIH and HC cohorts. Higher levels of CCR6 were observed in the MAIT cells compared to CD3+ cells. Lastly, IL-18r levels were much higher in MAIT cells compared to CD3+ cells in which IL-18r expression was near to zero. The MMI for surface markers was generally lower post-STIM compared to UNSTIM.
The CD3+ cells had a greater proportion of CD4+ cells and much higher expression of CD38 than total MAIT cells.

On review of the MAIT cell subsets, the MAIT CD4+ cells appear to be central memory in phenotype (T_{CM} cells) with a high expression of CD45R0 and CCR7 (Figure 4ac). Compared to MAIT CD8a+ and DN cells, MAIT CD4+ cells expressed higher levels of the cytokines IL-22 and GMCSF post-STIM, particularly in the PSC and HC cohorts for the latter. MAIT CD4+ cells also expressed higher levels of surface markers compared to MAIT CD8a+ and DN cells; higher CTLA-4, PD-1, CD95 (Fas), as well as higher CD38, CD27, and CD40L.
MAIT CD8a+ and DN cells on the other hand were effector memory in phenotype, (T_{EM}, CD45RO+ CCR7-) and expressed high levels of proinflammatory transcription factors and cytokines; higher Tbet, RORγt and PLZF, and higher TNF-α, IFNγ and Perforin levels. CCR5 and IL-18r were also expressed to a higher degree in MAIT CD8a+ and DN cells, in keeping with their proinflammatory nature.

4.7 Discussion

MAIT cells are the most abundant invariant T cell population in humans, constituting 1-10% of total peripheral blood and 30-40% of intrahepatic T lymphocytes in adults [38, 44]. Their enrichment at mucosal sites like the liver, gastrointestinal tract and lung suggests MAIT cells play an important role in the maintenance of mucosal integrity at these key sites of potential microbial entry [10, 11, 41]

4.7.1 Paediatric MAIT cell subset frequencies

Human MAIT cells are predominantly CD8+ve T cells with an effector memory phenotype (T_{EM}) of CD45RO+ CCR7- [8, 14, 67]. The residual are mainly double negative MAIT cells (CD4- CD8-), with CD4+ cells accounting for only a minority of this invariant population.
In health, total circulating MAIT cells increases steadily from birth to 20-40years of age before numbers start to decline [14, 192, 193]. Although MAIT cells are described to be up to 10% of total circulating CD3+ cells, most population-based studies found MAIT cells to represent 1-5% of total CD3+ cells [41, 92, 181]. There is a noticeable reduction of MAIT cell numbers by 60years of age [13, 192, 193]. MAIT cells were found in the fetal liver, gastrointestinal tract and lung from the second trimester onwards (Leeansyah 2014). These were mostly CD8aa homodimers and double negative (DN) cells and are similar to adult MAIT cell subsets [14, 194]. There are few studies investigating MAIT cell frequency and function in children. Decreased total MAIT cell numbers were reported in children with active infections of tuberculosis (TB), human immunodeficiency virus (HIV), cholera and in helicobacter pylori compared to healthy controls [195-197]. In terms of disease, reduced circulating MAIT cell numbers are reported in children with various conditions including

autoimmune hepatitis [64, 178, 196, 198].

In adults, circulating MAIT cell numbers are depleted in almost all conditions, including autoimmune diseases, viral and bacterial infections, and malignancy [12, 38, 181]. Circulating MAIT cell numbers are reduced in many chronic liver diseases aside from AILD and these include non-alcoholic fatty liver disease (NAFLD), viral hepatitis, and alcoholic hepatitis [19, 51, 80].

In our three cohorts, healthy children (HC) had the highest percentage of MAIT cells (0.97 – 5.61% of total CD3+ cells) followed by children with autoimmune hepatitis (AIH) (0.23 – 2.44%) and Primary sclerosing cholangitis (PSC) (0.08 – 2.71%) which is reflective of adult AILD studies. However, the post-STIM MAIT cell frequency was largely unchanged in AIH and PSC children compared to HC which saw a marked reduction. This differs from adults with AILD in which a significant reduction in MAIT cell numbers are speculated to result from activation-induced cell death [80, 81, 143].

MAIT cell subsets in all three cohorts were mostly DN and to a lesser extent CD8a+ cells and this contrasts with adult studies in which the majority of MAIT cells are CD8a+ cells. There is little difference in functionality reported between DN and CD8a+ MAIT cells in adults [14, 41, 177]. Subset frequencies were unaltered for MAIT DN and CD8a+ cells but a rise in the post-STIM MAIT CD4+ cells in the AIH and PSC children were observed. This is of interest as the MAIT CD4+ subset, although a minor population, differs in function in adults [13, 14]. Higher MAIT CD4+ cells were also reported in a study of children with Rheumatoid arthritis who were in remission compared to those with acute disease [199]. A quiescence of inflammatory activity as observed in disease remission may account for this

finding but on separating the AIH treatment naïve and the AIH treated patients, post-STIM MAIT CD4+ cell counts were increased in both AIH subgroups. This biological difference in MAIT CD4+ cell numbers and activity require further investigation to decipher the role of MAIT CD4+ cells in disease.

4.7.2 Paediatric MAIT cell IFNγ and TNF-α, and Tbet expression

Post-STIM TNFα production was higher in total MAIT cells compared to their total CD3+ counterparts. MAIT cells from children with PSC displayed the greatest TNFα production followed by healthy children (HC) and then AIH. Interestingly, compared to their total CD3+ T cells, MAIT cells from PSC children had a 40xfold higher TNFα production and MAIT cells from HC and AIH children were 20xfold higher. The highest post-STIM response was observed in the MAIT CD4+ cells, followed by MAIT DN and CD8a+ cells.
A reduction in activated MAIT cell TNFα production is reported in most studies and is in line with the concept of activation-induced cell exhaustion and dysfunction. Recent studies have contradicted this finding, with reports of unchanged or higher TNFα expression in activated MAIT cells [200, 201]. One paediatric study observed a 10xfold increase in TNFα production by MAIT cells in infants infected with mycobacterium compared to neonates [202].

Post-STIM total MAIT cell IFNγ expression was 20xfold higher than total CD3+ cells. The highest post-STIM total and MAIT cell subset IFNγ production was from HC followed by PSC and then the AIH group. This IFNγ expression impairment found in our AIH and PSC children mirrors that in adult AILD. Defective MAIT cell IFNγ production is reported in

various adult conditions including chronic liver disease [19, 80, 203]. Böttcher et al showed not only a reduction in blood MAIT cell frequency in adult AILD but repetitive cytokine stimulation led to a reduction in MAIT IFNγ and Tbet expression. Impaired IFNγ secretion from AILD intrahepatic MAIT cells were also shown along with a reduction in numbers [80]. MAIT cells from Rheumatoid arthritis and Systemic Lupus Erythematosis (SLE) patients had impaired IFNγ production as well as a reduction in cell numbers [204, 205]. No functional MAIT cell IFNγ data from children with AILD is reported in the literature.

Post-STIM Tbet expression was upregulated, most prominently in the HC, followed by the AIH and then PSC groups. Similar but much lower post-STIM Tbet expression was observed in the CD3+ cells from the same patients. Upregulated blood MAIT cell Tbet expression is described in infections [206, 207]. Coakley et al found patients with sepsis had a diminished Tbet response compared to those with infection without sepsis [206]. This suggests that the presence of disease and its severity impacts on the MAIT cell Tbet response, as observed in our AILD patients, in the blood MAIT cells from adults with AILD and in the septic patients reported by Coakley et al.

Interestingly, no difference was observed between the AIH treatment naïve (disease presentation) and treated children for TNF-α, IFNγ or Tbet expression. This suggests the pathways leading to their release i.e. preserved TNFα activity but IFNγ dysfunction, are affected as early on as childhood disease presentation.

The TNFα response from MAIT cells in children with PSC is much more pronounced compared to their Tbet response. Other pathways leading to MAIT cell TNFα secretion may be activated such as the tumour necrosis factor (TNF) superfamily which will be discussed further on in this chapter.

4.7.3 MAIT cell IL-17A and IL-22, and RORγt expression

Interleukin-17 (IL-17) producing MAIT cells, the so called MAIT17 phenotype is linked to many chronic inflammatory conditions including inflammatory bowel disease, rheumatoid arthritis, psoriasis and multiple sclerosis in adults and children [78, 184].
IL-17A is a chronic inflammatory cytokine which potentiates hepatic stellate cells/hepatic myofibroblasts proliferation in chronic liver disease [51, 80]. In AILD, Böttcher et al described increased Il-17 production and RORγt expression with chronic IL-12 stimulation. Furthermore, in MAIT- hepatic stellate cell (HSC) co-culture experiments, HSC proliferation was found to be partly IL-17 dependent. These findings were supported by Hedge et al who showed increased proliferation of hepatic fibrogenic cells when co-cultured with MAIT cells also in a cell-to-cell contact fashion. Here, hepatic fibroblast activity was blunted by MR1 blockade suggesting activation to be MR1 dependent. Moreover, higher MAIT IL-17 production was found in diseased livers (non-alcoholic steatohepatitis (NASH) and alcoholic hepatitis) [51]. Both Böttcher and Hedge concluded intrahepatic IL-17 producing MAIT cells to be profibrogenic. Double negative (DN) MAIT cells are reported to have the highest IL-17 production which is of importance as our patient and HC cohorts were found to have mainly DN blood MAIT cells [194, 208].

In our patients, IL-17A production was minimal in the CD3+ cells but a post-STIM IL-17A response was observed in the MAIT cells of all three groups, being most marked in the PSC, followed by the HC and then AIH group. On MAIT cell subset analysis, the post-STIM response was highest in the MAIT CD4+ and CD8a+ cells in PSC patients and in MAIT CD4+ cells in the HC. IL-17A expression was lowest in the AIH cohort. The MMI range is

low compared to IFNγ and TNFα expression but IL-17A production was evident in this short stimulation experiment; MAIT cell IL-17A production is generally low or absent in short stimulation assays, with increasing IL-17A activity reported in prolonged/chronic stimulation [80, 135]. The MAIT IL-17A response from our PSC patients and in the HC suggests early activation potential in these children which differs from the chronic stimulation required to elicit an IL-17A response in adults with AILD.

The RORγt post-STIM response in contrast was similar between the total CD3+ and MAIT cells. Higher post-STIM RORγt activity was observed in the HC and PSC cohorts in both cell populations but not in AIH. Only a marginal increase in post-STIM RORγt was observed in the MAIT CD8a+ cells of both the AIH treatment naive and treated children.

RORγt is the transcription factor which regulates IL-17 production [80, 209]. Upregulation in both as observed in the activated MAIT cells from our PSC patients and the HC demonstrates this relationship. The lack of IL-17A activity in the AIH children who also lack RORγt expression again highlights RORγt regulation of IL-17A production.
These findings suggests the RORγt - IL-17A pathway is preserved in the MAIT cells from children with PSC, as observed in healthy children (HC). This is in contrast to the MAIT cells from children with AIH in which either the pathway is disrupted or chronic stimulation is required to elicit a response as observed in adults with AILD.

Impaired IFNγ but preserved IL-17A activity in the MAIT cells of particularly children with PSC suggests a switch from a MAIT1 to MAIT17 phenotype. A higher ratio of MAIT17 to MAIT1 cells were described in patients with acute graft versus host disease (aGVHD) [210]. MAIT17 cells were also higher in sickle cell disease children compared to healthy controls

but no difference was observed in MAIT1 cells [77]. These findings along with those described by Böttcher et al, in which repetitive stimulation of blood MAIT cells decreased IFNγ and Tbet expression and paradoxically increased IL-17 and RORγt expression supports the theory of MAIT cell plasticity and a switch from an acute inflammatory MAIT1 to a chronic inflammatory and profibrogenic MAIT17 phenotype.

MAIT cell secretion of interleukin-22 (IL-22) is also governed by the transcription factor RORγt [28, 211]. Overall, IL-22 MAIT cell activity appears reduced in the children with AILD compared to the healthy cohort. Notably, in contrast to the absence of IL-17A activity, children with newly diagnosed AIH (treatment naïve) had greater IL-22 expression compared to children already on treatment. IL-22 is a member of the IL-10 cytokine superfamily and has an important anti-inflammatory role and tissue repair [44, 212]. In liver disease, upregulation of IL-22 has dampens hepatic stellate cell activity, reducing fibrosis [44, 213]. IL-22 is therefore hepatoprotective and anti-fibrotic [213, 214].
Our findings suggests both MAIT and CD3+ cells from children with AILD and in HC have anti-inflammatory and tissue reparative properties by their secretion of IL-22 at steady state, and this secretion is upregulated, particularly in the healthy children, upon stimulation. Furthermore, MAIT cells from children with newly diagnosed AIH have greater anti-inflammatory and tissue repair potential compared to those on treatment, reflecting the homeostatic and regenerative role of MAIT cells in acute disease onset.

4.7.4 MAIT cell cytotoxic activity

MAIT cells possess an innate-like ability to rapidly respond to virus infected cells with the release of granzyme and perforin proteins . MAIT cells express the transcription factor PLZF (promyelocytic leukemia zinc-finger) which is a known transcriptional regulator of iNKT cells [38]. High expression of PLZF drives MAIT cell maturation and is directly related to their innate-like capacity [38, 215].

PLZF expression is generally higher in MAIT cells compared to total CD3+ cells in our three cohorts. The PSC children had much lower PLZF expression compared to the AIH and HC. This trend is reflected in the MAIT cell subsets. Similarly, post-STIM total and MAIT cell subset granzyme expression is lowest in the PSC cohort and highest in the HC, a trend reflected in the CD3+ cells. AIH treatment naïve children had higher PLZF expression and granzyme production than those on treatment.

A variable response in granzyme expression is in hepatitis C (HCV) and hepatitis B (HBV) infection, with lower levels observed in severe disease [33, 216]. In hepatitis delta (HDV) infection, impaired cytolytic function was found in PLZF low MAIT cells [217]. Moreover, granzyme B expression is inversely correlated with the degree of liver fibrosis [80]

Decreased granzyme B release and PLZF transcription factor activity is observed in the MAIT cells from our children with AILD compared to healthy children. MAIT cells from the newly diagnosed AIH patients had preserved cytolytic function compared to those on treatment.

In addition to their cytolytic potential, MAIT cells also secrete GMCSF (granulocyte-macrophage colony-stimulating factor), a proinflammatory cytokine and white cell growth factor [185, 186]. Almost a reverse trend to granzyme B and PLZF is observed with GMCSF expression in our cohorts; PSC patients had the highest MAIT GMCSF production followed by the HC and AIH cohorts. Interestingly, amongst the subsets, CD8+ MAIT cells from

children with AIH had similar GMCSF expression to the PSC patients. Moreover, there was no GMCSF activity observed in the treated AIH children.

A recent study found MAIT cell activation to be a significant predictor of morbidity and mortality in COVID-19 patients and elevated levels of GMCSF were identified amongst the significant proinflammatory cytokines [186]. Preserved granzyme B, PLZF and GMCSF activity are observed in the AIH treatment naïve patients compared to treated patients. This reflects the heightened proinflammatory state of MAIT cells in newly diagnosed AIH. Dampened activity in the treated AIH patients may however reflect disease quiescence as these patients are in remission or it may reflect the immunosuppressive drug response. Higher MAIT cell GMCSF but lower granzyme B and PLZF expression suggests preserved colony-stimulating and growth factor capabilities but dysfunctional cytolysis in our PSC cohort.

Taken together, blood MAIT cells from children with PSC demonstrate pronounced TNF-α, IL-17A and GMCSF activity compared to healthy children. In addition, they have defective IFNγ production and cytolysis in granzyme B and PLZF expression [31, 32, 38]. This MAIT cell functional impairment may be of clinical significance in the immunopathogenesis of PSC.

4.7.5 MAIT cell and liver homing chemokine expression

The MAIT cell research from our group highlighted the increased expression of the chemokine receptors CXCR6 and CCR6 on intrahepatic MAIT cells from both diseased and donor livers [19]. Other investigators have also reported a higher expression of these liver-homing chemokine receptors in intrahepatic MAIT cells from different chronic liver disease

states [218, 219]. Liver homing chemokine expression enables immune cells to migrate to regions of inflammation within the liver sinusoidal and peribiliary regions in response to their respective ligands, CXCL16 and CCL20 [19, 219].

Total CD3+ and MAIT cell expression of CCR6 and CXCR6 was relatively low, being slightly higher in the HC and AIH cohorts. AIH treatment naïve patients had a higher MAIT CXCR6 expression compared to treated patients whereas CCR6 levels were similar, as was CCR9. Interestingly, AIH children had the highest expression of the gut homing chemokine receptor CCR9 in both the MAIT and CD3+ cell populations. This was reflected in the MAIT cell subsets. Increased CCR9 expression was observed in the MAIT CD8a+ subset in AIH and PSC. MAIT cells from the PSC group expressed higher levels of CCR6 than CXCR6.

The importance of CCR9 in liver disease is increasingly being studied [39, 220]. CCR9+ immune cells have been linked with hepatic stellate cell proliferation in murine models and impaired CCR9/CCL25 signaling has been reported in NASH [39, 210]. Aberrant expression of gut homing molecules resulting in liver recruitment of gut derived immune cells is postulated to occur in PSC but is now believed to be a feature of many chronic liver diseases [133]. The finding of upregulated CCR9 expression in our paediatric AIH as well as in the PSC cohort supports this finding.

MAIT cells with a Th1 effector memory phenotype express high levels of the inflammatory chemokine receptors CXCR3 and CCR5, and recruit to areas of inflammation [87, 221]. MAIT and CD3+ cells from the children with AIH had the highest CXCR3 and CCR5 expression compared to the PSC and HC cohorts; no difference was observed in the treatment naïve and treated children. This was reflected in the MAIT cell subsets. PSC

MAIT CD8a+ cells displayed higher expression of CXCR3 and CCR5 compared to MAIT CD4+ and DN cells, which reflects the heightened inflammatory homing abilities of cytotoxic CD8 cells.

4.7.6 MAIT cell activation and exhaustion status

Stimulated blood and intrahepatic MAIT cells are described to be in an activation-induced (CD69+, CD38+), cell exhausted (PD1+, CTLA-4+) state with impaired function (defective IFNγ and TNFα secretion) [80, 182]. Other studies reported unchanged PD1 expression in blood MAIT cells from patients with decompensated liver disease compared to patients with compensated liver disease and healthy subjects [222].

In our cohorts, post-STIM total CD3+ cells had higher CD38 expression compared to the MAIT cells. The reverse was observed with PD-1 expression, which was negligible in the CD3+ but highest in the PSC MAIT cells. CD38 expression was observed however, and was also highest in the PSC MAIT cells compared to AIH and HC.

CTLA-4 expression was observed in both MAIT and total CD3+ cells and was highest in the PSC group overall. MAIT CD4+ cells had the highest CTLA-4 expression which is consistent with conventional CD4+ cells.

The proliferative marker Ki67 was also examined; post-STIM MAIT cells and their subsets from the AIH group expressed Ki67 but with no expression observed in the PSC or HC cohorts. The AIH treatment naïve and treated patients had similar Ki67 expression levels.

Taken together, MAIT cells from the children with PSC were of an activated and cell exhausted state. MAIT cells from the AIH children displayed less activation and cell exhaustion but greater proliferative activity with no difference observed between newly

diagnosed and patients already on treatment.

4.7.7 MAIT cell TNF superfamily expression

CD40L is a costimulatory molecule belonging to the tumour necrosis factor ligand (TNFL) superfamily. It is chiefly expressed on activated CD4+ cells and regulates the immune response by augmenting macrophage and B lymphocyte activation. Our group described the upregulation of CD40L surface expression on blood MAIT cells from adult patients with chronic liver disease following antigen presentation by cholangiocytes [19].

Activated MAIT cell CD40L upregulation has since been demonstrated by other researchers [223, 224]. Humphreys et al had shown prior augmentation with CD40 was necessary for CD95 (FAS) dependent BEC cell death [137]. Functional deficiency of CD40L (CD154), the ligand for CD40, predisposes to the development of cholangiocarcinoma due to failure of apoptosis [225]. The surface expression of CD40L on immune cells are speculated to induce BEC apoptosis via the CD40-CD40L interaction and augmentation of FAS dependent cell death [19].

Post-STIM MAIT cell CD40L expression was highest in the PSC cohort followed by AIH and HC. PSC MAIT CD4+ cells had the highest CD40L expression compared to MAIT CD8+ and DN cells. Among the children with AIH, treatment naïve patients had slightly higher expression than treated patients.

MAIT cell CD40L expression induces dendritic cell maturation, increasing antigen presentation by upregulating costimulatory molecules and activation of CD8+ cytotoxic lymphocytes [190, 191]. The predominant location of MAIT cells in the biliary and periportal regions in chronic liver disease, combined with the finding of higher CD40L expression on MAIT cells in our PSC cohort, further supports MAIT cell induced biliary inflammation and epithelial damage.

CD27 is a costimulatory molecule of the tumour necrosis factor receptor (TNFR) superfamily [226]. It has an important role in clonal T cell expansion, promoting Th1 and cytotoxic T cell function [226, 227]. CD3+ CD27 expression was slightly greater than the MAIT cells in all three cohorts with PSC patients displaying the highest expression, followed by AIH and HC. MAIT cell subset CD27 expression followed the same trend, being highest in the PSC CD8+ cells. Amongst the AIH children, the treatment naïve generally had higher CD27 expression compared to treated patients. Findings suggests the TNFR superfamily pathway are implicated in the activation and function of MAIT cells from children with PSC, and to an extent, AIH treatment naïve children.

4.7.8 MAIT cell IL-12r and IL-18r expression

MAIT cells can be activated in a cytokine dependent manner by cytokine receptors on their cell surface [31, 32]. Optimal MAIT cell activation by MR1 triggering is achieved by cytokine co-stimulation, namely by interleukin-12 (IL-12) and IL-18 [33, 44]. Repetitive stimulation with IL-12 induced an IL-17 augmented profibrotic response [19].

MAIT cells from our PSC patients expressed the highest level of IL-18r, followed by the AIH and then the HC cohorts. In contrast, IL-12r, except for a few outliers were minimally expressed by the AIH and PSC compared to the healthy children. Both IL-18r and IL-12r were negligible in the CD3+ cells. On review of the subsets, PSC MAIT CD8a+ and DN had the highest expression of IL-18r followed by the AIH and then HC cohorts. AIH treatment naïve patients had significantly higher IL-18r expression than treated patients, whereas IL-12r expression was minimal. These findings show cytotoxic MAIT cells from children with PSC and MAIT cells from newly diagnosed AIH patients to express the highest IL-18

cytokine receptors compared to healthy children.

In conclusion, the results from my CyTOF research has highlighted similarities but also significant differences between MAIT cells in children with AILD compared to adult AILD and compared to healthy age matched children.

The greatest differences were observed in the MAIT cells from children with PSC which displayed enhanced TNF-α, IL-17A and GMCSF activity compared to healthy children. Impaired IFNγ production and dysfunctional cytolysis was observed in these PSC MAIT cells and mirrors that described in adult AILD. Impaired IFNγ but preserved IL-17A activity following relatively short stimulation suggests a switch from a MAIT1 to a profibrotic MAIT17 phenotype early on in the disease course of these children.

PSC MAIT cell TNFα secretion was much more pronounced than Tbet upregulation and the finding of high TNFL (CD40L) and TNFR (CD27) superfamily expression suggests TNF superfamily pathway activation may be the main driver in TNFα activity in this invariant cell population. The prevalence of MAIT cells in the biliary and periportal regions in PSC, combined with their higher CD40L expression lends support to the theory of MAIT cell induced biliary inflammation and epithelial damage. Lastly, although MAIT cells from children with AILD were of an activated and cell exhausted state and thus reflective of adult AILD, preserved MAIT cell frequency post-activation differs remarkably from adult studies. These clear cell survival and functional differences between MAIT cells in children with AILD compared adult AILD and compared to age-matched healthy children may be of crucial importance in the pathogenesis of this lifelong condition. Treatment in PSC lack efficacy and the only cure at present is liver transplantation which has a high disease recurrence rate. Further investigation into these differences may lead to novel targeted therapy development in this unresponsive progressive autoimmune cholangiopathy.

Chapter 5. Functional role of MAIT cells in autoimmune biliary disease in children and adults

5.1 MAIT cells and the liver

Portal venous blood imports a large amount of antigenic dietary compounds and commensal bacteria to the liver [37, 43]. Enrichment of effector immune cells within the liver such as mucosal-associated invariant T (MAIT) cells, enables immunosurveillance and action against potential pathogenic bacterial breaches [19, 150, 162].

In the adult human liver, MAIT cells are located around the bile ducts in the peribiliary and portal regions of explanted livers from patients with end-stage liver disease [19, 80]. Portal tract MAIT cell frequency were highest in explanted Primary Sclerosing cholangitis (PSC) livers compared to donor livers and other diseased liver explants [19]

MAIT cells were further shown to be located not just at the portal areas but also within the fibrous septae in explanted diseased livers including autoimmune (PSC, AIH, and PBC) [51, 80]. In contrast, MAIT cells in healthy donor livers and in acute liver injury mostly localized to sinusoids and the parenchyma [18, 19, 51].

Liver MAIT cells are speculated to be protective in health but their propensity and activity in the peribiliary and portal areas likely contributes to the biliary epithelial damage observed in the inflamed liver and diseased states [19, 44, 80].

Böttcher *et al* demonstrated reduced IFNγ expression following repetitive stimulation with interleukin 12 (Il-12) and IL-18 which led to higher MAIT cell expression of the cell death receptor and cell exhaustion markers PD-1 and TIM-3 respectively. Importantly, repetitive stimulation with IL-12 induced higher MAIT cell expression of IL-17A from patients with autoimmune liver disease (AILD) and in healthy controls. IL-17 is a cytokine of chronic inflammation and the upregulation of the Th17 profile in association with impaired Th1 cytokine function is frequently described in chronic inflammatory states [80].

Böttcher et al and Hedge et al separately demonstrated the profibrogenic potential of MAIT cells cocultured with HSC/hepatic myofibroblasts which was partially reversed with IL-17A and MR1 blockade respectively. Both studies showed MAIT cell enhanced hepatic myofibroblast proliferation to be cell-to-cell contact dependent [51, 80].

Hedge et al further demonstrated MR1 knockout mice to have less hepatic αSMA and Sirius red staining but MATI cell transgenic mice had enhanced staining compared to wild type mice, thus supporting the profibrotic potential of MAIT cells [51]. Chronic MAIT cell activation therefore drives liver fibrosis in chronic liver diseases like AILD.

5.2 MAIT cell activation via ‘non-classical’ antigen presentation by liver dendritic cells

Dendritic cells (DC) are classical antigen presenting cells and are considered the most effective at T lymphocyte activation [228, 229]. There are two main subtypes of dendritic cells: myeloid dendritic cells (mDC) and plasmacytoid dendritic cells (pDCs). mDCs are also termed conventional DCs Type 1 and 2 (cDC1, cDC2) [228, 229]. These DC subsets are

found in the human liver; mDCs are reportedly located around the portal tracts whereas pDCs are mostly found in the parenchyma [230] The majority of hepatic DCs are mDCs [231].

Hepatic DCs are tolerogenic and induces T lymphocyte hypo-responsiveness; they produce the immunosuppressive cytokines IL-4 and IL-10, have a low expression of costimulatory molecules (CD80, CD86), MHC II and a high expression of inhibitory receptors like PD-ligand 1 and indoleamine dioxygenase (IDO) [230, 232]. Liver MAIT cell activation by liver-derived monocytes, B lymphocytes and cholangiocytes were demonstrated in previous research from our group. Hepatocytes, liver sinusoidal endothelial cells (LSEC) and HSC has since been shown to also activate MAIT cells in a MR1-dependent manner. However, dendritic cell induced human liver MAIT cell activation has not been shown. In this chapter, I present my results of *E.coli* primed liver DCs cocultured with liver MAIT cells from the same liver, which led to MAIT cell proinflammatory cytokine secretion and proliferation.

5.2.1 Liver MAIT cell co-cultured with *E.coli* primed liver dendritic cells

In brief, viable liver derived CD3+ lymphocytes and dendritic cell (DC) subsets from the same human livers were cell sorted using the BD FACSAria Fusion cell sorter at the Institute of Biomedical Research. Cell sorted CD3+ T lymphocytes were co-cultured with *E.coli* primed liver DC subsets; mDCs (CD11c+ HLA DR+) and pDCs (CD123+ HLA DR+ CD11c-). MAIT cell specific antibody panels were applied to stain for intracellular and surface markers from the liver derived CD3+ T lymphocytes following the coculture

experiments. Samples were processed using the BD LSR Fortessa X-20 sixteen colour flow cytometer. Analysis of the results were performed using FlowJo V10 and GraphPad Prism 9.0. Figure 5a and Figure 5b shows the gating strategies used to isolate MAIT cells and DCs respectively.

Liver MAIT cell expression of IFNγ, CD107a (degranulation marker) and Ki67 (cell proliferation marker) were measured. The human monocyte cell line, THP-1 cells, sourced from the European Collection of Authenticated Cell cultures (ECACC), Public Health England, were cultured and used as a positive control in these experiments i.e. monocyte antigen presentation; *E.coli* primed THP-1 cells were cocultured with MAIT cells in parallel with the DC and MAIT coculture experiments.

In Figure 5c, the interferon gamma (IFNγ) response of MAIT cells (CD3+ Vα 7.2+ CD161++) gated from isolated lymphocytes of an explanted human PSC liver is shown; IFNγ expression increases from 13.3% to 33.3% in the presence of antigen presentation by liver dendritic cells which have been incubated with *E.coli* for a 12hour period. This is a 2.5 fold increase in liver MAIT cell IFNγ expression compared to its paired negative control (without *E.coli*). A higher response is observed in the positive control of the experiment when THP-1 cells are used as antigen presenting cells (monocyte lineage); IFNγ expression increased from 3.42% to 22.7%, giving it a 6.5 fold upregulation of IFNγ. From this experiment, I have demonstrated that *E.coli* primed liver dendritic cells can activate liver MAIT cells from the same liver. The IFNγ response is less than that of its THP-1 positive control. This finding supports the well described post-activation hypo-responsiveness of T lymphocytes induced by dendritic cell antigen presentation in the liver.

This trend however was not observed in repeated experiments in which the post-activation IFNγ response of MAIT cells by antigen presentation with DCs were similar to that elicited by THP-1 cells in PSC (N=3), AIH (N=2) and Donor livers (N=3) (Figure 5d). Experiment numbers are low and more experiments need to be performed to assess whether a significant difference in MAIT cell response exists between DC and monocyte (THP-1) antigen presentation. Limiting factors and further discussion will be analyzed in the Chapter Discussion of this section.

CD107a is a marker used in degranulation assays. It is a lysosomal associated membrane glycoprotein also referred to as LAMP-1 that surrounds granzymes and perforin within the cytoplasm of cytotoxic cells [233, 234]. Once these lytic proteins are released from the cells (degranulation), CD107a becomes incorporated into the cell surface. Therefore an upregulation of surface CD107a would indicate degranulation (of granzymes and perforin) to have occurred [233, 234]. In the MAIT cell-DC coculture experiment from the explanted PSC liver of Figure 5c, MAIT cell CD107a expression increased from 5.88% to 10.6%. This is a 2 fold increase in the liver MAIT cell CD107a response compared to its negative control (without *E.coli*) (Figure 5e). A higher response is also observed in the positive control arm with THP-1 cells in which a 10 fold increase is observed; CD107a increases from 1.71% to 18.2%.

Similar post-activation MAIT cell CD107a responses were observed in repeated experiments; PSC (N=2), AIH (N=2) and Donor livers (N=2) (Figure 5f); CD107a upregulation has been elicited in MAIT cells activated by DC and THP-1 antigen presentation.

Ki67, also known as MKI67, is a protein detected within the nucleus of actively dividing cells and is widely used as a marker of cell proliferation [187, 188]. Liver MAIT cell activation was associated with active cellular proliferation in our MAIT cell *E.coli* primed DC coculture in which a 2 fold rise of 14.7% to 31.8% is observed. This again is less than that of the positive control arm of *E.coli* primed THP-1 cells in which a 5 fold rise from 2.56% to 13.6% is seen (Figure 5g).

The MAIT cell Ki67 response was quite variable amongst the repeated experiments with autoimmune and donor livers; PSC N=3, AIH N=2 and Donor livers N=3 (Figure 5h). The degree (difference in %) of response observed in the PSC livers is less by DC antigen presentation compared to the THP-1 cells. The small numbers again make interpretation difficult especially with the outlying high response observed in the AIH liver by DC antigen presentation and the high response of the donor liver in the THP-1 positive control. It can only be interpreted that a higher post-activation MAIT cell Ki67 expression was observed in all three liver types.

Next, an assessment of whether the functional (cytokine) response observed in the LI-MAIT cells were MR1 dependent was carried out. Three treatment arms were set; LI-MAIT cells from an explanted PSC liver were a) cocultured with *E.coli* pre-treated LI-DC (from the same liver) and the response was compared to two other experimental conditions, b) untreated (without *E.coli*) and c) *E.coli* pre-treated LI-DC (from the same liver) with MR1 blockade. A reduction in expression of IFNγ, TNFα and CD107a degranulation was observed in the wells treated with anti-MR1 antibody in the LI-MAIT-DC coculture and in the positive control with THP-1 cells.

5.3 MAIT cell activation via ‘non-professional’ antigen presentation by cholangiocytes

Activated MAIT cells are potent producers of IFNy and TNFα and may account for a significant proportion of these proinflammatory cytokines within the liver, particularly in the peribiliary and portal regions [11, 12, 38]. As described, our group previously demonstrated the ability of cholangiocytes to act as ‘‘non-professional” antigen presenting cells to MAIT cells following exposure to *E. coli* by activating MAIT cells in a MR1- dependent manner [19]

Importantly, MAIT cell CD40L (CD154) expression were upregulated following BEC activation [19]. BECs in the diseased and normal liver are sensitive to CD40 augmented Fas dependent cell death [137, 225]. This BEC-MAIT cell interaction may induce CD40-Fas mediated BEC injury and cell death. This biliary epithelial damage potentially underlies the pathogenesis in autoimmune biliary disorders like Primary Sclerosing Cholangitis (PSC). In-vitro co-culture experiments of *E.coli* primed BECs and MAIT cells were performed to assess MAIT cell cytokine and CD40L expression. BEC expression of CD40 and FAS were assessed to investigate the CD40-CD40L association and FAS induced BEC death.

5.3.1 Paediatric MAIT cell co-culture with *E.coli* primed cholangiocytes

Cholangiocytes were cultured from donor liver to a passage stage of P3-P4 prior to use in the MAIT-BEC coculture experiments. Magnetic negative CD3+ selection using a Pan T cell isolation kit (Miltenyi Biotec) was performed on PBMCs from a paediatric patient with autoimmune hepatitis (AIH). Enriched T cells from the magnetic isolation was cocultured with BEC (with and without *E.coli*). A detailed description of the experimental methods can be found in Sections 2.14 to 2.17. Samples were processed using the BD LSR Fortessa X-20 sixteen colour flow cytometer. Analysis of cytokine and cell marker expression was gated on MAIT cells performed using FlowJo V10 (Figure 5j). A repeat of the experiment was carried out on PBMCs from an age matched unrelated healthy child. For these experiments, CytoStim, a cell stimulation containing polyclonal antibodies, were added (treated) to the blood PBMCs from both children as a positive control.

A 2.5 fold increase in cytokine response is detected from the MAIT cells of the AIH patient; an increase of 3.97% from 1.64% in IFNγ, 12.9% from 5.18% in Perforin, and 22.5% to 50.9% in IL-17A in the *E.coli* primed BEC coculture compared to the negative control (without *E.coli*) (Figure 5k). In this experiment, the CD40L expression remains largely unaltered from 4.1% to 5.16%.

In CytoStim treated positive control, a higher response is elicited in the cytokines; an increase of 17.3% from 1.37% in IFNγ, 10% from 1.93% in Perforin, and 4.34% to 19% in IL-17A compared to the negative control (untreated). With CytoStim activation, a rise of CD40L is observed from 6.11% to 11.4% (Figure 5l).

As an alternative to using CytoStim treatment for the positive control, CD14+ monocytes from PBMCs of a healthy child were isolated by magnetic positive selection and cocultured (+/- treatment with *E.coli*) with the enriched T cells from the same PBMC sample. The MAIT cell response from the PBMCs of this experiment was gated on flow cytometry. Enriched T cells from the same sample was cocultured with *E.coli* treated BEC as the main test experiment.

In both experiments, a high Perforin response was induced but minimal change in IFNγ expression observed. A small but appreciable IL-17A response was also observed. Interestingly, an impaired IFNγ response in the presence of IL-17A production would be in keeping with chronic stimulation for example in patients with autoimmune liver disease but not in a healthy child. A similarly low IFNγ response was observed in the HC blood MAIT – BEC coculture from Figure 5m, in which CytoStim elicited a much higher IFNγ response with blood MAIT cells from the same sample. Without repeated experiments, these responses are difficult to interpret.

5.3.2 MR1 blockade of paediatric MAIT cell co-culture with *E.coli* primed cholangiocytes

MR1 antibody was next introduced to assess whether the functional cytokine responses observed in paediatric peripheral blood MAIT cells were MR1-dependent. Here, magnetic selection enriched T cells from a healthy child was cocultured with *E.coli* treated BEC and anti-MR1 antibodies (Figure 5n). As opposed to using THP-1 cells or CytoStim as a positive control, the patient's own blood monocytes were isolated using magnetic positive CD14+ selection (Miltenyi Biotec) and cocultured (with/without *E.coli*) with the patient's blood MAIT cells. In both experiments, a marked perforin response was elicited but minimal change in IFNγ expression was observed. A small but appreciable IL-17A response is also observed. Importantly, the expression of all three cytokines are reduced in the presence of MR1 blockade, indicating these pathways are MR1-dependent. Repeat experiments are needed to establish whether the results are reproducible and comparisons be made with MAIT cells from autoimmune patients but time and sample availability were significant limiting factors which will be reviewed in the Chapter discussion.

5.4 Discussion

Human liver MAIT cell activation has been shown with monocytes and B lymphocytes as well as non-classical antigen presenters like hepatocytes, cholangiocytes, liver sinusoidal endothelial cells and hepatic stellate cells [18, 19, 44, 77]. Research from our group first demonstrated LI-MAIT cell activation by *E.coli* treated monocyte-derived macrophages, liver B lymphocytes and cholangiocytes, which induced LI-MAIT upregulation of the proinflammatory cytokine interferon gamma (IFNγ) and the degranulation marker CD107 in an MR1 dependent manner [19, 71]. Liver MAIT cell (LI- MAIT) activation by dendritic cell (DC) antigen presentation has not been described. My coculture experiments of LI-MAIT cells with *E.coli* primed DC were designed to investigate this previously unexplored pathway.

5.4.1 Liver dendritic cell antigen presentation induces liver MAIT cell proinflammatory cytokine secretion and proliferation in an MR1 dependent manner

Three functional expression markers were assessed in my LI-MAIT-*E.coli* primed DC coculture experiments; IFNγ, CD107a and the cellular proliferation marker Ki67. Impaired IFNγ response following MAIT cell activation is considered a hallmark of T cell exhaustion [11, 12, 80]. Reduced MAIT cell IFNγ production were found in association with high CD38, CTLA-4 and PD-1 expression. This activation-induced cell exhausted state is frequently observed in circulating MAIT cells in almost all disease conditions including chronic liver disease [44, 51, 80]. This post-activation MAIT cell exhausted pre-apoptotic

phenotype was most prominent in the paediatric PSC cohort of my Cytof experiments (Chapter 4).

In the liver mononuclear cell coculture studies from the explanted PSC cirrhotic liver, a lower LI-MAIT IFNγ response was induced by the *E.coli* treated liver DC experiment compared to the THP-1 positive control (monocyte cell lineage antigen presentation). This observation would support DC induced T lymphocyte hypo-responsiveness, a feature of hepatic DCs which are inherently tolerogenic given their low expression of the costimulatory molecules CD80, CD86 and MHC class-II, and a high expression of the immunosuppressive cytokines IL-4, IL-10 and TGF- β (Wirtz, Soltani, Dou).

This finding was not observed with repeated experiments however; similar MAIT cell IFNγ expression levels were induced by co-culture with *E.coli* treated DCs or *E.coli* treated THP-1 cells. Definite conclusions cannot be drawn due to the small number of experiments performed which does not allow for a true comparison to be made between the AIH and PSC explants, nor with the healthy donor livers.

There were significant limitations encountered in the research work of this Chapter. Several factors prevented further repeat experiments. Cell sorting was crucial in separating 'pure' liver MAIT and DC cell populations for coculturing. Low liver DC yields were consistently isolated from liver mononuclear cells per cell sort. This low starting cell population prevented adequate downstream experiments despite having optimized DC flow cytometry panels. This resulted in failed attempts at coculturing for the first six months of my research. I had to undertake the PhD part-time whilst I worked as a Clinical Fellow at the Liver Unit of Birmingham Children's Hospital. I tried to maximize my laboratory time throughout but this

was further cut short when I was re-deployed for an 8month period back to full-time hospital work at the height of the pandemic in 2020. There was another delay of 6months once my research resumed as we awaited for COVID safety and quality control measures to be put in place for the obtainment of blood and explant liver tissue for research.

Over the course of my research, only two paediatric autoimmune explant livers were available (one PSC and one AIH). Unfortunately, both children were transplanted on a weekend (one on a Friday night and one on Saturday). When I created the SOP (Standard Operating Procedure) and set up the transfer of paediatric samples from Birmingham Children's Hospital (BCH), it was decided, in conjunction with the Pathologists at BCH, that paediatric autoimmune livers explanted during the weekend (between 16:00hrs on a Friday and 12:00hrs on a Sunday) would be fixed in formalin to prioritize clinical assessment as no histopathology service was available during this time. Due to these challenging limiting factors and small experiment numbers, a true comparison of my MAIT cell coculture results cannot be made between the autoimmune explanted livers or with the donor livers. Hence, it can only be interpreted that IFNγ, CD107a and Ki67 upregulation was observed in the MAIT cell cocultures in both DC and THP-1 antigen presentation in all three liver types. CD107a, as described above, is a marker used in degranulation assays and cytotoxic activity. Its cell surface upregulation indicates degranulation has taken place with the cellular release of perforin and granzymes. In previous work from our group, CD107a upregulation was shown in the LI-MAIT coculture experiments with *E.coli* treated liver B lymphocytes and BECs [19]. In addition, higher Ki67 expression has been described in blood MAIT cells from patients with cirrhosis compared to healthy individuals [51].

Excitingly, a reduction in proinflammatory and cytotoxic activity (IFNγ, TNFα and CD107a

expression) was observed with MR1 blockade in the LI-MAIT-DC coculture from an explanted PSC liver. Taken together, my findings has shown that *E.coli* treated liver DCs induces MAIT cell expression of IFNγ, CD107a and Ki67 from AIH, PSC and donor livers. Additionally, the IFNγ, TNFα and CD107a response by LI-MAIT cells can be blunted by MR1 blockade.

5.4.2 Paediatric blood MAIT cell activation by biliary epithelial cell antigen presentation is MR1 dependent

Cholangiocytes are designated ‘non-classical’ antigen presenting cells due to their ability to present bacterial ligands and activate blood and liver MAIT cells from adult patients with chronic liver disease (PSC, PBC, NASH and alcoholic liver disease), healthy subjects and in donor livers [19]The propensity of MAIT cells in the peri-portal regions of diseased livers, most notably in PSC, compared to healthy donor livers, suggest they play a role in augmenting biliary epithelial damage [19, 33, 80]. To assess paediatric MAIT cell activation by BEC antigen presentation, blood MAIT cells from paediatric samples were cocultured with *E.coli* treated BEC. In addition to the aforementioned challenges in the MAIT-DC coculture section, this aspect of my research was dependent on BEC and THP-1 cell viability.

Biliary epithelial cell cultures were performed by a dedicated laboratory technician with expertise in tissue culture. I had the good fortune of learning the technique from her prior to her retirement. However, it took many months to grow BECs to confluency and passage to a stage ready for downstream experiments. I had tried to grow BEC isolated from adult

explanted PSC, AIH and PBC livers but these attempts failed due to a) failure of cell growth, b) suspected infection of cultured cells and c) concern that the BECs were transforming into myofibroblasts due to their change of phenotype under light microscopy examination. I was however, successful with growing BEC isolated from donor liver cells and used these for the downstream coculture experiments.

With regards to the THP-1 cells, batches were frozen and stored in liquid nitrogen during my re-deployment into clinical service during the COVID pandemic. On my return to the lab, I had difficulty resuscitating these cells even with different batches and obtaining expert advice from other research groups with experience in THP-1 cell culture. New samples of THP-1 cells were sourced from the European Collection of Authenticated Cell cultures (ECACC), Public Health England. However, by the time these were cultured to readiness for downstream experiments, time constraint was becoming a significant factor. As I had success with using CytoStim, a cell stimulation cocktail polyclonal antibodies, in my CyTOF experiments, I had elected to use CytoStim as a positive control for the MAIT cell-BEC coculture experiments instead of the THP-1 cells.

In this chapter, PBMCs from a paediatric patient with autoimmune hepatitis (AIH) was cocultured with *E.coli* treated BEC and the MAIT cell response was analyzed by flow cytometry. The same experiment was performed using PBMCs from an age matched unrelated healthy child. A 2.5 fold rise in cytokine response of IFNγ, Perforin, and IL-17A was observed in the blood activated MAIT cells from the AIH patient. Interestingly, a much higher Perforin response was elicited in the healthy control (HC) compared to the AIH patient which was in contrast to the IL-17A response being higher from the MAIT cells of the AIH patient.

Blood MAIT cells treated with CytoStim were used as a positive control and this also induced a more pronounced IFNγ as well as Perforin response from the MAIT cells of the HC.

IL-17A production again was higher in the activated blood MAIT cells from the AIH patient compared to the HC. The results suggests preserved Th1 function in MAIT cells from the HC but a switch to a Th17 phenotype in the MAIT cells from the child with AIH. Findings are in keeping with published adult MAIT cell studies in which impaired IFNγ production is a consistent finding of MAIT cells in disease and is considered a hallmark of T cell exhaustion [11, 12, 80].

IL-17A is a chronic inflammatory cytokine with profibrogenic potential e.g. inducing hepatic stellate cells/hepatic myofibroblasts proliferation [51, 78, 80]. Under 'normal' physiological conditions, MAIT cell IL-17 production is minimal in health [44, 185]. An impaired IFNγ response in the presence of IL-17A production would be in keeping with chronic stimulation and suggests the MAIT cells from this child with AIH are of a chronic inflammatory MAIT17 phenotype.

CD40L (CD154) expression was higher in the CytoStim treated MAIT cells from the AIH patient compared to the HC where no CD40L response was appreciated nor in the MAIT-BEC *E.coli* coculture. TCR stimulation by bacterial ligands such as *E.coli* are known to invoke a partial response as part of the MAIT cells' tissue repair signature; optimal response requires cytokine co-stimulation e.g. in the presence of inflammatory cues likes DAMPS or PAMPS [33, 44]. CytoStim initiates a stronger TCR response with its array of superantigens which is evident with the upregulation of markers like CD40L expression. Interestingly, CD40L expression is higher from the MAIT cells of the child with AIH compared to the HC.

CD40L a is tumour necrosis factor (TNF) ligand superfamily member which binds to CD40 [226, 235]. CD40 is a costimulatory receptor molecule present on antigen presenting cells but is also expressed by some non-immune cells like BEC [19, 226]. CD40L-CD40 ligation on BECs augments FAS (CD95) induced biliary cell death [137, 225]. Results of this experiment suggests MAIT cells in disease (AIH) has the potential to incur damage to BECs via the CD40L-CD40 interaction than MAIT cells in health.

Lastly, CD14+ monocytes obtained by magnetic positive selection of PBMCs from a healthy child was cocultured (with/without *E.coli*) with enriched T cells from the same PBMC sample. The MAIT cell response was assessed by flow cytometry. Enriched T cells from the same sample was separately cocultured with *E.coli* treated BEC. In both experiments, a high Perforin but minimal IFNγ response was elicited. A small but appreciable IL-17A response was also observed. Results shows antigen presentation by both BEC and the patient's own blood CD14+ monocytes can activate blood MAIT cells from this healthy child. Impaired IFNγ production and preserved cytolytic function was observed which implies Th1 dysfunction in the MAIT cells from this healthy child. Low IL-17A expression would be in keeping with normal physiological findings as opposed to the high IL-17A levels of the chronic inflammatory MAIT17 phenotype [44, 78].

A similarly low IFNγ response was observed in the HC blood MAIT-BEC coculture compared to CytoStim positive control of blood MAIT cells from the same patient. Without repeat experiments, conclusions cannot be drawn from these results.
It can be interpreted that *E.coli* treated donor liver BEC can activate blood MAIT cells from a) healthy children to induce cytotoxicity with perforin production and b) AIH children induces IL-17A production and CD40L upregulation. MR1 blockade in both leads to a

reduction in all three cytokines, suggesting these responses to be partially MR1-dependent. These findings are similar to the experimental result from the adult AILD cohort. Cytokine blockade could not be performed due to insufficient cell yield and therefore whether these functional responses could be elicited in an MR1-independent activation could not be assessed.

Findings from my research provides further evidence that MAIT cells safeguard the biliary mucosa which is in direct continuity with the gastrointestinal tract and it's large array of microbiota. Microbial derived compounds such as lipopolysaccharide from *E.coli* has been found in higher concentrations in portal venous blood compared to the systemic circulation.

Chapter 6. General discussion

Autoimmune liver disease (AILD) is a life-long immune mediated chronic liver condition which often starts in childhood [95, 96]. MAIT cells are the most abundant invariant T lymphocyte population in the adult liver and are speculated to augment biliary epithelial damage and fibrosis in AILD [19, 80]. Their enrichment at mucosal sites like the liver and gastrointestinal tract suggests MAIT cells play an important role in the gut-liver axis and in the maintenance of mucosal integrity at these key sites of potential microbial breach [37, 38, 41]. The findings of my MAIT cell research and their implications in the pathogenesis of paediatric autoimmune liver disease is summarized below. The limitation to liver tissue and blood sample access in our cohorts meant that this research was based on few patients per diagnostic category. Higher numbers of tissue and blood samples are needed to examine the reproducibility of my findings and had I more time and resources, I would like to have repeated my experiments, particularly in the confocal imaging and MAIT cell coculture studies. A higher ‘n’ number in addition to larger liver tissue sections and blood volume would ensure more representative sampling. Within the liver itself, it would be beneficial if access to different regions of the liver were available for comparison e.g. central (porta hepatis) vs. peripheral liver tissue.

6.1.1 Confirmation of intrahepatic MAIT cells in paediatric liver

The detection of mucosal-associated invariant T (MAIT) cells in paediatric liver tissue by immunofluorescence (IF) has not been described. Even in adult autoimmune liver explants, IF staining of MAIT cells has not been shown in AIH or PSC [19, 125].

In this research, Vα7.2+ MAIT cells in paediatric autoimmune hepatitis type 1 (AIH T1), autoimmune hepatitis type 2 (AIH T2), primary sclerosing cholangitis (PSC), and biliary atresia (BA) were identified and shown to be well delineated by IF staining. I went on to demonstrate CD8+ Vα7.2+ MAIT cell colocalization, which accounted for <5% of total CD8+ cells in a confocal image of interface hepatitis in AIH T1. Gargano et al also found CD8+ MAIT cells to represent only <5% of the total CD8+ cells in Multiple sclerosis CNS lesions [142]. Low CD8+ Vα7.2+ MAIT cell numbers may reflect low total MAIT cell count as opposed to a low proportion of CD8+ MAIT cells [142]. Given more time, I would examine for CD4+ Vα7.2 dual staining to investigate for this subset in the paediatric liver.

6.1.2 MAIT cells localize to periportal areas of paediatric biliary cholangiopathies

Higher Vα7.2+. MAIT cells were identified in the periportal regions compared to the hepatic parenchyma in the paediatric liver tissue assessed which included AIH T1, AIH T2, PSC, and BA. Paediatric liver MAIT cell frequency from my findings were lower than that reported in adult diseased and donor livers [19, 80]. This is in keeping with reported literature of lower peripheral blood MAIT cell count in children compared to adults with liver disease [63, 64].

Liver sections from the child with PSC had the highest number of Vα7.2+ MAIT cells in the periportal regions compared to the other conditions. This also reflects that described in adult livers [19, 51, 80]. To assess the consistency of this finding, repeat IF staining on PSC liver tissue from different paediatric patients would be needed but due to the lack of tissue availability I was not able to do this within the timeframe of my research.

6.1.3 Confocal image capture of MAIT cell Granzyme release

MAIT cell cytolytic function was next assessed. In addition to Th1 and Th17 cytokine profiles, MAIT cells possess cytotoxic potential [38, 80, 183]. MAIT cell cytolysis has not been assessed by this immunofluorescence staining. I examined for intrahepatic MAIT cell Granzyme B release which I found to be most evident in paediatric biliary atresia (BA) liver tissue; a rim of Granzyme B secretion can be clearly seen surrounding TCR Vα7.2+ staining in a BA liver section. To take this aspect of my research forward, I would perform IF staining for Perforin and the degranulation marker C107a expression in addition to Granzyme in different paediatric liver tissue.

6.1.4 MAIT cells and Tregs periportal distribution

Regulatory T cells (Tregs) are central in maintaining immunotolerance within the liver [162, 163]. Treg dysfunction and the resultant breakdown in immunotolerance are speculated to underly AILD immunopathogenesis which is aggravated by a higher ratio of T effector cells [151, 153, 164].

My research shows MAIT cells and Tregs to mainly populate around the portal tracts and periportal areas in paediatric AIH and PSC liver tissue. Enrichment of these two cell types in the portal tracts of newly diagnosed adult AIH patients have been reported [126]. The intrahepatic spatial relationship and interaction of these two different immune cell types maybe of pathological significance. Currently, besides the description of a higher frequency of both MAIT cells and Tregs in the periportal regions, there is insufficient evidence to support cellular crosstalk between these two cell types within the liver microenvironment within this research. To investigate further, I would assess for MAIT cell and Treg IF staining along with their respective cytokine and chemokine receptor profiles to investigate for cellular crosstalk between these two immune cell types in paediatric liver tissue.

6.1.5 Cell-in-cell structures in paediatric AILD and biliary atresia

During my research work with IF staining, emperipolesis of MAIT cells within cholangiocytes were captured in paediatric PSC liver tissue. Emperipolesis is a recognized histological feature of AIH and was recently described in PBC [158]. It’s identification in PSC in this research suggests a common pathway of bile duct injury in AILD. Within the

same paediatric PSC explant, FOXP3+ Tregs were identified to lie within the cytoplasm of hepatocytes, a phenomenon known as enclysis which refers to the capture and lysis of Tregs by hepatocytes [172]. Enclysis was also observed in paediatric AIH T1 liver tissue.

Enclysis is thought to contribute to the loss of tolerance in AIH [157, 159]. In addition to enclysis, a FOXP3+ Treg was imaged to be moving towards a hepatocyte in a paediatric AIH type 2 liver explant and in the paediatric PSC liver, cell-to-cell contact between a FOXP3+ Treg and a hepatocyte was captured in this research. Furthermore, dual CD4 and FOXP3 staining confirmed them to be CD4+ FOXP3+ Tregs. Lastly, Treg frequencies were found to be higher in the parenchyma of the biliary cholangiopathies; PSC and BA compared to AIH T1. This finding may be related to Treg enclysis in areas of active inflammation causing an apparent reduction in intrahepatic Treg frequency. Further investigation of this interesting finding is being carried out by our group.

6.2.1 Paediatric circulating MAIT cell subset frequencies identified by CyTOF

Compared to healthy individuals, circulating MAIT cell numbers are depleted in almost all diseases including autoimmune conditions [9, 12, 38]. Although MAIT cells account for up to 10% of circulating total CD3+ lymphocytes, most population-based studies have found MAIT cells to represent 1-4.5% of total CD3+ lymphocytes [12, 14, 41]. Decreased MAIT cell numbers are reported in children with asthma, coeliac disease, cerebral palsy and in active infections like tuberculosis (TB) and human immunodeficiency virus (HIV) [178, 195, 196, 198]. Only two MAIT cell studies in children with liver disease are reported in the literature and both describe lower blood and intrahepatic MAIT cell frequencies compared to adults [63, 64].

In my three cohorts, healthy children (HC) had the highest percentage of circulating MAIT cells (0.97 – 5.61% of total CD3+ cells) followed by children with AIH (0.23 – 2.44%) and

then PSC (0.08 – 2.71%). Interestingly, a significant post-STIM reduction in MAIT cell numbers were observed in the HC but not in children with AIH or PSC, wherein MAIT cell frequency were largely unchanged. A greater reduction in blood MAIT cell frequency in disease is speculated to be partly due to reduced survival caused by activation-induced cell exhaustion and cell death [80, 81, 182]. My findings of preserved MAIT cell numbers in children with AILD challenges this theory and perhaps MAIT cells in children with AILD are less susceptible to the cell exhausted phenotype.

MAIT cell subsets in all three paediatric cohorts were mostly double negative (DN) and to a lesser extent CD8a+ cells which contrasts with adult studies in which the majority of MAIT cells are CD8a+ cells [41, 177, 181]. Minimal functional difference is reported amongst DN and CD8a+ MAIT cells . As with total MAIT cell numbers, a post-STIM reduction in all MAIT subsets is observed in the HC but not the AILD children. Importantly, a rise in post-STIM MAIT CD4+ cells in AIH and PSC patients were observed. This is of interest as the MAIT CD4+ subset, although a minor population, is described to differ in their function to the MAIT CD8a+ and DN subsets [14, 182, 194]. Higher MAIT CD4+ cells were reported in a study of children with convalescent Rheumatoid fever compared to those with acute disease [199]. A quiescence of disease inflammatory activity may account for this finding but increased post-STIM MAIT CD4+ cell count was observed in both AIH subgroups (AIH treatment naïve and the AIH treated children (remission). The biological significance of a higher MAIT CD4+ cell count needs to be further investigated to decipher the role of MAIT CD4+ cells in disease.

6.2.2 Paediatric MAIT cell IFNγ and TNFα, and Tbet expression

Post-STIM TNFα production was higher in total MAIT cells compared to their total CD3+ counterparts (from the same blood sample) in all three cohorts. Moreover, MAIT cells from PSC children had a 40xfold higher TNFα production than total CD3+ cells and MAIT cells from AIH and healthy children were 20xfold higher. MAIT CD4+ cells displayed the highest TNFα production followed by MAIT DN and CD8a+ cells. Many adult MAIT cell studies report a reduction in TNFα production by activated MAIT cells but recent studies have contradicted this finding [200, 201] There is one paediatric study however that observed a 10xfold increase in TNFα expression by MAIT cells from infants infected with mycobacterium [202]. My findings suggest preserved TNFα secretion in activated MAIT cells from children with AILD, particularly in PSC.

Higher post-STIM MAIT cell IFNγ expression compared to CD3+ was also observed but this was much lower in the AILD children compared to HC and significantly lower than TNFα production. Defective MAIT cell IFNγ and Tbet expression in parallel with higher PD1 is reported in adults with AILD and supports the concept of activation-induced cell exhaustion [33, 80, 203]. In children, MAIT cells from patients with Rheumatoid arthritis and Systemic Lupus Erythematosus had impaired IFNγ production as well as a reduction in cell numbers [204, 205]. In addition, Coakley et al found patients with sepsis had a diminished Tbet response compared to those with infection without sepsis [206].

In my research, Tbet expression post-STIM in total and MAIT cell subsets were upregulated, most prominently from the HC, followed by the AIH and then PSC children. The TNFα response however was much more pronounced than Tbet upregulation.

Of note, no difference in Tbet, TNFα or IFNγ activity was observed between the AIH treatment naïve compared to the treated AIH children. This finding implies newly diagnosed AIH patients (treatment naïve) have similar MAIT1 function to patients on maintenance immunosuppression of Azathioprine and low dose prednisolone.

Importantly, the TNFα response was much more pronounced than Tbet upregulation. This taken together with the impaired IFNγ function, suggests TNFα production may be regulated by variables other than Tbet transcription e.g., from modulation of the tumour necrosis factor (TNF) superfamily.

6.2.3 Paediatric MAIT cell IL-17A and IL-22, and RORγt expression

Higher interleukin-17 (IL-17) production by MAIT cells (MAIT17) is described in many chronic inflammatory conditions [78, 184]. Double negative (CD4- CD8-) MAIT cells are reported to have the highest IL-17 production [194, 208]. This chronic inflammatory MAIT17 phenotype is observed in the bronchoalveolar lavage of children with acute asthma exacerbations and in pneumonia [236, 237]. In inflammatory bowel disease, MAIT cells in diseased bowel from patients with ulcerative colitis and Crohn's disease had higher IL-17 production than healthy adjacent bowel [135].

In AILD, Böttcher et al described increased Il-17 production and RORγt expression with chronic cytokine stimulation. In the same study, HSC proliferation was shown to be partly IL-17 dependent [80]. MAIT cell induced hepatic myofibroblast proliferation in the presence of IL-17 upregulation was shown to be MR1-dependent in non-alcoholic steatohepatitis (NASH) and alcoholic hepatitis [51]. Investigators from both studies concluded intrahepatic

IL-17 producing MAIT cells to be profibrogenic.

From my CyTOF experiments, IL-17A production was minimal in the total CD3+ cells but a post-STIM IL-17A response was observed in the MAIT cells of all three cohorts, being most marked in the PSC children. The highest post-STIM IL-17A response were from MAIT CD4+ and CD8a+ subsets in PSC and in MAIT CD4+ cells in the HC cohorts. IL-17A expression was lowest in the AIH patients. Increased post-STIM RORγt activity was observed in the HC and PSC cohorts but not in AIH either.

Böttcher et al demonstrated chronic stimulation of blood MAIT cells from healthy controls and patients with AILD to have impaired IFNγ and Tbet expression but an increase in IL-17 and RORγt expression [80]. Results from my paediatric CyTOF experiments supports these findings and the theory of MAIT cell plasticity with an altering phenotype from MAIT1 in situations of acute inflammation to a MAIT17 phenotype in chronic inflammation.

In addition, MAIT cell secretion of interleukin-22 is also governed by the transcription factor RORγt. IL-22 is a member of the IL-10 cytokine superfamily and in liver disease, IL-22 has been shown to dampen hepatic stellate cell activity and reduce fibrosis [44, 213]. IL-22 is therefore considered hepatoprotective and antifibrotic [213, 214]. Overall, IL-22 MAIT cell activity appears reduced in our children with AILD compared to the healthy cohort but strikingly, children with newly diagnosed AIH had significantly higher IL-22 production than AIH children on treatment. My results suggest children with AILD have less anti-inflammatory and tissue repair potential than healthy children. Moreover, this tissue repair potential appears dampened in children in remission (AIH on treatment); lower IL-22 in this instance may be due general lack of inflammatory activity or the presence of established

fibrosis e.g., loss of tissue repair potential.

6.2.4 Paediatric MAIT cell cytotoxic and GMCSF activity

MAIT cells have an innate-like ability to rapidly respond to virus infected cells with the release of granzyme and perforin proteins [31, 32, 34]. MAIT cells express the transcription factor PLZF (promyelocytic leukemia zinc-finger) which is a known transcriptional regulator of iNKT cells [38, 215]. High expression of PLZF drives MAIT cell maturation and is directly related to their innate-like capabilities [38, 215, 239].

PLZF and Granzyme B expression in the three paediatric cohorts were generally higher in the MAIT cells compared to total CD3+ cells. PSC total and MAIT cell subsets had lower PLZF and Granzyme B expression compared to the AIH and HC cohorts. AIH treatment naïve patients had higher PLZF and Granzyme expression than that of treated children. These results show PSC and to a lesser degree, AIH treated patients, have impaired PLZF transcription factor activity and functional release of Granzyme compared to healthy children. Newly diagnosed AIH children had preserved cytolytic function however compared to the treated ones.

Additionally, MAIT cells have been shown to secrete GMCSF (granulocyte-macrophage colony-stimulating factor), a proinflammatory cytokine and white cell growth factor [185, 186]. MAIT cell GMCSF production was found to be a predictor of morbidity and mortality in COVID-19 patients [186]. Almost a reverse trend to Granzyme B and PLZF was observed with GMCSF expression; PSC patients had the highest MAIT cell GMCSF production followed by the HC and AIH cohorts. Higher MAIT cell GMCSF but lower Granzyme B and

PLZF activity suggests preserved colony-stimulating and growth factor capabilities but dysfunctional cytolysis in our PSC cohort. AIH treatment naïve patients had preserved Granzyme B, PLZF and GMCSF expression compared to treated patients. This may reflect the proinflammatory nature of MAIT cells in newly diagnosed AIH patients compared to those in remission (treated). Dampened activity in the treated AIH patients may reflect disease quiescence in remission or it may reflect the immunosuppressive drug response.

Taken together, blood MAIT cells from children with PSC demonstrate heightened TNF-α, IL-17A and GMCSF activity but impaired IFNγ and cytolytic function. Although AIH patients had dampened Th1 and Th17 activity, AIH treatment naïve patients had preserved cytolytic function, GMCSF and IL-22 production.

6.2.5 Paediatric MAIT cell and liver homing chemokine expression

Intrahepatic MAIT cells are known to express higher level of the chemokine receptors CXCR6 and CCR6 from diseased and donor livers [218, 219]. These liver homing chemokine receptors enable immune cells to migrate to regions of inflammation within the liver sinusoidal and peribiliary regions in response to their ligands CXCL16 and CCL20 respectively [19, 218, 219].

From my CyTOF experiments, blood MAIT cell expression of CCR6 and CXCR6 was relatively low. MAIT cells from the PSC children expressed higher levels of CCR6 than CXCR6. The reverse was found in AIH treatment naïve patients who had higher CXCR6 expression and unchanged CCR6 levels. The AIH cohort had the highest expression of the gut homing chemokine receptor CCR9 in the MAIT and CD3+ cell populations. The

importance of CCR9 in liver disease is becoming increasingly recognized CCR9+ immune cells are linked to hepatic stellate cell proliferation in murine models and impaired CCR9/CCL25 signaling has been reported in NASH [220]. Aberrant expression of gut homing molecules resulting in liver recruitment of gut derived immune cells is postulated to occur in PSC but is now believed to be a feature of many chronic liver diseases [133]. Upregulation of CCR9 expression in our paediatric AIH and PSC cohorts supports this finding.

MAIT cells with a Th1 effector memory phenotype have a high expression of the inflammatory chemokine receptors CXCR3 and CCR5, and recruited to areas of inflammation [87, 221]. From our cohorts, AIH MAIT cells showed the highest CXCR3 and CCR5 expression compared to PSC and HC. AIH treatment naïve and treated patients had similar expression levels of both which is interesting and implies persistent upregulated inflammatory chemokine receptor expression on MAIT cells despite remission in the treated patients.

6.2.6 MAIT cell activation and exhaustion status

Peripheral blood and liver MAIT cells in chronic liver disease are described to be of a chronically activated, functionally impaired and cell-exhausted phenotype. Activated circulating and intrahepatic MAIT cells have high expression of the lymphocyte activation markers CD69+, CD38+ and cell exhaustion markers PD1+, CTLA-4+ in association with impaired IFNγ function [44, 80, 182]. On review of these cell status markers, MAIT cell CD38 expression was observed although to a lesser extent than total CD3+ cells. The reverse was observed with PD-1 which was negligible in the CD3+ cells but highest in the

PSC MAIT cells. CTLA-4 expression was also highest in the PSC cohort and of the subsets, MAIT CD4+ cells had the highest CTLA-4 expression. Only the post-STIM MAIT cells from the AIH patients expressed the proliferation marker Ki67 with minimal difference observed between the AIH treatment naïve and treated patients. These findings suggest MAIT cells from PSC children to be in an activated and cell exhausted state but AIH patients in contrast displayed an activated and proliferative phenotype regardless of treatment status.

6.2.7 MAIT cell TNF superfamily expression

CD40L is a costimulatory molecule of the tumour necrosis factor ligand (TNFL) superfamily. It is primarily expressed by activated CD4+ cells and regulates the immune response by augmenting macrophage and B lymphocyte activation [190, 235]. Our group first described the upregulation of CD40L surface expression on blood MAIT cells from adult patients with chronic liver disease following antigen presentation by cholangiocytes [19].

MAIT cell CD40L upregulation post activation has since been demonstrated by other researchers [191, 235]. Humphreys et al had shown BEC CD95 (FAS) dependent cell death required prior augmentation of CD40 which is expressed on the surface of BEC [137]. MAIT cell upregulation of CD40L is speculated to induce BEC apoptosis via this CD40-CD40L augmentation of FAS dependent cell death [19].

In my CyTOF research, I observed the post-STIM MAIT cell CD40L expression to be highest from the PSC children followed by AIH and HC. PSC MAIT CD4+ cells had the highest CD40L expression compared to the other subsets. Among the AIH subgroups, treatment naïve patients had marginally higher expression than treated patients.

The predominant location of MAIT cells in the portal regions in PSC, combined with the finding of higher CD40L expression on MAIT cells in our PSC cohort, further supports MAIT cell augmented biliary inflammation and epithelial damage in this autoimmune cholangiopathy, even in childhood.

CD27 is a costimulatory molecule of the tumour necrosis factor receptor(TNFR) superfamily. It has an important role in clonal T cell expansion, promoting Th1 and cytotoxic T cell function [226]. My observations show MAIT cell CD27 expression to follow the same trend as CD40L, being highest in the PSC group, but instead of MAIT CD4+, CD27 expression was highest in PSC MAIT CD8a+ cells. Within the AIH subgroups, treatment naïve patients also had higher CD27 expression than the treated patients.

As observed, PSC MAIT cell TNFα secretion was much more pronounced than Tbet upregulation and this finding of high TNFL (CD40L) and TNFR (CD27) superfamily expression suggests TNF superfamily pathway activation may be the main driver in TNFα activity in this invariant cell population

6.2.8 MAIT cell IL-12r and IL-18r expression

MAIT cells can be activated in a cytokine dependent manner by cytokine receptors on their cell surface [31, 32]. Optimal MAIT cell activation is achieved by cytokine co-stimulation, namely by interleukin-12 (IL-12) and IL-18 [33, 44, 76]. Moreover, an IL-17 augmented profibrotic response is brought on by chronic cytokine MAIT cell stimulation [80]. My research shows MAIT cells from the PSC children had the highest IL-

18r expression, followed by AIH and then HC. In contrast, IL-12r were minimally expressed by the autoimmune compared to healthy children. AIH treatment naïve patients had significantly higher IL-18r expression than treated patients. Of note both IL-18r and IL-12r were negligible in the CD3+ cells from these children.

These findings imply MAIT cell IL-18r expression and thus IL-18 cytokine activation to be of importance in paediatric PSC and in newly diagnosed acute AIH.

6.3.1. Liver dendritic cell antigen presentation induces liver MAIT cell proinflammatory cytokine secretion and proliferation which is MR1 dependent

Liver MAIT (LI-MAIT) cell activation by liver dendritic cell (DC) antigen presentation has not been investigated. Research from our group previously demonstrated LI-MAIT cell activation by *E.coli* treated monocyte-derived macrophages, liver B lymphocytes and cholangiocytes, which upregulated LI-MAIT secretion of the proinflammatory cytokine interferon gamma (IFNγ) and the degranulation marker CD107 in an MR1 dependent manner [19].

To explore this pathway further, I performed liver MAIT cell co-cultures with *E.coli* primed DC isolated from the same livers. Functional assessment undertaken include IFNγ, CD107a and the cellular proliferation marker Ki67 expression profiles.

My coculture experiments were successful in demonstrating LI-MAIT cell activation by liver DC antigen presentation (from the same livers). Activated MAIT cell upregulation of all three markers, IFNγ, CD107a and Ki67 were measured compared to the negative controls. This

was shown with autoimmune explanted livers of Primary sclerosing cholangitis (PSC) and autoimmune hepatitis (AIH) as well as in healthy donor livers. The IFNγ and CD107a MAIT cell response from the diseased explants interestingly, were higher compared to donor livers. This contrasts with the functional impairment described in MAIT cells in disease [10, 51, 80]. Repeat experiments are required to ascertain this finding.

Few studies have investigated the expression of Ki67 but higher blood MAIT Ki67 expression from cirrhotic patients compared to healthy individuals has been reported [51]. Due to small numbers, a true comparison cannot be made between the liver types but upregulation of Ki67 can be appreciated in all three (AIH, PSC and donor liver) from my experiments.

Liver DC induced LI-MAIT cell cytokine activity was shown to be MR1 dependent in the PSC explant experiment in which IFNγ, TNFα and CD107a expression was blunted by MR1 blockade. Given more time and tissue availability, I would carry out repeat MAIT-DC coculture experiments with PSC, AIH and donor livers to assess for cytokine, chemokine and cell activation markers with/without MR1 blockade.

Significant limitations were encountered in this aim of my research due to repeated low yields of liver DC numbers, unsuccessful co-culture experiments despite attempts at troubleshooting, and my redeployment back to clinical work at the height of the COVID pandemic. Had I more time and tissue availability, I would have performed repeat experiments with paediatric and adult autoimmune livers to allow for a true comparison of the data between the liver types.

6.3.2 AIH peripheral blood MAIT cell activation by cholangiocytes

The propensity of MAIT cells in the peribiliary and portal areas in disease, most notably in PSC, suggests they play a role in augmenting biliary epithelial damage. Cholangiocytes are designated ‘non-classical’ antigen presenting cells due to their ability to present bacterial ligands via MR1 to activate MAIT cells [19]. Paediatric MAIT cell response following BEC antigen presentation however has not been investigated.

I isolated peripheral blood mononuclear cells from a paediatric patient with AIH and co-cultured them with BEC tissue isolated from a donor liver. Results were compared to a repeat experiment performed with blood MAIT cells isolated from an age matched unrelated healthy child. The functional change in marker expression was measured for IFNγ, Perforin, IL-17A and CD40L.

Results show the healthy child to have preserved IFNγ and Perforin secretion on MAIT cell activation compared to the AIH patient, who in contrast, had higher IL-17A and CD40L expression. These results were most obvious in the CytoStim positive control arm. One interpretation of the results is that the MAIT cells from the AIH child has impaired MAIT1 (IFNγ) and cytotoxic function, and a switch to the chronic inflammatory and profibrotic MAIT17 phenotype has occurred. IL-17A is a chronic inflammatory which has been shown to potentiate hepatic stellate cell/hepatic myofibroblast proliferation [44, 78, 80]. Under physiological conditions, MAIT cell IL-17 production is minimal in health [44, 80]. An impaired IFNγ response in the presence of IL-17A upregulation would be in keeping with chronic stimulation and suggests the MAIT cells from this child with AIH has transformed into the chronic inflammatory MAIT17 phenotype. CD40L is a member of the tumour necrosis factor (TNF) ligand superfamily which binds to CD40 [190, 235]. Although the

costimulatory receptor molecule CD40 is mostly expressed by antigen presenting cells, it is a surface marker found on BECs [19]. Moreover, CD40L-CD40 ligation on BECs augments FAS (CD95) induced biliary cell death [225]. The higher CD40L expression from MAIT cells of the child with AIH has a greater potential to damage BECs compared to the MAIT cells from the healthy child. A higher expression of CD40L in MAIT cells from adult autoimmune liver explants has been described [19]. This MAIT-BEC interaction is thought to be pathological in causing biliary epithelial damage in disease.

Due to time constraints and time dedicated to the tissue culture of BECs to a confluent passage stage of P3-4 for downstream experiments in addition to THP-1 cell cultures, I was not able to repeat these experiments. I would have liked to repeat the experiments and assess the function of paediatric PSC blood MAIT cells as well as AIH and healthy donor blood MAIT cells.

6.3.3 Peripheral blood MAIT cell activation via CD14+ monocytes

Monocytes are classical antigen presenters and activators of MAIT cells [19, 240]. For this experiment, I isolated CD14+ monocytes from the peripheral blood sample of a healthy child which was then primed with *E.coli* and cocultured with MAIT cells from the same blood sample. For comparison, a repeat of the BEC-MAIT coculture experiment was performed with healthy donor blood MAIT cells. The MAIT cell functional response of IFNγ, Perforin and IL-17A was measured. Preserved cytotoxic function, measurable IL-17A expression and impaired IFNγ was demonstrated with both experiments which used blood MAIT cells from different healthy children. This finding suggests suboptimal MAIT cell Th1 activity even in healthy children but preserved cytotoxic activity. Low IL-17A expression would be in keeping with normal physiological levels in contrast to the high IL-17A secretion of the

chronic inflammatory MAIT17 phenotype observed in disease. The expression of all three cytokines were blunted by MR1 blockade in the MAIT - CD14+ and in the MAIT – BEC cocultures. Without repeat experiments however, conclusions cannot be drawn from these results.

6.4 Conclusion

Intrahepatic MAIT cells from paediatric liver explants were identified using immunofluorescent staining and confocal imaging. MAIT cells in paediatric autoimmune and biliary atresia livers predominantly located to the portal regions. MAIT cell emperipolesis observed in the paediatric PSC liver tissue suggests MAIT cell induces biliary epithelium damage. The CyTOF results show children with PSC had significantly higher MAIT cell TNFα secretion in association with upregulated TNF superfamily activity. These findings suggest preserved TNFα secretion by TNF superfamily pathway activation despite suboptimal Tbet expression and impaired IFNγ function.

The paediatric blood MAIT cell co-culture studies demonstrated higher IL-17A and CD40L expression and impaired IFNγ production in AILD compared to healthy controls. Crucially, PSC MAIT cells appear to display early polarization towards the chronic inflammatory MAIT17 phenotype with early IL-17A production upon acute activation. Higher MAIT cell GMCSF expression also suggests preserved colony-stimulating and growth factor capacity in PSC patients. Lastly, paediatric PSC MAIT cells had the highest expression of the cell-exhaustion markers PD1 and CTLA-4 which supports the theory of activation-induced cell exhaustion.

Collectively, these findings from MAIT cells of children with autoimmune liver disease may be of clinical significance and contribute to the biliary epithelial damage and progression of liver disease observed, particularly in PSC.

Lastly, the hepatoprotective and antifibrotic cytokine IL-22 expression observed in the MAIT cells from our paediatric PSC and AIH treatment naïve patients signifies homeostatic tissue repair despite acute disease activity. Taken together, results from my research highlight the important role of MAIT cells in the pathogenesis of paediatric autoimmune liver disease.

References

1. Porcelli, S., et al., *Analysis of T cell antigen receptor (TCR) expression by human peripheral blood CD4-8- alpha/beta T cells demonstrates preferential use of several V beta genes and an invariant TCR alpha chain.* J Exp Med, 1993. **178**(1): p. 1-16.
2. Treiner, E., et al., *Selection of evolutionarily conserved mucosal-associated invariant T cells by MR1.* Nature, 2003. **422**(6928): p. 164-9.
3. Reantragoon, R., et al., *Structural insight into MR1-mediated recognition of the mucosal associated invariant T cell receptor.* J Exp Med, 2012. **209**(4): p. 761-74.
4. Reantragoon, R., et al., *Antigen-loaded MR1 tetramers define T cell receptor heterogeneity in mucosal-associated invariant T cells.* J Exp Med, 2013. **210**(11): p. 2305-20.
5. Tilloy, F., et al., *An invariant T cell receptor alpha chain defines a novel TAP-independent major histocompatibility complex class Ib-restricted alpha/beta T cell subpopulation in mammals.* J Exp Med, 1999. **189**(12): p. 1907-21.
6. Takahashi, T., S. Dejbakhsh-Jones, and S. Strober, *Expression of CD161 (NKR-P1A) defines subsets of human CD4 and CD8 T cells with different functional activities.* J Immunol, 2006. **176**(1): p. 211-6.
7. Billerbeck, E., et al., *Analysis of CD161 expression on human CD8+ T cells defines a distinct functional subset with tissue-homing properties.* Proc Natl Acad Sci U S A, 2010. **107**(7): p. 3006-11.
8. Napier, R.J., et al., *The Role of Mucosal Associated Invariant T Cells in Antimicrobial Immunity.* Front Immunol, 2015. **6**: p. 344.
9. Martin, E., et al., *Stepwise development of MAIT cells in mouse and human.* PLoS Biol, 2009. **7**(3): p. e54.
10. Kurioka, A., et al., *MAIT cells: new guardians of the liver.* Clin Transl Immunology, 2016. **5**(8): p. e98.
11. D'Souza, C., Z. Chen, and A.J. Corbett, *Revealing the protective and pathogenic potential of MAIT cells.* Mol Immunol, 2018. **103**: p. 46-54.
12. Reantragoon, R., et al., *Mucosal-associated invariant T cells in clinical diseases.* Asian Pac J Allergy Immunol, 2016. **34**(1): p. 3-10.
13. Gherardin, N.A., et al., *Human blood MAIT cell subsets defined using MR1 tetramers.* Immunol Cell Biol, 2018. **96**(5): p. 507-525.
14. Leeansyah, E., et al., *Acquisition of innate-like microbial reactivity in mucosal tissues during human fetal MAIT-cell development.* Nat Commun, 2014. **5**: p. 3143.
15. Walker, L.J., et al., *Human MAIT and CD8αα cells develop from a pool of type-17 precommitted CD8+ T cells.* Blood, 2012. **119**(2): p. 422-33.
16. Konno, A., et al., *CD8alpha alpha memory effector T cells descend directly from clonally expanded CD8alpha +beta high TCRalpha beta T cells in vivo.* Blood, 2002. **100**(12): p. 4090-7.
17. Kjer-Nielsen, L., et al., *MR1 presents microbial vitamin B metabolites to MAIT cells.* Nature, 2012. **491**(7426): p. 717-23.
18. Lett, M.J., et al., *Stimulatory MAIT cell antigens reach the circulation and are efficiently metabolised and presented by human liver cells.* Gut, 2022. **71**(12): p. 2526-2538.
19. Jeffery, H.C., et al., *Biliary epithelium and liver B cells exposed to bacteria activate intrahepatic MAIT cells through MR1.* J Hepatol, 2016. **64**(5): p. 1118-1127.
20. Walker, L.J., H. Tharmalingam, and P. Klenerman, *The rise and fall of MAIT cells with age.* Scand J Immunol, 2014. **80**(6): p. 462-3.

21. Hashimoto, K., M. Hirai, and Y. Kurosawa, *A gene outside the human MHC related to classical HLA class I genes.* Science, 1995. **269**(5224): p. 693-5.
22. Le Bourhis, L., et al., *Antimicrobial activity of mucosal-associated invariant T cells.* Nat Immunol, 2010. **11**(8): p. 701-8.
23. Le Bourhis, L., et al., *MAIT cells detect and efficiently lyse bacterially-infected epithelial cells.* PLoS Pathog, 2013. **9**(10): p. e1003681.
24. Gold, M.C., et al., *MR1-restricted MAIT cells display ligand discrimination and pathogen selectivity through distinct T cell receptor usage.* J Exp Med, 2014. **211**(8): p. 1601-10.
25. Gold, M.C., et al., *Human mucosal associated invariant T cells detect bacterially infected cells.* PLoS Biol, 2010. **8**(6): p. e1000407.
26. Corbett, A.J., et al., *T-cell activation by transitory neo-antigens derived from distinct microbial pathways.* Nature, 2014. **509**(7500): p. 361-5.
27. Keller, A.N., et al., *Drugs and drug-like molecules can modulate the function of mucosal-associated invariant T cells.* Nat Immunol, 2017. **18**(4): p. 402-411.
28. Toussirot, É., et al., *Increased IL-22- and IL-17A-Producing Mucosal-Associated Invariant T Cells in the Peripheral Blood of Patients With Ankylosing Spondylitis.* Front Immunol, 2018. **9**: p. 1610.
29. Kawachi, I., et al., *MR1-restricted V alpha 19i mucosal-associated invariant T cells are innate T cells in the gut lamina propria that provide a rapid and diverse cytokine response.* J Immunol, 2006. **176**(3): p. 1618-27.
30. Chua, W.J., et al., *Polyclonal mucosa-associated invariant T cells have unique innate functions in bacterial infection.* Infect Immun, 2012. **80**(9): p. 3256-67.
31. Ussher, J.E., et al., *CD161++ CD8+ T cells, including the MAIT cell subset, are specifically activated by IL-12+IL-18 in a TCR-independent manner.* Eur J Immunol, 2014. **44**(1): p. 195-203.
32. van Wilgenburg, B., et al., *MAIT cells are activated during human viral infections.* Nat Commun, 2016. **7**: p. 11653.
33. Binder, B., R. Thimme, and M. Hofmann, *MAIT Cells in Viral Hepatitis and Liver Diseases.* Crit Rev Immunol, 2021. **41**(5): p. 37-47.
34. Ussher, J.E., C.B. Willberg, and P. Klenerman, *MAIT cells and viruses.* Immunol Cell Biol, 2018. **96**(6): p. 630-641.
35. Lamichhane, R., et al., *Type I interferons are important co-stimulatory signals during T cell receptor mediated human MAIT cell activation.* Eur J Immunol, 2020. **50**(2): p. 178-191.
36. Lamichhane, R., et al., *TCR- or Cytokine-Activated CD8(+) Mucosal-Associated Invariant T Cells Are Rapid Polyfunctional Effectors That Can Coordinate Immune Responses.* Cell Rep, 2019. **28**(12): p. 3061-3076 e5.
37. Atif, M., S. Warner, and Y.H. Oo, *Linking the gut and liver: crosstalk between regulatory T cells and mucosa-associated invariant T cells.* Hepatol Int, 2018. **12**(4): p. 305-314.
38. Provine, N.M. and P. Klenerman, *MAIT Cells in Health and Disease.* Annu Rev Immunol, 2020. **38**: p. 203-228.
39. Chu, P.S., et al., *C-C motif chemokine receptor 9 positive macrophages activate hepatic stellate cells and promote liver fibrosis in mice.* Hepatology, 2013. **58**(1): p. 337-50.
40. Lee, C.H., et al., *C/EBPδ drives interactions between human MAIT cells and endothelial cells that are important for extravasation.* Elife, 2018. **7**.
41. Nel, I., et al., *MAIT cells, guardians of skin and mucosa?* Mucosal Immunol, 2021. **14**(4): p. 803-814.

42. Hann, A., Y.H. Oo, and M. Perera, *Regulatory T-Cell Therapy in Liver Transplantation and Chronic Liver Disease.* Front Immunol, 2021. **12**: p. 719954.
43. Bozward, A.G., et al., *Gut-Liver Immune Traffic: Deciphering Immune-Pathogenesis to Underpin Translational Therapy.* Front Immunol, 2021. **12**: p. 711217.
44. Mehta, H., et al., *MAIT cells in liver inflammation and fibrosis.* Semin Immunopathol, 2022. **44**(4): p. 429-444.
45. Klenerman, P., T.S.C. Hinks, and J.E. Ussher, *Biological functions of MAIT cells in tissues.* Mol Immunol, 2021. **130**: p. 154-158.
46. Constantinides, M.G., et al., *MAIT cells are imprinted by the microbiota in early life and promote tissue repair.* Science, 2019. **366**(6464).
47. Leng, T., et al., *TCR and Inflammatory Signals Tune Human MAIT Cells to Exert Specific Tissue Repair and Effector Functions.* Cell Rep, 2019. **28**(12): p. 3077-3091 e5.
48. Salou, M. and O. Lantz, *A TCR-Dependent Tissue Repair Potential of MAIT Cells.* Trends Immunol, 2019. **40**(11): p. 975-977.
49. Hinks, T.S.C., et al., *Activation and In Vivo Evolution of the MAIT Cell Transcriptome in Mice and Humans Reveals Tissue Repair Functionality.* Cell Rep, 2019. **28**(12): p. 3249-3262 e5.
50. Vaishnavi, C., et al., *Estimation of endotoxin in infected bile from patients with biliary diseases.* Trop Gastroenterol, 2006. **27**(1): p. 22-5.
51. Hegde, P., et al., *Mucosal-associated invariant T cells are a profibrogenic immune cell population in the liver.* Nat Commun, 2018. **9**(1): p. 2146.
52. Mariotti, V., et al., *Animal models of biliary injury and altered bile acid metabolism.* Biochim Biophys Acta Mol Basis Dis, 2018. **1864**(4 Pt B): p. 1254-1261.
53. Strazzabosco, M., et al., *Pathophysiologic implications of innate immunity and autoinflammation in the biliary epithelium.* Biochim Biophys Acta Mol Basis Dis, 2018. **1864**(4 Pt B): p. 1374-1379.
54. Curbishley, S.M., et al., *CXCR 3 activation promotes lymphocyte transendothelial migration across human hepatic endothelium under fluid flow.* Am J Pathol, 2005. **167**(3): p. 887-99.
55. Lalor, P.F. and D.H. Adams, *Adhesion of lymphocytes to hepatic endothelium.* Mol Pathol, 1999. **52**(4): p. 214-9.
56. Lalor, P.F., et al., *Association between receptor density, cellular activation, and transformation of adhesive behavior of flowing lymphocytes binding to VCAM-1.* Eur J Immunol, 1997. **27**(6): p. 1422-6.
57. Grant, A.J., et al., *Homing of mucosal lymphocytes to the liver in the pathogenesis of hepatic complications of inflammatory bowel disease.* Lancet, 2002. **359**(9301): p. 150-7.
58. Heydtmann, M., et al., *CXC chemokine ligand 16 promotes integrin-mediated adhesion of liver-infiltrating lymphocytes to cholangiocytes and hepatocytes within the inflamed human liver.* J Immunol, 2005. **174**(2): p. 1055-62.
59. Grimaldi, D., et al., *Specific MAIT cell behaviour among innate-like T lymphocytes in critically ill patients with severe infections.* Intensive Care Med, 2014. **40**(2): p. 192-201.
60. Haga, K., et al., *MAIT cells are activated and accumulated in the inflamed mucosa of ulcerative colitis.* J Gastroenterol Hepatol, 2016. **31**(5): p. 965-72.
61. Kim, M., et al., *TNFα and IL-1β in the synovial fluid facilitate mucosal-associated invariant T (MAIT) cell migration.* Cytokine, 2017. **99**: p. 91-98.

62. Willing, A., et al., *CD8⁺MAIT cells infiltrate into the CNS and alterations in their blood frequencies correlate with IL-18 serum levels in multiple sclerosis.* Eur J Immunol, 2014. **44**(10): p. 3119-28.
63. Yuksel, M., et al., *Examining the Hepatic Immune System in Children With Liver Disease With Fine Needle Aspiration.* J Pediatr Gastroenterol Nutr, 2022. **74**(2): p. 200-207.
64. Yuksel, M., et al., *Standard immunosuppressive treatment reduces regulatory B cells in children with autoimmune liver disease.* Front Immunol, 2022. **13**: p. 1053216.
65. Huang, W., et al., *Mucosal-associated invariant T-cells are severely reduced and exhausted in humans with chronic HBV infection.* J Viral Hepat, 2020. **27**(11): p. 1096-1107.
66. Barathan, M., et al., *Peripheral loss of CD8(+) CD161(++) TCRVα7·2(+) mucosal-associated invariant T cells in chronic hepatitis C virus-infected patients.* Eur J Clin Invest, 2016. **46**(2): p. 170-80.
67. Bolte, F.J., et al., *Intra-Hepatic Depletion of Mucosal-Associated Invariant T Cells in Hepatitis C Virus-Induced Liver Inflammation.* Gastroenterology, 2017. **153**(5): p. 1392-1403 e2.
68. Spaan, M., et al., *Frequencies of Circulating MAIT Cells Are Diminished in Chronic HCV, HIV and HCV/HIV Co-Infection and Do Not Recover during Therapy.* PLoS One, 2016. **11**(7): p. e0159243.
69. Xue, H., et al., *Mucosal-associated invariant T cells in hepatitis B virus-related liver failure.* World J Gastroenterol, 2020. **26**(31): p. 4703-4717.
70. Yong, Y.K., et al., *Hyper-Expression of PD-1 Is Associated with the Levels of Exhausted and Dysfunctional Phenotypes of Circulating CD161(++)TCR iVα7.2(+) Mucosal-Associated Invariant T Cells in Chronic Hepatitis B Virus Infection.* Front Immunol, 2018. **9**: p. 472.
71. Boeijen, L.L., et al., *Mucosal-Associated Invariant T Cells Are More Activated in Chronic Hepatitis B, but Not Depleted in Blood: Reversal by Antiviral Therapy.* J Infect Dis, 2017. **216**(8): p. 969-976.
72. Li, W., et al., *Alcohol Abstinence Does Not Fully Reverse Abnormalities of Mucosal-Associated Invariant T Cells in the Blood of Patients With Alcoholic Hepatitis.* Clin Transl Gastroenterol, 2019. **10**(6): p. e00052.
73. Hengst, J., et al., *Nonreversible MAIT cell-dysfunction in chronic hepatitis C virus infection despite successful interferon-free therapy.* Eur J Immunol, 2016. **46**(9): p. 2204-10.
74. Hofmann, M. and R. Thimme, *MAIT be different-persisting dysfunction after DAA-mediated clearance of chronic hepatitis C virus infection.* Eur J Immunol, 2016. **46**(9): p. 2099-102.
75. Li, Y., et al., *Mucosal-Associated Invariant T Cells Improve Nonalcoholic Fatty Liver Disease Through Regulating Macrophage Polarization.* Front Immunol, 2018. **9**: p. 1994.
76. Magalhaes, I., et al., *Mucosal-associated invariant T cell alterations in obese and type 2 diabetic patients.* J Clin Invest, 2015. **125**(4): p. 1752-62.
77. Allali, S., et al., *Innate-like T cells in children with sickle cell disease.* PLoS One, 2019. **14**(6): p. e0219047.
78. Pisarska, M.M., et al., *Interleukin-17 producing mucosal associated invariant T cells - emerging players in chronic inflammatory diseases?* Eur J Immunol, 2020. **50**(8): p. 1098-1108.
79. Yan, J., et al., *MAIT Cells Promote Tumor Initiation, Growth, and Metastases via Tumor MR1.* Cancer Discov, 2020. **10**(1): p. 124-141.

80. Böttcher, K., et al., *MAIT cells are chronically activated in patients with autoimmune liver disease and promote profibrogenic hepatic stellate cell activation.* Hepatology, 2018. **68**(1): p. 172-186.
81. Chiba, A., G. Murayama, and S. Miyake, *Mucosal-Associated Invariant T Cells in Autoimmune Diseases.* Front Immunol, 2018. **9**: p. 1333.
82. Lamichhane, R., et al., *Human liver-derived MAIT cells differ from blood MAIT cells in their metabolism and response to TCR-independent activation.* Eur J Immunol, 2021. **51**(4): p. 879-892.
83. Zhang, X., et al., *Interleukin-26 promotes the proliferation and activation of hepatic stellate cells to exacerbate liver fibrosis by the TGF-β1/Smad2 signaling pathway.* Int J Clin Exp Pathol, 2019. **12**(12): p. 4271-4279.
84. Kong, X., et al., *Hepatoprotective and anti-fibrotic functions of interleukin-22: therapeutic potential for the treatment of alcoholic liver disease.* J Gastroenterol Hepatol, 2013. **28 Suppl 1**(0 1): p. 56-60.
85. Wang, K., et al., *Angelica sinensis polysaccharide attenuates CCl(4)-induced liver fibrosis via the IL-22/STAT3 pathway.* Int J Biol Macromol, 2020. **162**: p. 273-283.
86. Weng, H., et al., *IFN-gamma abrogates profibrogenic TGF-beta signaling in liver by targeting expression of inhibitory and receptor Smads.* J Hepatol, 2007. **46**(2): p. 295-303.
87. Ibidapo-Obe, O., et al., *Mucosal-Associated Invariant T Cells Redistribute to the Peritoneal Cavity During Spontaneous Bacterial Peritonitis and Contribute to Peritoneal Inflammation.* Cell Mol Gastroenterol Hepatol, 2020. **9**(4): p. 661-677.
88. Niehaus, C.E., et al., *MAIT Cells Are Enriched and Highly Functional in Ascites of Patients With Decompensated Liver Cirrhosis.* Hepatology, 2020. **72**(4): p. 1378-1393.
89. Keenan, B.P., L. Fong, and R.K. Kelley, *Immunotherapy in hepatocellular carcinoma: the complex interface between inflammation, fibrosis, and the immune response.* J Immunother Cancer, 2019. **7**(1): p. 267.
90. Yang, Y.M., S.Y. Kim, and E. Seki, *Inflammation and Liver Cancer: Molecular Mechanisms and Therapeutic Targets.* Semin Liver Dis, 2019. **39**(1): p. 26-42.
91. Duan, M., et al., *Activated and Exhausted MAIT Cells Foster Disease Progression and Indicate Poor Outcome in Hepatocellular Carcinoma.* Clin Cancer Res, 2019. **25**(11): p. 3304-3316.
92. Healy, K., et al., *Human MAIT cells endowed with HBV specificity are cytotoxic and migrate towards HBV-HCC while retaining antimicrobial functions.* JHEP Rep, 2021. **3**(4): p. 100318.
93. Mack, C.L., et al., *Diagnosis and Management of Autoimmune Hepatitis in Adults and Children: 2019 Practice Guidance and Guidelines From the American Association for the Study of Liver Diseases.* Hepatology, 2020. **72**(2): p. 671-722.
94. Trivedi, P.J. and G.M. Hirschfield, *Recent advances in clinical practice: epidemiology of autoimmune liver diseases.* Gut, 2021. **70**(10): p. 1989-2003.
95. Di Giorgio, A., et al., *Seamless Management of Juvenile Autoimmune Liver Disease: Long-Term Medical and Social Outcome.* J Pediatr, 2020. **218**: p. 121-129 e3.
96. Mieli-Vergani, G., et al., *Diagnosis and Management of Pediatric Autoimmune Liver Disease: ESPGHAN Hepatology Committee Position Statement.* J Pediatr Gastroenterol Nutr, 2018. **66**(2): p. 345-360.
97. Lleo, A., et al., *The Pathogenesis of Primary Biliary Cholangitis: A Comprehensive Review.* Semin Liver Dis, 2020. **40**(1): p. 34-48.
98. Trivedi, P.J. and G.M. Hirschfield, *Review article: overlap syndromes and autoimmune liver disease.* Aliment Pharmacol Ther, 2012. **36**(6): p. 517-33.

99. Boberg, K.M., et al., *Overlap syndromes: the International Autoimmune Hepatitis Group (IAIHG) position statement on a controversial issue.* J Hepatol, 2011. **54**(2): p. 374-85.
100. Kerkar, N. and A. Chan, *Autoimmune Hepatitis, Sclerosing Cholangitis, and Autoimmune Sclerosing Cholangitis or Overlap Syndrome.* Clin Liver Dis, 2018. **22**(4): p. 689-702.
101. Roepe, I.G., et al., *Presentation and Outcomes of Autoimmune Hepatitis Type 1 and Type 2 in Children: A Single-center Study.* J Pediatr Gastroenterol Nutr, 2021. **72**(1): p. 101-107.
102. Ferri Liu, P.M., et al., *Autoimmune hepatitis in childhood: the role of genetic and immune factors.* World J Gastroenterol, 2013. **19**(28): p. 4455-63.
103. M, L.V. and N. Reau, *Diagnosis and Management of Autoimmune Hepatitis in Adults and Children: A Patient-Friendly Summary of the 2019 AASLD Guidelines.* Clin Liver Dis (Hoboken), 2021. **17**(2): p. 85-89.
104. *EASL Clinical Practice Guidelines: Autoimmune hepatitis.* J Hepatol, 2015. **63**(4): p. 971-1004.
105. Hennes, E.M., et al., *Simplified criteria for the diagnosis of autoimmune hepatitis.* Hepatology, 2008. **48**(1): p. 169-76.
106. Deneau, M.R., et al., *The natural history of primary sclerosing cholangitis in 781 children: A multicenter, international collaboration.* Hepatology, 2017. **66**(2): p. 518-527.
107. Gregorio, G.V., et al., *Autoimmune hepatitis/sclerosing cholangitis overlap syndrome in childhood: a 16-year prospective study.* Hepatology, 2001. **33**(3): p. 544-53.
108. Fricker, Z.P. and D.R. Lichtenstein, *Primary Sclerosing Cholangitis: A Concise Review of Diagnosis and Management.* Dig Dis Sci, 2019. **64**(3): p. 632-642.
109. Di Giorgio, A., D. Vergani, and G. Mieli-Vergani, *Cutting edge issues in juvenile sclerosing cholangitis.* Dig Liver Dis, 2022. **54**(4): p. 417-427.
110. Mataya, L., N. Patel, and R.K. Azzam, *Autoimmune Liver Diseases in Children.* Pediatr Ann, 2018. **47**(11): p. e452-e457.
111. Wiecek, S., et al., *Analysis of the Clinical Course of Primary Sclerosing Cholangitis in Paediatric Population-Single Center Study.* Medicina (Kaunas), 2021. **57**(7).
112. Carbone, M. and J.M. Neuberger, *Autoimmune liver disease, autoimmunity and liver transplantation.* J Hepatol, 2014. **60**(1): p. 210-23.
113. Chapman, M.H., et al., *British Society of Gastroenterology and UK-PSC guidelines for the diagnosis and management of primary sclerosing cholangitis.* Gut, 2019. **68**(8): p. 1356-1378.
114. Di Giorgio, A., et al., *Biliary features in liver histology of children with autoimmune liver disease.* Hepatol Int, 2019. **13**(4): p. 510-518.
115. Tanaka, A., *Autoimmune Hepatitis: 2019 Update.* Gut Liver, 2020. **14**(4): p. 430-438.
116. Laborda, T.J., et al., *Treatment of primary sclerosing cholangitis in children.* World J Hepatol, 2019. **11**(1): p. 19-36.
117. Komori, A., *Recent updates on the management of autoimmune hepatitis.* Clin Mol Hepatol, 2021. **27**(1): p. 58-69.
118. Czaja, A.J., *Advancing Biologic Therapy for Refractory Autoimmune Hepatitis.* Dig Dis Sci, 2022. **67**(11): p. 4979-5005.
119. Terziroli Beretta-Piccoli, B., G. Mieli-Vergani, and D. Vergani, *Autoimmune hepatitis: Standard treatment and systematic review of alternative treatments.* World J Gastroenterol, 2017. **23**(33): p. 6030-6048.

120. Milkiewicz, P., et al., *Primary Sclerosing Cholangitis With Features of Autoimmune Hepatitis: Exploring the Global Variation in Management.* Hepatol Commun, 2020. **4**(3): p. 399-408.
121. Deneau, M., et al., *Primary sclerosing cholangitis, autoimmune hepatitis, and overlap in Utah children: epidemiology and natural history.* Hepatology, 2013. **58**(4): p. 1392-400.
122. Ben Merabet, Y., et al., *Sustained Remission After Treatment Withdrawal in Autoimmune Hepatitis: A Multicenter Retrospective Study.* Dig Dis Sci, 2021. **66**(6): p. 2107-2117.
123. Çavuş, B., et al., *Is there any predictor for relapse after treatment withdrawal in autoimmune hepatitis patients in the real life?* Int J Immunopathol Pharmacol, 2022. **36**: p. 3946320221077860.
124. Deneau, M., et al., *Outcome after discontinuation of immunosuppression in children with autoimmune hepatitis: a population-based study.* J Pediatr, 2014. **164**(4): p. 714-719 e2.
125. Chen, Z., et al., *CXCL12-CXCR4-Mediated Chemotaxis Supports Accumulation of Mucosal-Associated Invariant T Cells Into the Liver of Patients With PBC.* Front Immunol, 2021. **12**: p. 578548.
126. Renand, A., et al., *Immune Alterations in Patients With Type 1 Autoimmune Hepatitis Persist Upon Standard Immunosuppressive Treatment.* Hepatol Commun, 2018. **2**(8): p. 968-981.
127. von Seth, E., et al., *Primary sclerosing cholangitis leads to dysfunction and loss of MAIT cells.* Eur J Immunol, 2018. **48**(12): p. 1997-2004.
128. Ancona, G., et al., *The Interplay between Gut Microbiota and the Immune System in Liver Transplant Recipients and Its Role in Infections.* Infect Immun, 2021. **89**(11): p. e0037621.
129. Zheng, Z. and B. Wang, *The Gut-Liver Axis in Health and Disease: The Role of Gut Microbiota-Derived Signals in Liver Injury and Regeneration.* Front Immunol, 2021. **12**: p. 775526.
130. Berglin, L., et al., *In situ characterization of intrahepatic non-parenchymal cells in PSC reveals phenotypic patterns associated with disease severity.* PLoS One, 2014. **9**(8): p. e105375.
131. Setsu, T., et al., *Persistent reduction of mucosal-associated invariant T cells in primary biliary cholangitis.* J Gastroenterol Hepatol, 2018. **33**(6): p. 1286-1294.
132. Jiang, X., et al., *The immunobiology of mucosal-associated invariant T cell (MAIT) function in primary biliary cholangitis: Regulation by cholic acid-induced Interleukin-7.* J Autoimmun, 2018. **90**: p. 64-75.
133. Graham, J.J., et al., *Aberrant hepatic trafficking of gut-derived T cells is not specific to primary sclerosing cholangitis.* Hepatology, 2022. **75**(3): p. 518-530.
134. Quraishi, M.N., et al., *The gut-adherent microbiota of PSC-IBD is distinct to that of IBD.* Gut, 2017. **66**(2): p. 386-388.
135. Serriari, N.E., et al., *Innate mucosal-associated invariant T (MAIT) cells are activated in inflammatory bowel diseases.* Clin Exp Immunol, 2014. **176**(2): p. 266-74.
136. Alabraba, E.B., et al., *Coculture of human liver macrophages and cholangiocytes leads to CD40-dependent apoptosis and cytokine secretion.* Hepatology, 2008. **47**(2): p. 552-62.
137. Humphreys, E.H., et al., *Primary and malignant cholangiocytes undergo CD40 mediated Fas dependent apoptosis, but are insensitive to direct activation with exogenous Fas ligand.* PLoS One, 2010. **5**(11): p. e14037.

138. Maroni, L., et al., *Functional and structural features of cholangiocytes in health and disease.* Cell Mol Gastroenterol Hepatol, 2015. **1**(4): p. 368-380.
139. Marchesi, J.R., et al., *The gut microbiota and host health: a new clinical frontier.* Gut, 2016. **65**(2): p. 330-9.
140. Schrumpf, E., et al., *The gut microbiota contributes to a mouse model of spontaneous bile duct inflammation.* J Hepatol, 2017. **66**(2): p. 382-389.
141. Shaheen, W.A., M.N. Quraishi, and T.H. Iqbal, *Gut microbiome and autoimmune disorders.* Clin Exp Immunol, 2022. **209**(2): p. 161-174.
142. Gargano, F., et al., *Proinflammatory mucosal-associated invariant CD8+ T cells react to gut flora yeasts and infiltrate multiple sclerosis brain.* Front Immunol, 2022. **13**: p. 890298.
143. Torre, P., et al., *Mucosal-Associated Invariant T Cells in T-Cell Non-Hodgkin Lymphomas: A Case Series.* Cancers (Basel), 2022. **14**(12).
144. Hartley, J., A. Harnden, and D. Kelly, *Biliary atresia.* BMJ, 2010. **340**: p. c2383.
145. Lakshminarayanan, B. and M. Davenport, *Biliary atresia: A comprehensive review.* J Autoimmun, 2016. **73**: p. 1-9.
146. Guo, C., et al., *Combinatory effects of hepatic CD8+ and NK lymphocytes in bile duct injury from biliary atresia.* Pediatr Res, 2012. **71**(6): p. 638-44.
147. Zheng, S., et al., *CD8+ T lymphocyte response against extrahepatic biliary epithelium is activated by epitopes within NSP4 in experimental biliary atresia.* Am J Physiol Gastrointest Liver Physiol, 2014. **307**(2): p. G233-40.
148. Hill, R., et al., *Th-17 cells infiltrate the liver in human biliary atresia and are related to surgical outcome.* J Pediatr Surg, 2015. **50**(8): p. 1297-303.
149. Moris, D., L. Lu, and S. Qian, *Mechanisms of liver-induced tolerance.* Curr Opin Organ Transplant, 2017. **22**(1): p. 71-78.
150. Schramm, C., Y.H. Oo, and A.W. Lohse, *Tolerance and autoimmunity in the liver.* Semin Immunopathol, 2022. **44**(4): p. 393-395.
151. Longhi, M.S., G. Mieli-Vergani, and D. Vergani, *Regulatory T cells in autoimmune hepatitis: an updated overview.* J Autoimmun, 2021. **119**: p. 102619.
152. Osei-Bordom, D., A.G. Bozward, and Y.H. Oo, *The hepatic microenvironment and regulatory T cells.* Cell Immunol, 2020. **357**: p. 104195.
153. Assis, D.N., *Immunopathogenesis of Autoimmune Hepatitis.* Clin Liver Dis (Hoboken), 2020. **15**(3): p. 129-132.
154. Benseler, V., et al., *Hepatocyte entry leads to degradation of autoreactive CD8 T cells.* Proc Natl Acad Sci U S A, 2011. **108**(40): p. 16735-40.
155. Sierro, F., et al., *Suicidal emperipolesis: a process leading to cell-in-cell structures, T cell clearance and immune homeostasis.* Curr Mol Med, 2015. **15**(9): p. 819-27.
156. Davies, S.P., et al., *Hepatocytes Delete Regulatory T Cells by Enclysis, a CD4(+) T Cell Engulfment Process.* Cell Rep, 2019. **29**(6): p. 1610-1620 e4.
157. Davies, S.P., et al., *Cell-in-Cell Structures in the Liver: A Tale of Four E's.* Front Immunol, 2020. **11**: p. 650.
158. Zhao, S.X., et al., *Emperipolesis mediated by CD8(+) T cells correlates with biliary epithelia cell injury in primary biliary cholangitis.* J Cell Mol Med, 2020. **24**(2): p. 1268-1275.
159. Aghabi, Y.O., et al., *Targeting Enclysis in Liver Autoimmunity, Transplantation, Viral Infection and Cancer.* Front Immunol, 2021. **12**: p. 662134.
160. Kelly, D., M. Samyn, and K.B. Schwarz, *Biliary Atresia in Adolescence and Adult Life: Medical, Surgical and Psychological Aspects.* J Clin Med, 2023. **12**(4).
161. Scaravaglio, M., M. Carbone, and P. Invernizzi, *Autoimmune liver diseases.* Minerva Gastroenterol (Torino), 2023. **69**(1): p. 7-9.

162. Kubes, P. and C. Jenne, *Immune Responses in the Liver.* Annu Rev Immunol, 2018. **36**: p. 247-277.
163. Richardson, N., et al., *Challenges and opportunities in achieving effective regulatory T cell therapy in autoimmune liver disease.* Semin Immunopathol, 2022. **44**(4): p. 461-474.
164. Vuerich, M., et al., *Dysfunctional Immune Regulation in Autoimmune Hepatitis: From Pathogenesis to Novel Therapies.* Front Immunol, 2021. **12**: p. 746436.
165. Liang, M., et al., *The Imbalance between Foxp3(+)Tregs and Th1/Th17/Th22 Cells in Patients with Newly Diagnosed Autoimmune Hepatitis.* J Immunol Res, 2018. **2018**: p. 3753081.
166. Schwinge, D., et al., *Dysfunction of hepatic regulatory T cells in experimental sclerosing cholangitis is related to IL-12 signaling.* J Hepatol, 2017. **66**(4): p. 798-805.
167. Sebode, M., et al., *Reduced FOXP3(+) regulatory T cells in patients with primary sclerosing cholangitis are associated with IL2RA gene polymorphisms.* J Hepatol, 2014. **60**(5): p. 1010-6.
168. Liu, L.W., et al., *[Dysregulated proportion of intrahepatic Treg cells and Th17 along with CD8+ T lymphocytes drives disease progression after kasai biliary atresia surgery].* Zhonghua Gan Zang Bing Za Zhi, 2021. **29**(2): p. 150-155.
169. Wen, J., et al., *Interactions between Th1 cells and Tregs affect regulation of hepatic fibrosis in biliary atresia through the IFN-γ/STAT1 pathway.* Cell Death Differ, 2017. **24**(6): p. 997-1006.
170. Tucker, R.M., et al., *Regulatory T cells inhibit Th1 cell-mediated bile duct injury in murine biliary atresia.* J Hepatol, 2013. **59**(4): p. 790-6.
171. Rastogi, V., et al., *Emperipolesis - a review.* J Clin Diagn Res, 2014. **8**(12): p. ZM01-2.
172. Hu, Y., et al., *Emperipolesis is a potential histological hallmark associated with chronic hepatitis B.* Curr Mol Med, 2015. **15**(9): p. 873-81.
173. Mitsialis, V., et al., *Single-Cell Analyses of Colon and Blood Reveal Distinct Immune Cell Signatures of Ulcerative Colitis and Crohn's Disease.* Gastroenterology, 2020. **159**(2): p. 591-608 e10.
174. Paleja, B., et al., *Systemic Sclerosis Perturbs the Architecture of the Immunome.* Front Immunol, 2020. **11**: p. 1602.
175. Dai, W., et al., *Influence of adipose tissue immune dysfunction on childhood obesity.* Cytokine Growth Factor Rev, 2022. **65**: p. 27-38.
176. Warner, S., et al., *Understanding COVID-19: are children the key?* BMJ Paediatr Open, 2021. **5**(1): p. e001063.
177. Garner, L.C., P. Klenerman, and N.M. Provine, *Insights Into Mucosal-Associated Invariant T Cell Biology From Studies of Invariant Natural Killer T Cells.* Front Immunol, 2018. **9**: p. 1478.
178. Chandra, S., et al., *Development of Asthma in Inner-City Children: Possible Roles of MAIT Cells and Variation in the Home Environment.* J Immunol, 2018. **200**(6): p. 1995-2003.
179. Malka-Ruimy, C., et al., *Mucosal-Associated Invariant T Cell Levels Are Reduced in the Peripheral Blood and Lungs of Children With Active Pulmonary Tuberculosis.* Front Immunol, 2019. **10**: p. 206.
180. Tian, J., et al., *Peripheral and intestinal mucosal-associated invariant T cells in premature infants with necrotizing enterocolitis.* Front Pharmacol, 2022. **13**: p. 1008080.

181. Magalhaes, I., M. Solders, and H. Kaipe, *MAIT Cells in Health and Disease.* Methods Mol Biol, 2020. **2098**: p. 3-21.
182. Leeansyah, E., et al., *Activation, exhaustion, and persistent decline of the antimicrobial MR1-restricted MAIT-cell population in chronic HIV-1 infection.* Blood, 2013. **121**(7): p. 1124-35.
183. Zinser, M.E., et al., *Human MAIT cells show metabolic quiescence with rapid glucose-dependent upregulation of granzyme B upon stimulation.* Immunol Cell Biol, 2018. **96**(6): p. 666-674.
184. Berry, S.P.D., et al., *The role of IL-17 and anti-IL-17 agents in the immunopathogenesis and management of autoimmune and inflammatory diseases.* Int Immunopharmacol, 2022. **102**: p. 108402.
185. Carnero Contentti, E., M.F. Farez, and J. Correale, *Mucosal-Associated Invariant T Cell Features and TCR Repertoire Characteristics During the Course of Multiple Sclerosis.* Front Immunol, 2019. **10**: p. 2690.
186. Youngs, J., et al., *Identification of immune correlates of fatal outcomes in critically ill COVID-19 patients.* PLoS Pathog, 2021. **17**(9): p. e1009804.
187. Menon, S.S., et al., *Ki-67 protein as a tumour proliferation marker.* Clin Chim Acta, 2019. **491**: p. 39-45.
188. Sun, X. and P.D. Kaufman, *Ki-67: more than a proliferation marker.* Chromosoma, 2018. **127**(2): p. 175-186.
189. Chen, S., et al., *Reciprocal alterations in circulating and hepatic gamma-delta T cells in patients with primary biliary cholangitis.* Hepatol Int, 2022. **16**(1): p. 195-206.
190. Clarke, S.R., *The critical role of CD40/CD40L in the CD4-dependent generation of CD8+ T cell immunity.* J Leukoc Biol, 2000. **67**(5): p. 607-14.
191. Dulong, J., et al., *CD40L-expressing CD4(+) T cells prime adipose-derived stromal cells to produce inflammatory chemokines.* Cytotherapy, 2022. **24**(5): p. 500-507.
192. Chen, P., et al., *Circulating Mucosal-Associated Invariant T Cells in a Large Cohort of Healthy Chinese Individuals From Newborn to Elderly.* Front Immunol, 2019. **10**: p. 260.
193. Novak, J., et al., *The decrease in number and change in phenotype of mucosal-associated invariant T cells in the elderly and differences in men and women of reproductive age.* Scand J Immunol, 2014. **80**(4): p. 271-5.
194. Dias, J., et al., *The CD4(-)CD8(-) MAIT cell subpopulation is a functionally distinct subset developmentally related to the main CD8(+) MAIT cell pool.* Proc Natl Acad Sci U S A, 2018. **115**(49): p. E11513-E11522.
195. Booth, J.S., et al., *Mucosal-Associated Invariant T Cells in the Human Gastric Mucosa and Blood: Role in Helicobacter pylori Infection.* Front Immunol, 2015. **6**: p. 466.
196. Khaitan, A., et al., *HIV-Infected Children Have Lower Frequencies of CD8+ Mucosal-Associated Invariant T (MAIT) Cells that Correlate with Innate, Th17 and Th22 Cell Subsets.* PLoS One, 2016. **11**(8): p. e0161786.
197. Leung, D.T., et al., *Circulating mucosal associated invariant T cells are activated in Vibrio cholerae O1 infection and associated with lipopolysaccharide antibody responses.* PLoS Negl Trop Dis, 2014. **8**(8): p. e3076.
198. Dunne, M.R., et al., *Persistent changes in circulating and intestinal γδ T cell subsets, invariant natural killer T cells and mucosal-associated invariant T cells in children and adults with coeliac disease.* PLoS One, 2013. **8**(10): p. e76008.
199. Ozkaya, M., et al., *The number and activity of CD3(+)TCR Vα7.2(+)CD161(+) cells are increased in children with acute rheumatic fever.* Int J Cardiol, 2021. **333**: p. 174-183.

200. Jiang, X., et al., *MAIT cells ameliorate liver fibrosis by enhancing the cytotoxicity of NK cells in cholestatic murine models.* Liver Int, 2022. **42**(12): p. 2743-2758.
201. Kumar, V. and A. Ahmad, *Role of MAIT cells in the immunopathogenesis of inflammatory diseases: New players in old game.* Int Rev Immunol, 2018. **37**(2): p. 90-110.
202. Swarbrick, G.M., et al., *Postnatal Expansion, Maturation, and Functionality of MR1T Cells in Humans.* Front Immunol, 2020. **11**: p. 556695.
203. Huang, W., et al., *Activated but impaired IFN-γ production of mucosal-associated invariant T cells in patients with hepatocellular carcinoma.* J Immunother Cancer, 2021. **9**(11).
204. Cho, Y.N., et al., *Mucosal-associated invariant T cell deficiency in systemic lupus erythematosus.* J Immunol, 2014. **193**(8): p. 3891-901.
205. Koppejan, H., et al., *Altered composition and phenotype of mucosal-associated invariant T cells in early untreated rheumatoid arthritis.* Arthritis Res Ther, 2019. **21**(1): p. 3.
206. Coakley, J.D., et al., *Innate Lymphocyte Th1 and Th17 Responses in Elderly Hospitalised Patients with Infection and Sepsis.* Vaccines (Basel), 2020. **8**(2).
207. Terpstra, M.L., et al., *Circulating mucosal-associated invariant T cells in subjects with recurrent urinary tract infections are functionally impaired.* Immun Inflamm Dis, 2020. **8**(1): p. 80-92.
208. Ueyama, A., et al., *Potential role of IL-17-producing CD4/CD8 double negative αβ T cells in psoriatic skin inflammation in a TPA-induced STAT3C transgenic mouse model.* J Dermatol Sci, 2017. **85**(1): p. 27-35.
209. Castro, G., et al., *RORγt and RORα signature genes in human Th17 cells.* PLoS One, 2017. **12**(8): p. e0181868.
210. Gao, M.G., et al., *The Potential Roles of Mucosa-Associated Invariant T Cells in the Pathogenesis of Gut Graft-Versus-Host Disease After Hematopoietic Stem Cell Transplantation.* Front Immunol, 2021. **12**: p. 720354.
211. Lamb, D., et al., *RORγt inhibitors block both IL-17 and IL-22 conferring a potential advantage over anti-IL-17 alone to treat severe asthma.* Respir Res, 2021. **22**(1): p. 158.
212. Yamana, S., et al., *Mucosal-associated invariant T cells have therapeutic potential against ocular autoimmunity.* Mucosal Immunol, 2022. **15**(2): p. 351-361.
213. Wu, Y., et al., *Interleukin 22 in Liver Injury, Inflammation and Cancer.* Int J Biol Sci, 2020. **16**(13): p. 2405-2413.
214. Caparrós, E. and R. Francés, *The Interleukin-20 Cytokine Family in Liver Disease.* Front Immunol, 2018. **9**: p. 1155.
215. Gérart, S., et al., *Human iNKT and MAIT cells exhibit a PLZF-dependent proapoptotic propensity that is counterbalanced by XIAP.* Blood, 2013. **121**(4): p. 614-23.
216. Yong, Y.K., et al., *Decrease of CD69 levels on TCR Vα7.2(+)CD4(+) innate-like lymphocytes is associated with impaired cytotoxic functions in chronic hepatitis B virus-infected patients.* Innate Immun, 2017. **23**(5): p. 459-467.
217. Dias, J., et al., *Chronic hepatitis delta virus infection leads to functional impairment and severe loss of MAIT cells.* J Hepatol, 2019. **71**(2): p. 301-312.
218. Boisvert, J., et al., *Liver-infiltrating lymphocytes in end-stage hepatitis C virus: subsets, activation status, and chemokine receptor phenotypes.* J Hepatol, 2003. **38**(1): p. 67-75.
219. Dusseaux, M., et al., *Human MAIT cells are xenobiotic-resistant, tissue-targeted, CD161hi IL-17-secreting T cells.* Blood, 2011. **117**(4): p. 1250-9.

220. Nakamoto, N., *[Role of inflammatory macrophages and CCR9/CCL25 chemokine axis in the pathogenesis of liver injury as a therapeutic target].* Nihon Rinsho Meneki Gakkai Kaishi, 2016. **39**(5): p. 460-467.
221. Oo, Y.H., et al., *CXCR3-dependent recruitment and CCR6-mediated positioning of Th-17 cells in the inflamed liver.* J Hepatol, 2012. **57**(5): p. 1044-51.
222. Zhang, Y., et al., *Persistent deficiency of mucosa-associated invariant T (MAIT) cells during alcohol-related liver disease.* Cell Biosci, 2021. **11**(1): p. 148.
223. Azzout, M., et al., *IL-33 Enhances IFNγ and TNFα Production by Human MAIT Cells: A New Pro-Th1 Effect of IL-33.* Int J Mol Sci, 2021. **22**(19).
224. Wang, J.J., et al., *Mucosal-associated invariant T cells are reduced and functionally immature in the peripheral blood of primary Sjögren's syndrome patients.* Eur J Immunol, 2016. **46**(10): p. 2444-2453.
225. Afford, S.C., et al., *CD40 activation-induced, Fas-dependent apoptosis and NF-kappaB/AP-1 signaling in human intrahepatic biliary epithelial cells.* FASEB J, 2001. **15**(13): p. 2345-54.
226. So, T. and N. Ishii, *The TNF-TNFR Family of Co-signal Molecules.* Adv Exp Med Biol, 2019. **1189**: p. 53-84.
227. Idriss, H.T. and J.H. Naismith, *TNF alpha and the TNF receptor superfamily: structure-function relationship(s).* Microsc Res Tech, 2000. **50**(3): p. 184-95.
228. O'Keeffe, M., W.H. Mok, and K.J. Radford, *Human dendritic cell subsets and function in health and disease.* Cell Mol Life Sci, 2015. **72**(22): p. 4309-25.
229. Ueno, H., et al., *Dendritic cell subsets in health and disease.* Immunol Rev, 2007. **219**: p. 118-42.
230. Wirtz, T.H., E.F. Brandt, and M.L. Berres, *Liver DCs in health and disease.* Int Rev Cell Mol Biol, 2019. **348**: p. 263-299.
231. Soltani, S., M. Mahmoudi, and E. Farhadi, *Dendritic Cells Currently under the Spotlight; Classification and Subset Based upon New Markers.* Immunol Invest, 2021. **50**(6): p. 646-661.
232. Thomson, A.W., et al., *Immunobiology of liver dendritic cells.* Immunol Cell Biol, 2002. **80**(1): p. 65-73.
233. Alter, G., J.M. Malenfant, and M. Altfeld, *CD107a as a functional marker for the identification of natural killer cell activity.* J Immunol Methods, 2004. **294**(1-2): p. 15-22.
234. Lorenzo-Herrero, S., et al., *CD107a Degranulation Assay to Evaluate Immune Cell Antitumor Activity.* Methods Mol Biol, 2019. **1884**: p. 119-130.
235. Karnell, J.L., et al., *Targeting the CD40-CD40L pathway in autoimmune diseases: Humoral immunity and beyond.* Adv Drug Deliv Rev, 2019. **141**: p. 92-103.
236. Lezmi, G., et al., *Circulating IL-17-producing mucosal-associated invariant T cells (MAIT) are associated with symptoms in children with asthma.* Clin Immunol, 2018. **188**: p. 7-11.
237. Lu, B., et al., *IL-17 production by tissue-resident MAIT cells is locally induced in children with pneumonia.* Mucosal Immunol, 2020. **13**(5): p. 824-835.
238. He, Y., et al., *Immunopathobiology and therapeutic targets related to cytokines in liver diseases.* Cell Mol Immunol, 2021. **18**(1): p. 18-37.
239. Liu, T., et al., *MicroRNA-155 Regulates MAIT1 and MAIT17 Cell Differentiation.* Front Cell Dev Biol, 2021. **9**: p. 670531.
240. Shey, M.S., et al., *Contribution of APCs to mucosal-associated invariant T cell activation in infectious disease and cancer.* Innate Immun, 2018. **24**(4): p. 192-202.

Figure 1a. Intrahepatic MAIT cells express the semi-invariant T cell receptor Vα7.2 and the C-type lectin-like receptor CD161. They have come to be defined as CD3+ Vα7.2+ CD161++. Cell surface expression of the homing chemokine receptors CCR2, CCR5, CCR6, CCR9 and CXCR6 has been described. Known MAIT cell transcription factors include Tbet, RORγt, PLZF and the multidrug resistance transporter ABCB1. MAIT cells express a range of cytokine receptors like interleukin-12 receptor (IL-12R) and IL-18R which can trigger MAIT cell activation in an MR1-independent (cytokine dependent) manner.

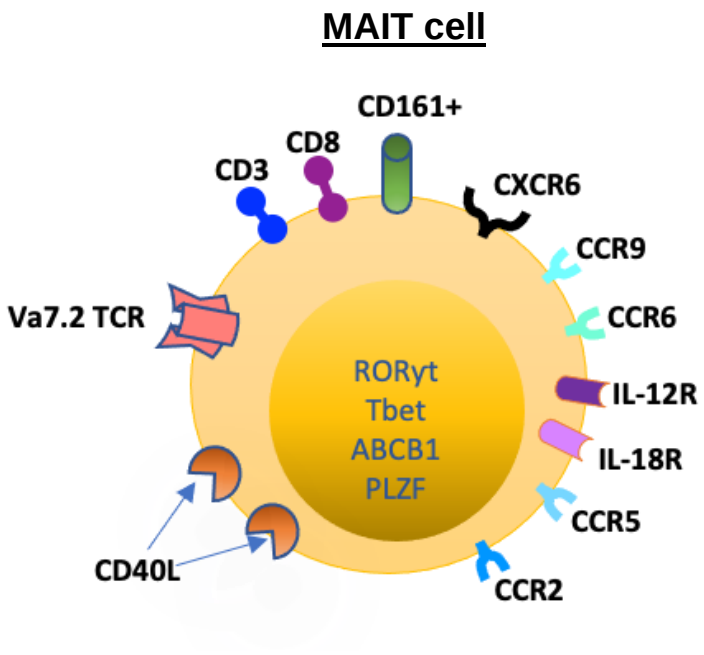

201

Figure 1b. Cholangiocytes possess the MHC class-1 related molecule, MR1. The semi-invariant T cell receptor Vα7.2 is restricted by ligands presented by MR1, which binds to microbial-derived vitamin B metabolites in its antigen presenting cleft. In the illustration, a cholangiocyte (green) presents a microbial vitamin B ligand via the MR1 molecule which then activates the MAIT cell (yellow) via restriction of the TCR Vα7.2.

The activated MAIT cell releases the proinflammatory cytokines IFNγ, TNFα, IL-17 and de- granulate Granzymes and Perforin

(Atif et al, Hepatol Int 2018).

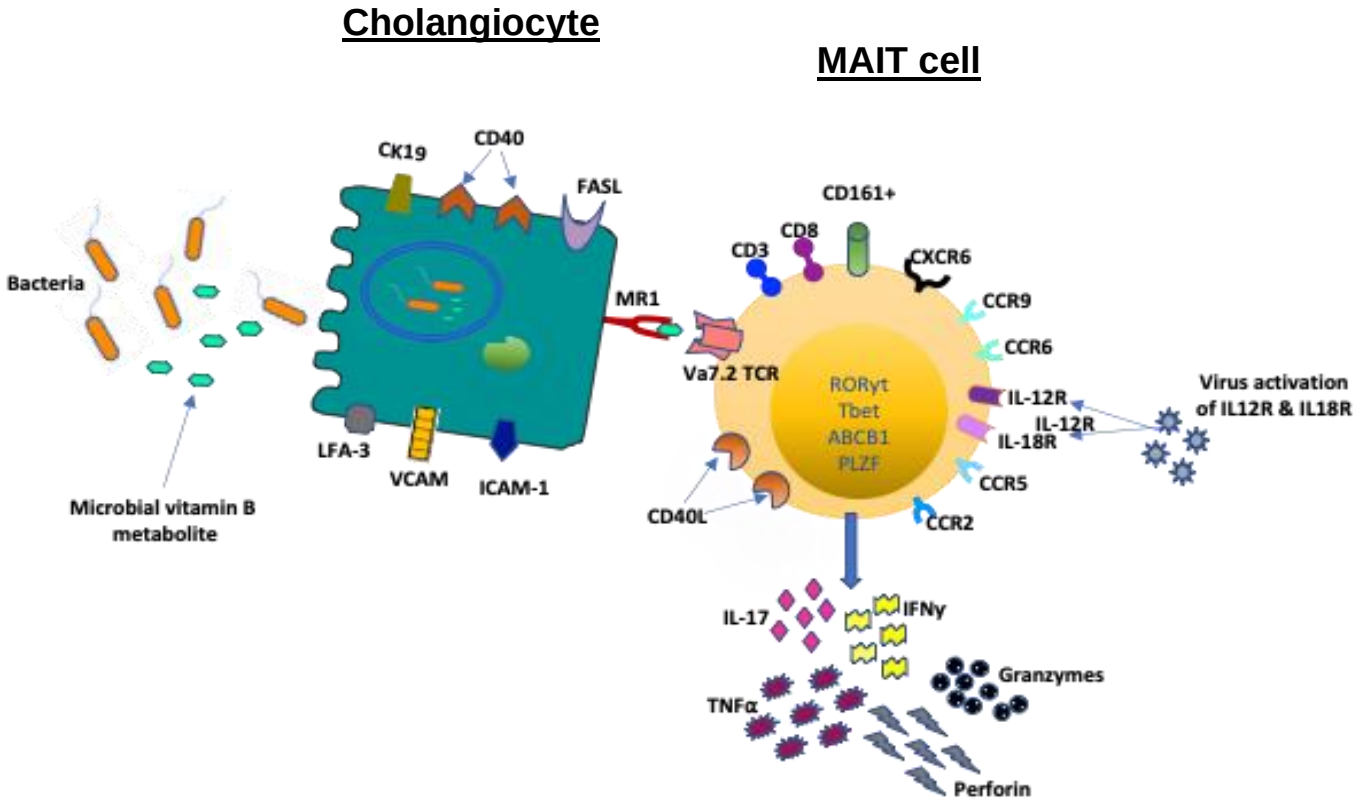

202

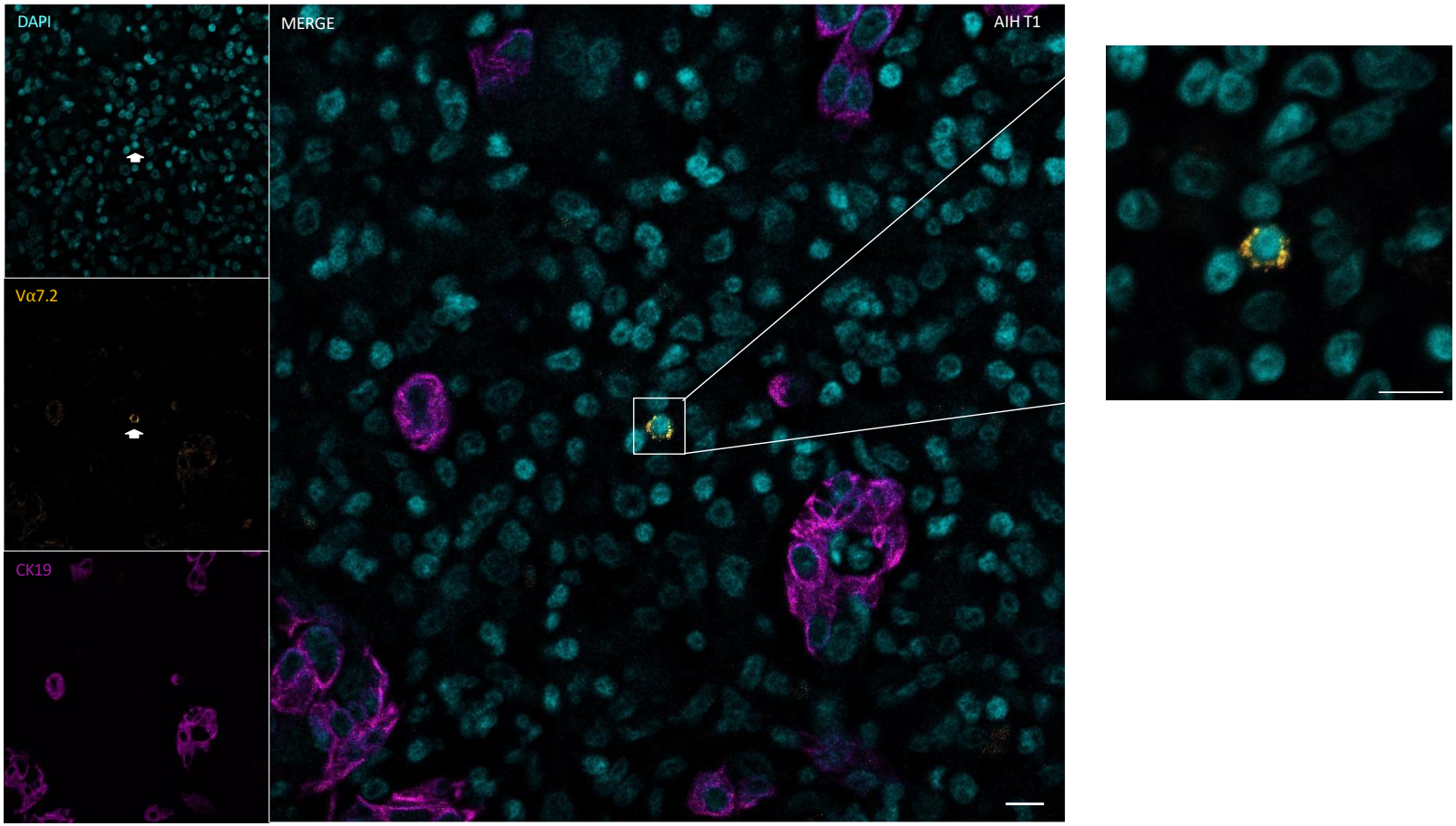

Figure 3a. Confocal micrograph of a section of liver explant tissue from a paediatric patient with autoimmune hepatitis type 1 (AIH T1).
Clear and well-defined cell surface immunofluorescence (IF) staining of the semi-invariant T cell receptor, TCR Vα7.2+ (orange), is shown (MERGE), with the inset displaying the magnified image. The nuclei are stained with 4′,6-diamidino-2-phenylindole (DAPI, blue) and the bile ducts with CK19, a biliary epithelial cell marker (magenta). Individual channels are displayed on the left hand side. Arrows in the individual channels point to the area of TCR Vα7.2+ staining observed in the MERGE image; (Vα7.2+) and cyan (DAPI) channels. Scale bars: 10μm.

203

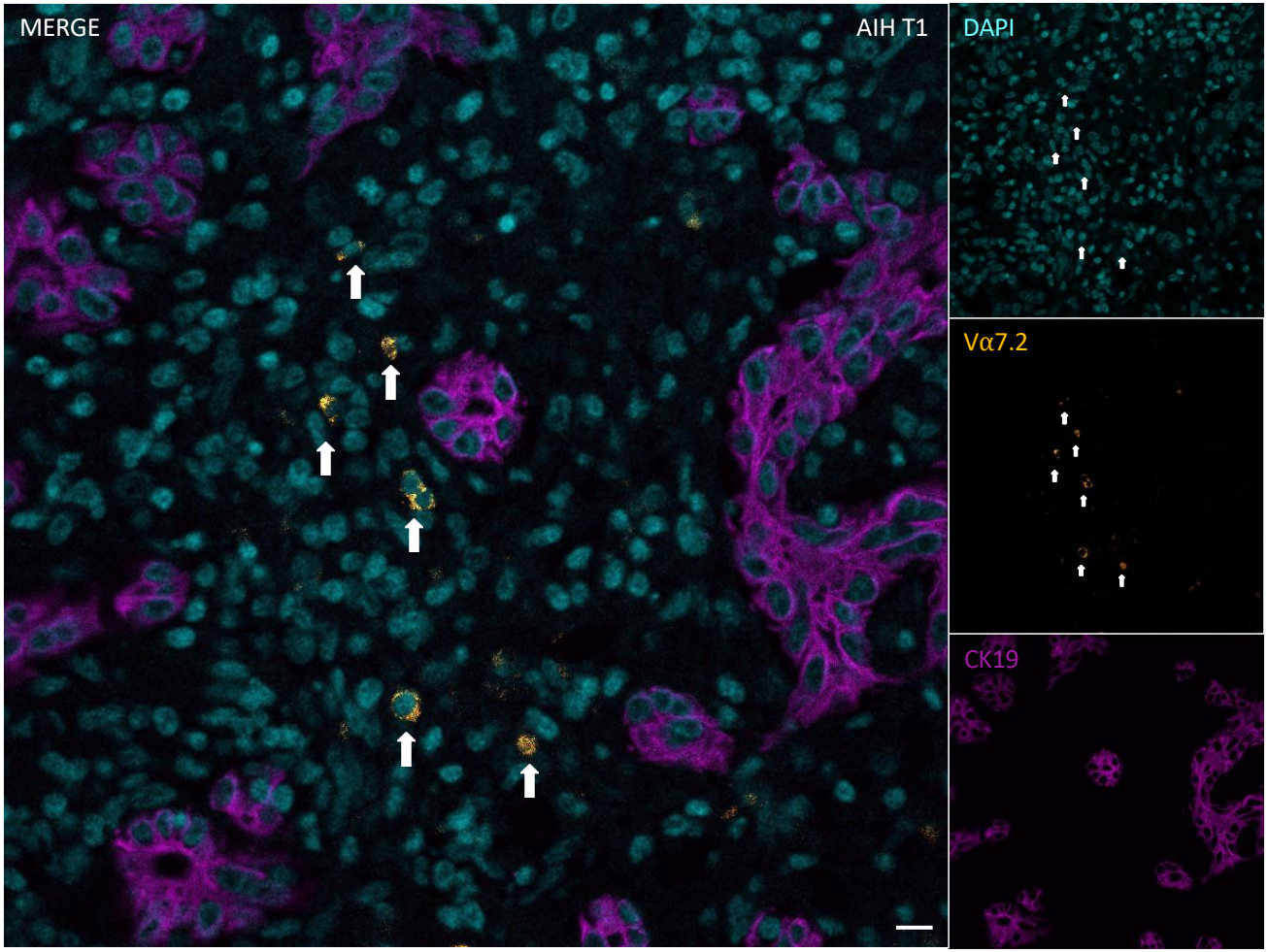

Figure 3b. Confocal micrograph displaying multiple cell surface TCR Vα7.2+ staining (orange) in an area of interface hepatitis in the liver explant of a second paediatric patient with autoimmune hepatitis type 1 (AIH T1). IF staining of TCR Vα7.2+ (orange), CK19 (magenta) and all nucleated cells in DAPI (cyan). Individual channels are displayed on the right-hand side. Arrows in the individual channels point to the area of TCR Vα7.2+ staining observed in the MERGE image. Scale bars: 10μm.

204

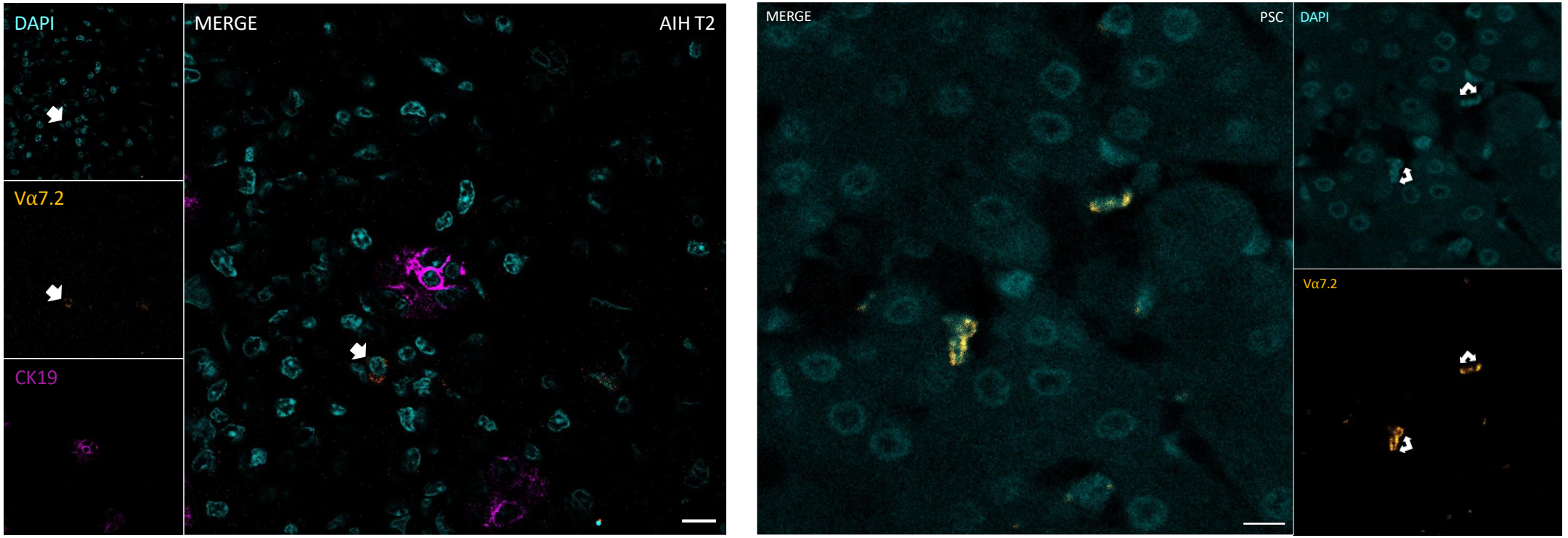

Figure 3c. Confocal micrographs of liver explant tissue from a child with AIH T2 (left) and a child with PSC (right). IF staining of TCR Vα7.2+ (orange), CK19 (magenta) and nucleated cells in DAPI (cyan) is shown. Multiple IF staining of Vα7.2+ MAIT cells are seen from the PSC confocal micrograph. Arrows in the individual channels point to the area of TCR Vα7.2+ staining observed in the MERGE image for the AIH T2 and the PSC patient accordingly. Scale bars: 10µm.

205

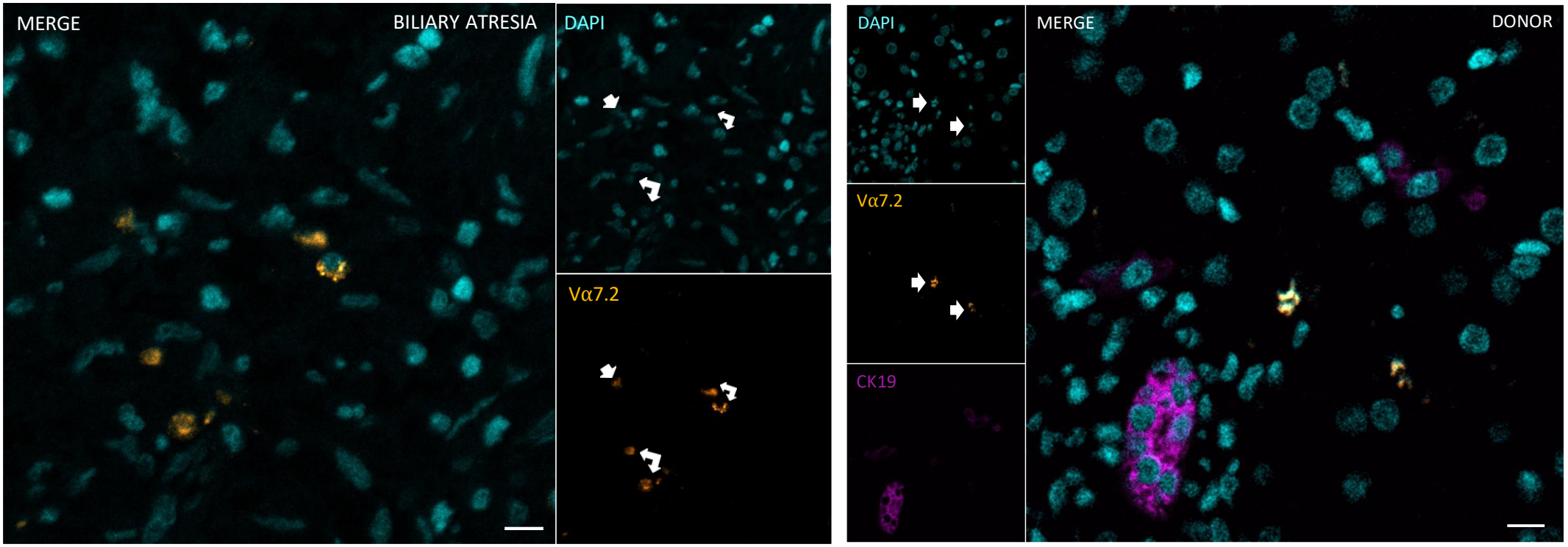

Figure 3d. Confocal micrographs of liver explant tissue from a child with biliary atresia (left) and an adult donor liver (right). Multiple IF staining of Vα7.2+ MAIT cells are observed in both images. Arrows in the individual channels point to the area of TCR Vα7.2+ staining seen in the corresponding MERGE images. IF staining of Vα7.2+ is in orange, CK19 in magenta and DAPI in cyan. Scale bars: 10µm.

206

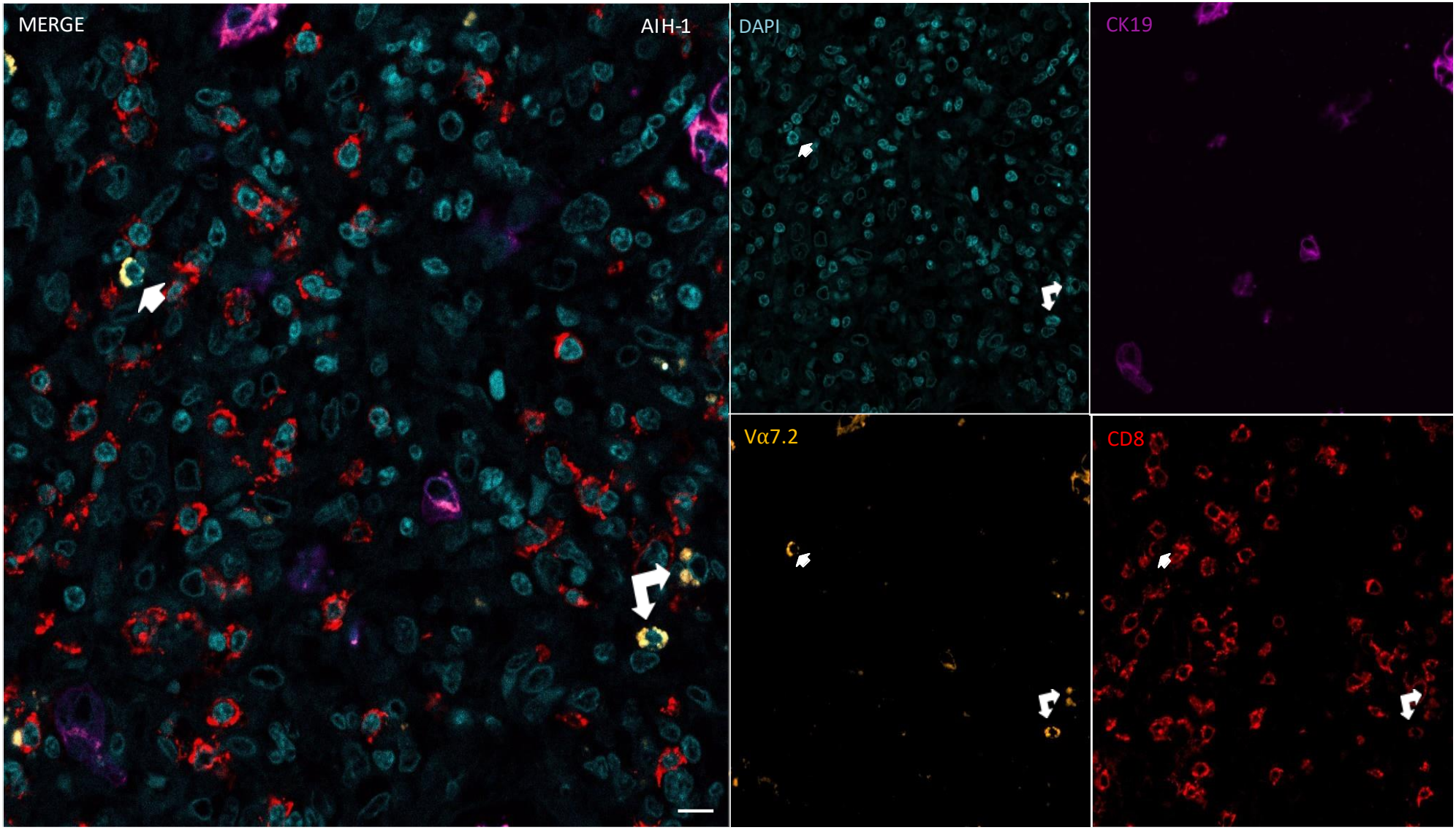

Figure 3e. Confocal micrograph of an area of interface hepatitis from a paediatric AIH T1 liver explant. Numerous CD8+ cells (red) are present in the inflammatory infiltrate. The single and double arrowheads points to areas of dual Vα7.2 + (orange) and CD8+ (red) IF staining in the MERGE and individual channels. Bile ducts are stained magenta (CK19+) and nucleated cells in cyan (DAPI). Scale bar; 10um.

207

Figure 3f (i)

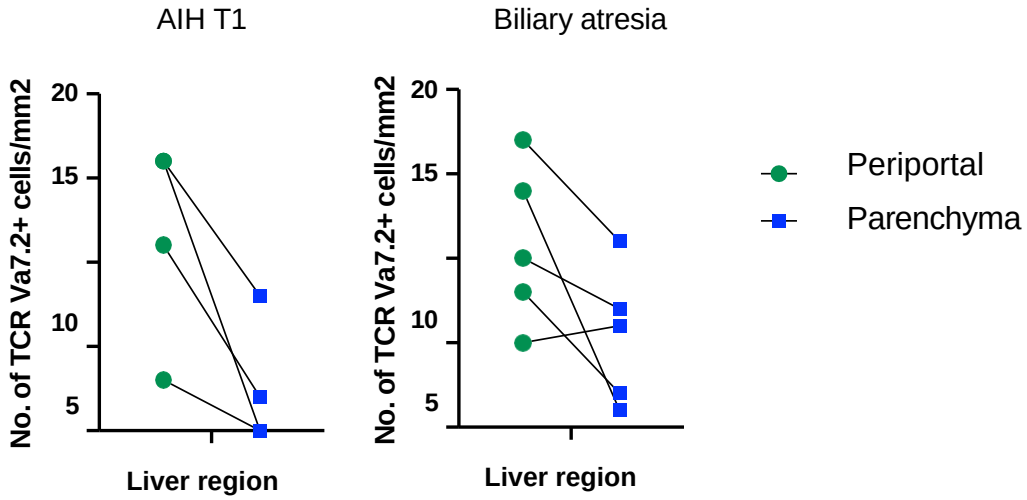

Figure 3f (ii)

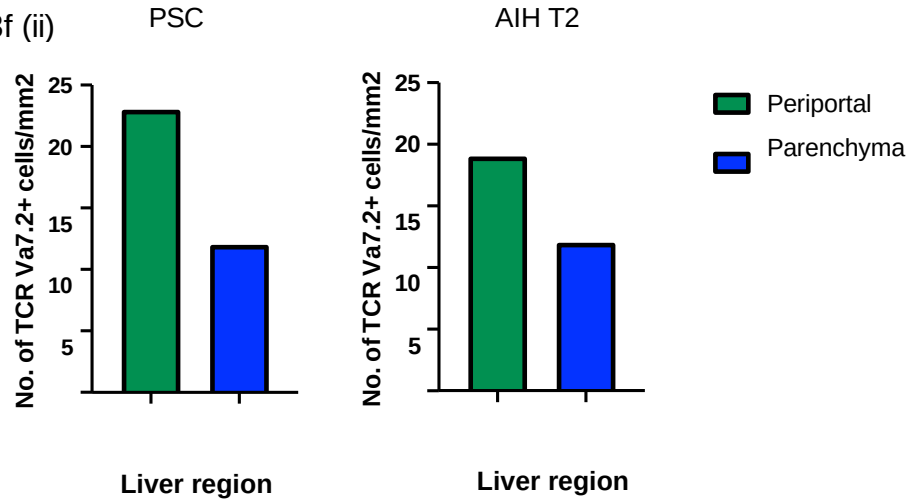

Figure 3f. MAIT cell distribution in different regions of the paediatric liver in

a) AIH T1 formalin fixed paraffin embedded (FFPE) liver explant sections N=4,
b) biliary atresia FFPE liver N=5,
c) AIH T2 FFPE liver N=1
d) PSC FFPE liver N=1.

In all 4 conditions, MAIT cell frequency was higher in the periportal regions compared to the hepatic parenchyma. This finding was of statistical significance in the AIH T1 patients (p=0.04). The child with PSC had the highest Vα7.2+ MAIT cell count in the periportal area compared to AIH T1, AIH T2 and biliary atresia. MAIT cell count was performed from Vα7.2+ IF stained liver explant tissue.

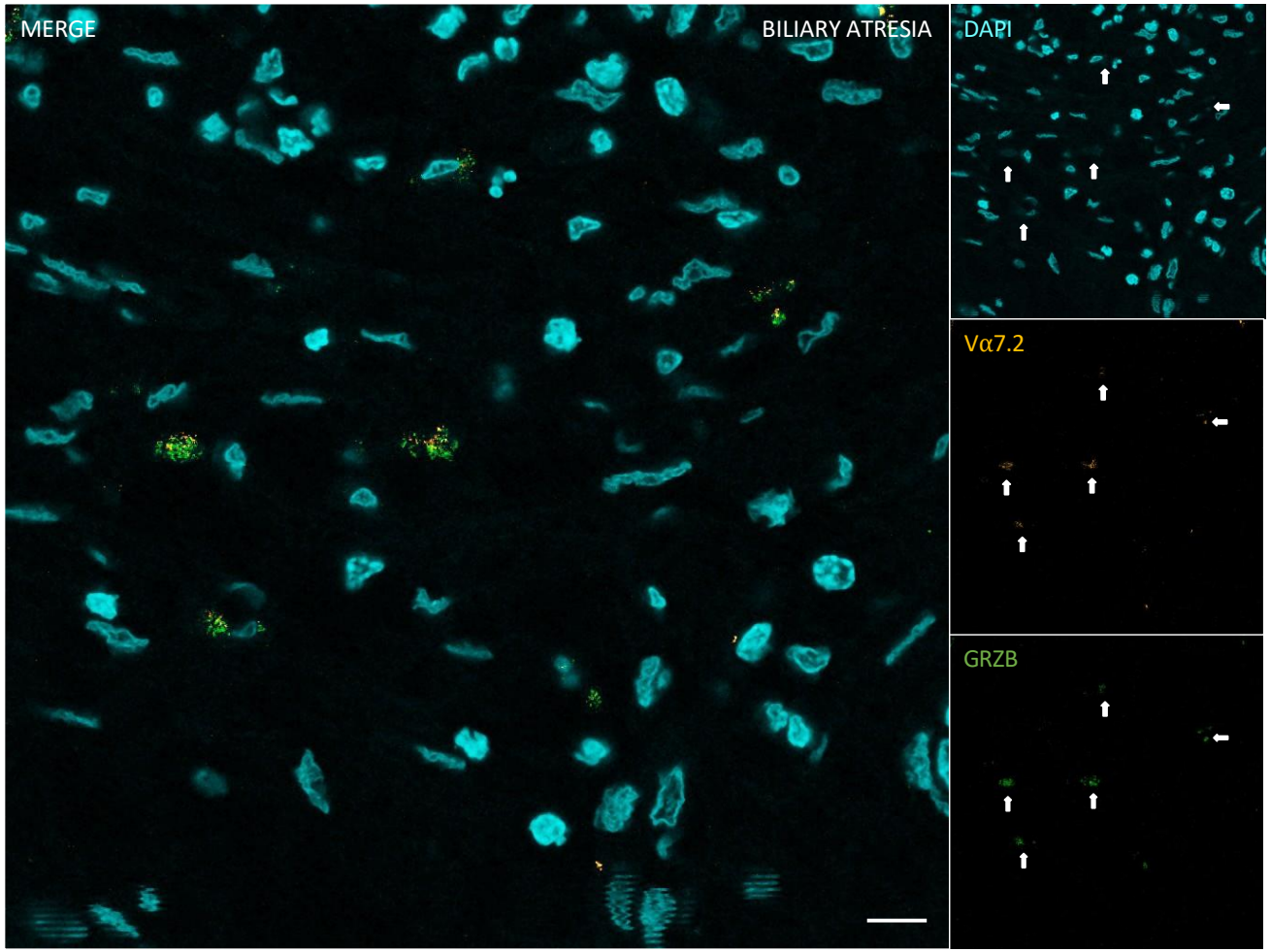

Figure 3g. Granzyme B (GRZB) (green) release by MAIT cells were captured in this liver explant confocal micrograph from a biliary atresia patient. Rims of green immunofluorescence are seen surrounding surface orange TCR Vα7.2+ staining.

Arrows in the individual channels point to the area of dual GRZB and Vα7.2+ staining observed in the MERGE image. Nucleated cells are stained cyan (DAPI). Scale bars: 10μm.

Figure 3h (i)

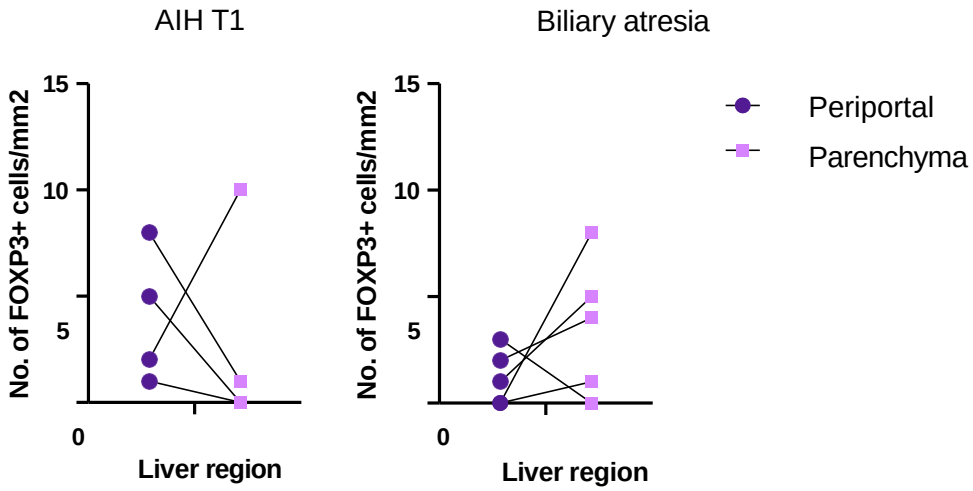

Figure 3h (ii)

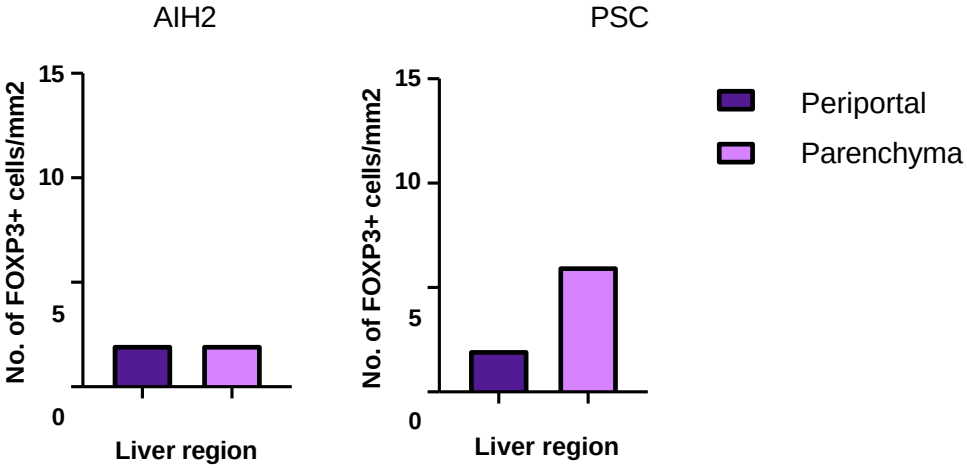

Figure 3h. FOXP3+ Treg distribution in different regions of paediatric liver explant tissue from (i) AIH T1 FFPE liver explant sections N=4, (ii) biliary atresia FFPE liver N=5, (iii) AIH T2 FFPE liver N=1 and (iv) PSC FFPE liver N=1.
Treg frequencies were higher in the parenchyma of the biliary cholangiopathies; biliary atresia and PSC. This contrasts with AIH T1 in which Treg frequencies were higher in the periportal region except in one patient.

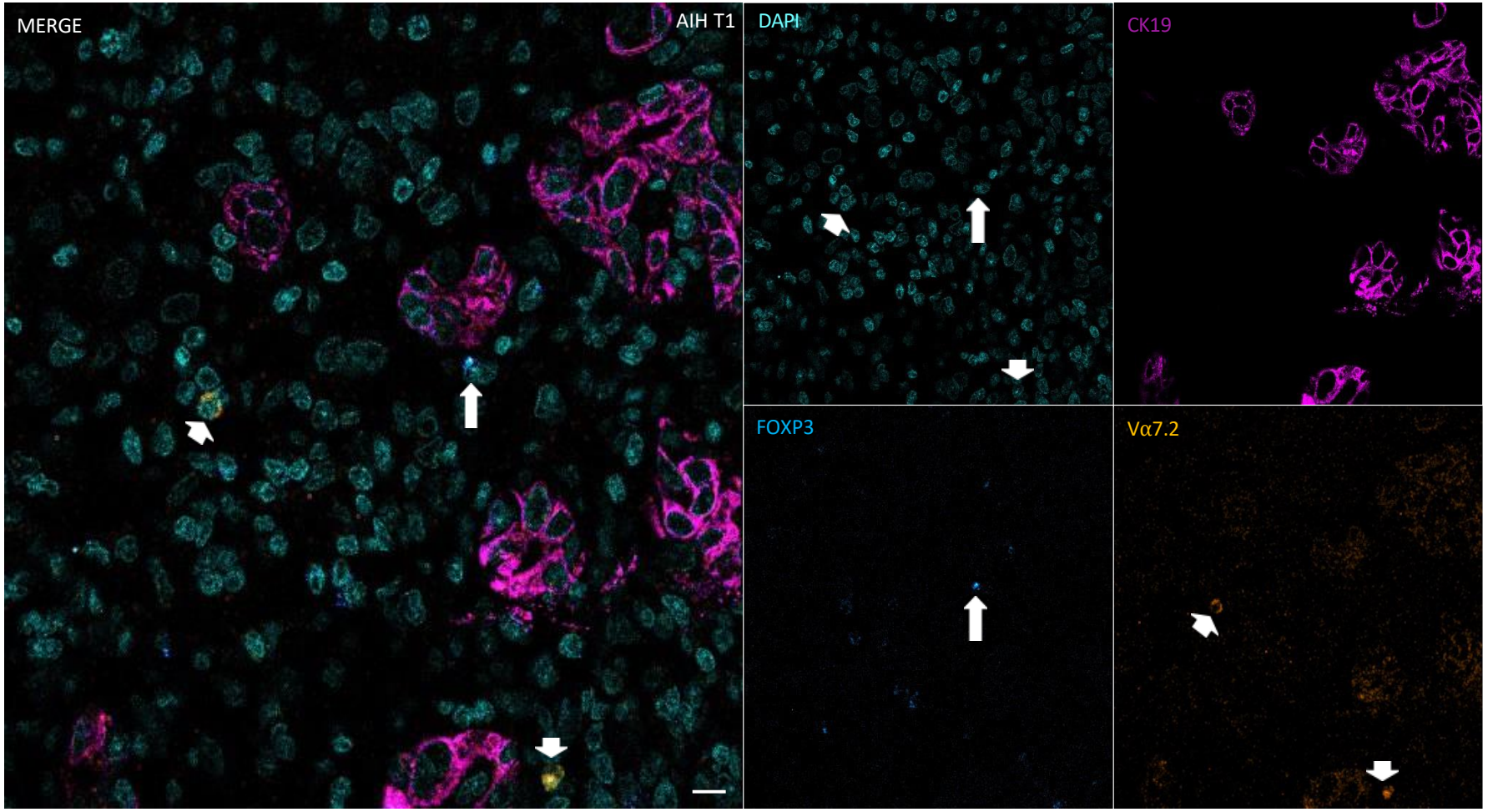

Figure 3i. Separate cells stained with TCR Vα7.2+ (orange) (arrowhead) and FOXP3+ (blue) (arrow) were identified in a confocal micrograph of liver explant tissue from a paediatric AIH T1 patient. Corresponding arrowheads and arrow from the MERGE image are shown in the individual channels. Bile ducts are stained magenta (CK19+) and nucleated cells in cyan (DAPI). Scale bar; 10um.

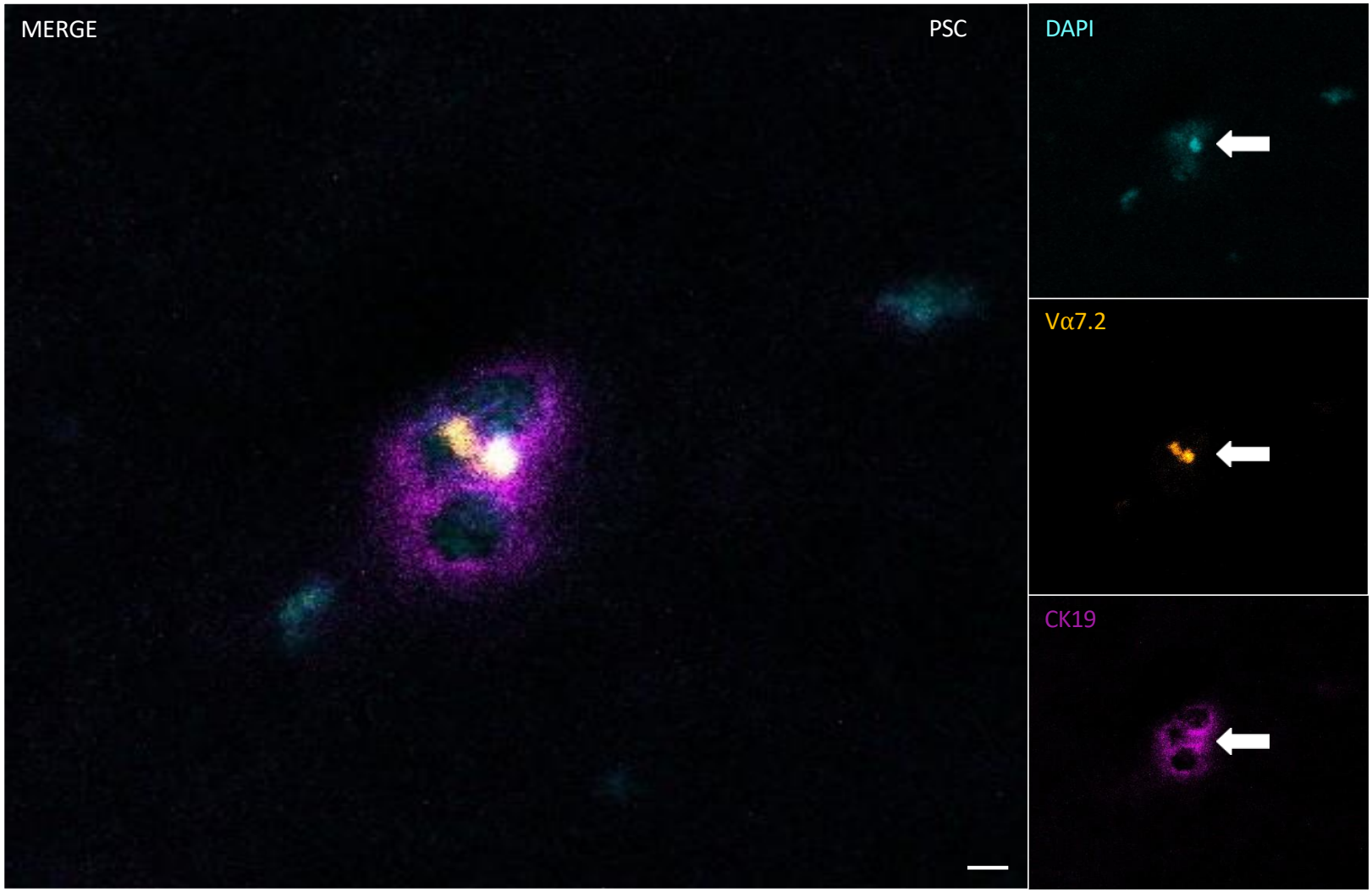

Figure 3j. Emperipolesis of MAIT cells within the bile ducts of a paediatric PSC explant liver; two TCR Vα7.2+ cells (orange) can be seen within the cytoplasm of cholangiocytes stained with CK19+ (magenta). Arrows in the individual channels point to the area of TCR Vα7.2+ staining observed in the MERGE image. Nucleated cells are stained with DAPI (cyan). Scale bars: 10μm.

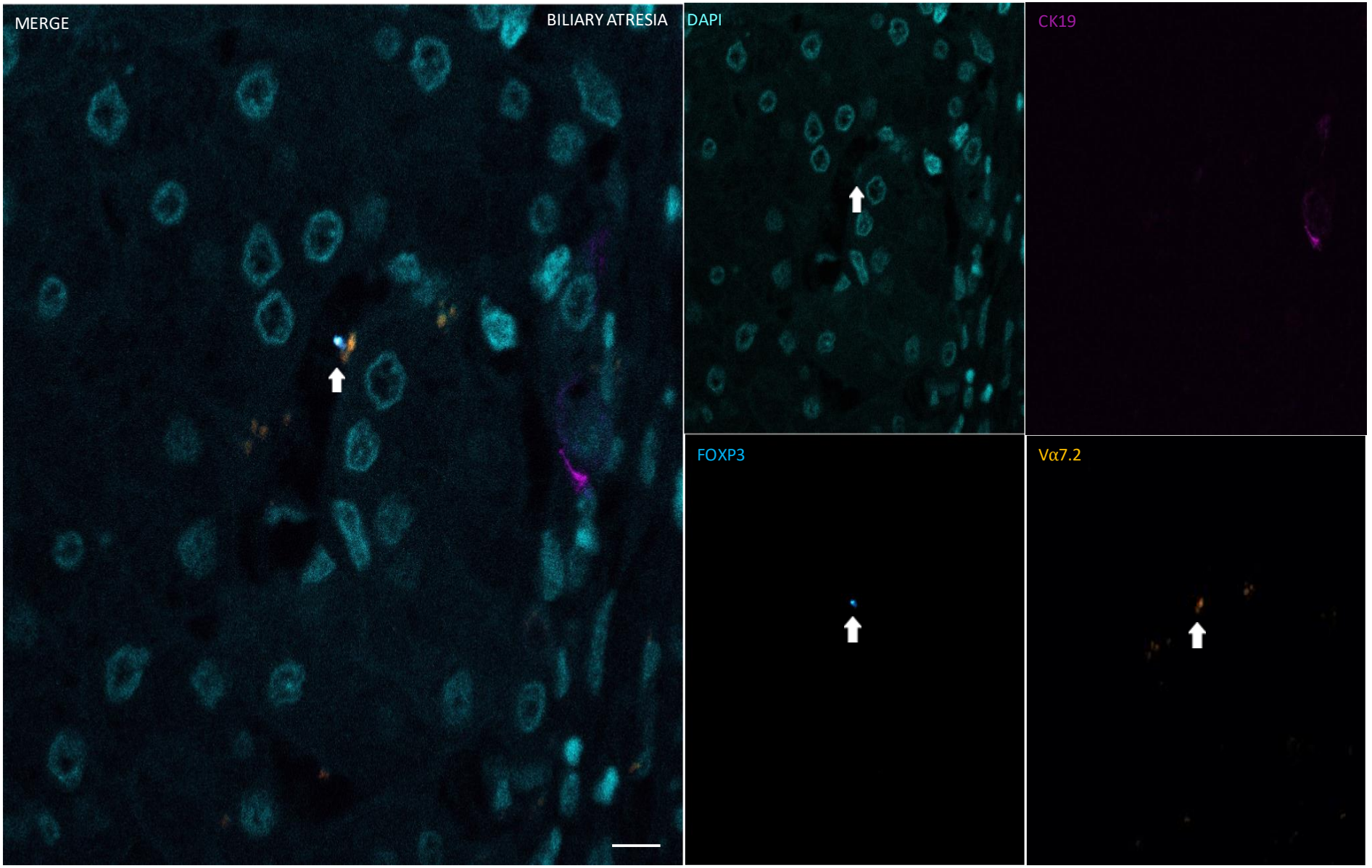

Figure 3k. Confocal image capture of what appears to be cell-to-cell contact between a TCR Vα7.2+ cell and a FOXP3+ cell in the liver explant of a patient with biliary atresia. Corresponding arrows from the MERGE image are shown in the individual channels. Bile ducts are stained magenta (CK19+) and nucleated cells in cyan (DAPI). Scale bar; 10um.

.

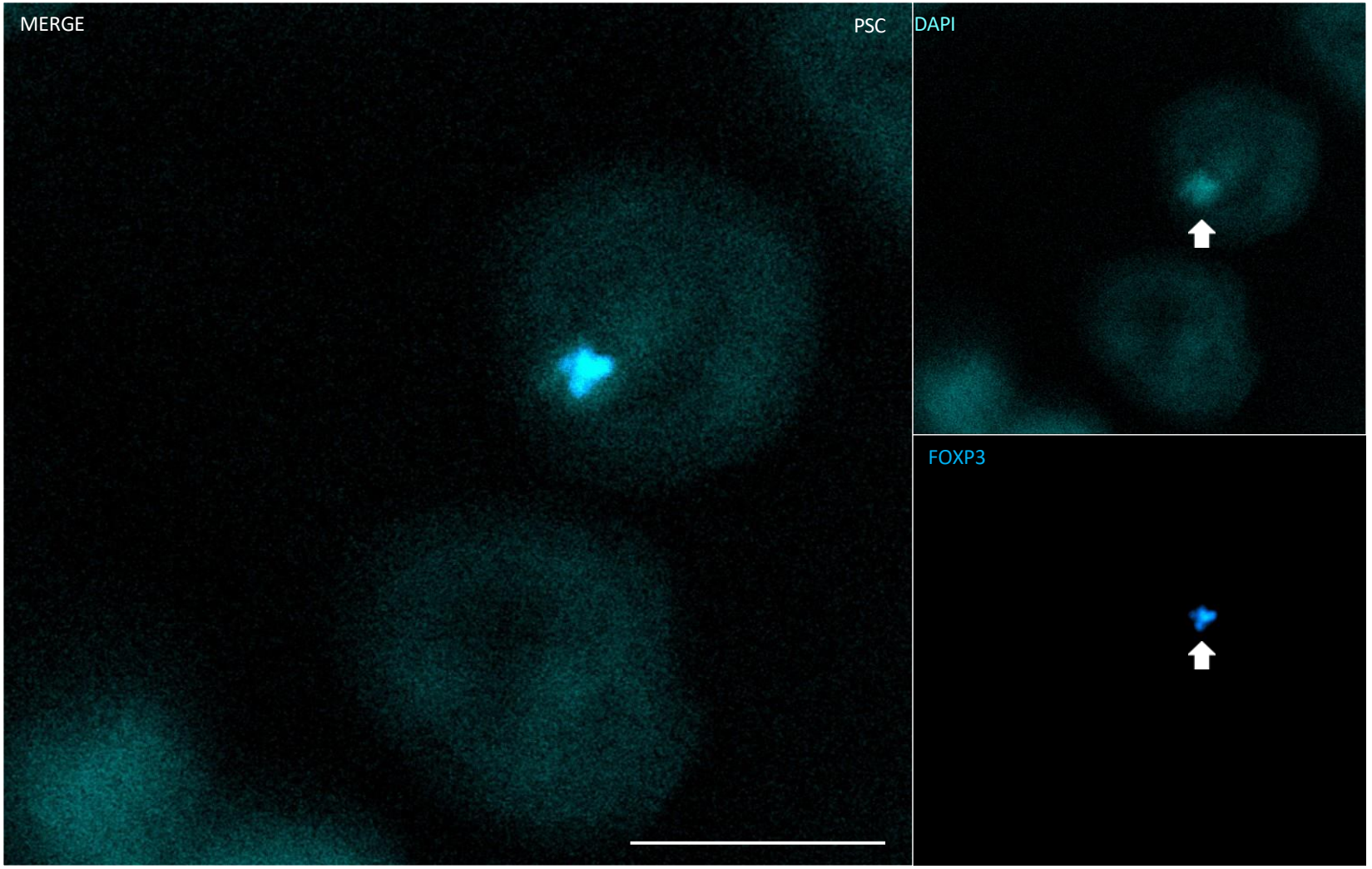

Figure 3l. Confocal micrograph of enclysis; a FOXP3+ Treg (blue) is captured inside a hepatocyte in the paediatric PSC liver explant. Arrows in the individual channels point to the area of FOXP3+ staining observed in the MERGE image. Nucleated cells are stained with DAPI (cyan).

Scale bars: 10μm.

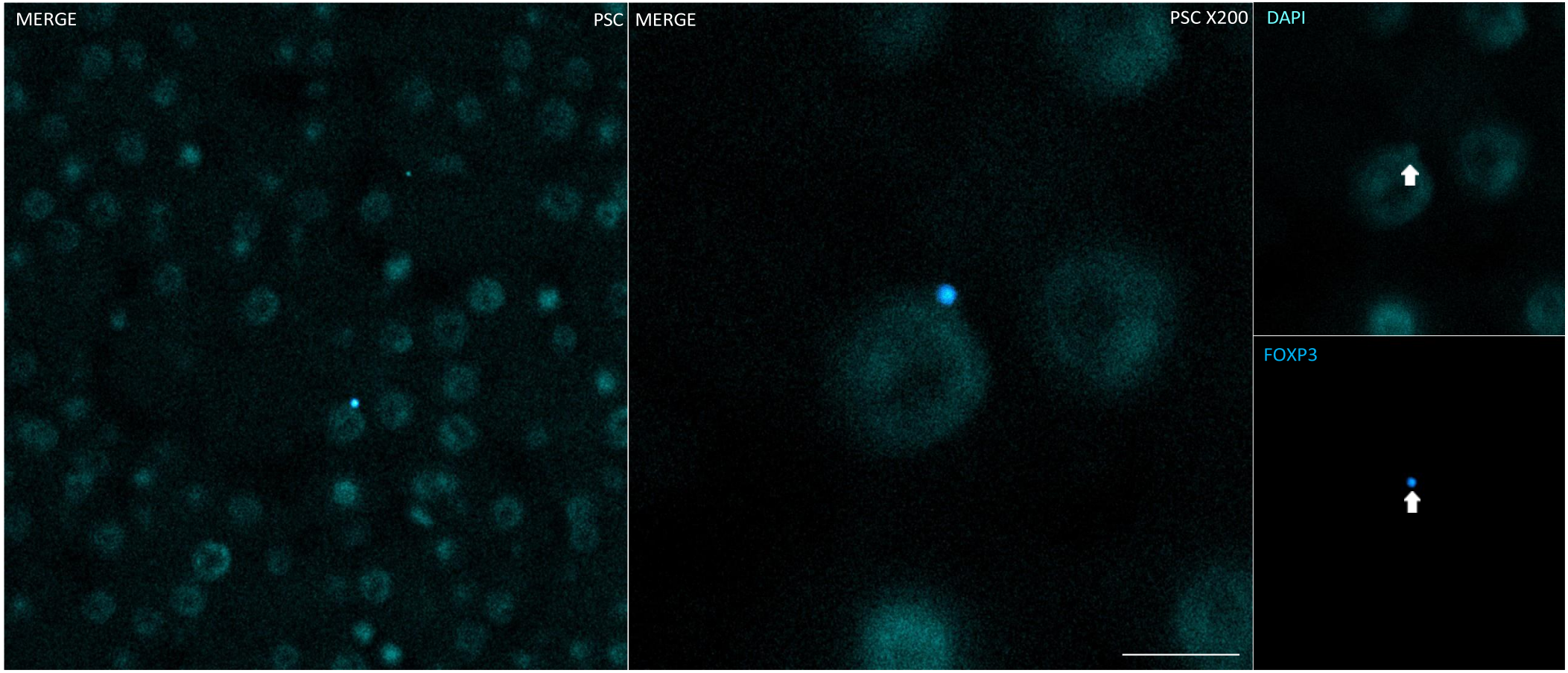

Figure 3m. Confocal image capture of cell-to-cell contact between a FOXP3+ (blue) Treg and a hepatocyte in the liver explant from a paediatric PSC patient. The magnified MERGE image is shown on the right-hand side. Arrows in the individual channels point to the area of FOXP3+ staining observed in the MERGE images. Nucleated cells are stained with DAPI (cyan). Scale bars: 10µm.

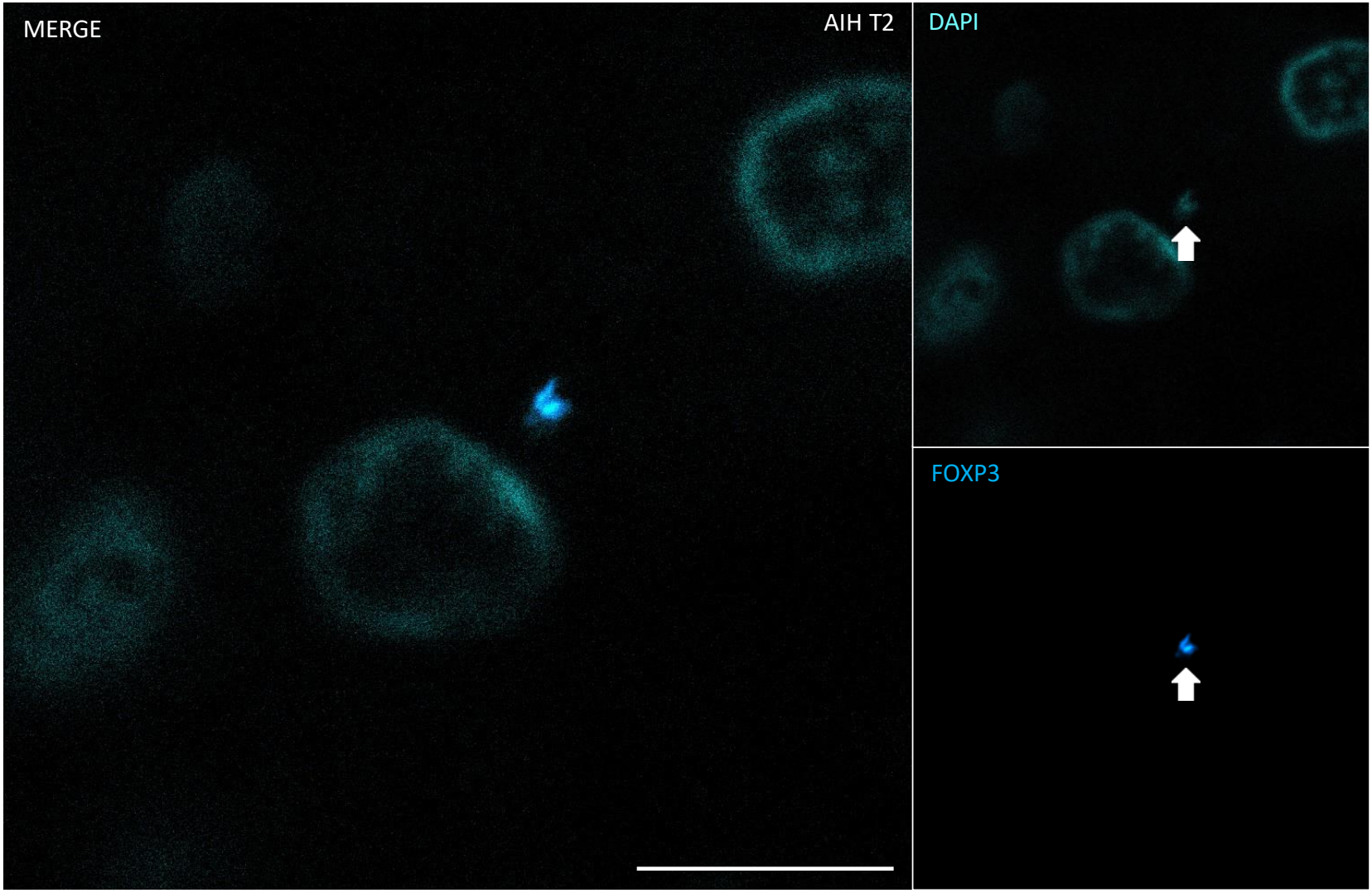

Figure 3n. Confocal micrograph of a cell with intracellular FOXP3+ staining which appears to be approaching a hepatocyte in the liver explant tissue of a paediatric AIH T2 patient. Arrows in the individual channels point to the area of FOXP3+ staining observed in the MERGE image. Nucleated cells are in DAPI (cyan). Scale bars: 10µm.

.

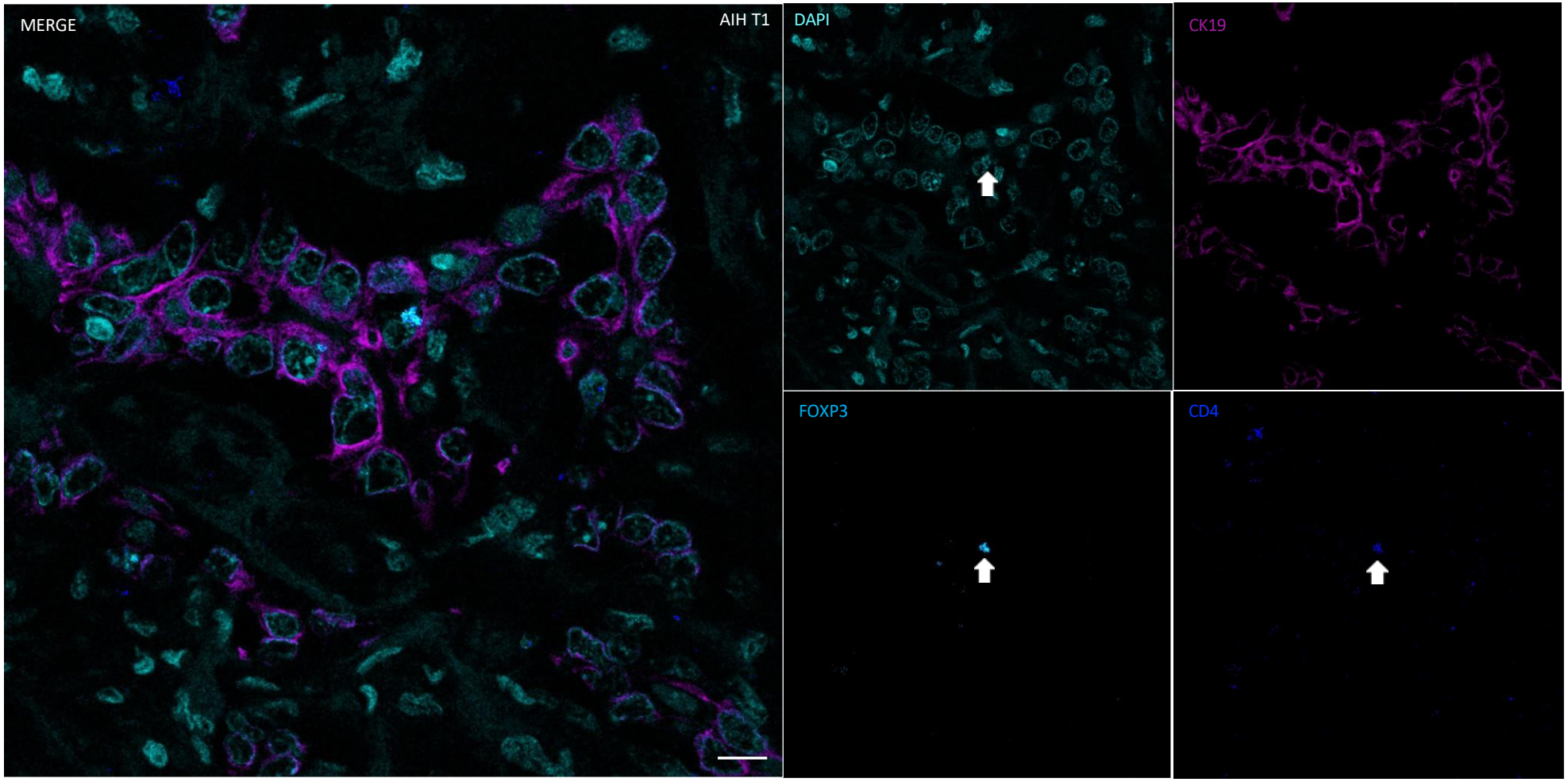

Figure 3o. Confocal micrograph of enclysis within the biliary epithelium identified in the liver explant tissue from a paediatric AIH T1 patient. A cell with dual IF staining of CD4+ (blue) and FOXP3+ (light blue) lies inside the cytoplasm of a biliary epithelial cell. Bile ducts are stained magenta (CK19+) and nucleated cells in cyan (DAPI). Scale bar; 10um.

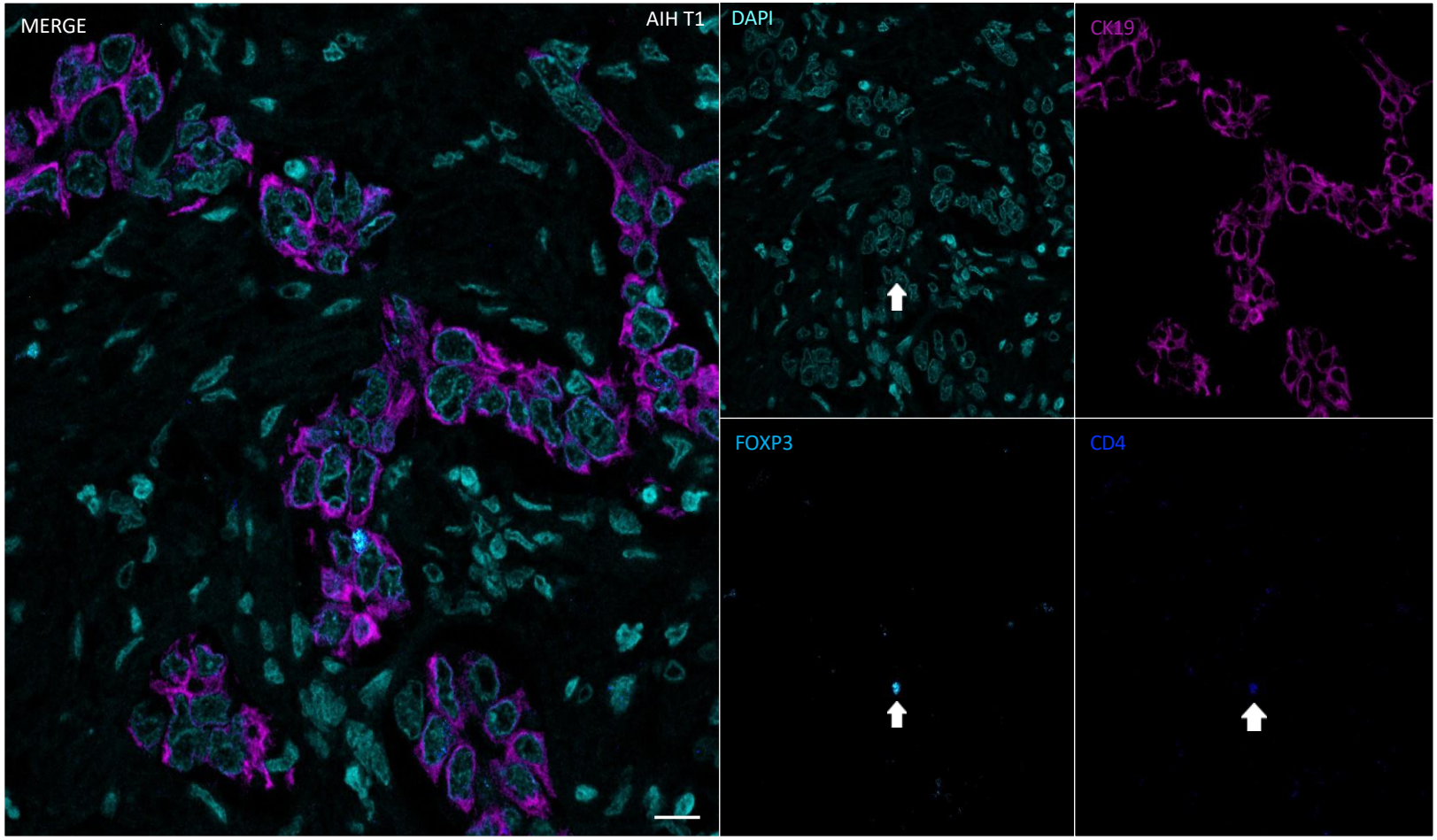

Figure 3p. Confocal micrograph of enclysis within the biliary epithelium. A cell with dual IF staining of CD4+ (blue) and FOXP3+ (light blue) lies inside the cytoplasm of a biliary epithelial cell in another area of the liver explant tissue from the same AIH T1 patient as Figure 3o. Bile ducts are stained magenta (CK19+) and nucleated cells in cyan (DAPI). Scale bar; 10um.

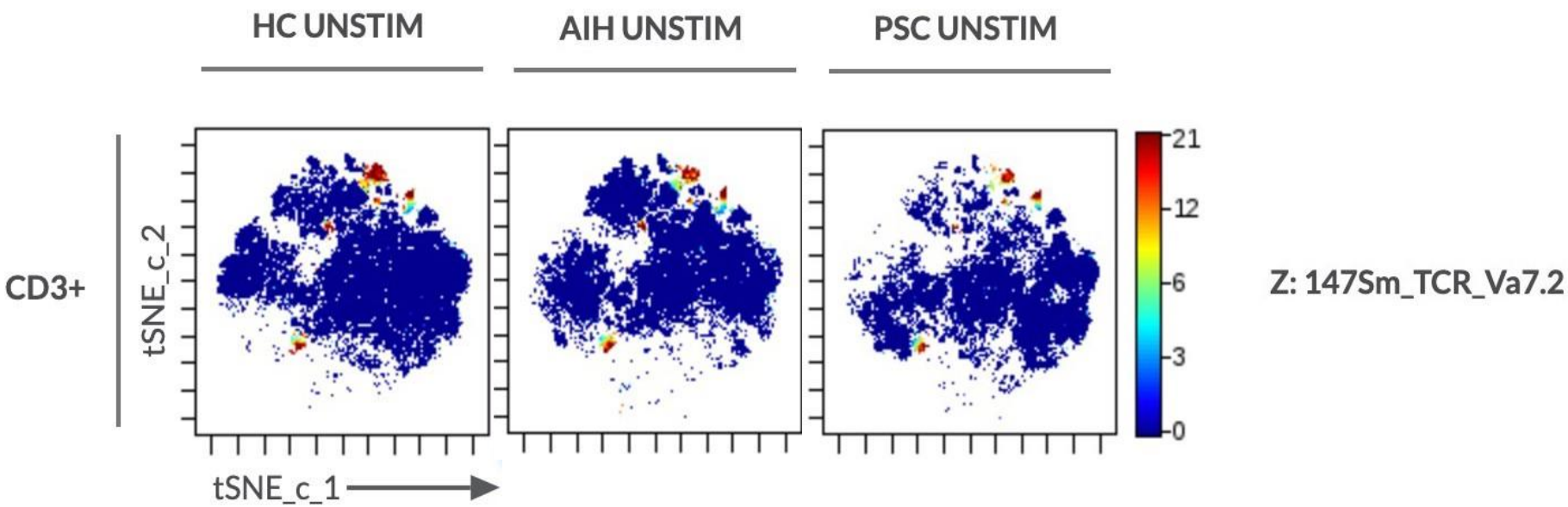

Figure 4a. tSNE plot of TCR Vα7.2+ cells gated on CD3+ lymphocytes. The colour scale bar is sited on the right; red = strongly positive, blue = strongly negative. Green arrows point out the area of Vα7.2+ clustering in the healthy child (HC); less dense clustering of the same regions is observed in the AIH and PSC patients. The TCR Vα7.2 is metal-conjugated to the samarium isotope 147 (147Sm) which is displayed on the z-axis. AIH; autoimmune hepatitis, PSC; primary sclerosing cholangitis, HC;
healthy children, STIM; stimulated, UNSTIM; unstimulated.

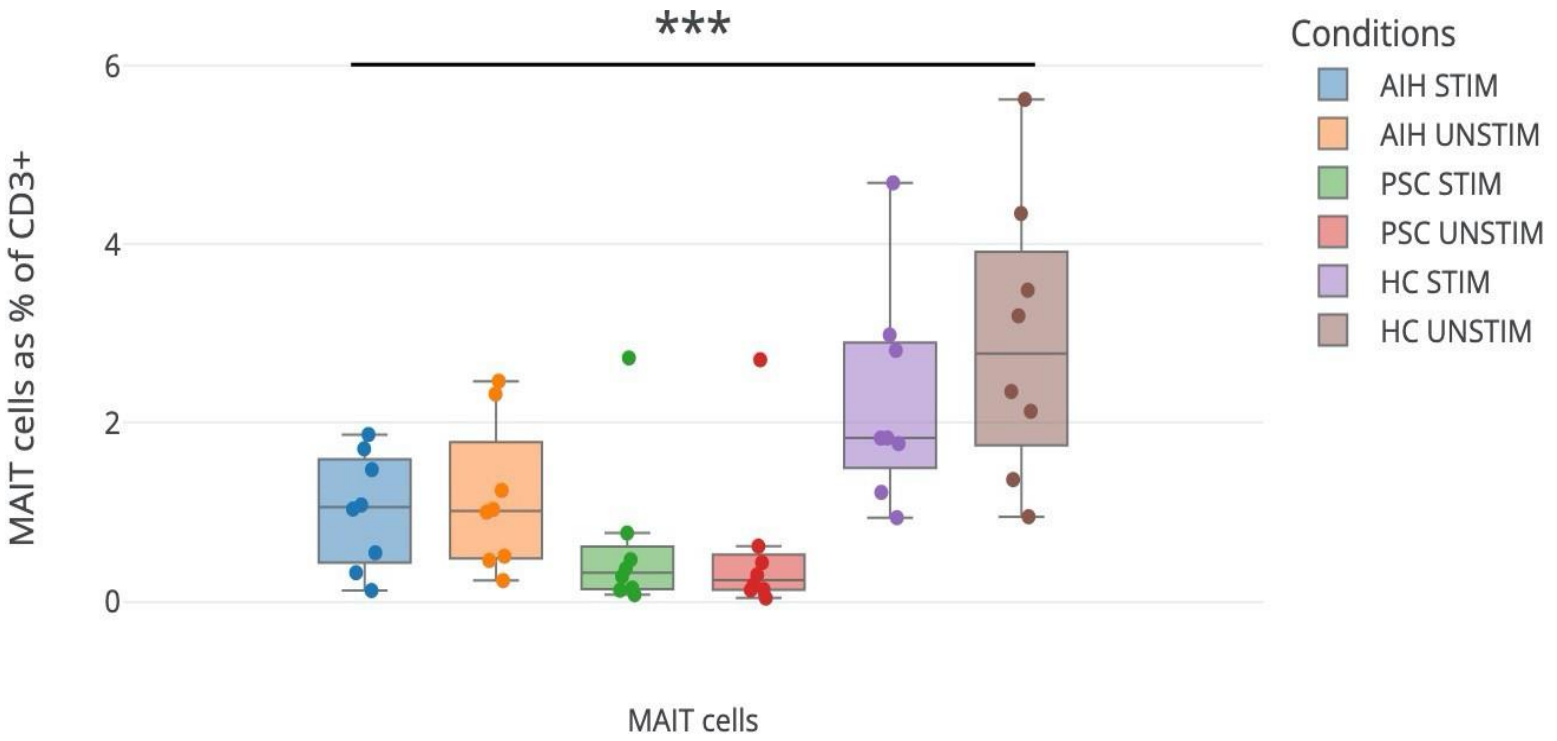

Kruskal-Wallis H test

Population	I.V.	p-value	Significance p-value
MAIT cells	Conditions	0.0004475	***

Figure 4b. Box - and - Whisker plot of peripheral blood MAIT cell frequencies (% of total CD3+ T lymphocytes) in paediatric patients with AIH N=8, PSC N=8, and healthy children (HC) N=8. PBMCs were treated with CytoStim; post-treatment (STIM; stimulated) results are shown along with their paired negative controls (UNSTIM; unstimulated). MAIT cell; mucosal-associated invariant T cell, AIH; autoimmune hepatitis, PSC; primary sclerosing cholangitis, HC; healthy children, PBMC; peripheral blood mononuclear cells. Data are presented as median +/- interquartile range. Results of the Kruskal-Wallis H test is displayed below the graph; ****p* <0.001

Figure 4c (i)

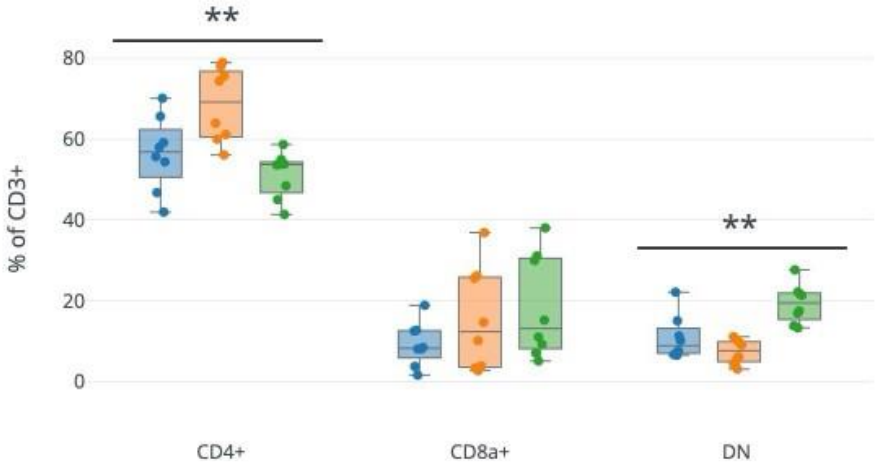

Kruskal-Wallis H test

Population	I.V.	p-value	Significance p-value
CD4+	Conditions	0.001994	**
DN	Conditions	0.001243	**
CD8a+	Conditions	0.332	ns

Figure 4c (ii)

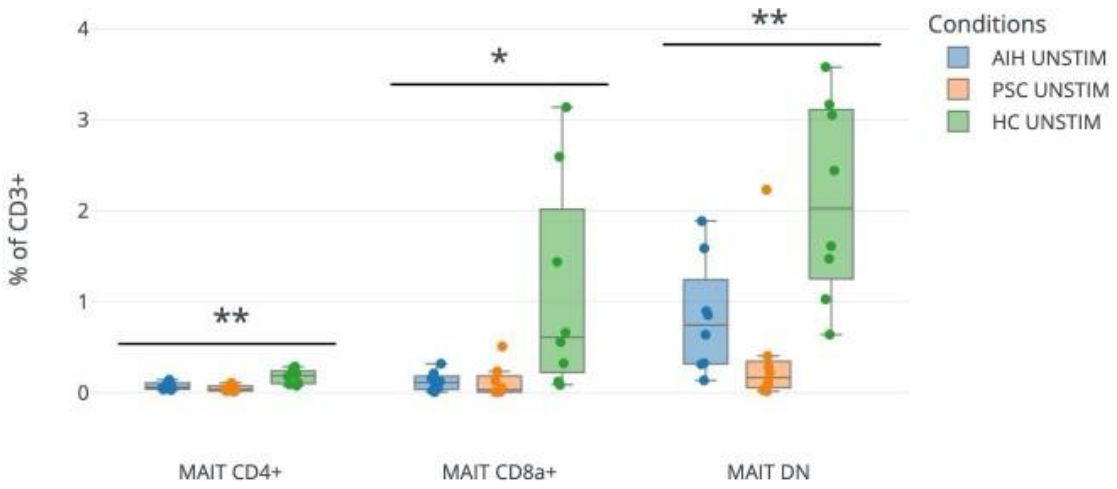

Kruskal-Wallis H test

Population	I.V.	p-value	Significance p-value
MAIT CD4+	Conditions	0.003272	**
MAIT CD8a+	Conditions	0.01133	*
MAIT DN	Conditions	0.002399	**

Figure 4c. Box - and - Whisker plot of peripheral blood CD3+ T lymphocyte subset frequencies in paediatric patients with AIH N=8, PSC N=8, and HC N=8; baseline cell counts of CD4+, CD8a+ and DN cells are shown (UNSTIM).

Figure 4c (ii) shows the MAIT cell subset frequencies; baseline UNSTIM cell counts of MAIT CD4+, MAIT CD8a+ and MAIT DN are shown. MAIT cell; mucosal-associated invariant T cell, AIH; autoimmune hepatitis, PSC; primary sclerosing cholangitis, HC; healthy children, DN; double negative, I.V.; independent variable, ns; not statistically significant. Data are presented as median +/- interquartile range. Results of the Kruskal-Wallis H test are displayed below the graphs;*p<0.05, **p<0.01.

Figure 4d (i)

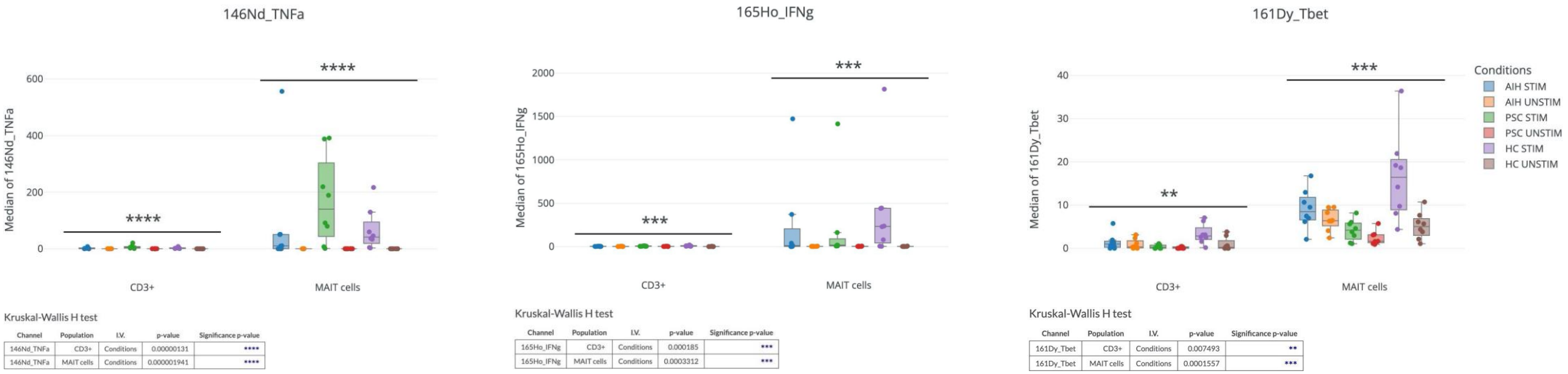

Figure 4d (i). Box - and - Whisker plots showing the total MAIT cell expression of the Th1 profile cytokines TNFα and IFNγ, and its transcription factor Tbet compared to the conventional CD3+ lymphocytes from the peripheral blood of the same children; AIH N=8, PSC N=8 and HC N=8. PBMCs were treated with CytoStim; post-treatment (STIM; stimulated) results are shown along with their paired negative controls (UNSTIM; unstimulated). MAIT cell; mucosal-associated invariant T cell, AIH; autoimmune hepatitis, PSC; primary sclerosing cholangitis, HC; healthy control, PBMC; peripheral blood mononuclear cells, I.V.; independent variable, ns; not statistically significant. The y-axis shows the median metal intensity (MMI). Kruskal-Wallis H test results are displayed below each graph.
Data are presented as median +/- interquartile range; ***p* <0.01, ****p* <0.001, *****p* <0.0001.

Figure 4d (ii)

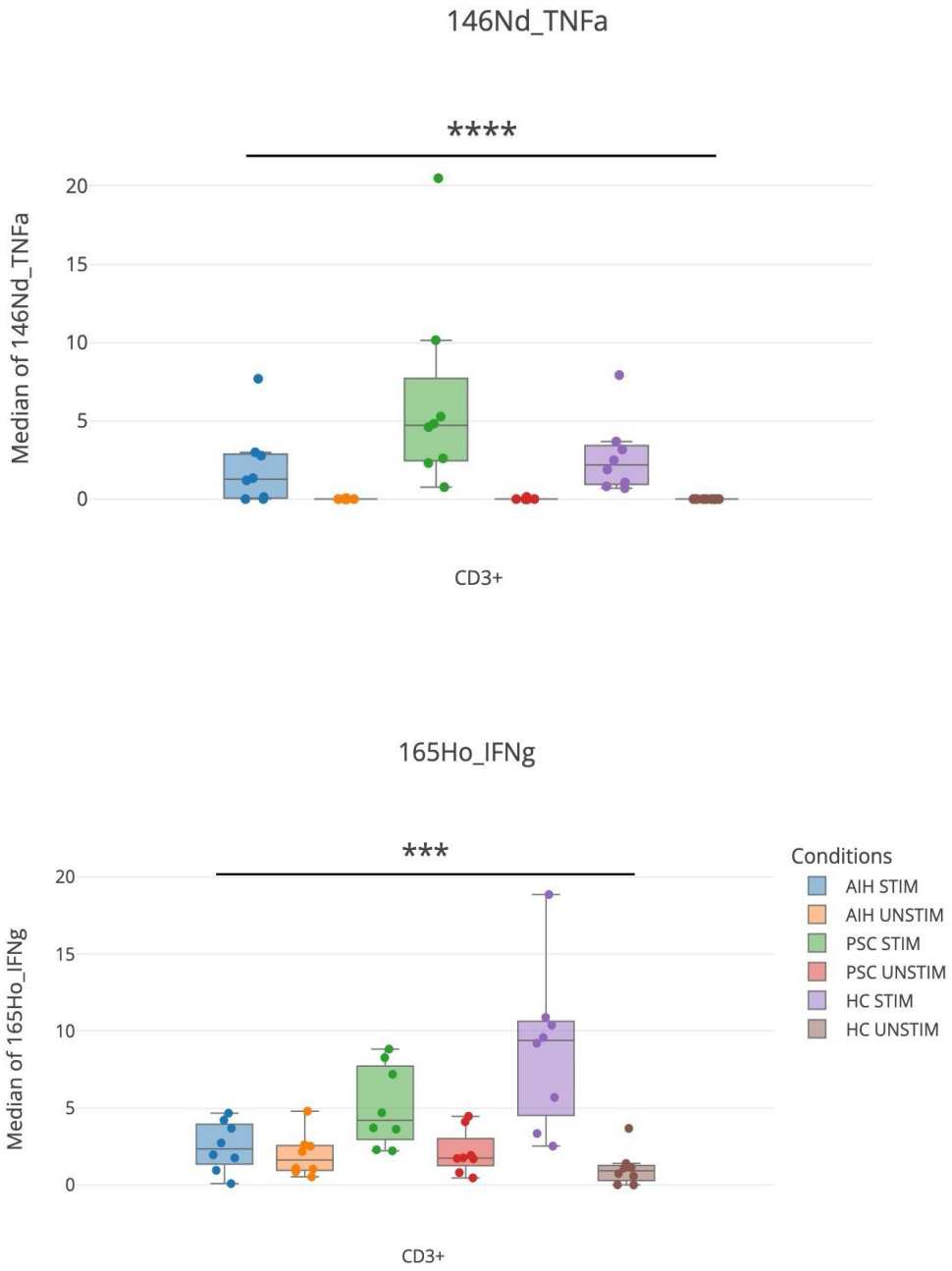

Figure 4d (ii). 'zoomed in' image of the Box - and - Whisker plots of TNFα and IFNγ expression in peripheral blood CD3+ lymphocytes from children with AIH N=8, PSC N=8 and in HC N=8. Results of PBMCs treated with CytoStim are shown; baseline (UNSTIM) and post-treatment (STIM). AIH; autoimmune hepatitis, PSC; primary sclerosing cholangitis, HC; healthy control, PBMC; peripheral blood mononuclear cells. Y-axis displays the median metal intensity (MMI). Data are presented as median +/- interquartile range; ****p* <0.001, *****p* <0.0001.

Figure 4d (iii)

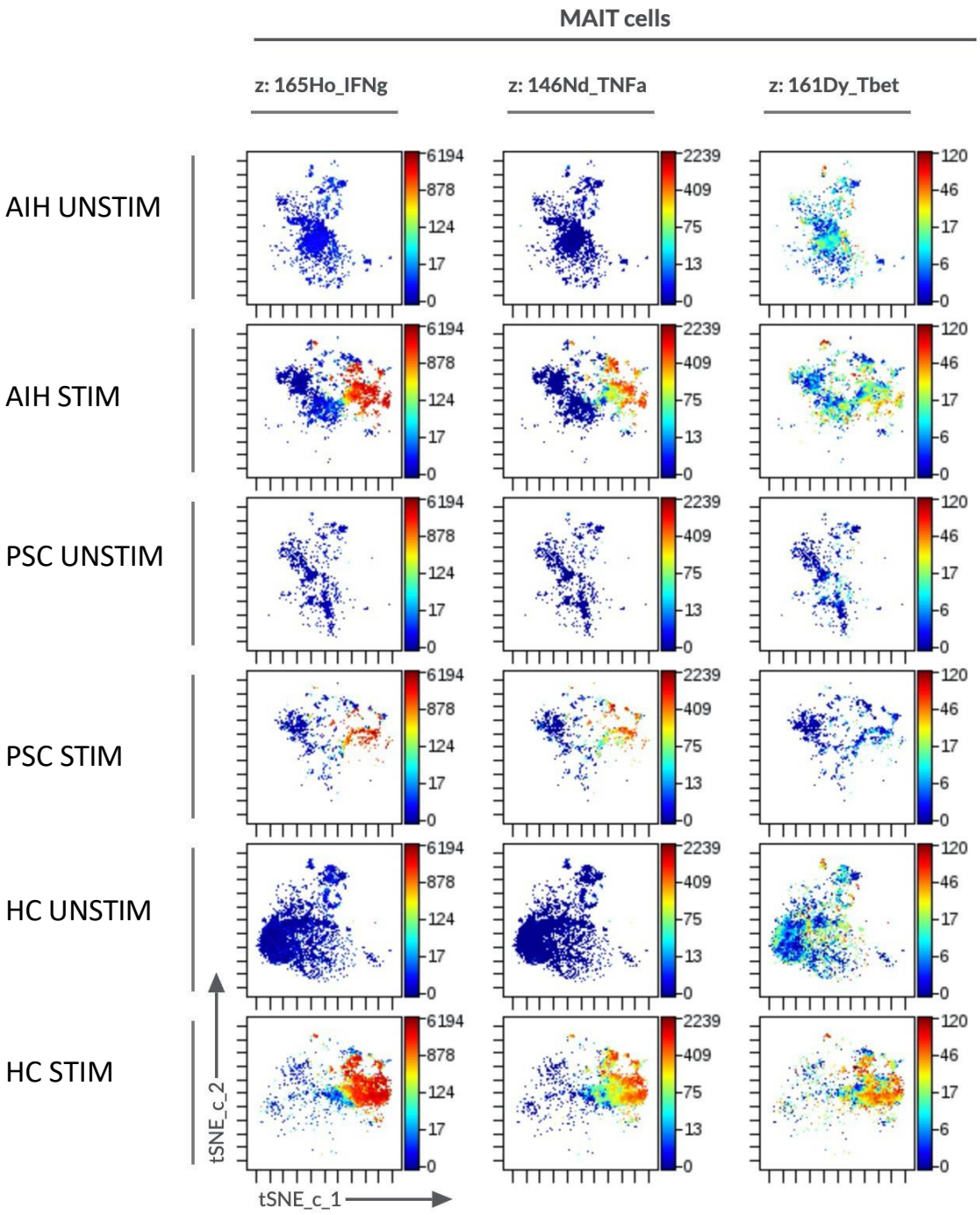

Figure 4d (iii). tSNE plots displaying MAIT cell expression levels of the Th1 proinflammatory cytokines IFNγ, TNFα, and the transcription factor Tbet in CytoStim treated PBMCs (STIM) and their paired baseline (UNSTIM) levels from three children; one AIH and one PSC patient and a healthy child. Colour scale bar on the right; red = strongly positive, blue = strongly negative.

Figure 4e (i)

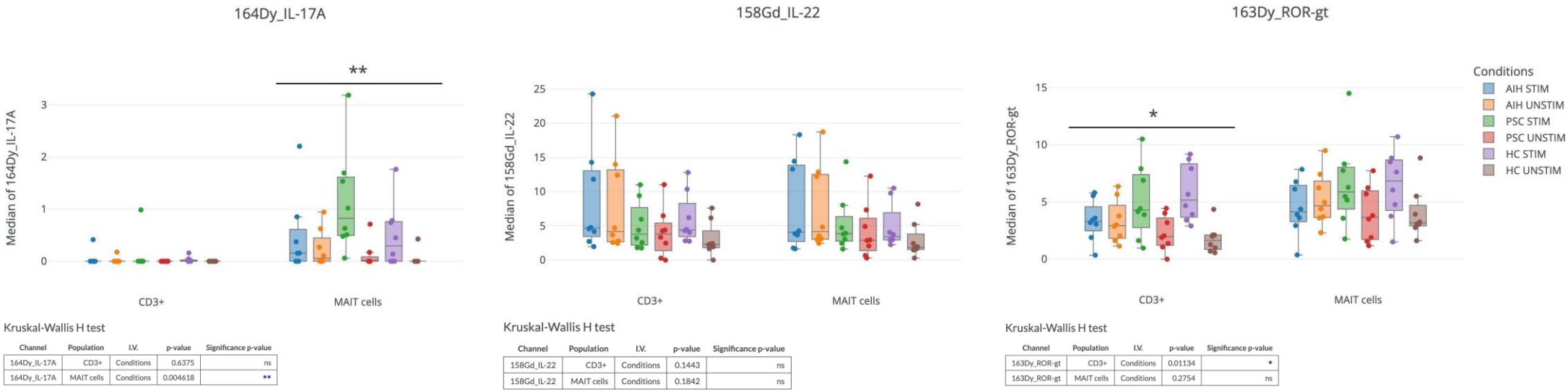

Kruskal-Wallis H test

Channel	Population	I.V.	p-value	Significance p-value
164Dy_IL-17A	CD3+	Conditions	0.6375	ns
164Dy_IL-17A	MAIT cells	Conditions	0.004618	**

Kruskal-Wallis H test

Channel	Population	I.V.	p-value	Significance p-value
158Gd_IL-22	CD3+	Conditions	0.1443	ns
158Gd_IL-22	MAIT cells	Conditions	0.1842	ns

Kruskal-Wallis H test

Channel	Population	I.V.	p-value	Significance p-value
163Dy_ROR-gt	CD3+	Conditions	0.01134	*
163Dy_ROR-gt	MAIT cells	Conditions	0.2754	ns

Figure 4e (i) Peripheral blood total MAIT cell and CD3+ lymphocyte expression of the Th17 profile cytokines IL-17A, IL-22 and its transcription factor RORγt from children with AIH N=8, PSC N=8 and HC N=8. Results of PBMCs treated with CytoStim, and their paired negative controls are shown; baseline (UNSTI; unstimulated) and post- treatment (STIM; stimulated). MAIT cell; mucosal-associated invariant T cell, AIH; autoimmune hepatitis, PSC; primary sclerosing cholangitis, HC; healthy children, PBMC; peripheral blood mononuclear cells, I.V.; independent variable, ns; not statistically significant. Y-axis shows the median metal intensity (MMI). Kruskal-Wallis H test results are given below each graph. Data are presented as median +/- interquartile range; *p <0.05, **p <0.01

Figure 4e (ii)

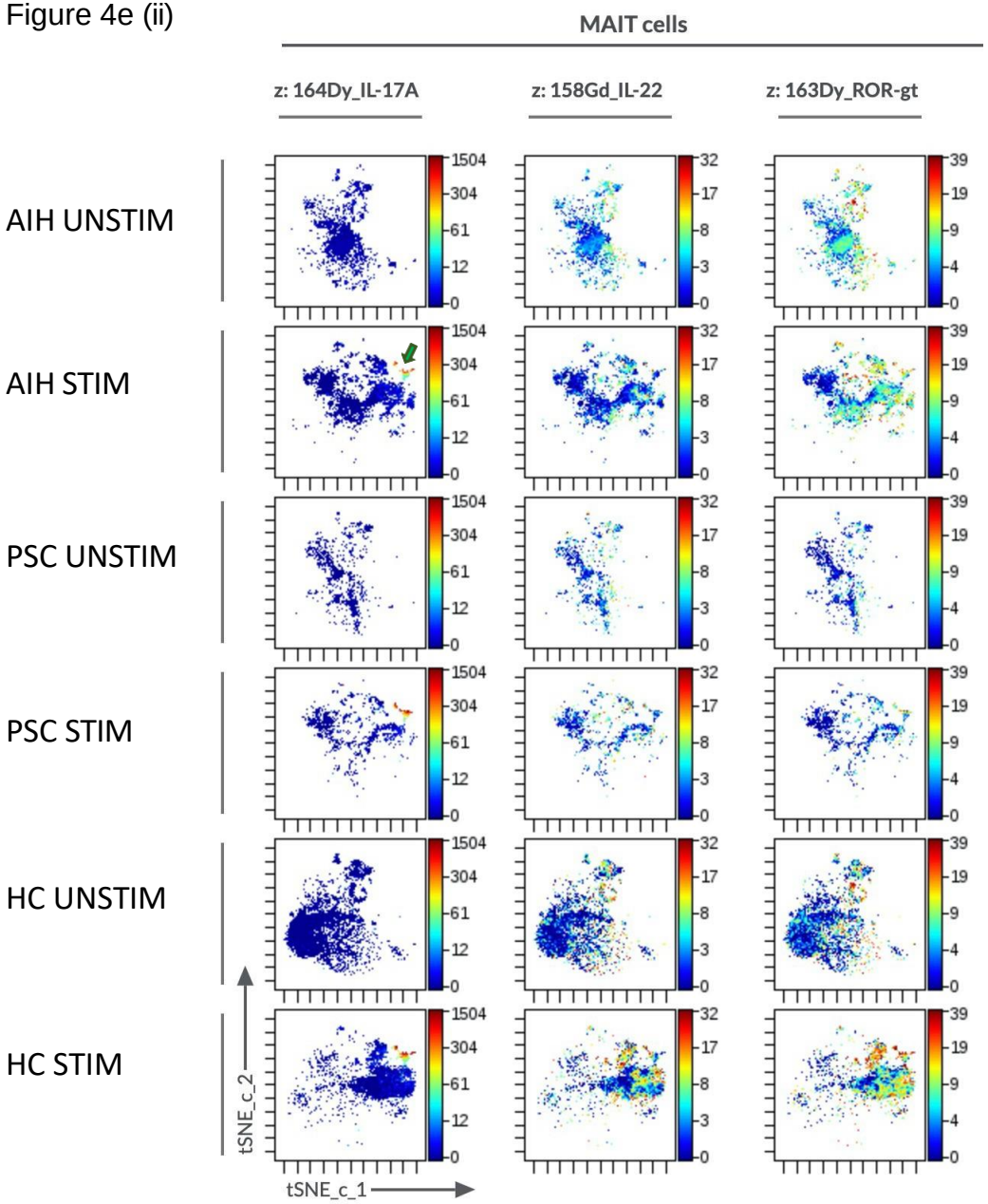

Figure 4e (ii). tSNE plots displaying expression levels of the Th17 cytokines IL-17A, IL-22 and the transcription factor RORγt in CytoStim treated PBMCs (STIM) and their paired baseline (UNSTIM) levels from three individuals; a paediatric patient with AIH, a paediatric patient with PSC and a healthy child. The green arrow points to the IL-17A clustering observed in the AIH STIM tSNE plot. Colour scale bar on the right; red = strongly positive, blue = strongly negative.

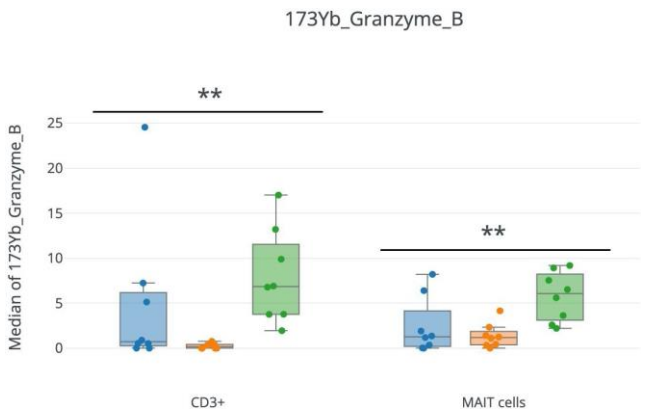

Kruskal-Wallis H test

Channel	Population	I.V.	p-value	Significance p-value
173Yb_Granzyme_B	CD3+	Conditions	0.002236	**
173Yb_Granzyme_B	MAIT cells	Conditions	0.008521	**

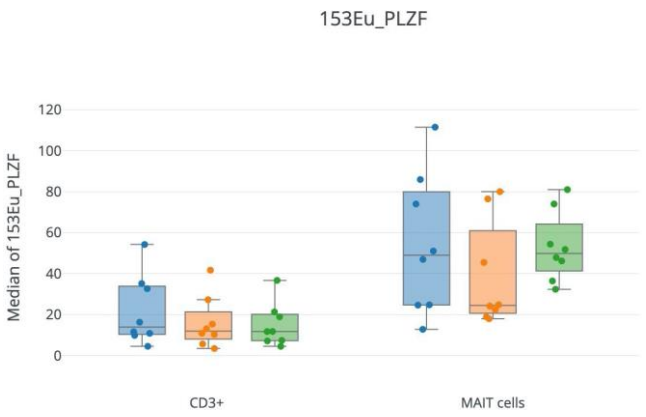

Kruskal-Wallis H test

Channel	Population	I.V.	p-value	Significance p-value
153Eu_PLZF	CD3+	Conditions	0.7965	ns
153Eu_PLZF	MAIT cells	Conditions	0.2573	ns

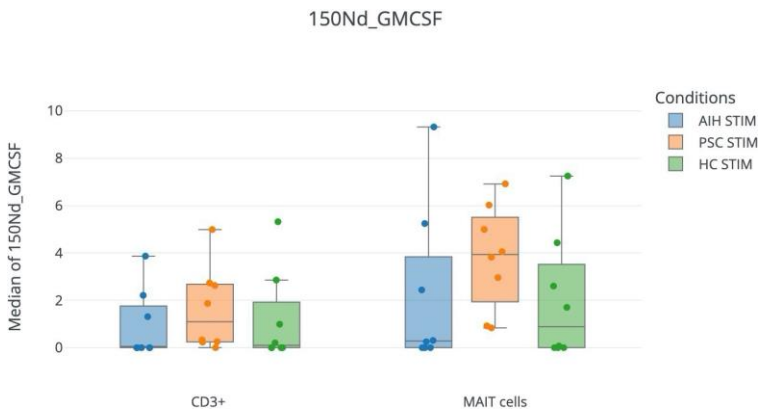

Kruskal-Wallis H test

Channel	Population	I.V.	p-value	Significance p-value
150Nd_GMCSF	CD3+	Conditions	0.3084	ns
150Nd_GMCSF	MAIT cells	Conditions	0.1605	ns

Figure 4f. Peripheral blood total MAIT cell and CD3+ lymphocyte expression of the cytolytic markers Granzyme B and PLZF, and GMCSF from children with AIH N=8, PSC N=8 and HC N=8. Results of PBMCs treated with CytoStim are shown (STIM; stimulated). MAIT cell; mucosal-associated invariant T cell, AIH; autoimmune hepatitis, PSC; primary sclerosing cholangitis, HC; healthy children, PBMC; peripheral blood mononuclear cells, I.V.; independent variable, ns; not statistically significant. Y-axis displays the median metal intensity (MMI). Kruskal-Wallis H test results are shown. Data are presented as median +/- interquartile range; ***p* <0.01

Figure 4g. Peripheral blood total MAIT cell and CD3+ lymphocyte expression of CD38, Ki67, PD-1 and CTLA-4 from children with AIH N=8, PSC N=8 and HC N=8. Results of PBMCs treated with CytoStim are shown (STIM). MAIT cell; mucosal- associated invariant T cell, AIH; autoimmune hepatitis, PSC; primary sclerosing cholangitis, HC; healthy children, PBMC; peripheral blood mononuclear cells, I.V.; independent variable, ns; not statistically significant.

Y-axis shows the median metal intensity (MMI). Kruskal-Wallis H test results are shown. Data are presented as median +/- interquartile range; *p <0.05, **p <0.01

145Nd_CD38

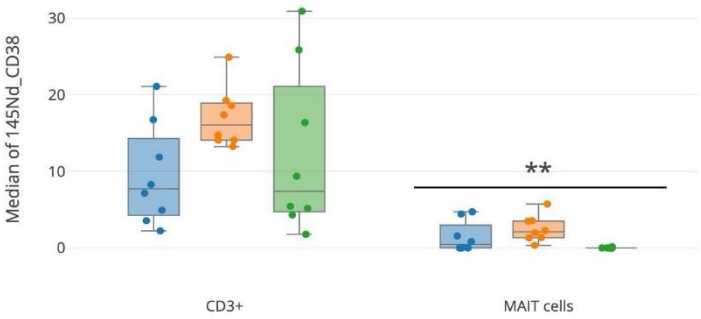

Kruskal-Wallis H test

Channel	Population	I.V.	p-value	Significance p-value
145Nd_CD38	CD3+	Conditions	0.1128	ns
145Nd_CD38	MAIT cells	Conditions	0.002101	**

172Yb_Ki-67

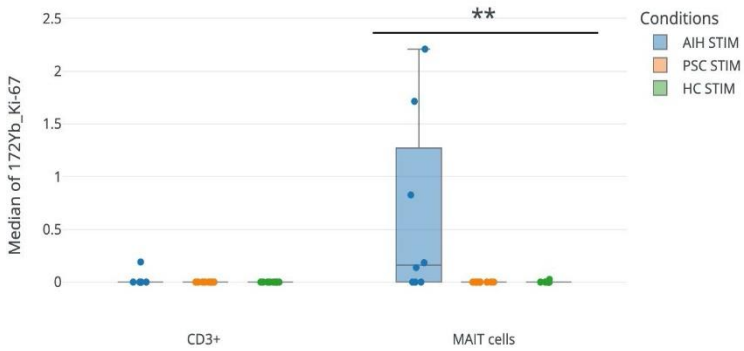

Kruskal-Wallis H test

Channel	Population	I.V.	p-value	Significance p-value
172Yb_Ki-67	CD3+	Conditions	0.3679	ns
172Yb_Ki-67	MAIT cells	Conditions	0.007446	**

175Lu_CD279_PD-1

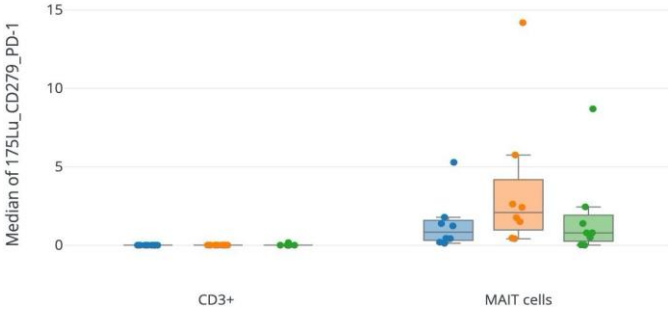

Kruskal-Wallis H test

Channel	Population	I.V.	p-value	Significance p-value
175Lu_CD279_PD-1	CD3+	Conditions	0.3679	ns
175Lu_CD279_PD-1	MAIT cells	Conditions	0.2248	ns

170Er_CD152_CTLA-4

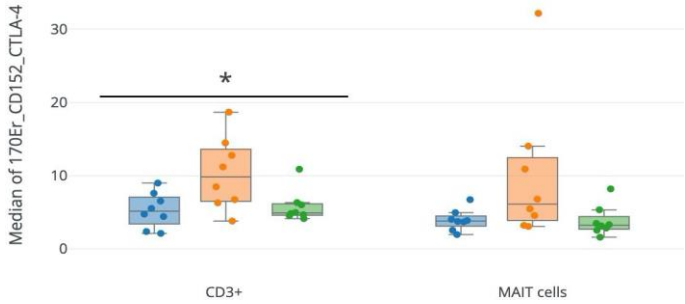

Kruskal-Wallis H test

Channel	Population	I.V.	p-value	Significance p-value
170Er_CD152_CTLA-4	CD3+	Conditions	0.04929	*
170Er_CD152_CTLA-4	MAIT cells	Conditions	0.0719	ns

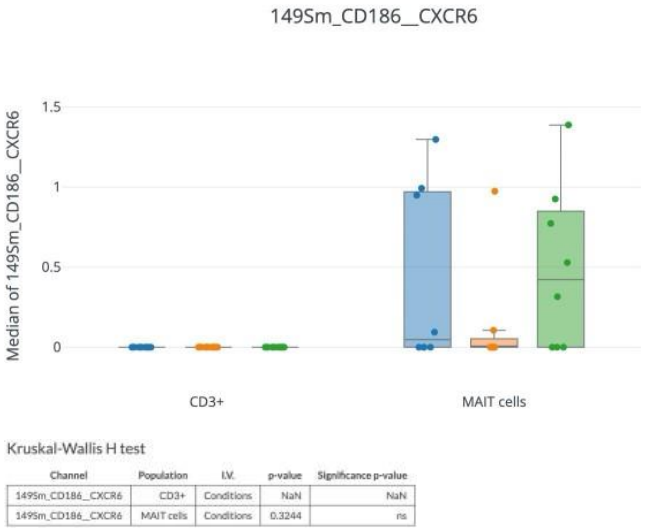

Kruskal-Wallis H test

Channel	Population	I.V.	p-value	Significance p-value
149Sm_CD186__CXCR6	CD3+	Conditions	NaN	NaN
149Sm_CD186__CXCR6	MAIT cells	Conditions	0.3244	ns

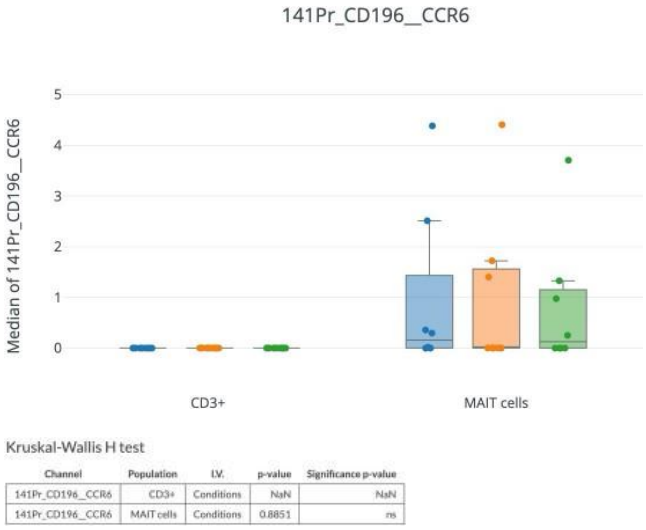

Kruskal-Wallis H test

Channel	Population	I.V.	p-value	Significance p-value
141Pr_CD196__CCR6	CD3+	Conditions	NaN	NaN
141Pr_CD196__CCR6	MAIT cells	Conditions	0.8851	ns

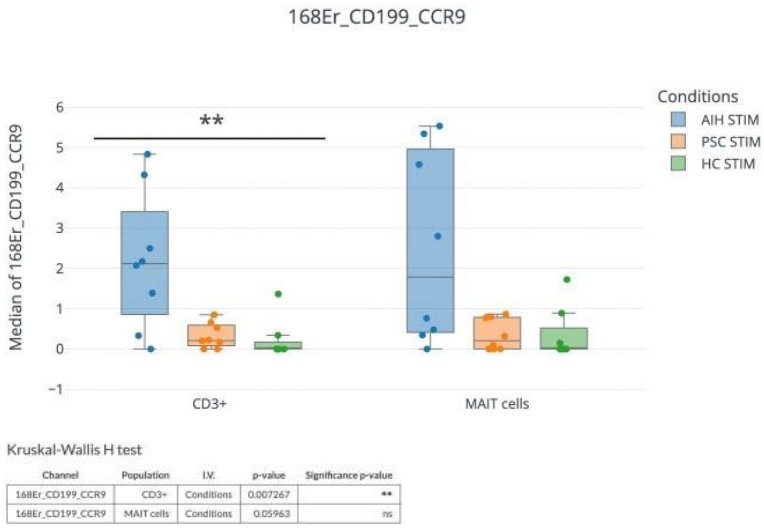

Kruskal-Wallis H test

Channel	Population	I.V.	p-value	Significance p-value
168Er_CD199_CCR9	CD3+	Conditions	0.007267	**
168Er_CD199_CCR9	MAIT cells	Conditions	0.05963	ns

Figure 4h. Peripheral blood total MAIT cell and CD3+ lymphocyte expression of the liver and gut homing chemokine receptors CXCR6, CCR6 and CCR9 respectively, from children with AIH N=8, PSC N=8 and HC N=8. Results of PBMCs treated with CytoStim are shown (STIM). MAIT cell; mucosal-associated invariant T cell, AIH; autoimmune hepatitis, PSC; primary sclerosing cholangitis, HC; healthy children, PBMC; peripheral blood mononuclear cells, I.V.; independent variable, ns; not statistically significant, NaN; not a number. Y-axis shows the median metal intensity (MMI). Kruskal-Wallis H test results are shown. Data are presented as median +/- interquartile range; ***p* <0.01

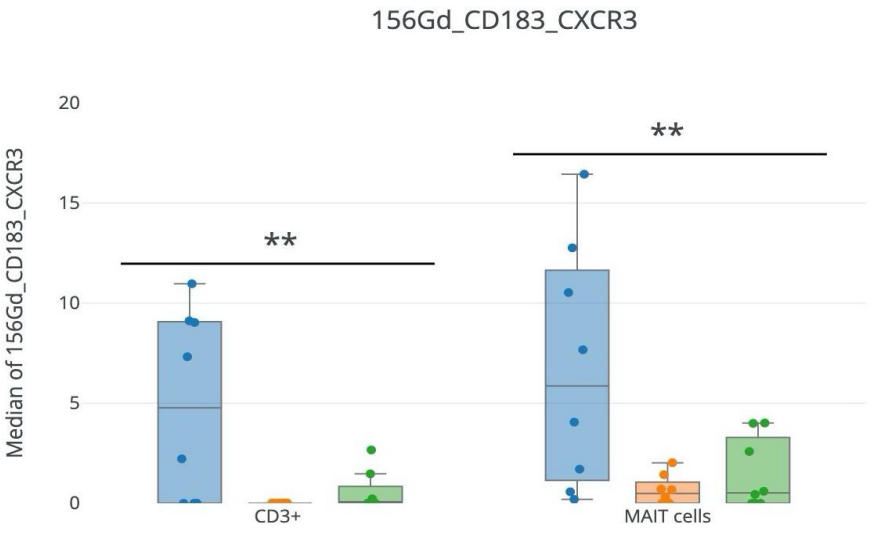

One-way analysis of variance

Channel	Population	I.V.	p-value	Significance p-value
156Gd_CD183_CXCR3	CD3+	Conditions	0.004177	**
156Gd_CD183_CXCR3	MAIT cells	Conditions	0.006506	**

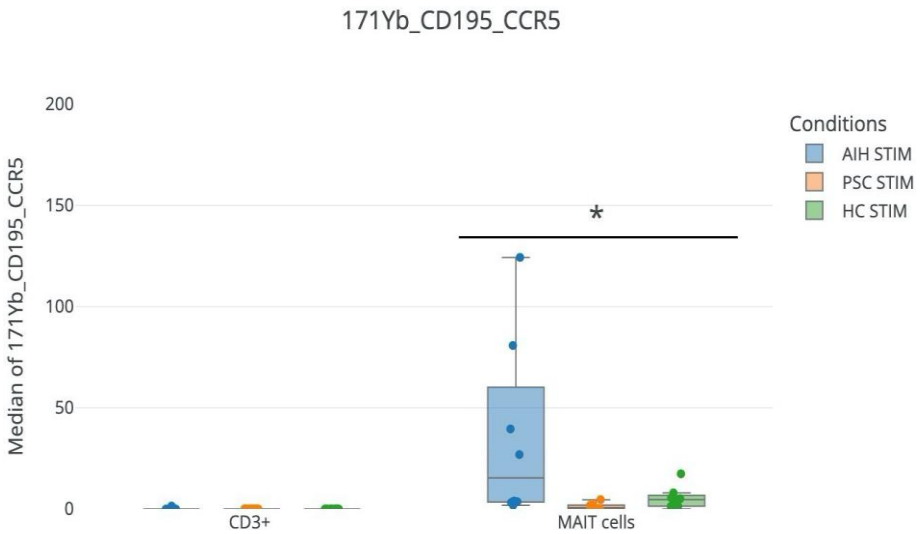

One-way analysis of variance

Channel	Population	I.V.	p-value	Significance p-value
171Yb_CD195_CCR5	CD3+	Conditions	0.3847	ns
171Yb_CD195_CCR5	MAIT cells	Conditions	0.03139	*

Figure 4i. Peripheral blood total MAIT cell and CD3+ lymphocyte expression of the inflammatory chemokine receptors CXCR3 and CCR5 from children with AIH N=8, PSC N=8 and HC N=8. Results of PBMCs treated with CytoStim are displayed (STIM). MAIT cell; mucosal-associated invariant T cell, AIH; autoimmune hepatitis, PSC; primary sclerosing cholangitis, HC; healthy children, PBMC; peripheral blood mononuclear cells, I.V.; independent variable, ns; not statistically significant. Y-axis shows the median metal intensity (MMI). Kruskal-Wallis H test results are shown. Data are presented as median +/- interquartile range; *p <0.05

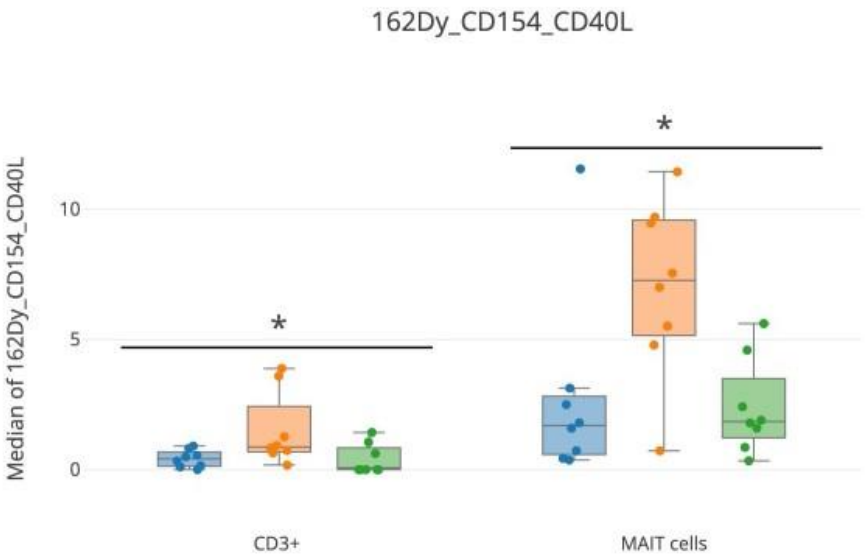

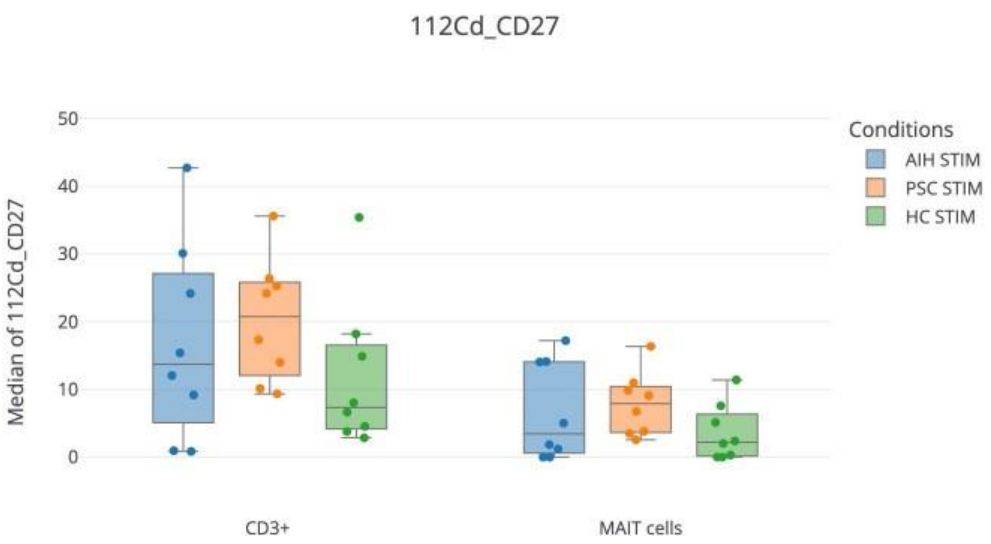

Kruskal-Wallis H test

Channel	Population	I.V.	p-value	Significance p-value
162Dy_CD154_CD40L	CD3+	Conditions	0.03125	*
162Dy_CD154_CD40L	MAIT cells	Conditions	0.03652	*

Kruskal-Wallis H test

Channel	Population	I.V.	p-value	Significance p-value
112Cd_CD27	CD3+	Conditions	0.1675	ns
112Cd_CD27	MAIT cells	Conditions	0.2257	ns

Figure 4j. Peripheral blood total MAIT cell and CD3+ lymphocyte expression of the TNF superfamily costimulatory molecules CD154 (CD40L) and CD27 for AIH N=8, PSC N=8 and HC N=8. Results of PBMCs treated with CytoStim are shown (STIM; stimulated). MAIT cell; mucosal-associated invariant T cell, AIH; autoimmune hepatitis, PSC; primary sclerosing cholangitis, HC; healthy children, PBMC; peripheral blood mononuclear cells, I.V.; independent variable, ns; not statistically significant. Y-axis shows the median metal intensity (MMI). Kruskal-Wallis H test results are shown. Data are presented as median +/- interquartile range; *p <0.05

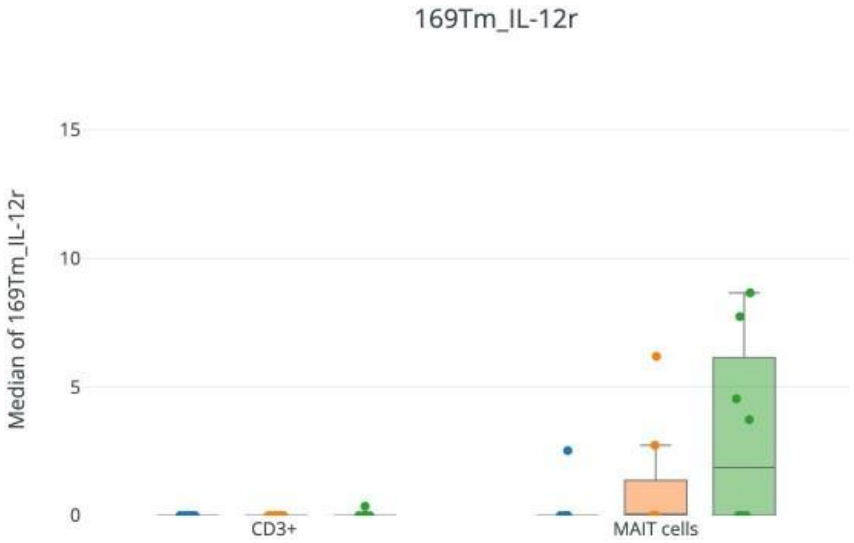

One-way analysis of variance

Channel	Population	I.V.	p-value	Significance p-value
169Tm_IL-12r	CD3+	Conditions	0.3847	ns
169Tm_IL-12r	MAIT cells	Conditions	0.1036	ns

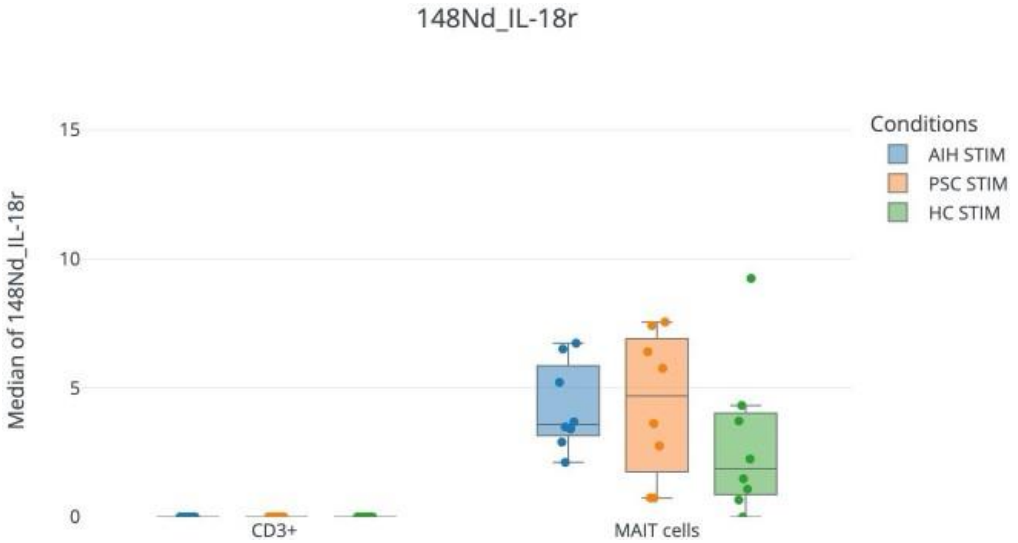

One-way analysis of variance

Channel	Population	I.V.	p-value	Significance p-value
148Nd_IL-18r	CD3+	Conditions	NaN	NaN
148Nd_IL-18r	MAIT cells	Conditions	0.4276	ns

Figure 4k. Peripheral blood total MAIT cell and CD3+ lymphocyte expression of the cytokine receptors IL-12r and IL-18r from children with AIH N=8, PSC N=8 and HC N=8. Results of PBMCs treated CytoStim are shown (STIM; stimulated). MAIT cell; mucosal-associated invariant T cell, AIH; autoimmune hepatitis, PSC; primary sclerosing cholangitis, HC; healthy children, PBMC; peripheral blood mononuclear cells, I.V.; independent variable, ns; not statistically significant, NaN; not a number. Y-axis shows the median metal intensity (MMI). Kruskal-Wallis H test results are shown. Data are presented as median +/- interquartile range.

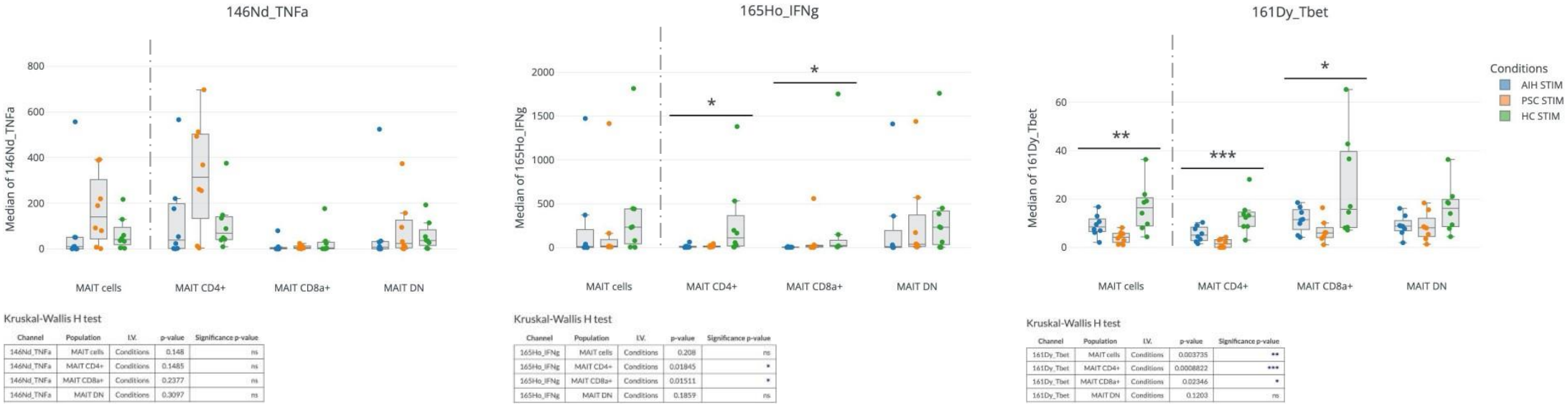

Kruskal-Wallis H test

Channel	Population	I.V.	p-value	Significance p-value
146Nd_TNFa	MAIT cells	Conditions	0.148	ns
146Nd_TNFa	MAIT CD4+	Conditions	0.1485	ns
146Nd_TNFa	MAIT CD8a+	Conditions	0.2377	ns
146Nd_TNFa	MAIT DN	Conditions	0.3097	ns

Kruskal-Wallis H test

Channel	Population	I.V.	p-value	Significance p-value
165Ho_IFNg	MAIT cells	Conditions	0.208	ns
165Ho_IFNg	MAIT CD4+	Conditions	0.01845	*
165Ho_IFNg	MAIT CD8a+	Conditions	0.01511	*
165Ho_IFNg	MAIT DN	Conditions	0.1859	ns

Kruskal-Wallis H test

Channel	Population	I.V.	p-value	Significance p-value
161Dy_Tbet	MAIT cells	Conditions	0.003735	**
161Dy_Tbet	MAIT CD4+	Conditions	0.0008822	***
161Dy_Tbet	MAIT CD8a+	Conditions	0.02346	*
161Dy_Tbet	MAIT DN	Conditions	0.1203	ns

Figure 4l. Box– and - whisker plots showing the total 'MAIT cells' and MAIT cell subset (CD4+, CD8a+, DN) expression of the Th1 profile cytokines TNFα and IFNγ and its transcription factor Tbet from the peripheral blood of children with AIH N=8, PSC N=8 and HC N=8. Results of PBMCs were treated with CytoStim are shown (STIM). MAIT cell; mucosal-associated invariant T cell, AIH; autoimmune hepatitis, PSC; primary sclerosing cholangitis, HC; healthy control, PBMC; peripheral blood mononuclear cells, I.V.; independent variable, ns; not statistically significant. The y-axis shows the median metal intensity (MMI). Kruskal-Wallis H test results are displayed below each graph. Data are presented as median +/- interquartile range; *p <0.05

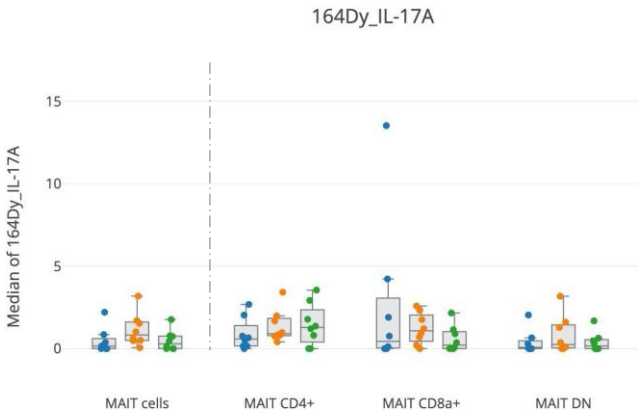

Kruskal-Wallis H test

Channel	Population	I.V.	p-value	Significance p-value
164Dy_IL-17A	MAIT cells	Conditions	0.1245	ns
164Dy_IL-17A	MAIT CD4+	Conditions	0.3682	ns
164Dy_IL-17A	MAIT CD8a+	Conditions	0.378	ns
164Dy_IL-17A	MAIT DN	Conditions	0.5485	ns

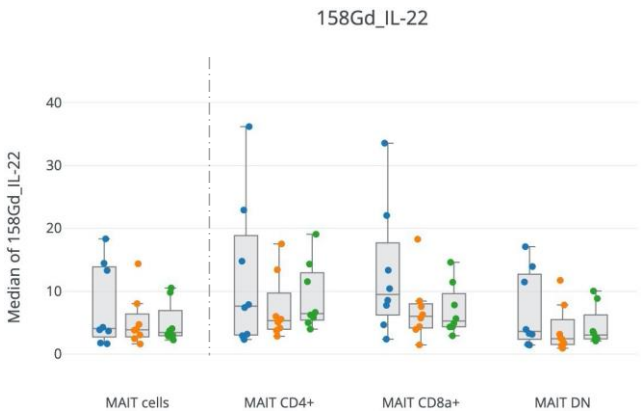

Kruskal-Wallis H test

Channel	Population	I.V.	p-value	Significance p-value
158Gd_IL-22	MAIT cells	Conditions	0.7464	ns
158Gd_IL-22	MAIT CD4+	Conditions	0.6126	ns
158Gd_IL-22	MAIT CD8a+	Conditions	0.2808	ns
158Gd_IL-22	MAIT DN	Conditions	0.357	ns

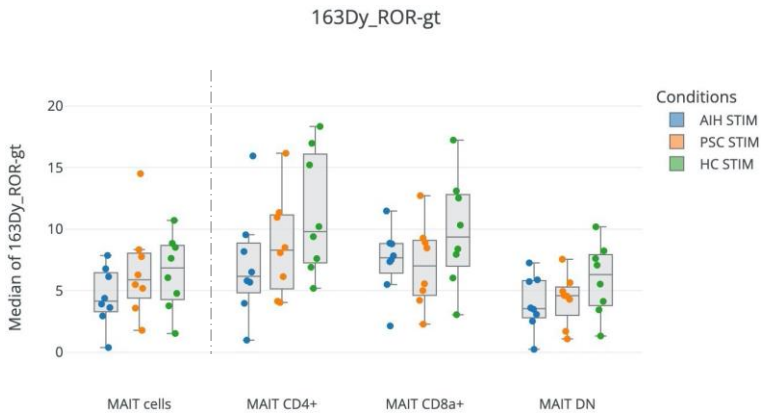

Kruskal-Wallis H test

Channel	Population	I.V.	p-value	Significance p-value
163Dy_ROR-gt	MAIT cells	Conditions	0.3597	ns
163Dy_ROR-gt	MAIT CD4+	Conditions	0.2096	ns
163Dy_ROR-gt	MAIT CD8a+	Conditions	0.3706	ns
163Dy_ROR-gt	MAIT DN	Conditions	0.3526	ns

Figure 4m. Peripheral blood total ‘MAIT cells’ and MAIT cell subset expression of the Th17 profile cytokines IL-17A, IL-22 and its transcription factor RORγt from children with AIH N=8, PSC N=8 and HC N=8. Results of PBMCs treated with CytoStim are shown (STIM). MAIT cell; mucosal-associated invariant T cell, AIH; autoimmune hepatitis, PSC; primary sclerosing cholangitis, HC; healthy children, PBMC; peripheral blood mononuclear cells, I.V.; independent variable, ns; not statistically significant. Y-axis; median metal intensity (MMI). Kruskal-Wallis H test results are shown. Data are presented as median +/- interquartile range.

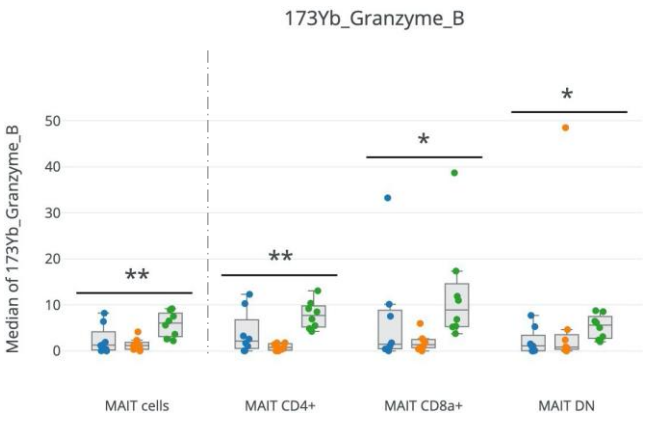

Kruskal-Wallis H test

Channel	Population	I.V.	p-value	Significance p-value
173Yb_Granzyme_B	MAIT cells	Conditions	0.008521	**
173Yb_Granzyme_B	MAIT CD4+	Conditions	0.002393	**
173Yb_Granzyme_B	MAIT CD8a+	Conditions	0.01474	*
173Yb_Granzyme_B	MAIT DN	Conditions	0.04188	*

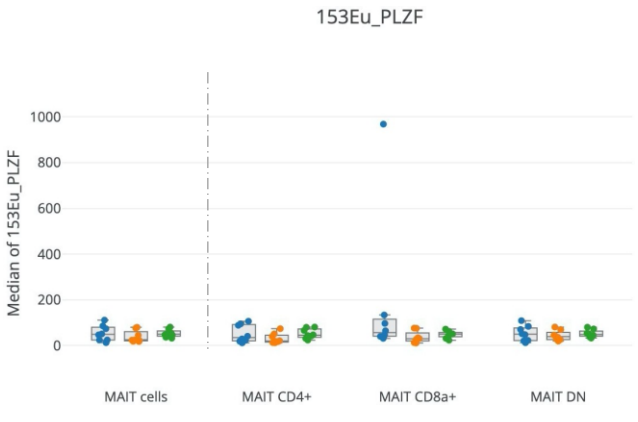

Kruskal-Wallis H test

Channel	Population	I.V.	p-value	Significance p-value
153Eu_PLZF	MAIT cells	Conditions	0.2573	ns
153Eu_PLZF	MAIT CD4+	Conditions	0.1377	ns
153Eu_PLZF	MAIT CD8a+	Conditions	0.1023	ns
153Eu_PLZF	MAIT DN	Conditions	0.5813	ns

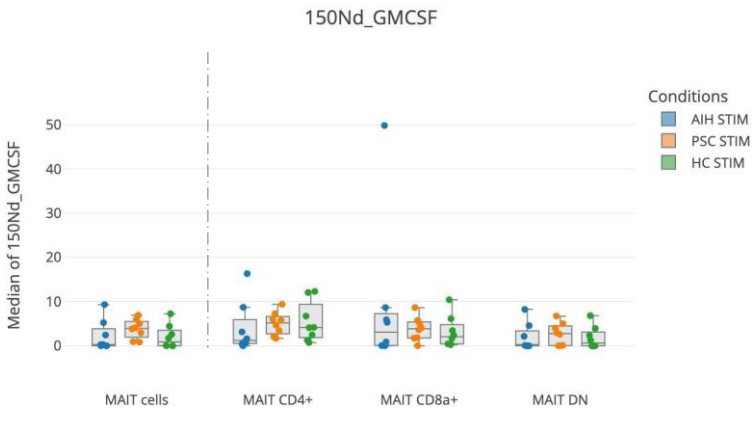

Kruskal-Wallis H test

Channel	Population	I.V.	p-value	Significance p-value
150Nd_GMCSF	MAIT cells	Conditions	0.1605	ns
150Nd_GMCSF	MAIT CD4+	Conditions	0.2472	ns
150Nd_GMCSF	MAIT CD8a+	Conditions	0.9412	ns
150Nd_GMCSF	MAIT DN	Conditions	0.5197	ns

Figure 4n. Peripheral blood total 'MAIT cells' and MAIT cell subset expression of Granzyme B and PLZF, and GMCSF from children with AIH N=8, PSC N=8 and HC N=8. Results of PBMCs treated with CytoStim are shown (STIM). MAIT cell; mucosal-associated invariant T cell, AIH; autoimmune hepatitis, PSC; primary sclerosing cholangitis, HC; healthy children, PBMC; peripheral blood mononuclear cells, I.V.; independent variable, ns; not statistically significant. Y-axis; median metal intensity (MMI). Kruskal-Wallis H test results are shown. Data are presented as median +/- interquartile range; *p <0.05, **p <0.01

Figure 4o (i). Peripheral blood MAIT cell subset expression of CD38, Ki67, PD-1 and CTLA-4 from children with AIH N=8, PSC N=8 and HC N=8. Results of PBMCs treated with CytoStim are shown (STIM). MAIT cell; mucosal-associated invariant T cell, AIH; autoimmune hepatitis, PSC; primary sclerosing cholangitis, HC; healthy children, PBMC; peripheral blood mononuclear cells, CTLA-4; cytotoxic T-lymphocyte associated protein 4, I.V.; independent variable, ns; not statistically significant. Y-axis; median metal intensity (MMI). Kruskal-Wallis H test are shown. Data are presented as median +/- interquartile range; *p <0.05

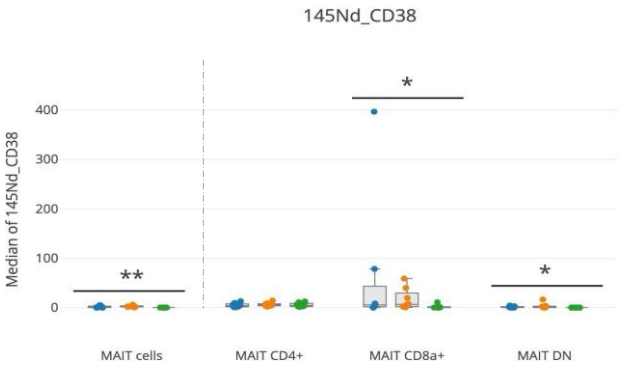

Kruskal-Wallis H test

Channel	Population	I.V.	p-value	Significance p-value
145Nd_CD38	MAIT cells	Conditions	0.002101	**
145Nd_CD38	MAIT CD4+	Conditions	0.7065	ns
145Nd_CD38	MAIT CD8a+	Conditions	0.02877	*
145Nd_CD38	MAIT DN	Conditions	0.01053	*

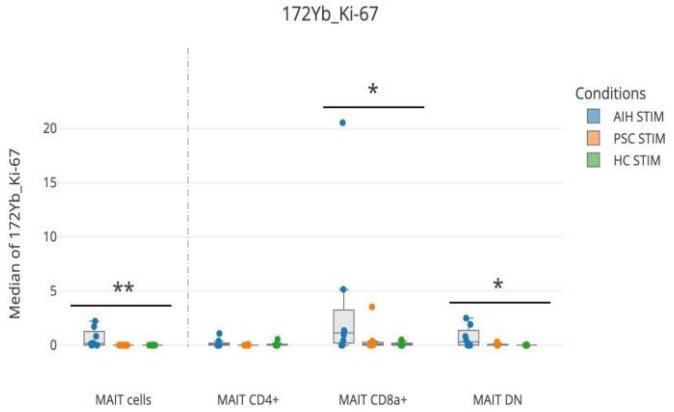

Kruskal-Wallis H test

Channel	Population	I.V.	p-value	Significance p-value
172Yb_Ki-67	MAIT cells	Conditions	0.007446	**
172Yb_Ki-67	MAIT CD4+	Conditions	0.6861	ns
172Yb_Ki-67	MAIT CD8a+	Conditions	0.04267	*
172Yb_Ki-67	MAIT DN	Conditions	0.03662	*

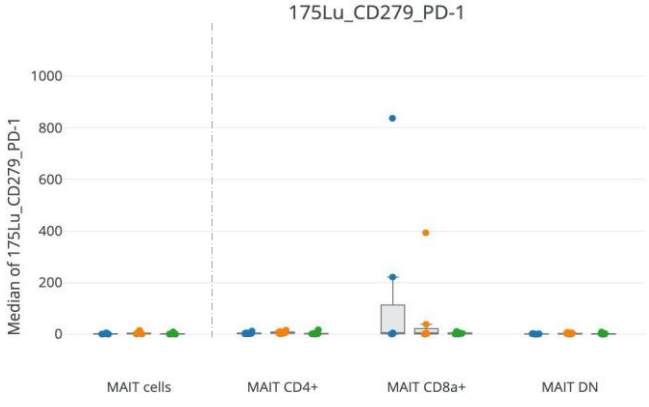

Kruskal-Wallis H test

Channel	Population	I.V.	p-value	Significance p-value
175Lu_CD279_PD-1	MAIT cells	Conditions	0.2248	ns
175Lu_CD279_PD-1	MAIT CD4+	Conditions	0.1367	ns
175Lu_CD279_PD-1	MAIT CD8a+	Conditions	0.6557	ns
175Lu_CD279_PD-1	MAIT DN	Conditions	0.6209	ns

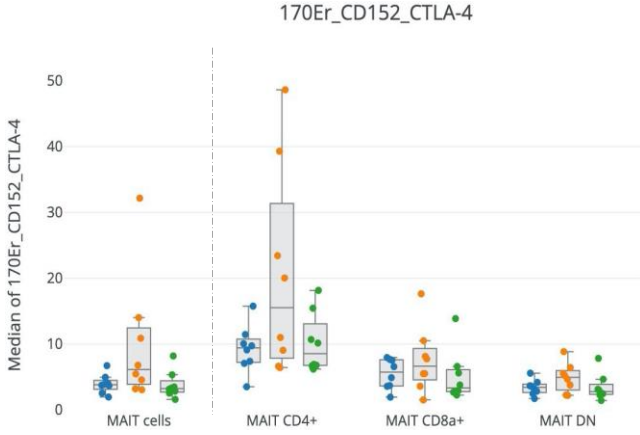

Kruskal-Wallis H test

Channel	Population	I.V.	p-value	Significance p-value
170Er_CD152_CTLA-4	MAIT cells	Conditions	0.0719	ns
170Er_CD152_CTLA-4	MAIT CD4+	Conditions	0.3688	ns
170Er_CD152_CTLA-4	MAIT CD8a+	Conditions	0.3858	ns
170Er_CD152_CTLA-4	MAIT DN	Conditions	0.2787	ns

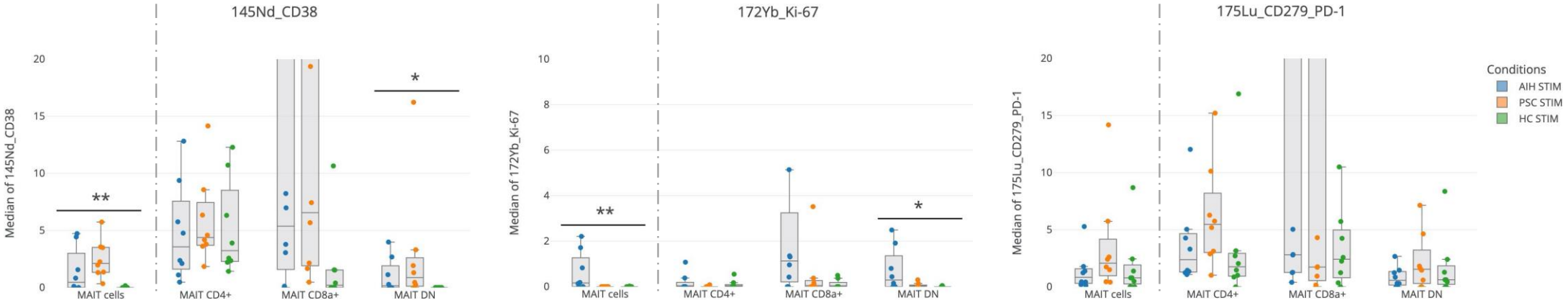

Figure 4o (ii). 'zoomed in' image of MAIT cell subset CD38, Ki67 and PD-1 expression with a lower y-axis scale. All results are displayed apart from the outlier results in Figure 4o. Data are presented as median +/- interquartile range; *p <0.05, **p <0.01

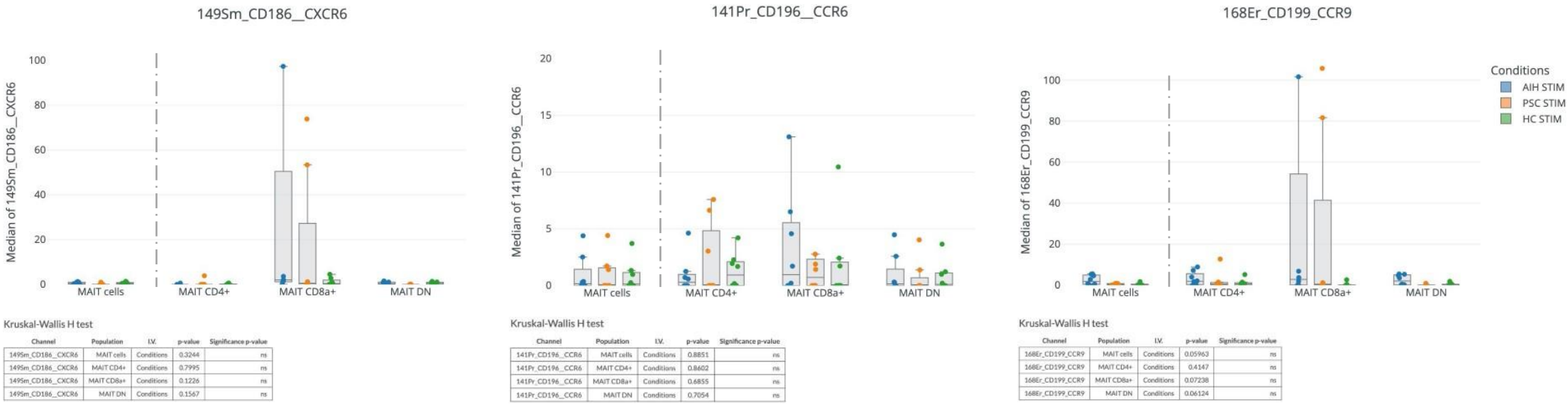

Channel	Population	I.V.	p-value	Significance p-value
149Sm_CD186__CXCR6	MAIT cells	Conditions	0.3244	ns
149Sm_CD186__CXCR6	MAIT CD4+	Conditions	0.7995	ns
149Sm_CD186__CXCR6	MAIT CD8a+	Conditions	0.1226	ns
149Sm_CD186__CXCR6	MAIT DN	Conditions	0.1567	ns

Channel	Population	I.V.	p-value	Significance p-value
141Pr_CD196__CCR6	MAIT cells	Conditions	0.8851	ns
141Pr_CD196__CCR6	MAIT CD4+	Conditions	0.8602	ns
141Pr_CD196__CCR6	MAIT CD8a+	Conditions	0.6855	ns
141Pr_CD196__CCR6	MAIT DN	Conditions	0.7054	ns

Channel	Population	I.V.	p-value	Significance p-value
168Er_CD199_CCR9	MAIT cells	Conditions	0.05963	ns
168Er_CD199_CCR9	MAIT CD4+	Conditions	0.4147	ns
168Er_CD199_CCR9	MAIT CD8a+	Conditions	0.07238	ns
168Er_CD199_CCR9	MAIT DN	Conditions	0.06124	ns

Figure 4p. Peripheral blood total ‘MAIT cells’ and MAIT cell subset expression of the liver and gut homing chemokine receptors CXCR6, CCR6 and CCR9 respectively are shown from children with AIH N=8, PSC N=8 and HC N=8. Results of PBMCs treated with CytoStim are displayed (STIM). MAIT cell; mucosal-associated invariant T cell, AIH; autoimmune hepatitis, PSC; primary sclerosing cholangitis, HC; healthy children, PBMC; peripheral blood mononuclear cells, I.V.; independent variable, ns; not statistically significant. Y-axis; median metal intensity (MMI). Kruskal-Wallis H test results are shown. Data are presented as median +/- interquartile range.

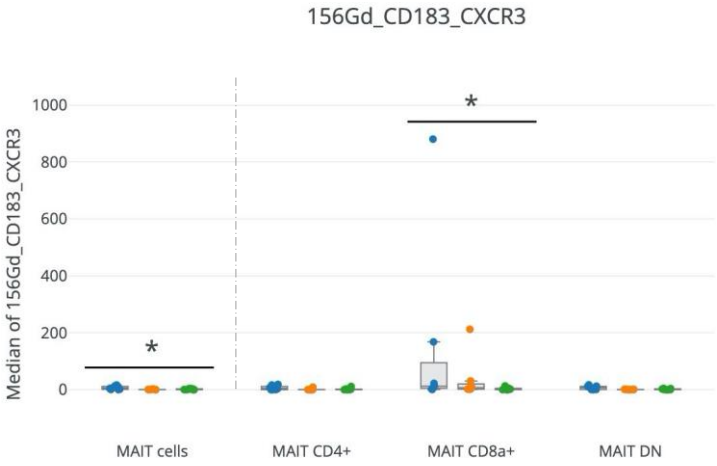

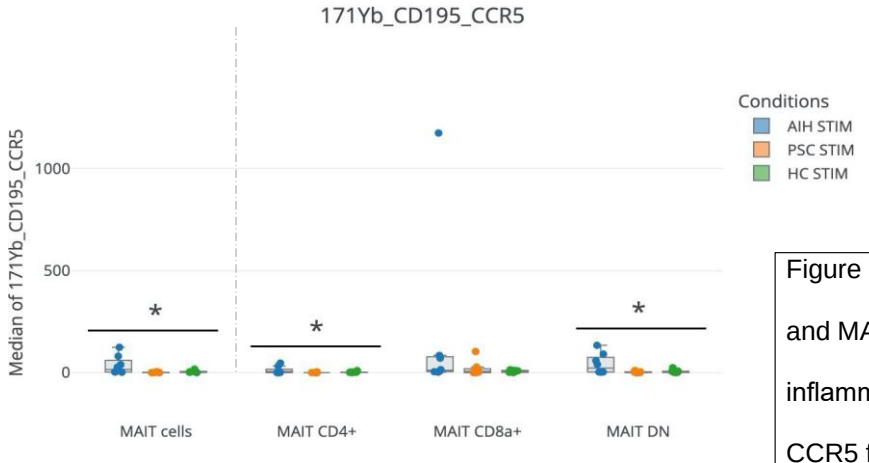

Kruskal-Wallis H test

Channel	Population	I.V.	p-value	Significance p-value
156Gd_CD183_CXCR3	MAIT cells	Conditions	0.03221	*
156Gd_CD183_CXCR3	MAIT CD4+	Conditions	0.1911	ns
156Gd_CD183_CXCR3	MAIT CD8a+	Conditions	0.03626	*
156Gd_CD183_CXCR3	MAIT DN	Conditions	0.05351	ns

Kruskal-Wallis H test

Channel	Population	I.V.	p-value	Significance p-value
171Yb_CD195_CCR5	MAIT cells	Conditions	0.01076	*
171Yb_CD195_CCR5	MAIT CD4+	Conditions	0.01908	*
171Yb_CD195_CCR5	MAIT CD8a+	Conditions	0.1619	ns
171Yb_CD195_CCR5	MAIT DN	Conditions	0.03865	*

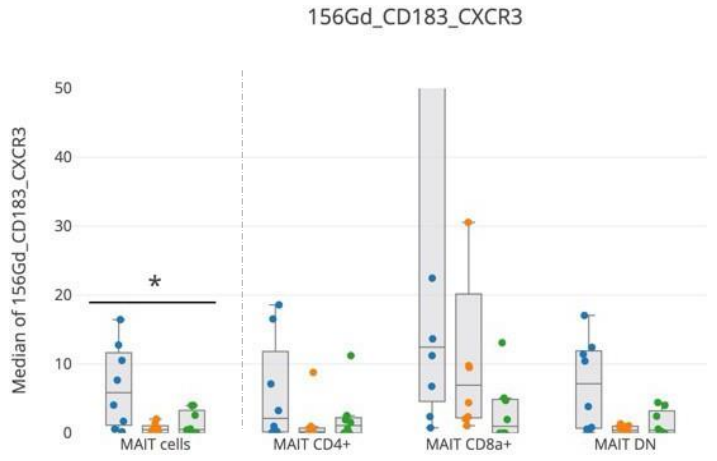

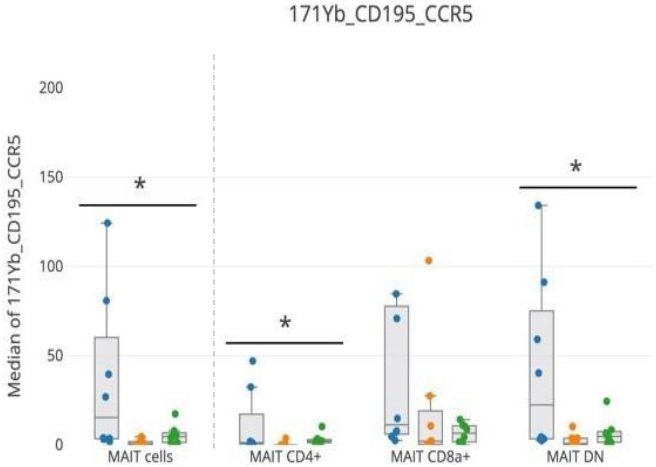

Figure 4q (i). Peripheral blood total 'MAIT cells' and MAIT cell subset expression of the inflammatory chemokine receptors CXCR3 and CCR5 from children with AIH N=8, PSC N=8 and HC N=8. Results of PBMCs treated with CytoStim are shown (STIM). Figure 4q (ii). Total 'MAIT cells' and subset expressions of CXCR3 and CCR5 with y-axis scale lowered to show the distribution of individual MMIs. MAIT cell; mucosal-associated invariant T cell, AIH; autoimmune hepatitis, PSC; primary sclerosing cholangitis, HC; healthy children, PBMC; peripheral blood mononuclear cells, I.V.; independent variable, ns; not statistically significant. Y-axis; median metal intensity (MMI). Kruskal-Wallis H test results are shown. Data are presented as median +/- interquartile range; *p <0.05

Figure 4r (i)

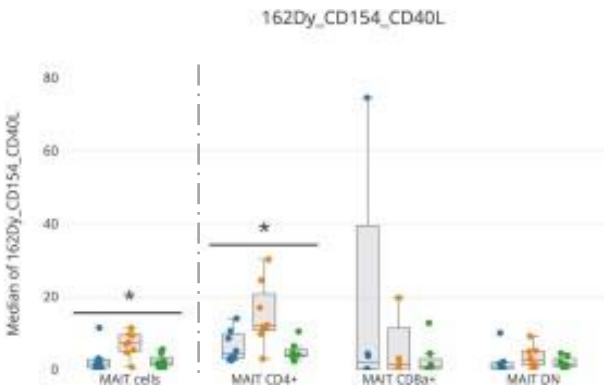

Kruskal-Wallis H test

Channel	Population	I.V.	p-value	Significance p-value
162Dy_CD154_CD40L	MAIT cells	Conditions	0.03652	*
162Dy_CD154_CD40L	MAIT CD4+	Conditions	0.02176	*
162Dy_CD154_CD40L	MAIT CD8a+	Conditions	0.9925	ns
162Dy_CD154_CD40L	MAIT DN	Conditions	0.38	ns

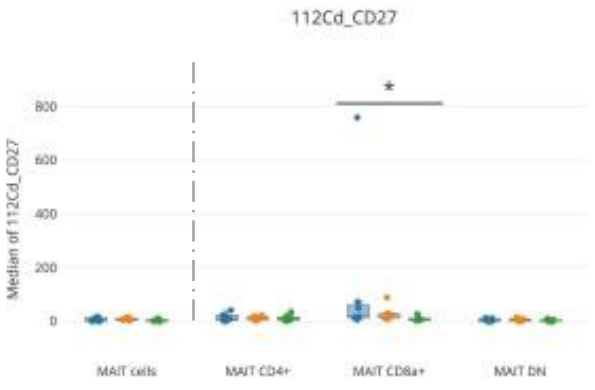

Kruskal-Wallis H test

Channel	Population	I.V.	p-value	Significance p-value
112Cd_CD27	MAIT cells	Conditions	0.2337	ns
112Cd_CD27	MAIT CD4+	Conditions	0.9254	ns
112Cd_CD27	MAIT CD8a+	Conditions	0.0133	*
112Cd_CD27	MAIT DN	Conditions	0.7278	ns

Figure 4r (ii)

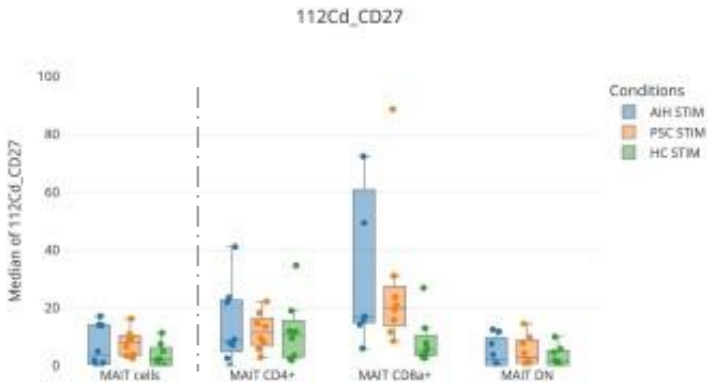

Figure 4r (i). Peripheral blood total 'MAIT cells' and subset expression of the costimulatory molecules CD154 (CD40L) and CD27 of the tumour necrosis factor ligand (TNFL) and receptor (TNFR) superfamily respectively, for AIH N=8, PSC N=8 and HC N=8. Results of PBMCs treated with CytoStim are shown (STIM).

Figure 4r (ii) 'zoomed in' image of CD27 expression with a lower y-axis scale; all results are displayed apart from the outlier in Figure 4r (i). MAIT cell; mucosal-associated invariant T cell, AIH; autoimmune hepatitis, PSC; primary sclerosing cholangitis, HC; healthy children, PBMC; peripheral blood mononuclear cells, I.V.; independent variable, ns; not statistically significant. Y-axis shows the median metal intensity (MMI). Kruksal-Wallis H test results are shown. Data are presented as median +/- interquartile range; *p <0.05

Figure 4s (i)

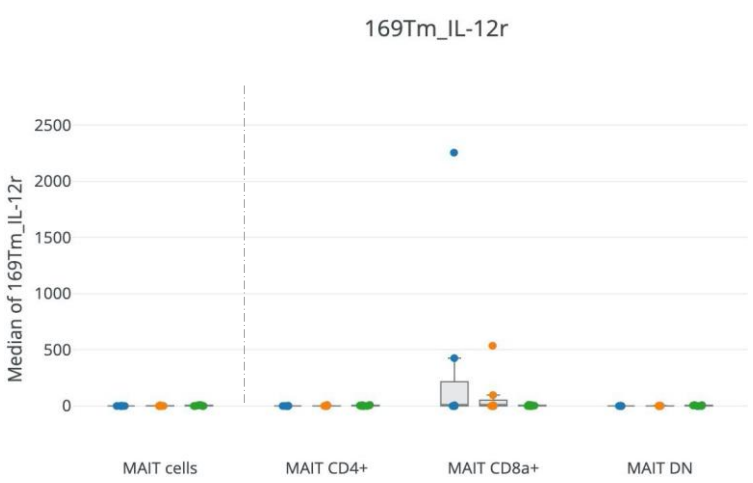

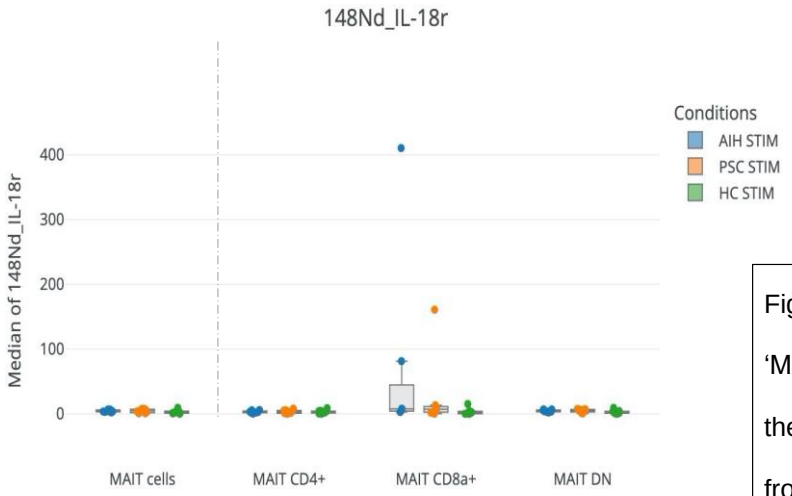

Kruskal-Wallis H test

Channel	Population	I.V.	p-value	Significance p-value
169Tm_IL-12r	MAIT cells	Conditions	0.1551	ns
169Tm_IL-12r	MAIT CD4+	Conditions	0.2026	ns
169Tm_IL-12r	MAIT CD8a+	Conditions	0.9451	ns
169Tm_IL-12r	MAIT DN	Conditions	0.122	ns

Kruskal-Wallis H test

Channel	Population	I.V.	p-value	Significance p-value
148Nd_IL-18r	MAIT cells	Conditions	0.3706	ns
148Nd_IL-18r	MAIT CD4+	Conditions	0.9536	ns
148Nd_IL-18r	MAIT CD8a+	Conditions	0.07086	ns
148Nd_IL-18r	MAIT DN	Conditions	0.2215	ns

Figure 4s (ii)

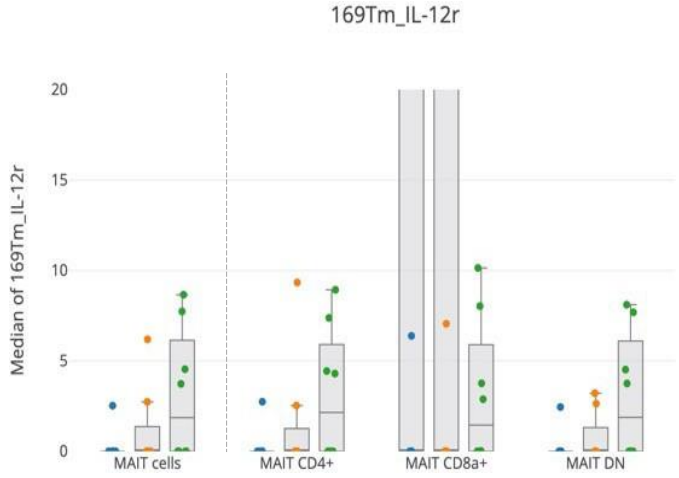

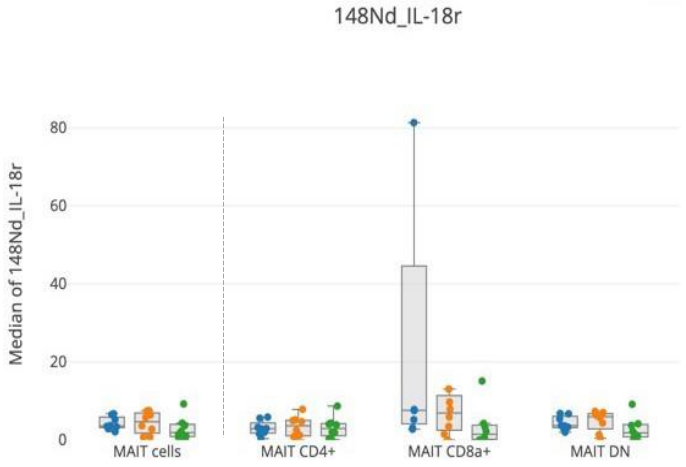

Figure 4s (i). Peripheral blood total 'MAIT cells' and subset expression of the cytokine receptors IL-12r and IL-18r from children with AIH N=8, PSC N=8 and HC N=8. Results of PBMCs treated with CytoStim are shown (STIM). Figure 4s (ii) 'zoomed in' images of IL-12r and IL-18r expression. MAIT cell; mucosal-associated invariant T cell, AIH; autoimmune hepatitis, PSC; primary sclerosing cholangitis, HC; healthy children, PBMC; peripheral blood mononuclear cells, I.V.; independent variable, ns; not statistically significant. Y-axis shows the median metal intensity (MMI). Kruskal-Wallis H test results are shown. Data are presented as median +/- interquartile range.

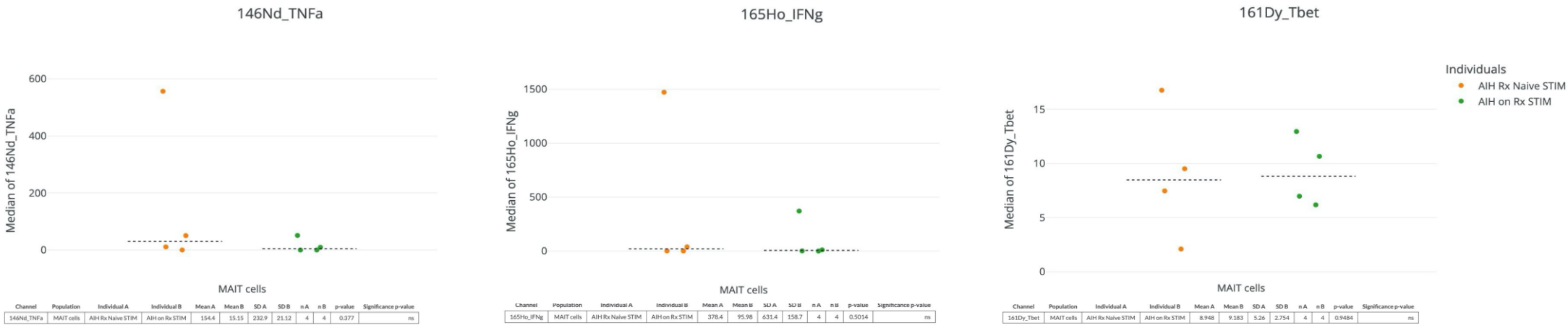

Channel	Population	Individual A	Individual B	Mean A	Mean B	SD A	SD B	n A	n B	p-value	Significance p-value
146Nd_TNFa	MAIT cells	AIH Rx Naive STIM	AIH on Rx STIM	154.4	15.15	232.9	21.12	4	4	0.377	ns

Channel	Population	Individual A	Individual B	Mean A	Mean B	SD A	SD B	n A	n B	p-value	Significance p-value
165Ho_IFNg	MAIT cells	AIH Rx Naive STIM	AIH on Rx STIM	378.4	95.98	631.4	158.7	4	4	0.5014	ns

Channel	Population	Individual A	Individual B	Mean A	Mean B	SD A	SD B	n A	n B	p-value	Significance p-value
161Dy_Tbet	MAIT cells	AIH Rx Naive STIM	AIH on Rx STIM	8.948	9.183	5.26	2.754	4	4	0.9484	ns

Figure 4t. Summary dot plots showing peripheral blood total MAIT cell expression of TNFα and IFNγ and the transcription factor Tbet from the AIH cohort. Analysis of the cohort is split into children with newly diagnosed AIH (treatment naïve, Rx Naïve STIM, N=4) and those already on therapy (on Rx STIM, N=4). Results of PBMCs stimulated with CytoStim are shown. MAIT cell; mucosal-associated invariant T cell, AIH; autoimmune hepatitis, PSC; primary sclerosing cholangitis, HC; healthy control, PBMC; peripheral blood mononuclear cells, ns; not statistically significant. The y-axis shows the median metal intensity (MMI). Mann-Whitney U test results are displayed below each graph. Data are presented as median +/- interquartile range.

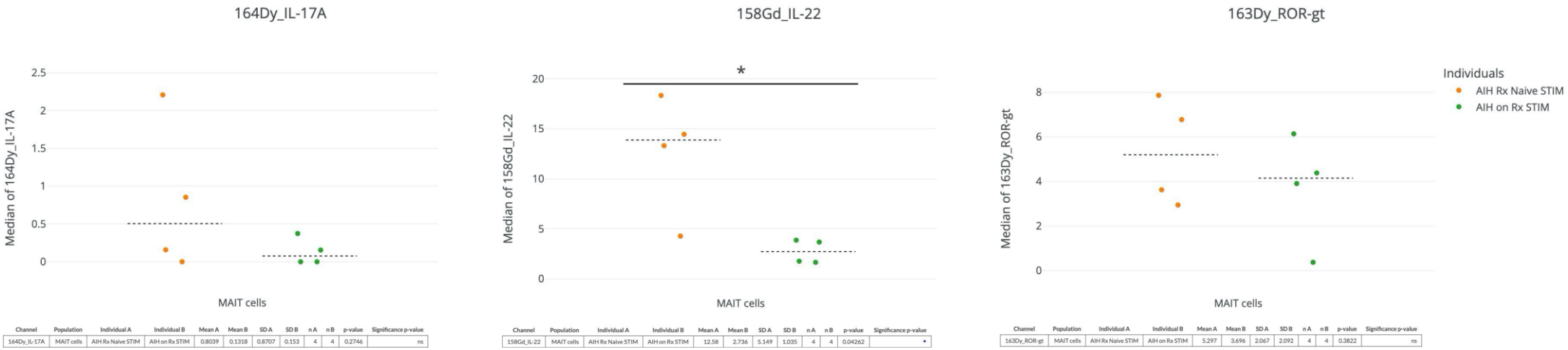

Channel	Population	Individual A	Individual B	Mean A	Mean B	SD A	SD B	n A	n B	p-value	Significance p-value
164Dy_IL-17A	MAIT cells	AIH Rx Naive STIM	AIH on Rx STIM	0.8039	0.1318	0.8707	0.153	4	4	0.2746	ns

Channel	Population	Individual A	Individual B	Mean A	Mean B	SD A	SD B	n A	n B	p-value	Significance p-value
158Gd_IL-22	MAIT cells	AIH Rx Naive STIM	AIH on Rx STIM	12.58	2.736	5.149	1.035	4	4	0.04262	*

Channel	Population	Individual A	Individual B	Mean A	Mean B	SD A	SD B	n A	n B	p-value	Significance p-value
163Dy_ROR-gt	MAIT cells	AIH Rx Naive STIM	AIH on Rx STIM	5.297	3.696	2.067	2.092	4	4	0.3822	ns

Figure 4u. Summary dot plots showing peripheral blood total MAIT cell expression of IL-17A, IL-22 and the transcription factor RORγt from the AIH cohort; children with newly diagnosed AIH (treatment naïve, Rx Naïve STIM, N=4) and those already on therapy (on Rx STIM, N=4). Results of PBMCs stimulated with CytoStim are shown.

MAIT cell; mucosal-associated invariant T cell, AIH; autoimmune hepatitis, PSC; primary sclerosing cholangitis, HC; healthy control, PBMC; peripheral blood mononuclear cells, ns; not statistically significant. Y-axis shows the median metal intensity (MMI). Mann-Whitney U test results are displayed below each graph. Data are presented as median +/- interquartile range; *p<0.05

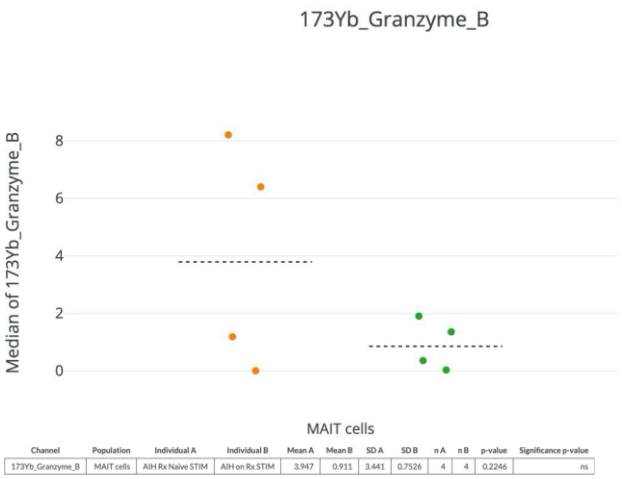

Channel	Population	Individual A	Individual B	Mean A	Mean B	SD A	SD B	n A	n B	p-value	Significance p-value
173Yb_Granzyme_B	MAIT cells	AIH Rx Naive STIM	AIH on Rx STIM	3.947	0.911	3.441	0.7526	4	4	0.2246	ns

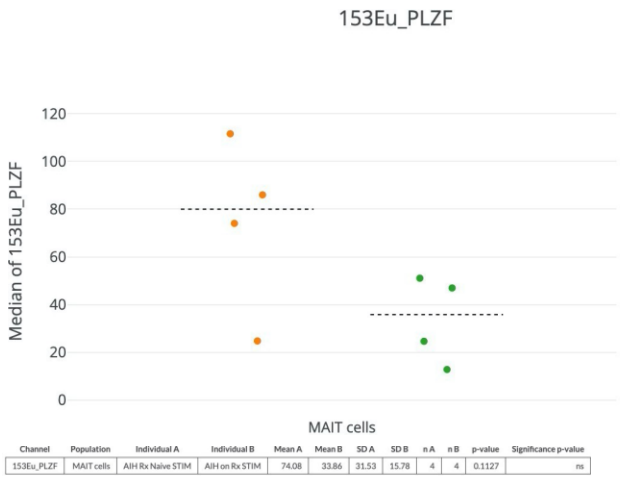

Channel	Population	Individual A	Individual B	Mean A	Mean B	SD A	SD B	n A	n B	p-value	Significance p-value
153Eu_PLZF	MAIT cells	AIH Rx Naive STIM	AIH on Rx STIM	74.08	33.86	31.53	15.78	4	4	0.1127	ns

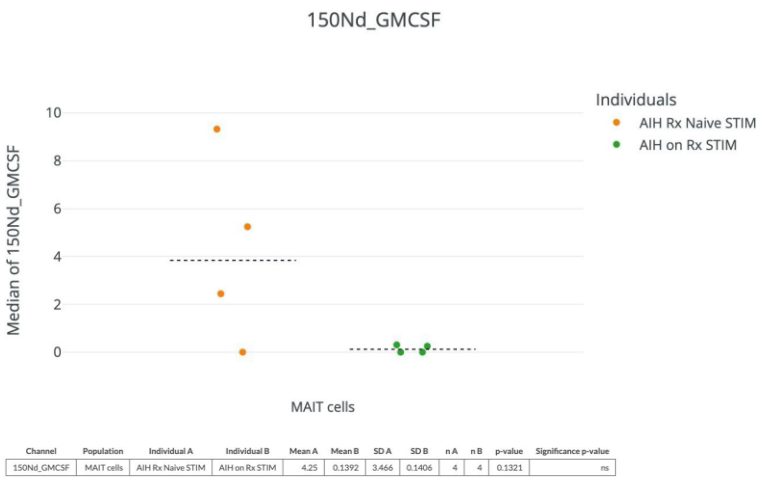

Channel	Population	Individual A	Individual B	Mean A	Mean B	SD A	SD B	n A	n B	p-value	Significance p-value
150Nd_GMCSF	MAIT cells	AIH Rx Naive STIM	AIH on Rx STIM	4.25	0.1392	3.466	0.1406	4	4	0.1321	ns

Figure 4v. Summary dot plots showing peripheral blood total MAIT cell expression of Granzyme B, PLZF and GMCSF from the AIH cohort; children with newly diagnosed AIH (treatment naïve, Rx Naïve STIM, N=4) and treated patients (on Rx STIM, N=4). Results of PBMC stimulated with CytoStim are shown. MAIT cell; mucosal-associated invariant T cell, AIH; autoimmune hepatitis, PSC; primary sclerosing cholangitis, HC; healthy control, PBMC; peripheral blood mononuclear cells, ns; not statistically significant. Y-axis shows the median metal intensity (MMI). Mann-Whitney U test results are displayed below each graph. Data are presented as median +/- interquartile range.

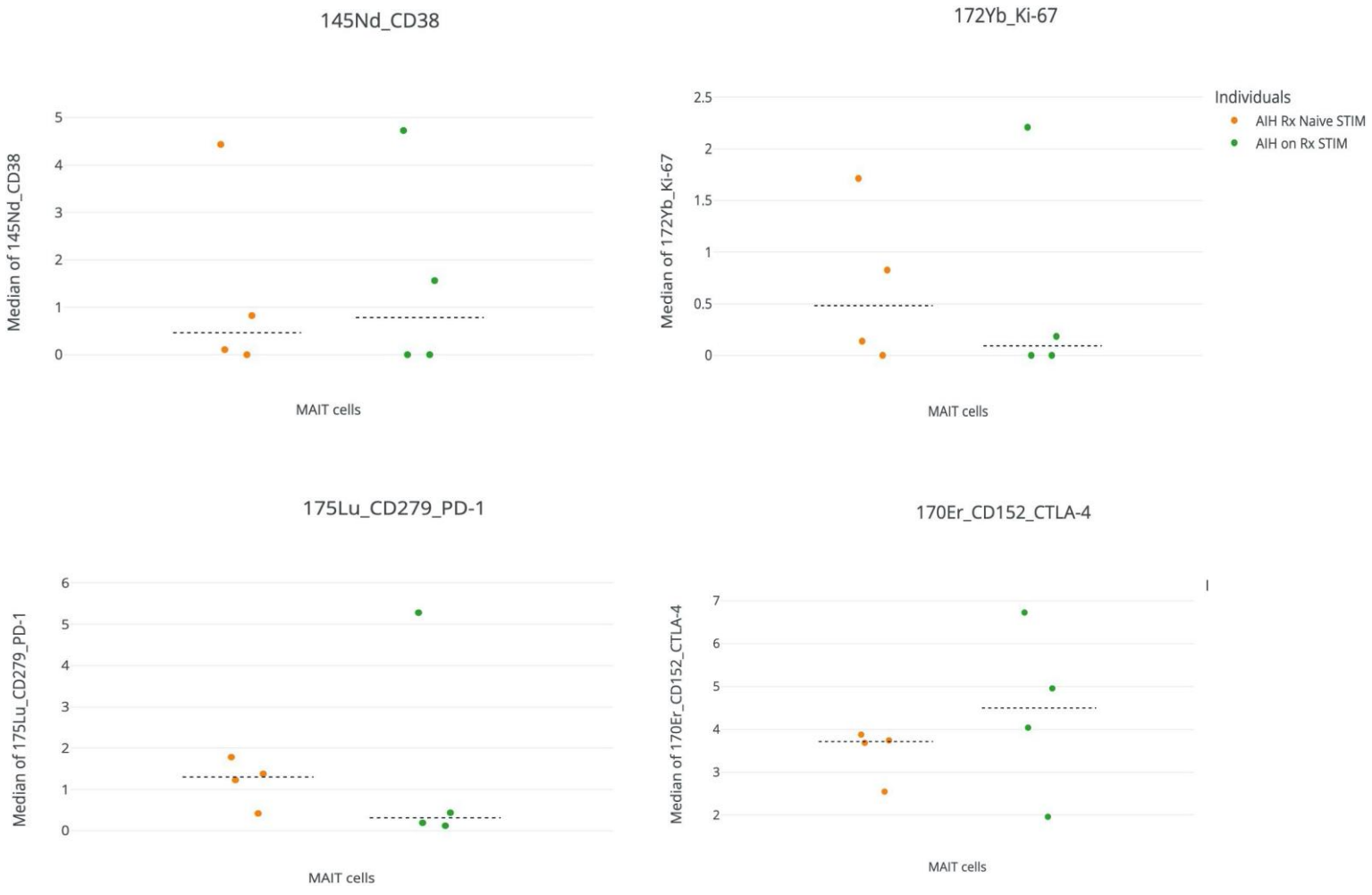

Figure 4w. Summary dot plots showing peripheral blood total MAIT cell expression of CD38, Ki67, PD-1, and CTLA-4 from the AIH cohort; children with newly diagnosed AIH (treatment naïve, Rx Naïve STIM, N=4) and treated patients (on Rx STIM, N=4). Results of PBMC stimulated with CytoStim are shown. MAIT cell; mucosal-associated invariant T cell, AIH; autoimmune hepatitis, PSC; primary sclerosing cholangitis, HC; healthy control, PBMC; peripheral blood mononuclear cells, ns; not statistically significant. Y-axis shows the median metal intensity (MMI).

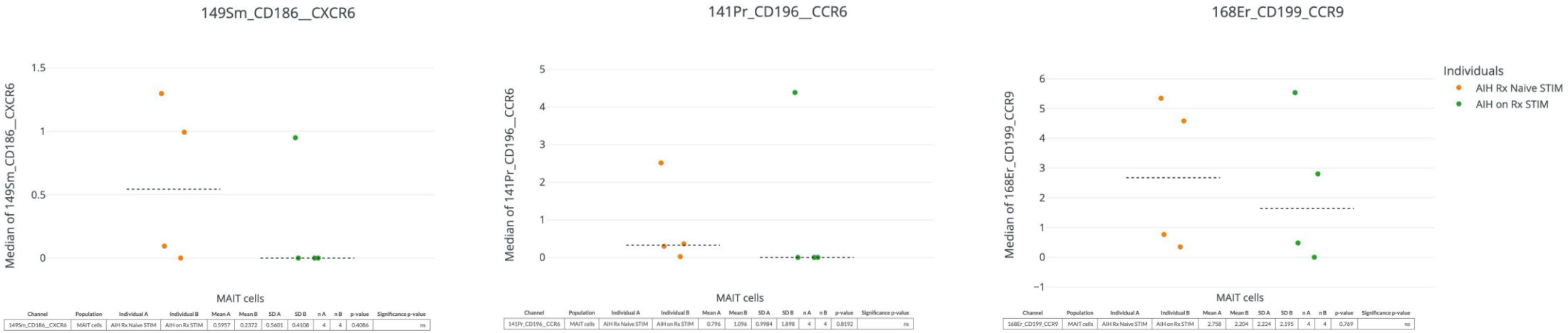

Channel	Population	Individual A	Individual B	Mean A	Mean B	SD A	SD B	n A	n B	p-value	Significance p-value
149Sm_CD186__CXCR6	MAIT cells	AIH Rx Naive STIM	AIH on Rx STIM	0.5957	0.2372	0.5601	0.4108	4	4	0.4086	ns

Channel	Population	Individual A	Individual B	Mean A	Mean B	SD A	SD B	n A	n B	p-value	Significance p-value
141Pr_CD196__CCR6	MAIT cells	AIH Rx Naive STIM	AIH on Rx STIM	0.796	1.096	0.9984	1.898	4	4	0.8192	ns

Channel	Population	Individual A	Individual B	Mean A	Mean B	SD A	SD B	n A	n B	p-value	Significance p-value
168Er_CD199_CCR9	MAIT cells	AIH Rx Naive STIM	AIH on Rx STIM	2.758	2.204	2.224	2.195	4	4	0.769	ns

Figure 4x. Summary dot plots showing peripheral blood total MAIT cell expression of the chemokine receptors CXCR6, CCR6 and CCR9 from the AIH cohort; children with newly diagnosed AIH (treatment naïve, Rx Naïve STIM, N=4) and treated patients (on Rx STIM, N=4). Results of PBMC stimulated with CytoStim are shown. MAIT cell; mucosal-associated invariant T cell, AIH; autoimmune hepatitis, PSC; primary sclerosing cholangitis, HC; healthy control, PBMC; peripheral blood mononuclear cells, ns; not statistically significant. Y-axis shows the median metal intensity (MMI). Mann-Whitney U test results are displayed below each graph. Data are presented as median +/- interquartile range.

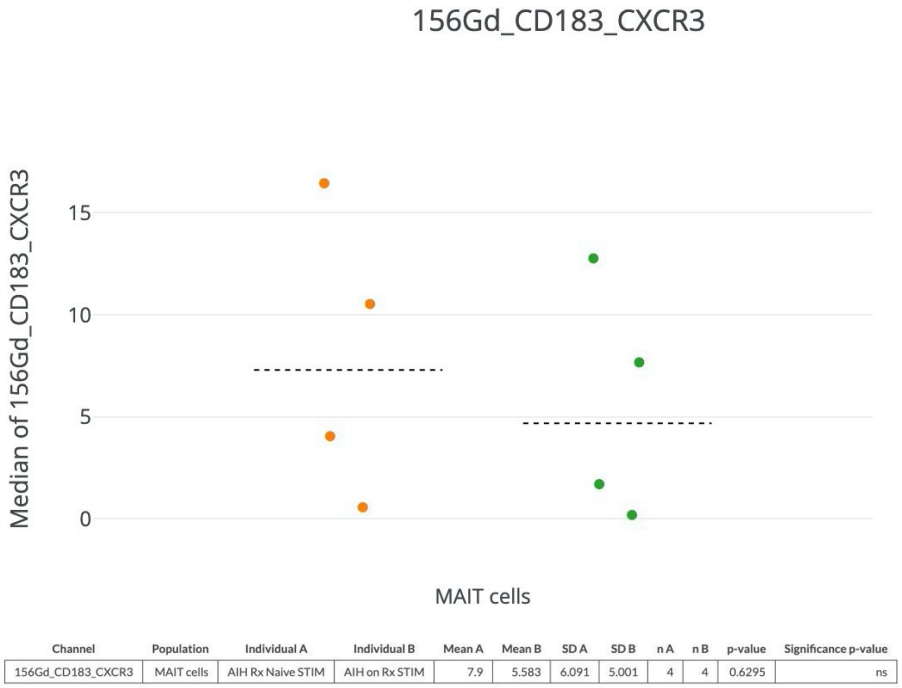

Channel	Population	Individual A	Individual B	Mean A	Mean B	SD A	SD B	n A	n B	p-value	Significance p-value
156Gd_CD183_CXCR3	MAIT cells	AIH Rx Naive STIM	AIH on Rx STIM	7.9	5.583	6.091	5.001	4	4	0.6295	ns

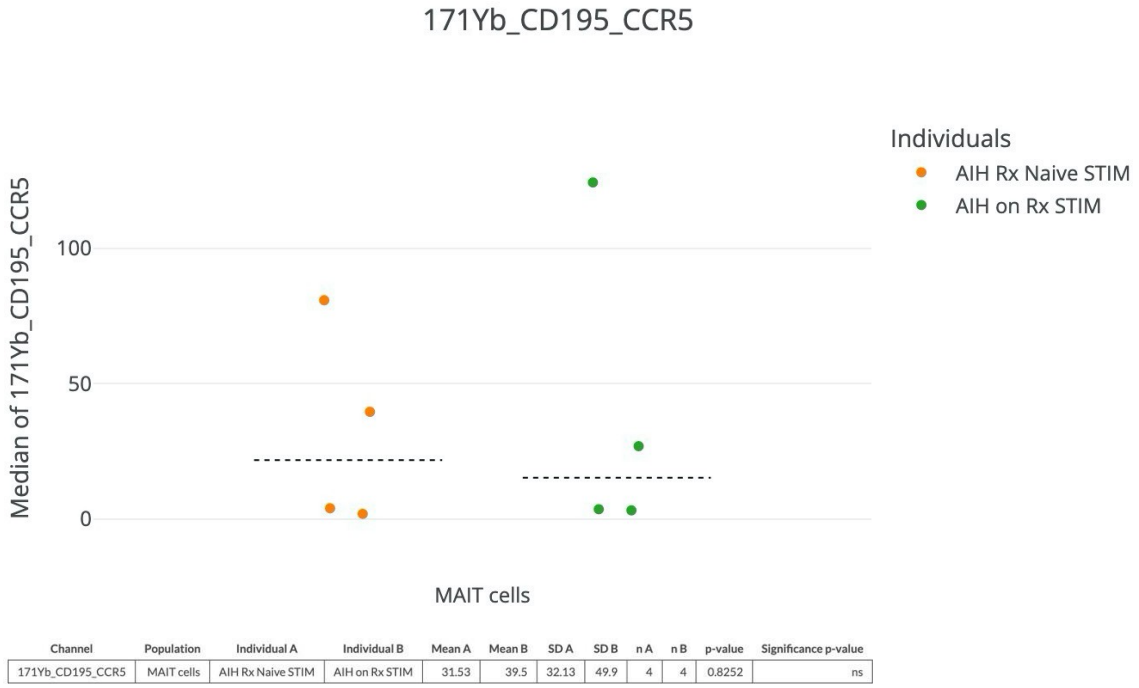

Channel	Population	Individual A	Individual B	Mean A	Mean B	SD A	SD B	n A	n B	p-value	Significance p-value
171Yb_CD195_CCR5	MAIT cells	AIH Rx Naive STIM	AIH on Rx STIM	31.53	39.5	32.13	49.9	4	4	0.8252	ns

Figure 4y. Summary dot plots showing peripheral blood total MAIT cell expression of the chemokine receptors CXCR3 and CCR5 from the AIH cohort; children with newly diagnosed AIH (treatment naïve, Rx Naïve STIM, N=4) and treated patients (on Rx STIM, N=4). Results of PBMC stimulated with CytoStim are shown. MAIT cell; mucosal- associated invariant T cell, AIH; autoimmune hepatitis, PSC; primary sclerosing cholangitis, HC; healthy control, PBMC; peripheral blood mononuclear cells, ns; not statistically significant. Y-axis shows the median metal intensity (MMI). Mann-Whitney U test results are displayed below each graph. Data are presented as median +/- interquartile range.

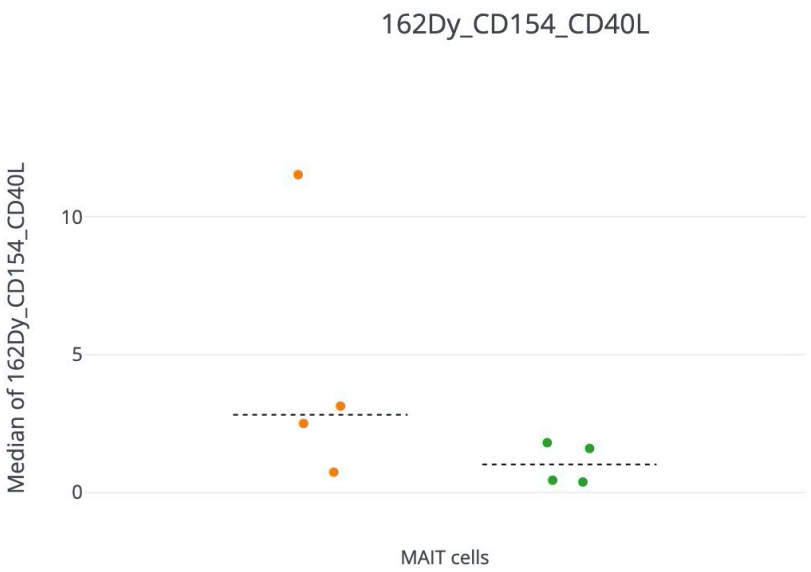

Channel	Population	Individual A	Individual B	Mean A	Mean B	SD A	SD B	n A	n B	p-value	Significance p-value
162Dy_CD154_CD40L	MAIT cells	AIH Rx Naive STIM	AIH on Rx STIM	4.475	1.048	4.176	0.6508	4	4	0.2509	ns

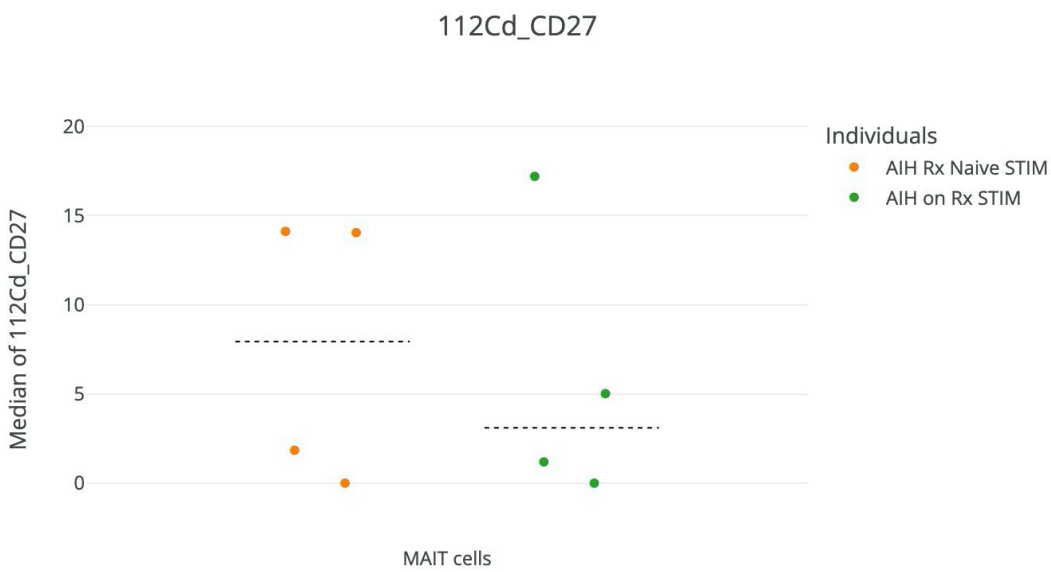

Channel	Population	Individual A	Individual B	Mean A	Mean B	SD A	SD B	n A	n B	p-value	Significance p-value
112Cd_CD27	MAIT cells	AIH Rx Naive STIM	AIH on Rx STIM	7.499	5.851	6.609	6.806	4	4	1	ns

Figure 4z. Summary dot plots showing peripheral blood total MAIT cell expression of the TNF superfamily costimulatory molecules CD40L and CD27 from the AIH cohort; children with newly diagnosed AIH (treatment naïve, Rx Naïve STIM, N=4) and treated patients (on Rx STIM, N=4). Results of PBMC stimulated with CytoStim are shown. MAIT cell; mucosal-associated invariant T cell, AIH; autoimmune hepatitis, PSC; primary sclerosing cholangitis, HC; healthy control, PBMC; peripheral blood mononuclear cells, ns; not statistically significant. Y-axis shows the median metal intensity (MMI). Mann-Whitney U test results are displayed below each graph. Data are presented as median +/- interquartile range.

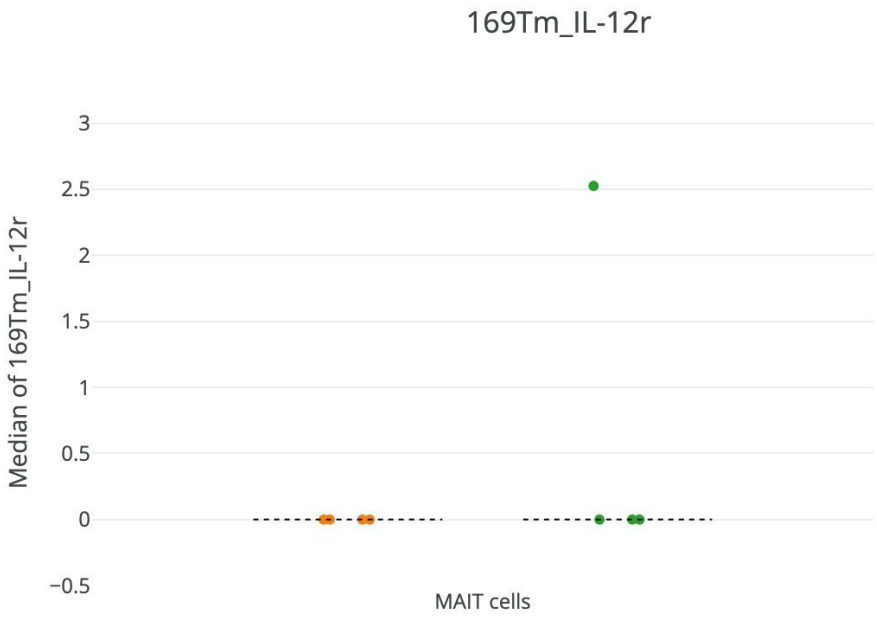

Channel	Population	Individual A	Individual B	Mean A	Mean B	SD A	SD B	n A	n B	p-value	Significance p-value
169Tm_IL-12r	MAIT cells	AIH Rx Naive STIM	AIH on Rx STIM	0	0.6313	0	1.093	4	4	0.391	ns

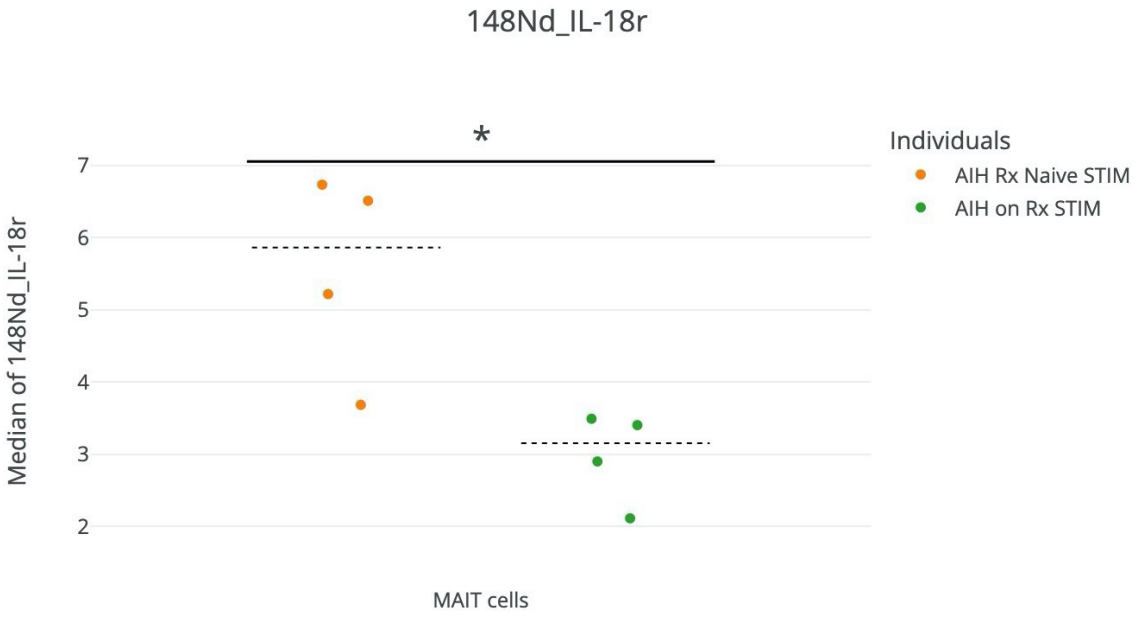

Channel	Population	Individual A	Individual B	Mean A	Mean B	SD A	SD B	n A	n B	p-value	Significance p-value
148Nd_IL-18r	MAIT cells	AIH Rx Naive STIM	AIH on Rx STIM	5.534	2.978	1.215	0.547	4	4	0.02752	*

Figure 4aa. Summary dot plots showing peripheral blood total MAIT cell expression of the cytokine receptors IL-12r and IL-18r from the AIH cohort; children with newly diagnosed AIH (treatment naïve, Rx Naïve STIM, N=4) and treated patients (on Rx STIM, N=4). Results of PBMC stimulated with CytoStim are shown. MAIT cell; mucosal- associated invariant T cell, AIH; autoimmune hepatitis, PSC; primary sclerosing cholangitis, HC; healthy control, PBMC; peripheral blood mononuclear cells, ns; not statistically significant. Y-axis shows the median metal intensity (MMI). Mann-Whitney U test results are displayed below each graph. Data are presented as median +/- interquartile range; *p<0.05

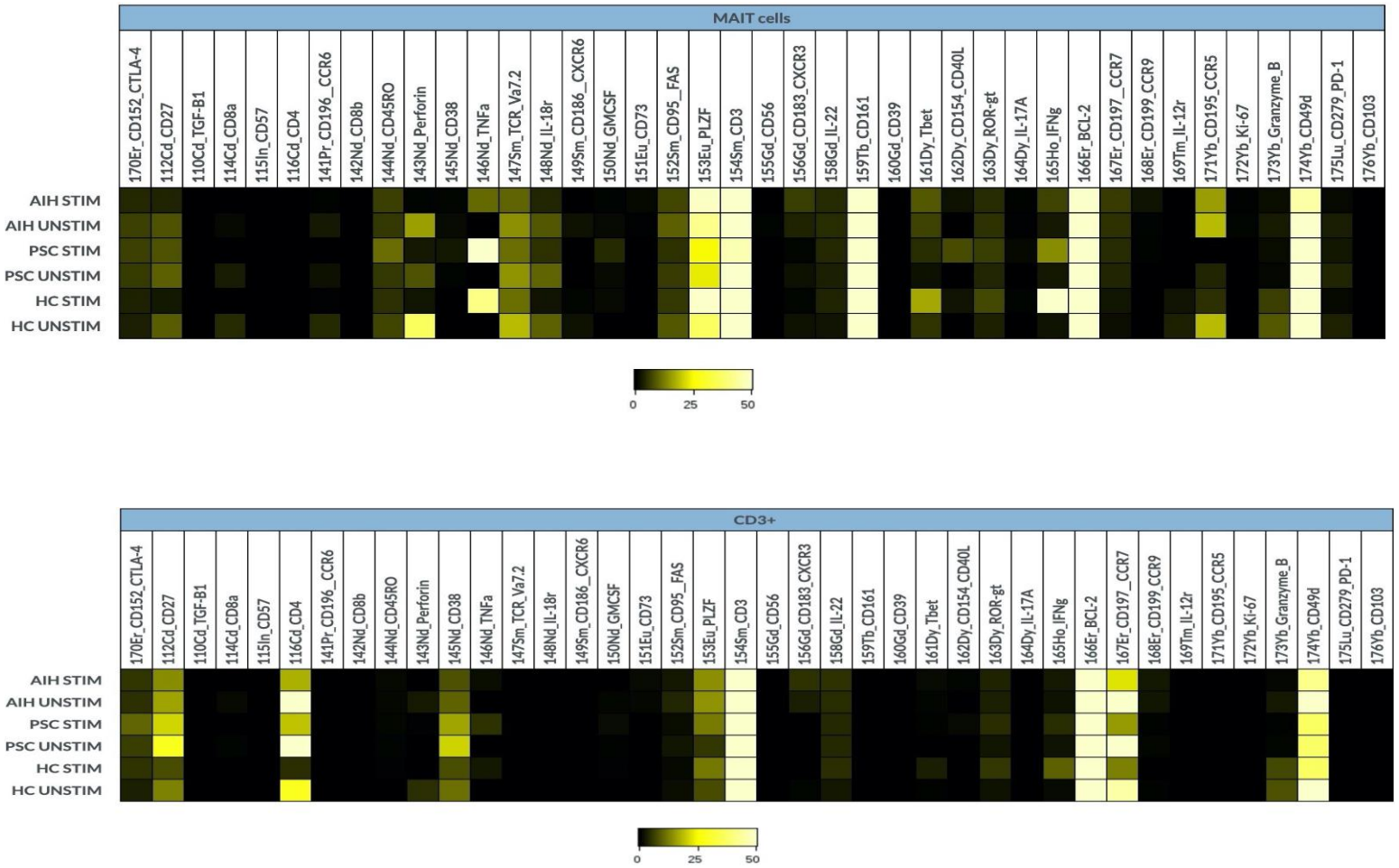

Figure 4ab. Heatmap of the cumulative surface and intracellular marker expression (column) in total MAIT cells (top) and CD3+ T lymphocytes (bottom) from paediatric patients with AIH N=8, PSC N=8 and healthy children N=8. Results of PBMCs treated with CytoStim (STIM) and their paired negative controls (UNSTIM) are shown (rows). The colour scale is shown at the bottom of each heatmap, with the median metal intensity (MMI) range set at 0-50; Pale yellow = strongly positive, black = strongly negative.

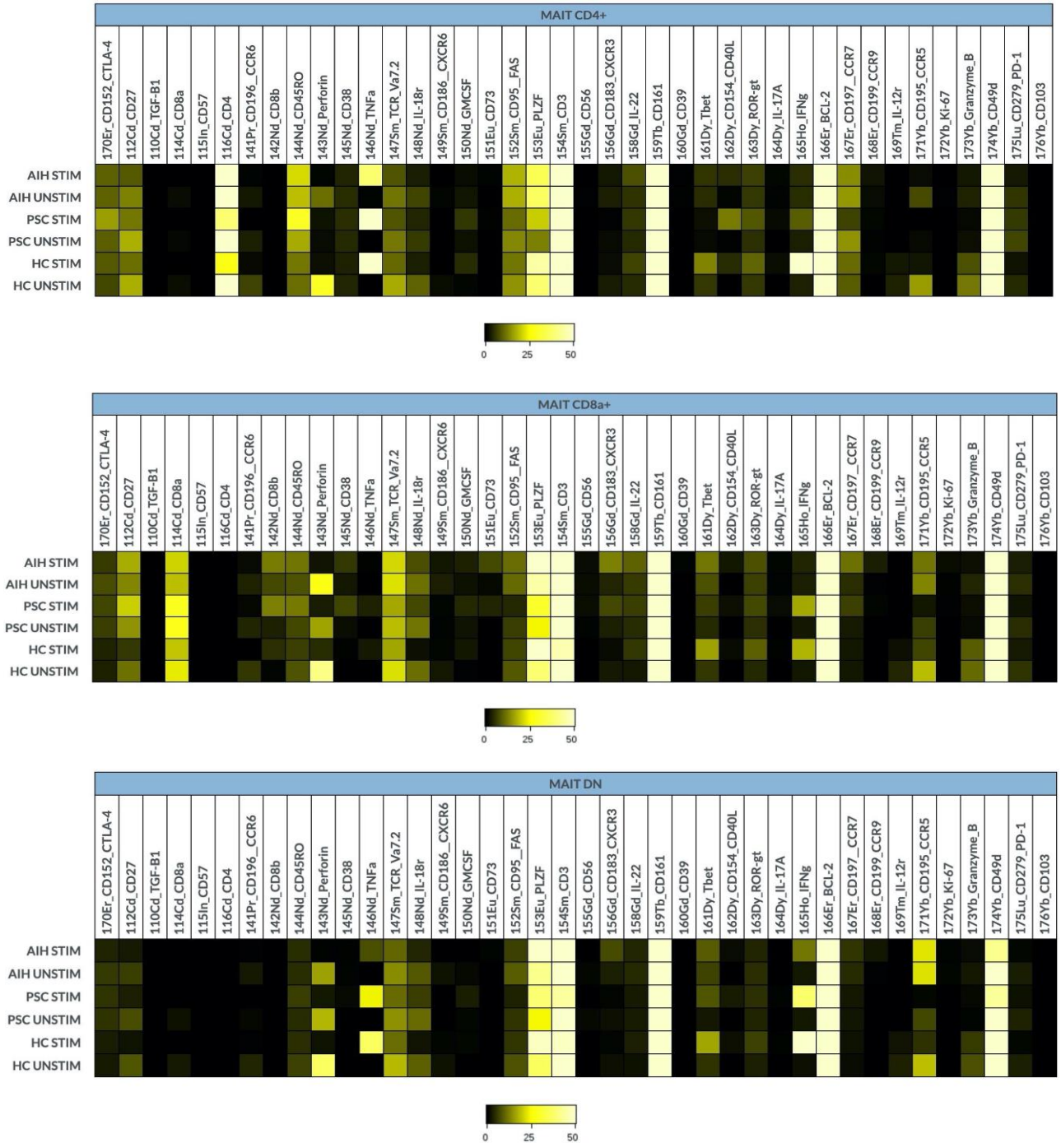

Figure 4ac. Heatmap of the cumulative surface and intracellular marker expression (column) in MAIT CD4+, CD8+ and DN cells from paediatric patients with AIH N=8, PSC N=8 and healthy children N=8.

Results of PBMCs treated with CytoStim (STIM) and their paired negative controls (UNSTIM) are shown (rows). The colour scale is shown at the bottom of each heatmap, with the median metal intensity (MMI) range set at 0-50;

Pale yellow = strongly positive, black = strongly negative.

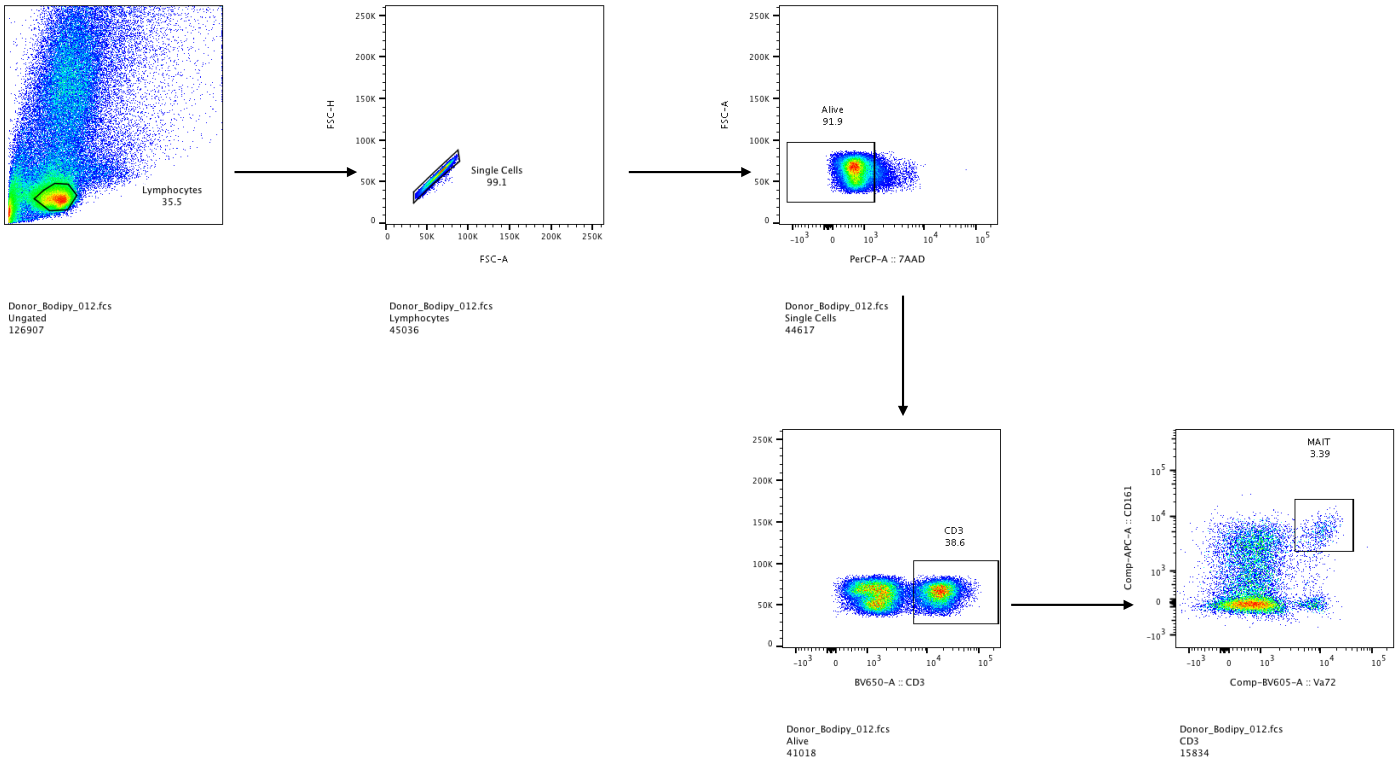

Figure 5a. Gating strategy for MAIT cells. Isolated lymphocytes from a donor liver were acquired using the BD LSR Fortessa X-20 sixteen colour flow cytometer. Analysis of the results were performed using FlowJo V10. Single cells were initially gated from lymphocytes to exclude doublet cells prior to the isolation of viable cells (7AAD negative) and then CD3+ cells. MAIT cells were gated from viable CD3+ cells (CD3+ Vα7.2+ CD161++).

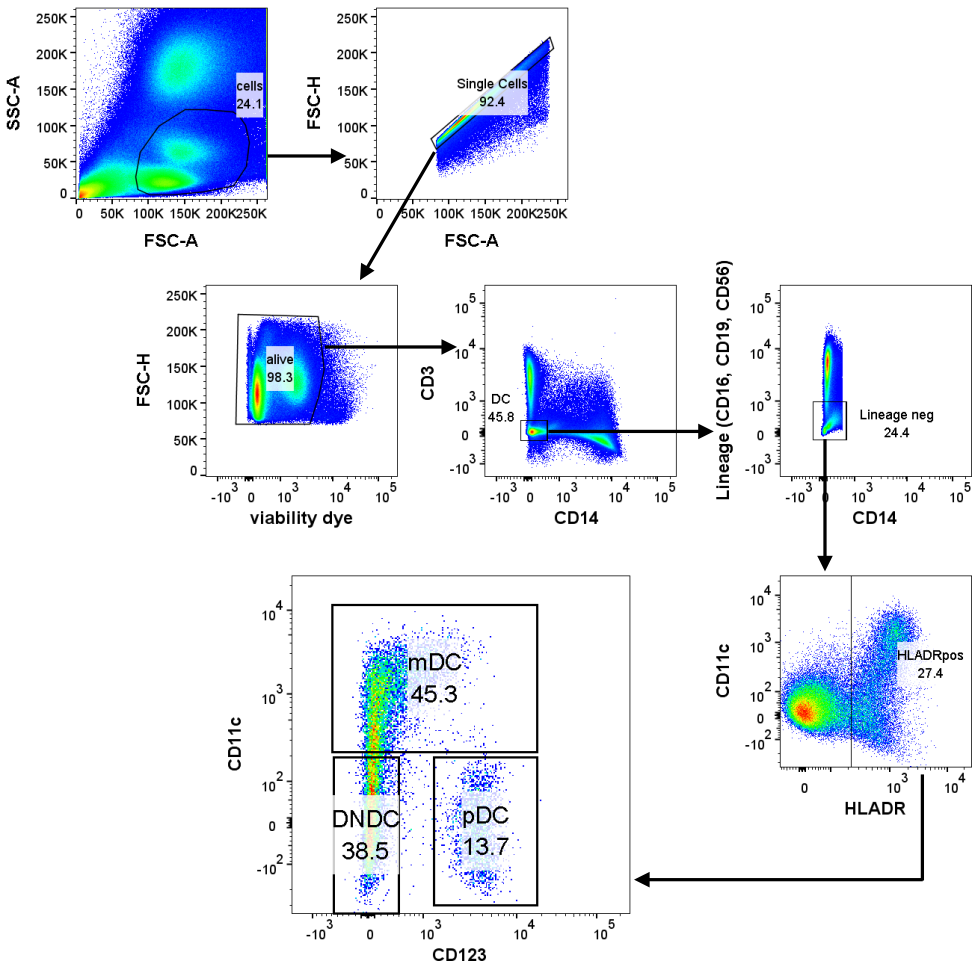

Figure 5b. Gating strategy for dendritic cells (DCs). Single cells were gated from liver derived monocytes and lymphocytes. Viable cells (e506 negative) were gated from the singlets prior to downstream gating of CD3- CD14-, lineage negative (CD16- CD19- CD56-) cells and onwards to obtain myeloid dendritic cells, mDC (CD11c++ HLADR+) and plasmacytoid dendritic cells, pDC (CD123+ HLADR+ CD11c-).

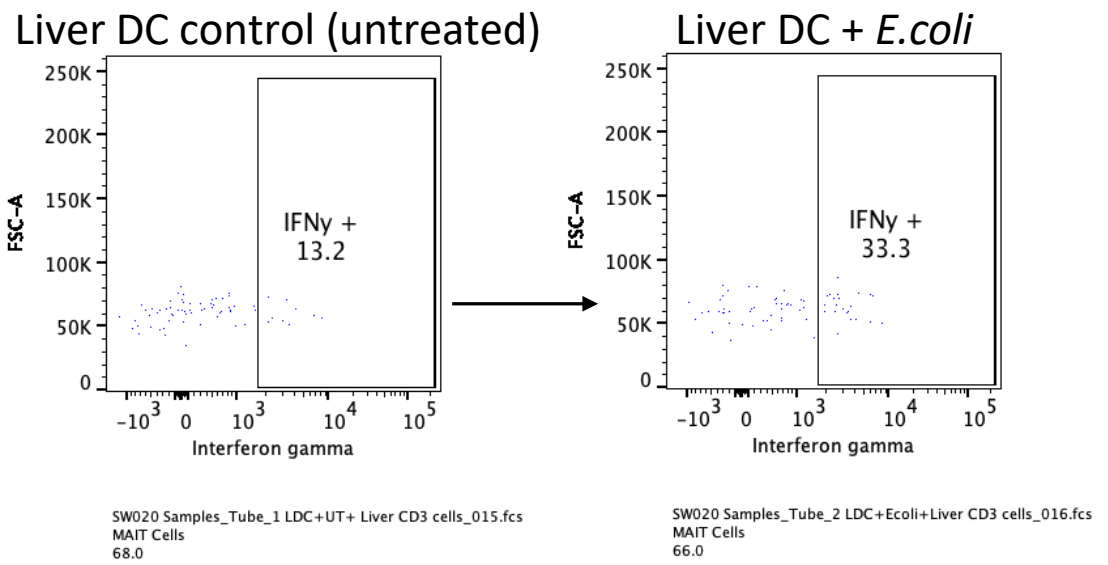

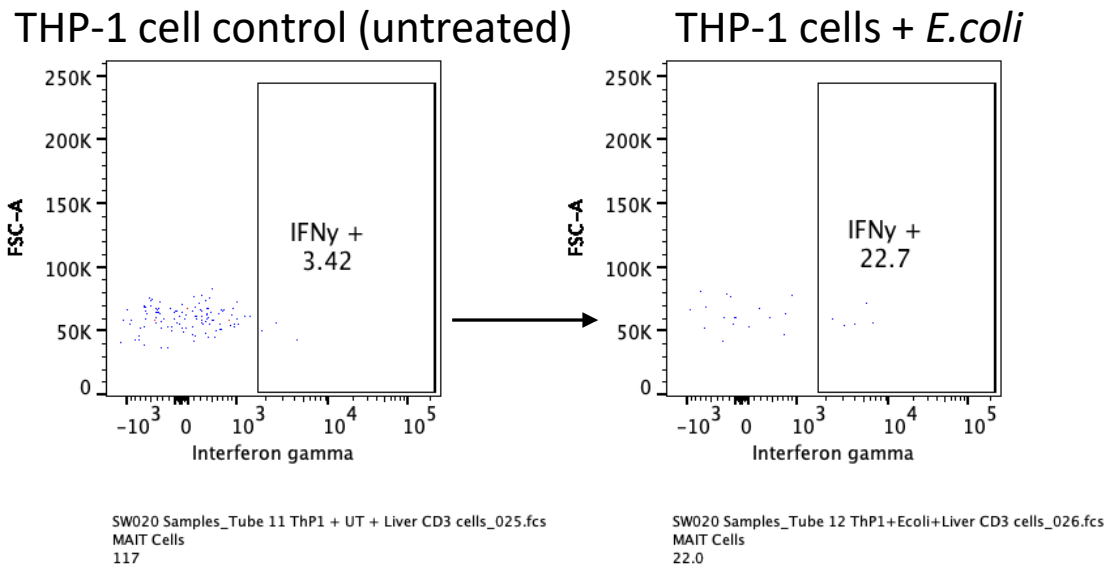

Figure 5c. *E.coli* primed liver derived dendritic cells can activate liver MAIT cells (gated CD3+, Vα 7.2+, CD161+); a 2.5 fold increase in liver MAIT cell interferon gamma (IFNγ) expression by *E.coli* primed dendritic cells is observed compared to its paired negative control (without *E.coli*). An even higher response of 6.5 fold increase in IFNγ is elicited in the experiment positive control (THP-1 cells with and without *E.coli*). Liver mononuclear cells were isolated from a human PSC liver explanted due to end-stage liver disease. Samples were processed using the BD LSR Fortessa X-20 sixteen colour flow cytometer. Analysis of the results were performed using FlowJo.

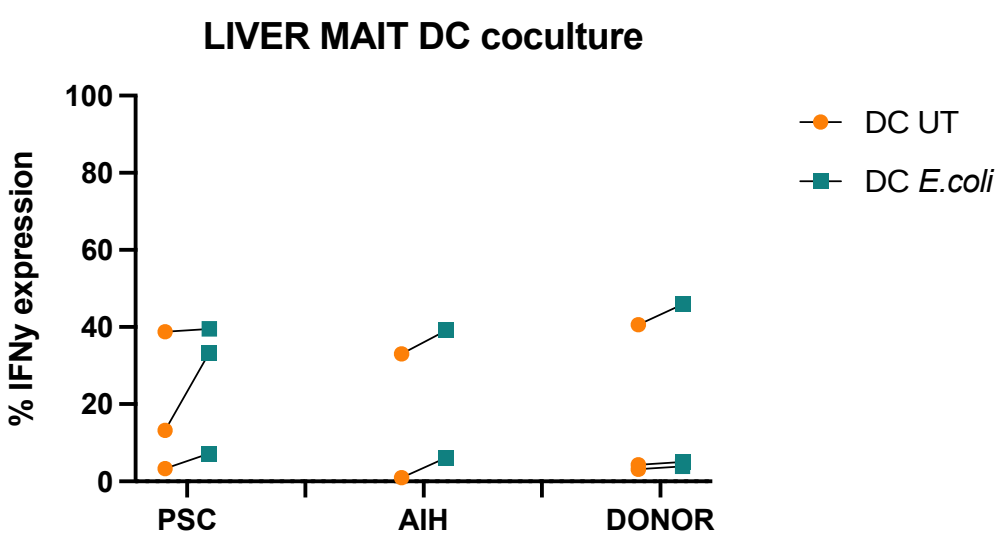

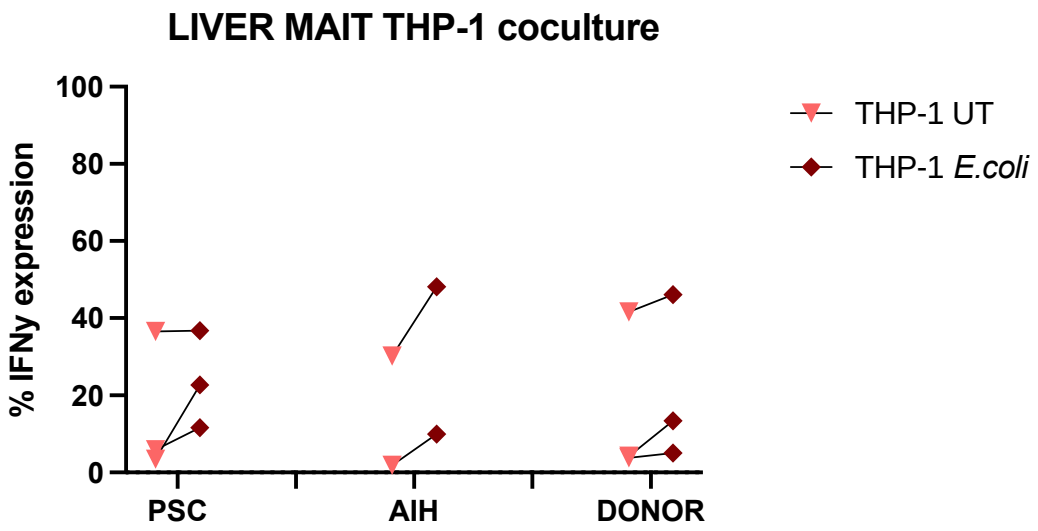

Figure 5d. Dot plots showing the liver MAIT cell interferon gamma (IFNγ) response following coculture with a) *E.coli* primed liver dendritic cells (DC) from the same liver and b) *E.coli* primed THP-1 cells (positive control) along with their paired negative controls (UT; untreated). Explanted livers; PSC, N=3, AIH, N=2. Donor livers N=3.

Liver DC control (untreated)

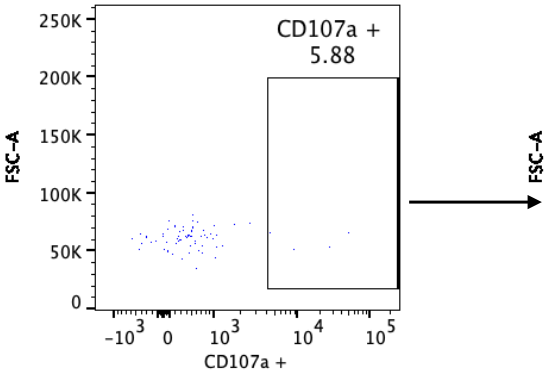

SW020 Samples_Tube_1 LDC+UT+ Liver CD3 cells_015.fcs
MAIT Cells
68.0

Liver DC + *E.coli*

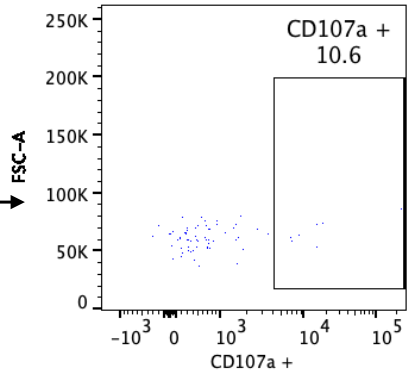

SW020 Samples_Tube_2 LDC+Ecoli+Liver CD3 cells_016.fcs
MAIT Cells
66.0

THP-1 cell control (untreated)

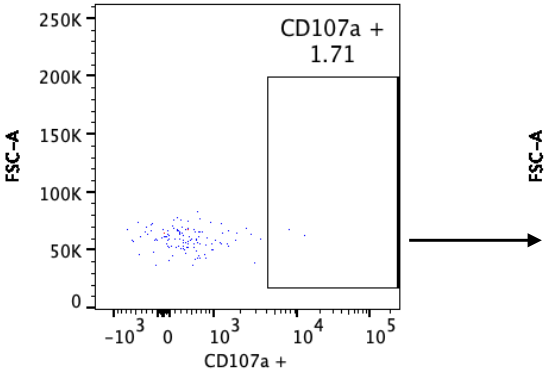

SW020 Samples_Tube 11 ThP1 + UT + Liver CD3 cells_025.fcs
MAIT Cells
117

THP-1 cells + *E.coli*

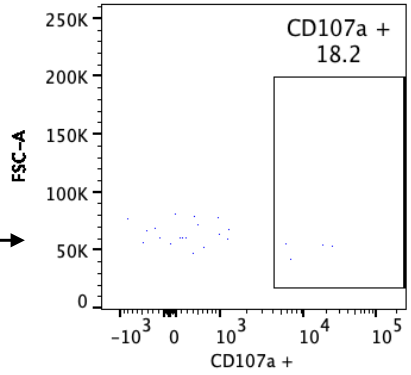

SW020 Samples_Tube 12 ThP1+Ecoli+Liver CD3 cells_026.fcs
MAIT Cells
22.0

Figure 5e. Liver MAIT cell CD107a (degranulation marker) expression is increased by 2 fold with *E.coli* primed liver DC and 10 fold by *E.coli* primed THP-1 cells compared to their negative controls (without *E.coli*).) Liver mononuclear cells were isolated from a human PSC liver explanted due to end-stage liver disease.

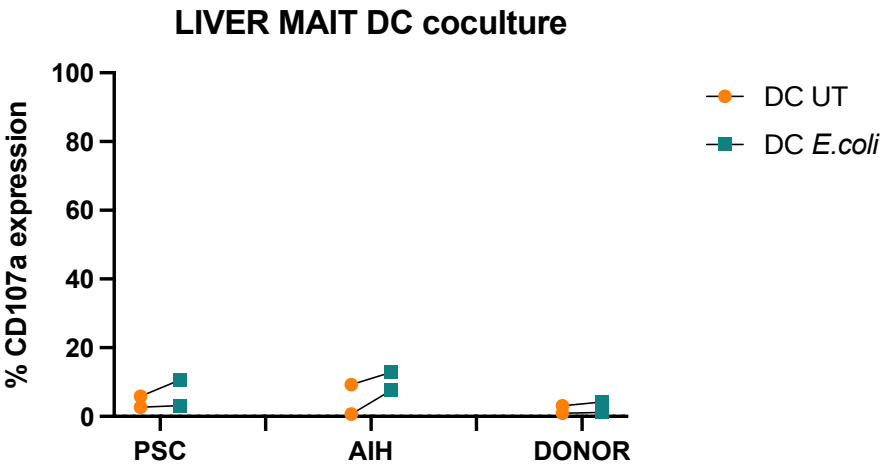

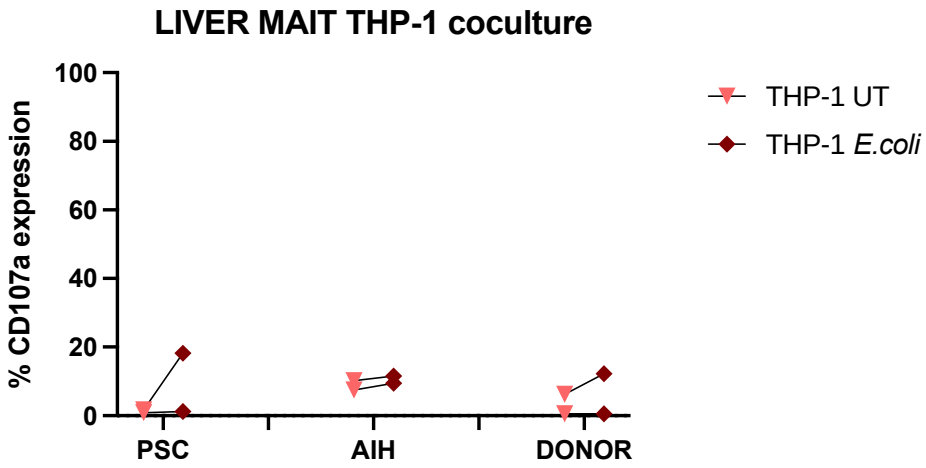

Figure 5f. Paired dot plots showing liver MAIT cell CD107a expression following coculture with a) *E.coli* primed liver dendritic cells (DC) from the same liver and b) *E.coli* primed THP-1 cells (positive control) along with their paired negative controls (UT; untreated). Explanted livers; PSC, N=2, AIH, N=2. Donor livers N=2.

Liver DC control (untreated)

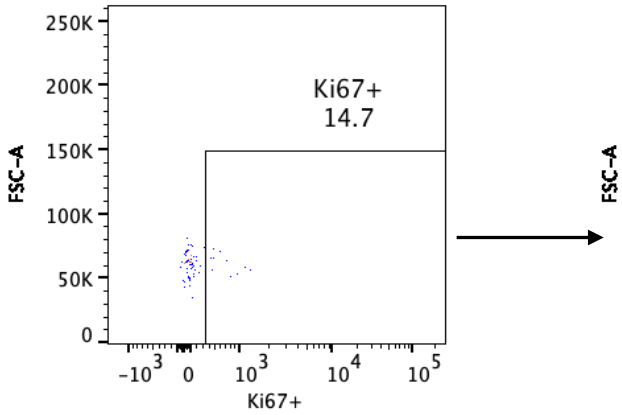

SW020 Samples_Tube_1 LDC+UT+ Liver CD3 cells_015.fcs
MAIT Cells
68.0

Liver DC + *E.coli*

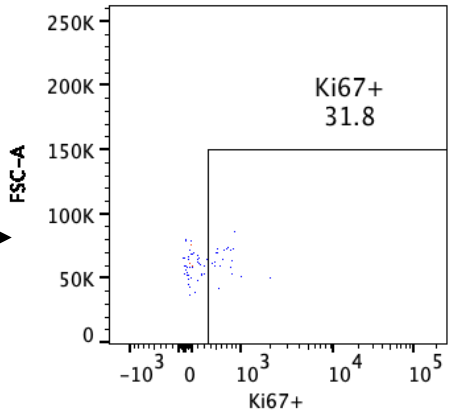

SW020 Samples_Tube_2 LDC+Ecoli+Liver CD3 cells_016.fcs
MAIT Cells
66.0

THP-1 cell control (untreated)

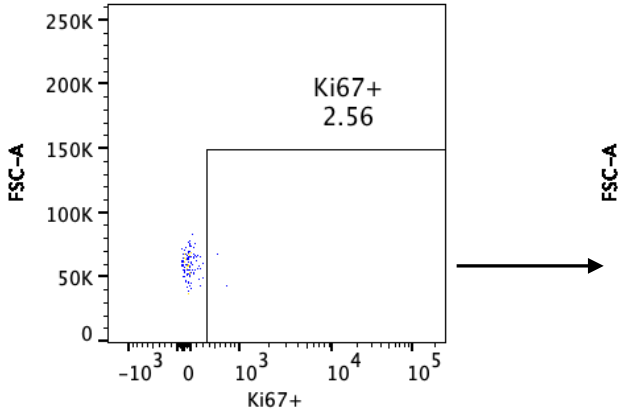

SW020 Samples_Tube 11 ThP1 + UT + Liver CD3 cells_025.fcs
MAIT Cells
117

THP-1 cells + *E.coli*

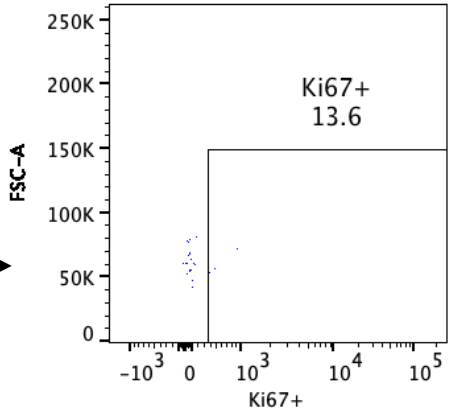

SW020 Samples_Tube 12 ThP1+Ecoli+Liver CD3 cells_026.fcs
MAIT Cells
22.0

Figure 5g. Liver MAIT cell Ki67 (cell proliferation marker) expression is increased by 2 fold with *E.coli* primed liver DC and 5 fold by *E.coli* primed THP-1 cells compared to their negative controls (without E.coli). Liver mononuclear cells were isolated from a human PSC liver explanted due to end-stage liver disease.

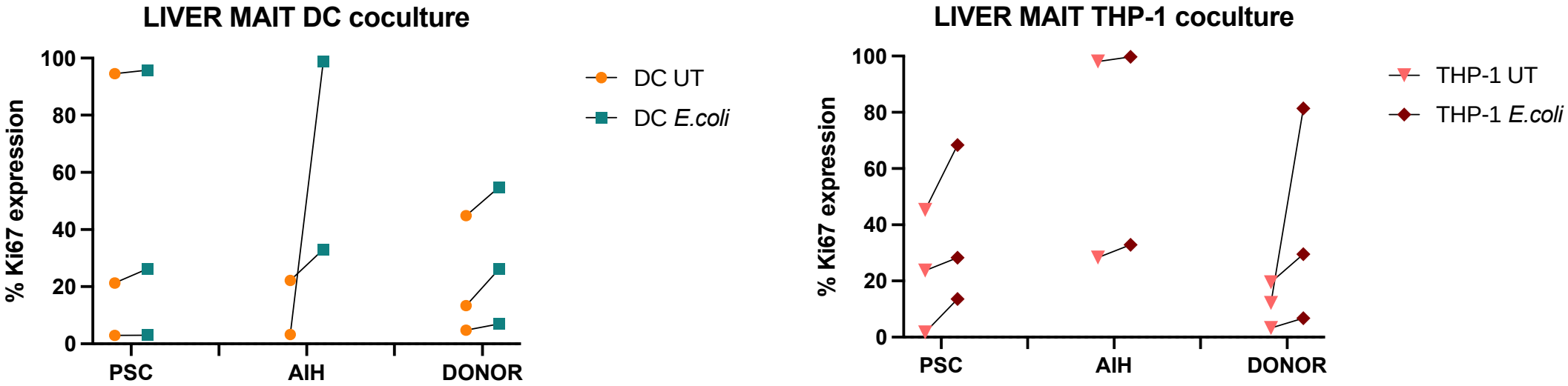

Figure 5h. Paired dot plots of liver MAIT cell Ki67+ expression following coculture with a) *E.coli* primed liver dendritic cells (DC) from the same liver and b) *E.coli* primed THP-1 cells (positive control) along with their respective negative controls (UT; untreated). Explanted livers; PSC, N=3, AIH, N=2. Donor livers N=3.

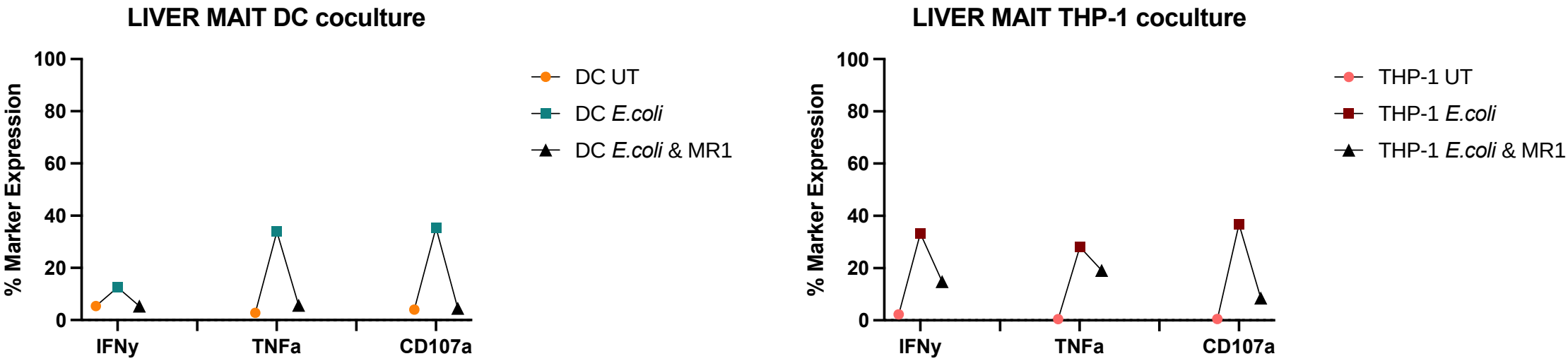

Figure 5i. MR1 blockade was introduced to a LI-MAIT coculture experiment from an explanted PSC liver. A reduction in expression of IFNγ, TNFα and CD107a is observed in the LI-MAIT cocultures in the presence of anti-MR1 antibodies with DC and with THP-1 antigen presentation.

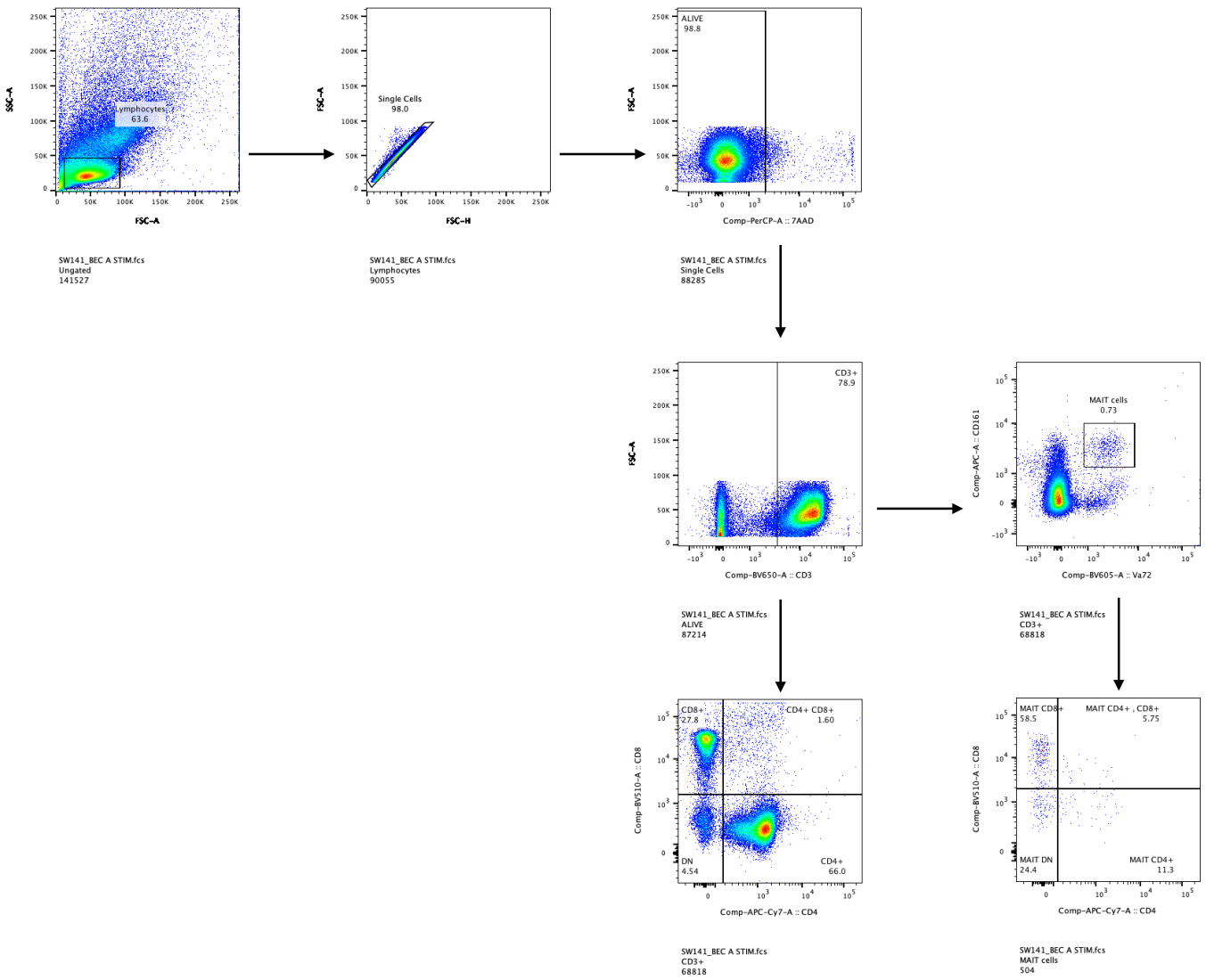

Figure 5j. Gating strategy of MAIT cells from lymphocytes isolated from a paediatric patient with autoimmune hepatitis. Viable cells were gated from lymphocyte singlets prior to CD3+ and then MAIT cell gating. Total CD3+ lymphocytes and MAIT cells (CD3+ Vα 7.2+ CD161++) are displayed along with their respective subsets (CD8+, CD4+, double negative DN, and CD8+ CD4+ lymphocytes).

BEC without *E.coli*

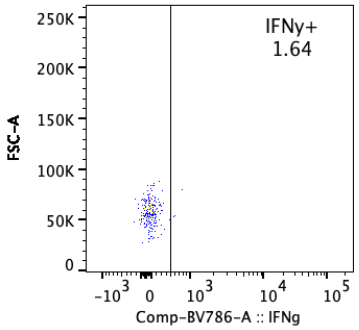

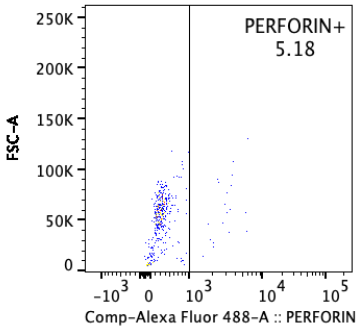

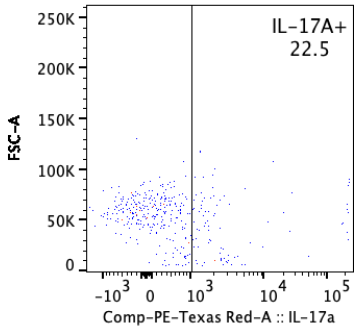

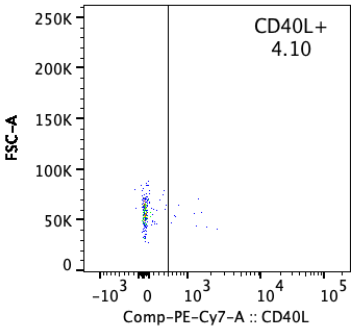

BEC with *E.coli*

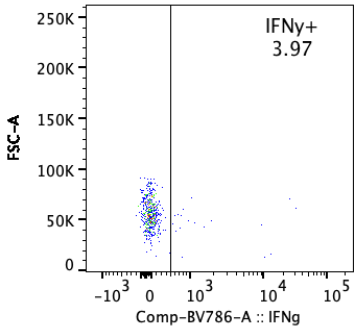

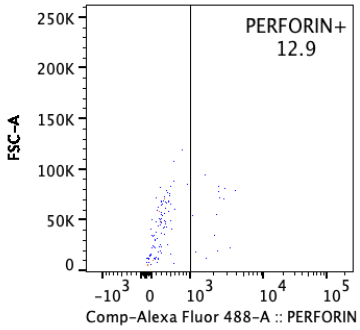

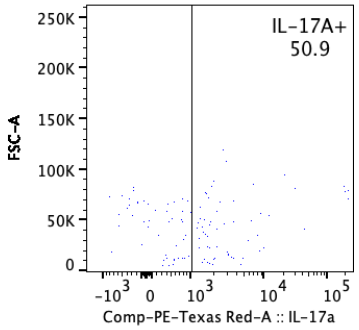

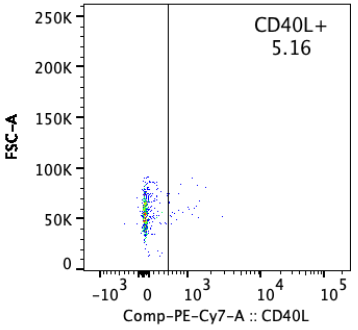

Figure 5k. Enriched T cells isolated from PBMCs of a paediatric patient with autoimmune hepatitis was cocultured with BEC (with and without *E.coli*). A 2.5 fold rise in MAIT cell cytokine response was demonstrated in the *E.coli* primed BEC coculture compared to the negative control (without *E.coli*). The CD40L expression in this experiment was unaltered. BEC; biliary epithelial cells.

Untreated

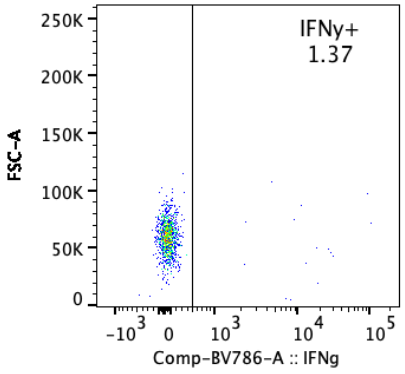

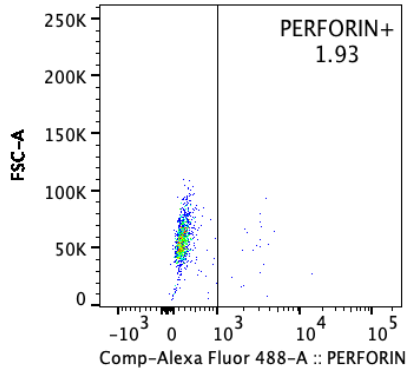

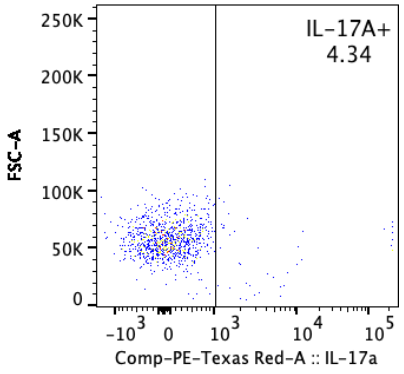

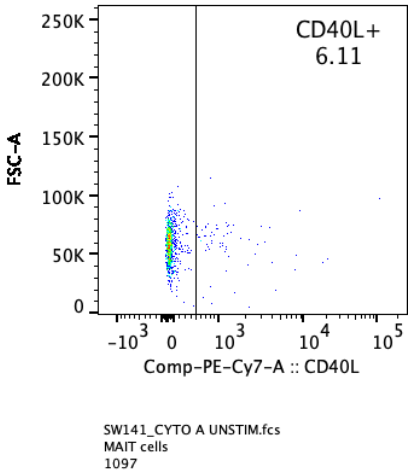

Treated (Cytostim)

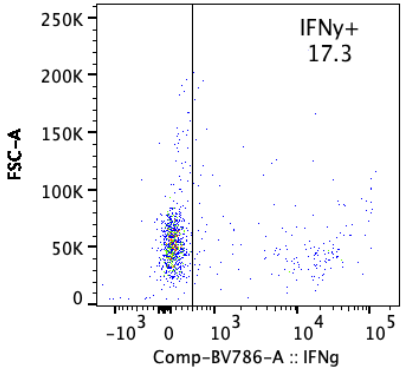

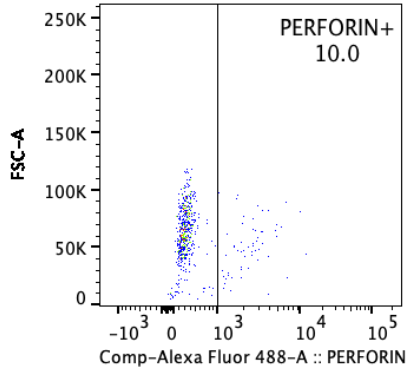

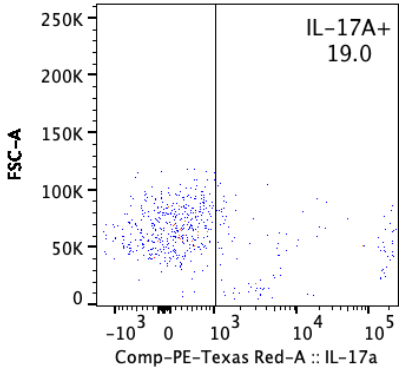

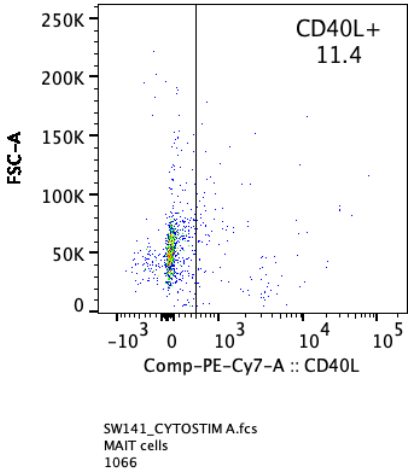

Figure 5l. Enriched T cells isolated from PBMCs of a paediatric patient with autoimmune hepatitis was treated with CytoStim, a cell stimulation cocktail containing polyclonal antibodies. A higher response is elicited in the cytokines IFNγ, Perforin and IL-17A compared to their paired untreated negative control and to that of the *E.coli* primed BEC coculture (Figure 5k). A rise in CD40L expression with CytoStim treatment was observed from 6.11% to 11.4%.

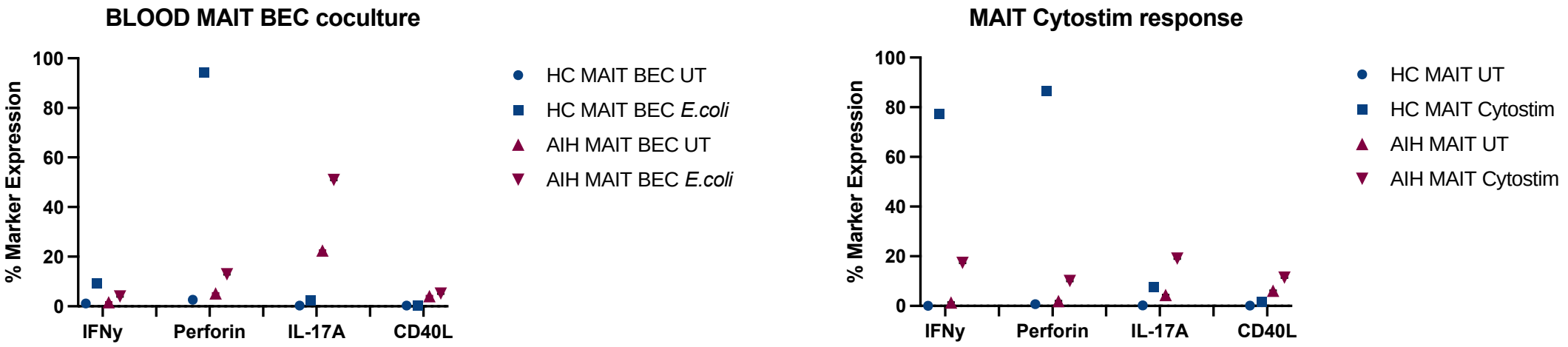

Figure 5m. Dot plots showing the blood MAIT cell response from an aged matched healthy control (HC) and an autoimmune hepatitis (AIH) paediatric patient.

In the MAIT-BEC cocultures (left dot plot), *E.coli* treated BEC induced a higher Perforin response in the HC. In contrast the IL-17A response is higher from the AIH patient. A similar pattern is observed in the positive control with CytoStim treatment (right dot plot) except a more pronounced response is observed in the IFNγ as well as Perforin expression in the HC. CD40L expression is increased in the MAIT cells of the AIH patient with CytoStim.

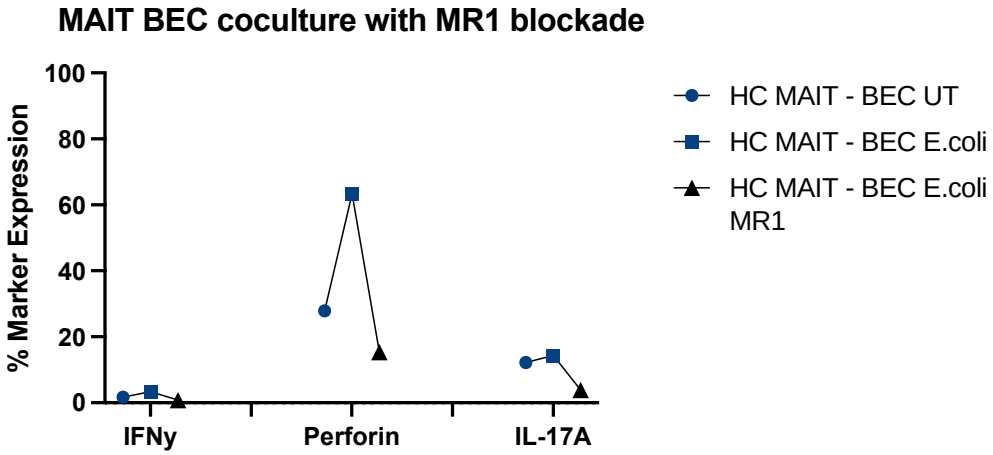

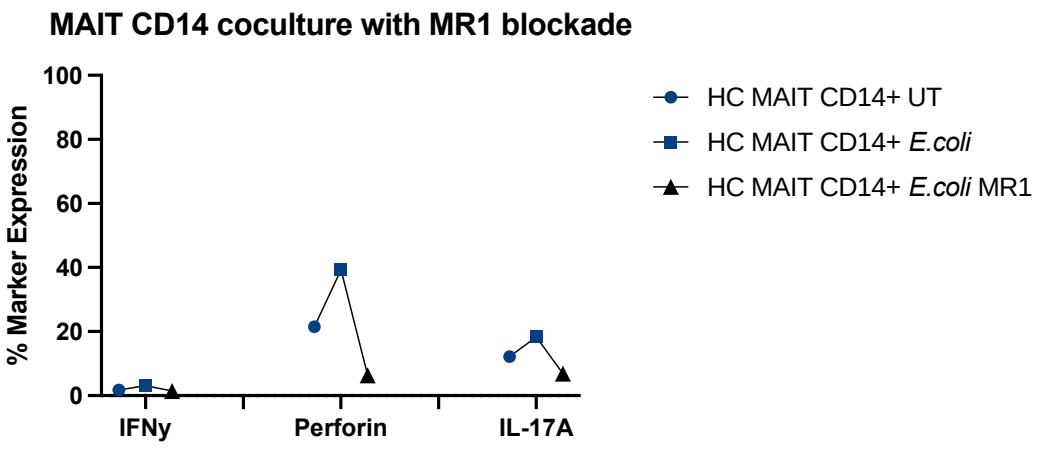

Figure 5n. Dot plots showing the blood MAIT cell response from a healthy child (HC). Three antigen presenting cell conditions were set; i) with *E.coli*, ii) with *E.coli* & MR1 antibody and iii) without *E.coli* or MR1. In the MAIT-BEC cocultures (left dot plot), *E.coli* treated BEC induced higher MAIT cell Perforin but minimal IFNγ response. A small IL-17A response is also demonstrated. A similar pattern is observed in the MAIT-CD14+ coculture in which blood MAIT cells were cocultured with CD14+ monocytes isolated from the same blood sample of the healthy child via magnetic positive CD14+ selection. In both cocultures, the MAIT cell IFNγ, Perforin and IL-17A response were shown to be MR1-dependent with a reduction in cytokines seen.